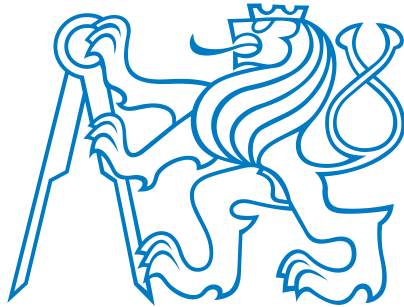


**CZECH TECHNICAL UNIVERSITY IN PRAGUE**

**Faculty of Electrical Engineering  
Department of Radioelectronics**



# **Design of Modulations for Wireless (Physical-Layer) Network Coding**

Doctoral Thesis

**Miroslav Hekrdla**

Prague, 2013

Ph.D. Programme: Electrical Engineering and Information Technology  
Branch of Study: Radioelectronics

Supervisor: **Prof. Ing. Jan Sýkora, CSc.**







*I don't want to achieve immortality through my work ... I want to achieve it through not dying.*

Woody Allen



# Abstract

This thesis is focused on a modulation design for emerging Wireless Network Coding (WNC) relaying strategy respecting various practical and theoretical conditions. Our work concerns three main topics.

The first topic is a constellation design for WNC in a simple AWGN 2-Way Relay Channel (2-WRC). The constellation design for WNC is generally challenging and sparsely investigated since the error performance of WNC processing at the relay (asymptotically determined by the minimal distance) does not depend only on a particular modulation alphabet but also on a network coding function used by the relay. Among other findings, we reveal the important property that *the constellations taken from a common lattice which are indexed in a suitable way* (indices form an arithmetic progression along each lattice dimension) *has the minimal distance equal to the minimal distance as in the point-to-point channel* (the important condition is that the modulo-sum network coding function is used by the relay). Based on this result, we have designed the constellations with the maximal possible minimal distance. The optimality of the proposed constellations are supported by error performance simulations as well as mutual information (Alphabet-Constrained Capacity (ACC)) curves.

The second topic targets a unique phenomenon of WNC in a wireless 2-WRC with perfect channel state information at the receiver – a new type of fading denoted as a *relative-fading*. Its name is derived by the fact that the relative-fading appears when a ratio of the channel gains is close to certain critical values no matter what are the actual values of the channel gains. The well-known relay processing method (using popular 4QAM) eliminates the relative-fading by the extended-cardinality network coding adaptation (the cardinality extension is undesirable since it introduces redundancy decreasing the data rates). We design and propose *special constellations* (e.g. *4HEX constellation*) *suitable for this method where the relative-fading is eliminated without the use of extended-cardinality adaptation*. As an alternative way how to combat the relative-fading, we introduce *constellations immune to the relative-fading without any adaptation* denoted as Uniformly Most Powerful (UMP). We identify some important features of the UMP systems like a) the use of bit-wise XOR network coding function is necessary but not a sufficient condition for the UMP condition, b) any orthogonal and bi-orthogonal alphabet is UMP and c) generally only multi-dimensional constellations can be UMP. We optimise naturally multi-dimensional modulations such as Frequency Shift Keying (FSK) and full-response Continuous Phase Modulation (CPM) to yield UMP alphabets. The found UMP alphabets provide considerable gains in a Rayleigh/Rice fading 2-WRC, although they require always more bandwidth than in the point-to-point case. They serve mainly as a performance benchmark identifying the schemes which perform close to the utmost UMP case but do not require more bandwidth. In the next chapter, we use robust non-linear optimisation tools to design general multi-dimensional UMP constellations with the highest possible minimal distance for given available bandwidth. It turns out that the UMP condition cannot be apparently fulfilled when the constellation spectral-efficiency is higher than 1 [bits/dimension]. Therefore, we propose a different type of alphabets called weak UMP which possess an unlimited spectral-efficiency but fulfil the UMP condition only for parameter ratios with absolute value equal to 1. This implies robustness to the Rician-type of fading.

The third topic is focused on the widely unexplored area of *the extension of WNC to more complicated network topologies*. We show that it is feasible to achieve additional considerable capacity gains in a 3-terminal 1-relay network with the carefully optimised multiple-access stage. We propose the ASK modulation, the modulo-sum network coding function and the  $\pi/3$  constellation prerotation for this scenario. It keeps the same minimal distance as in the point-to-point case providing the highest ACC performance among the other modulation, coding and prerotation types.





# Acknowledgements

It is my neat pleasure to thank Prof. Ing. Jan Sýkora, CSc for his supervising as well as for great experiences I have had a chance to participate as a member of Digital Radio Communication (DiRaC) research group. I have enjoyed the collaboration with him and with other DiRaC team members. My acknowledgement belongs to all my close friends and relatives as well.



# Proclamation

This PhD thesis “Design of modulations for wireless (physical-layer) network coding” has been made self-containedly and as a result of my research activities in the DiRaC group based on the collaboration with my supervisor and other team members. I have no objections against lending, publishing and any other utilization as long as the Department of Radioelectronics, FEE CTU in Prague, is in agreement.



# Contents

<b>1</b>	<b>Preface</b>	<b>21</b>
1.1	Goals of the Thesis . . . . .	21
1.2	Thesis Content . . . . .	21
<b>I</b>	<b>Introduction: Wireless (Physical-Layer) Network Coding</b>	<b>23</b>
<b>2</b>	<b>Introduction to Wireless Network Coding</b>	<b>25</b>
2.1	Historical Background: Mature P2P Communication . . . . .	25
2.1.1	Beginning of Modern Communication Theory . . . . .	25
2.1.2	Impact of Information Theory . . . . .	25
2.1.3	Road to the Capacity . . . . .	26
2.1.4	Besides the Capacity Challenge . . . . .	26
2.1.5	Point-to-Point Communication is Becoming Mature . . . . .	27
2.2	Historical Background: Challenging Networks . . . . .	27
2.2.1	Suboptimal Layered Architecture . . . . .	27
2.2.2	Notation Conventions for Network Topologies . . . . .	28
2.2.3	Troubles of Network Information Theory . . . . .	28
2.2.4	Cooperation and Relaying . . . . .	29
2.2.5	Network coding and Wireless Network Coding . . . . .	30
2.2.6	Other Emerging and Promising Research Areas . . . . .	30
2.3	Network Coding . . . . .	32
2.3.1	Non-optimality of Source-Separation Theorem in Communication Networks . . . . .	32
2.3.2	Network Coding Achieves Max-Flow Min-Cut Bound . . . . .	32
2.3.3	Linear and Random Linear Network Coding . . . . .	33
2.3.4	Non-Linear and Non-Coherent Network Coding . . . . .	33
2.3.5	Gains of Network Coding . . . . .	33
2.3.6	Possible Applications of Network Coding . . . . .	34
2.3.7	Tutorial Examples . . . . .	34
2.4	Wireless (Physical-Layer) Network Coding . . . . .	37
2.4.1	Discoveries Leading to WNC . . . . .	37
2.4.2	Origin of WNC . . . . .	37
2.4.3	Information Theoretical Considerations of WNC . . . . .	38
2.4.4	Ambiguous Names Describing WNC . . . . .	38
2.4.5	Tutorial Example: WNC in a 2-WRC . . . . .	39
2.4.6	Channel Coded WNC . . . . .	39
2.4.7	Fading Channel Parametrization Effects . . . . .	40
2.4.8	Constellation Design for WNC in an AWGN 2-WRC . . . . .	42
2.4.9	WNC in other than 2-WRC Network Topology . . . . .	42
2.4.10	WNC in a General Network Topology . . . . .	43
2.4.11	Real Implementation of WNC . . . . .	43

<b>II</b>	<b>Contribution: Modulation Design for Wireless Network Coding</b>	<b>45</b>
<b>3</b>	<b>Design of Lattice-Constellations and Constellation-Indexing for WNC</b>	<b>47</b>
3.1	Introduction . . . . .	47
3.1.1	Motivation & Related Work . . . . .	47
3.2	System Model . . . . .	48
3.2.1	2-Way Relay Channel Model . . . . .	48
3.2.2	Used Notation . . . . .	48
3.2.3	Wireless Network Coding in a 2-Way Relay Channel . . . . .	49
3.3	Affine Indexing for Modulo-Sum Decoding . . . . .	50
3.3.1	Impact of indexing . . . . .	50
3.3.2	Suitability of Affine Indexing . . . . .	50
3.3.3	Existence of AI for Canonical Lattice-Constellations . . . . .	53
3.3.4	Greedy-Sphere Packing for Constellation Shape Design which Ensures AI . . . . .	55
3.3.5	Generalisation for $N_A$ -terminal WNC MA stage . . . . .	57
3.3.6	Generalisation for Asymmetric Alphabet Cardinalities . . . . .	57
3.4	Error Performance Evaluation . . . . .	57
3.4.1	Analytical Symbol Pair-wise Error Approximation . . . . .	57
3.4.2	Average Number of Nearest Neighbours for WNC Method . . . . .	59
3.5	Alphabet-Constrained Capacity Evaluation . . . . .	61
3.6	Conclusion . . . . .	61
<b>4</b>	<b>Design of Constellations for Adaptive Minimum-Cardinality WNC</b>	<b>64</b>
4.1	Introduction . . . . .	64
4.1.1	Motivation & Related Work . . . . .	64
4.2	System Model . . . . .	65
4.2.1	Signal Space Model and Used Notation . . . . .	65
4.2.2	2-Way Relay Channel and Model Assumptions . . . . .	65
4.2.3	Adaptive WNC in a wireless 2-WRC . . . . .	66
4.3	Analysis of 4QAM Singularities . . . . .	67
4.4	Proposed Hexagonal Constellations . . . . .	68
4.4.1	4-ary HEX Constellation . . . . .	68
4.4.2	Unconventional 3-ary and 7-ary HEX Constellations . . . . .	72
4.5	Performance Evaluation . . . . .	73
4.6	Conclusion . . . . .	74
<b>5</b>	<b>Design of UMP Frequency Modulations</b>	<b>75</b>
5.1	Introduction . . . . .	75
5.1.1	Motivation & Related Work . . . . .	75
5.2	System Model . . . . .	76
5.2.1	Constellation Space Model and Used Notation . . . . .	76
5.2.2	Model Assumptions . . . . .	76
5.2.3	WNC Strategy . . . . .	76
5.2.4	Network Coding Operation . . . . .	77
5.2.5	Parametric Superimposed Constellation . . . . .	77
5.3	Minimal Distance Performance Measure and the Impact of Singularities . . . . .	78
5.3.1	Minimal Distance . . . . .	78
5.3.2	Singular Channel Parameters . . . . .	78
5.3.3	Network Coding Function Not Implying Singularities . . . . .	80
5.3.4	Non-Binary Linear Modulations are never UMP . . . . .	80
5.4	Uniformly Most Powerful Alphabet . . . . .	81
5.4.1	Minimal Distance Upper-bound . . . . .	81
5.4.2	UMP Alphabet Definition . . . . .	81
5.4.3	UMP Alphabet Properties . . . . .	81

5.4.4	Binary Modulation is UMP . . . . .	82
5.4.5	Non-Binary Orthonormal Modulation is UMP . . . . .	82
5.5	Design of UMP Frequency Modulations . . . . .	83
5.5.1	Design of UMP Frequency Shift Keying Modulation . . . . .	83
5.5.2	Bi-Orthonormal Modulation is UMP . . . . .	85
5.5.3	Design of UMP Continuous Phase Modulation . . . . .	85
5.6	Numerical Results . . . . .	92
5.6.1	Error Performance of Memoryless Modulations . . . . .	92
5.6.2	Error Performance of Full-response CPM . . . . .	92
5.6.3	Bandwidth Comparison . . . . .	94
5.7	Conclusion and Discussions . . . . .	96
<b>6</b>	<b>Design of General UMP Alphabets</b> . . . . .	<b>100</b>
6.1	Introduction . . . . .	100
6.1.1	Motivation & Related Work . . . . .	100
6.2	System Model . . . . .	101
6.2.1	Constellation Space Model and Used Notation . . . . .	101
6.2.2	Model Assumptions . . . . .	101
6.2.3	Wireless Network Coding Two-Way Relaying . . . . .	101
6.3	Error Performance at the MA Stage . . . . .	102
6.3.1	Nearest Neighbour Approximation of ML Metric . . . . .	102
6.3.2	Pairwise Error Union-Bound and Its Parametrization . . . . .	102
6.4	Uniformly Most Powerful Alphabet . . . . .	103
6.4.1	Problem of Parametric Performance at the MA stage . . . . .	103
6.4.2	UMP Definition and Properties . . . . .	104
6.5	UMP Alphabets Designed by Non-linear Optimization Tools . . . . .	105
6.5.1	Optimization Goal . . . . .	105
6.5.2	Energy Conditions . . . . .	106
6.5.3	Optimization Problem . . . . .	106
6.5.4	Problem Classification . . . . .	106
6.5.5	Problem Settings . . . . .	107
6.5.6	Non-linear Optimization Methods . . . . .	107
6.6	Numerical Results . . . . .	107
6.7	Conclusion . . . . .	113
<b>7</b>	<b>Impact of Relative-Fading in WNC 2-Way Relaying with Diversity Reception</b> . . . . .	<b>114</b>
7.1	Introduction . . . . .	114
7.1.1	Motivation & Related Work . . . . .	114
7.2	WNC in Diversity SIMO 2-WRC . . . . .	115
7.2.1	Model Assumptions . . . . .	115
7.2.2	Signal Space Model . . . . .	115
7.2.3	Bidirectional Relaying based on WNC . . . . .	115
7.3	Minimal Distance Analysis . . . . .	116
7.3.1	Minimal Distance of WNC . . . . .	116
7.3.2	Absolute-Fading and Relative-Fading . . . . .	117
7.3.3	Minimal Distance Upper-Bound Suppressing Relative-Fading . . . . .	117
7.4	Alphabet-Constrained Capacity . . . . .	119
7.4.1	Parametric ACC . . . . .	119
7.4.2	Ergodic ACC . . . . .	119
7.5	Numerical Results . . . . .	120
7.6	Conclusion . . . . .	123

<b>8</b>	<b>Optimised Constellation-Prerotation for WNC in 3T-1R Network</b>	<b>124</b>
8.1	Introduction . . . . .	124
8.1.1	Motivation & Related Work . . . . .	124
8.2	System Model . . . . .	126
8.2.1	3-Terminal 1-Relay Network . . . . .	126
8.2.2	Constellation Space Model and Used Notation . . . . .	126
8.2.3	Considered MA strategies . . . . .	126
8.3	WNC Strategy in a 3T-1R Network . . . . .	126
8.3.1	Two-stage MA strategy . . . . .	127
8.3.2	One-stage MA strategy . . . . .	127
8.3.3	Optimised Constellation Prerotation for the 1-stage MA Strategy . . . . .	127
8.3.4	Generalisation for a multi-source network . . . . .	128
8.4	Performance Evaluation . . . . .	130
8.5	Conclusion . . . . .	130
<b>9</b>	<b>Conclusion</b>	<b>131</b>
	<b>Bibliography</b>	<b>133</b>



# Acronyms

<b>2-WRC</b>	2-Way Relay Channel
<b>3T-1R</b>	3-Terminal 1-Relay network
<b>4QAM</b>	4-ary Quadrature Amplitude Modulation
<b>4HEX</b>	4-ary constellation taken from HEXagonal lattice
<b>ACC</b>	Alphabet-Constrained Capacity
<b>AF</b>	Amplify-and-Foward/Absolute-Fading
<b>AI</b>	Affine-Indexing
<b>ANC</b>	Analog Network Coding
<b>ASK</b>	Amplitude Shift Keying
<b>AWGN</b>	Additive White Gaussian Noise
<b>BC</b>	Broadcast Channel/ BroadCast
<b>BER</b>	Bit Error Rate
<b>BICM</b>	Bit-Interleaved Coded Modulation
<b>BPSK</b>	Binary Phase Shift Keying
<b>CF</b>	Compress-and-Forward/Compute-and-Forward
<b>CSI</b>	Channel State Information
<b>CSIR</b>	Channel State Information at the Receiver side
<b>CSIT</b>	Channel State Information at the Transceiver side
<b>CP</b>	Cyclic-Prefix
<b>CPM</b>	Continuous Phase Modulation
<b>DF</b>	Decode-and-Forward
<b>DNF</b>	DeNoise-and-Forward
<b>FG-SPA</b>	Factor Graph Sum-Product Algorithm
<b>FSK</b>	Frequency Shift Keying
<b>HDF</b>	Hierarchical Decode-and-Forward
<b>ISI</b>	Inter-Symbol Interference
<b>JDF</b>	Joint Decode-and-Forward
<b>LDPC</b>	Low-Density Parity-Check
<b>M2M</b>	Multipoint-to-multipoint
<b>MA</b>	Multiple Access
<b>MAC</b>	Multiple Access Channel
<b>MANET</b>	Mobile Ad-hoc NETwork
<b>MIMO</b>	Multiple-Input Multiple-Output
<b>ML</b>	Maximum Likelihood
<b>MSK</b>	Minimum Shift Keying
<b>NC</b>	Network Coding
<b>P2P</b>	Point-to-point

<b>PDF</b>	Probability Density Function
<b>PHY</b>	Physical
<b>PLNC</b>	Physical-Layer Network Coding a.k.a. WNC
<b>QAM</b>	Quadrature Amplitude Modulation
<b>QPSK</b>	Quaternary Phase Shift Keying
<b>RF</b>	Relative-Fading
<b>SER</b>	Symbol Error Rate
<b>SNR</b>	Signal-to-Noise Rate
<b>SIMO</b>	Single-Input Multiple-Output
<b>TCM</b>	Trellis Coded Modulation
<b>UMP</b>	Uniformly Most Powerful
<b>USRP</b>	Universal Software Radio Peripheral
<b>WNC</b>	Wireless Network Coding a.k.a. PLNC
<b>XOR</b>	eXclusive OR

# List of Used Symbols

$\star^{(i)}$	upper-index stresses a concrete variable value
$\oplus$	bit-wise XOR operation
$\langle \star, \star \rangle$	inner product
$\ \star, \star\ $	vector norm
$\mathbf{a}$	column lattice-coordinate vector of constellation alphabet $\mathcal{A}_A$
$A_2$	two-dimensional hexagonal lattice
$\mathcal{A}_A$	constellation alphabet of terminal $A$
$\mathcal{A}_{A+B}$	superimposed-constellation alphabet
$\alpha$	ratio of channel parameters $h_B/h_A$
$\mathbf{c}$	vector of common increments of modulo arithmetic progression
$C$	channel capacity
$C^*$	alphabet-constrained capacity
$\mathbb{C}$	complex field
$d_A$	data symbol of terminal $A$
$d_{AB}$	network coded data symbol
$D_2$	two-dimensional checkboard lattice
$D_4$	four-dimensional checkboard lattice
$\delta_{\min,A}$	minimal Euclidean distance of primary constellation $\mathcal{A}_A$
$\Delta_{\min}$	minimal Euclidean distance of network coded symbol decoding
$E_8$	eight-dimensional Gosset lattice
$E_{h_A}[\star]$	average over random value $h_A$
$\bar{\mathcal{E}}_s$	mean symbol energy
$\mathbb{F}$	finite field
$\mathbf{G}$	lattice generator matrix
$h_A$	frequency-flat fading channel coefficient
$\mathcal{I}$	indexing mapper
$\Im\{\star\}$	imaginary part
$j$	complex unit
$\kappa$	modulation index
$K$	Rician coefficients
$L$	diversity degree
$\Lambda$	lattice-modulation mapper/ lattice
$M_A$	data symbol cardinality of terminal $A$
$M_{AB}$	cardinality of network coded data symbols
$\mathcal{M}$	modulation mapper
mod	modulo operation
$N_s$	signal space dimensionality
$\mathbf{N}$	Latin square defining network coding function $\mathcal{N}$

$\mathcal{N}$	network coding function
$\mathcal{N}_{\text{adapt}}(\star)$	adaptive network coding function
$\sigma^2$	variance of complex AWGN sample
$p(\star)$	probability density function
$p(\star \star)$	conditional probability density function
$P[\star]$	vector permutation operator
$Q(\star)$	$Q$ -function
$\mathbb{R}$	real field
$\Re\{\star\}$	real part
$\mathbf{s}_A$	constellation space signal of constellation alphabet $\mathcal{A}_A$
$\mathcal{S}$	set of lattice coordinate vectors
$\gamma$	signal-to-noise ratio
$T_s$	symbol period
$\mathbf{u}$	superimposed-constellation point
$\mathbf{w}$	complex $N_s$ -dimensional AWGN
$W$	bandwidth
$\mathbf{x}$	received signal at the relay
$Z^2$	two-dimensional rectangular lattice
$\mathbb{Z}_M$	set of non-negative integers with elements lower than $M$
$\mathbb{Z}$	ring of integers

# Chapter 1

## Preface

### 1.1 Goals of the Thesis

The thesis “Design of modulations for wireless (physical-layer) network coding” is primarily submitted as a partial fulfilment of the requirements for the PhD degree. It summarizes my up-to-date research activities as a PhD candidate at the Faculty of Electrical Engineering, the Czech Technical University in Prague. There are two major goals of the thesis. Particularly, the thesis is intended to

1. introduce **current state-of-the-art of WNC strategy** supported by a detailed and actual list of **references**. We tried to support the introduction by sufficient number of basic examples and illustrations to explain the most important parts also to the readers not working in the field.
2. **Present our original contributions** and map them to the current state-of-the-art of WNC research.

### 1.2 Thesis Content

The thesis is divided into two parts corresponding to the goals of the thesis.

The first part is focused on the introduction to WNC serving also as a comprehensive source of references. We briefly introduce a historical background of communication development and describe the current-state-of-the-art in communication research today with an emphasis to the invention of network coding and wireless network coding. We write the introduction w.r.t. the thesis assignment: *modulation design for WNC*. The majority of our proposed solutions are supported by publication records which are integrated to the presented current-state-of-the-art. The first part is intended to be written for the broad audience not necessarily working in the field.

The second part consisting of six chapters is a summary of our original contributions related to the WNC research. The work was published mainly in [1, 2, 3, 4, 5, 6]. We keep individual chapters as a detailed stand alone text each describing a single result. Therefore, the chapters sometimes contain overlaps such as our notation conventions and system model descriptions. We believe that this is a more easily accessible way how to present the contributions than a single huge chapter with all the contributions mixed together (however without the redundant overlaps). Certainly, we have cleaned up the text to minimize the amount of redundancy and we have synchronised the system descriptions and used notations.

In particular, the third chapter deals with a constellation, indexing and network coding function design for WNC in a simple AWGN 2-WRC. The fourth chapter uses the properties discovered in the preceding chapter and based on them it designs a suitable modulations for the adaptive WNC method eliminating the effect of the relative-fading. The next two chapters are devoted to the design of multi-dimensional modulations immune to the relative-fading without any form of adaptation. The impact of relative-fading in diversity relaying system is studied in the next chapter. The eighth chapter targets generalisation of WNC into a more complex 3-terminal 1-relay network topology for which we present an optimised constellation, network coding function and linear precoding. We conclude our work in the last chapter where potential directions for the future research and possible practical implementations are discussed.



## **Part I**

# **Introduction: Wireless (Physical-Layer) Network Coding**

---

The first part of our thesis is focused on the introduction to WNC supported by a rich list of recommended references. At the beginning, we briefly introduce our general view of the historical background of communication development. Thereafter, we shortly describe the current-state-of-the-art of communication research (at least the related parts and these which seems to be the most promising and popular today). A special attention is given to the invention of network coding because it is the cornerstone of the aimed WNC strategy. The last section is solely intended to the WNC strategy. Particularly, we write the introduction w.r.t. the problems we dealt with: *a modulation design for WNC*. The majority of our proposed solutions are supported by publication records and these are integrated to the current-state-of-the-art.

The introduction is intended to be written for the broad audience not necessary working in the field. We try to avoid too detailed descriptions as well as mathematical details, rather we illustrate some important features by several basic examples. The essential details are introduced in the latter part dealing solely with our contributions.



## Chapter 2

# Introduction to Wireless Network Coding

## 2.1 Historical Background: Mature Point-to-Point Communication

### 2.1.1 Beginning of Modern Communication Theory

People perpetually wish to communicate between each other. In the history of communication, the value of information exchange triggered development of various information transmission techniques over various physical medium, depending on what technology was available at that time. Even the antique civilisations used sophisticated signalling based on light and/or sound medium. It has been more a century since the first radio pioneers started to utilise electromagnetic waves to transmit information. Theory of modern communication began to form by important personalities such as G. Marconi, N. Tesla, A. G. Bell and many others. Substantial progress and the real born of modern communication theory is deeply related to the origin of information theory. Information theory is based on outstanding pioneering work of C. Shannon utilising key ideas of the personalities of that time like H. Nyquist and R. Hartley. Information theory introduced a new way to look at communication, it brought solid mathematical formalism (probabilistic description) and it provides many answers to the fundamental communication problems.

### 2.1.2 Impact of Information Theory

Although information theory does not consider some important practical assumptions (like e.g. delay induced by communication and system complexity), it influences communication theory at the most. Particularly, it provides essential theoretical limits like the *channel capacity* (the maximal reliable information rate over a communication channel) and the *entropy* of an information source (the minimal rate of an errorless source-compression) [7]. Surprisingly, it often shows how to achieve these fundamental limits under practical constraints. It means that even if the results are purely theoretical with number of unrealistic assumptions, it often shows the way how to proceed in solving. For instance, source and channel separation theorem states (simply said) that source encoding and channel encoding can be theoretically designed separately without losing any performance. This caused the origin of theory of source and channel coding as separate research fields which greatly simplifies its design. Success of information theory is significantly supported by the fast grow of capabilities of electronic devices alleviating the impact of system complexity (not treated by information theory). Communication theory as well as information theory has undergone considerable development until today with plenty of key milestones. It is interesting that often many of the milestones have completely changed and broken the long standing and widely accepted believes.

### 2.1.3 Road to the Capacity

One of the most fundamental milestones, if we restrict on PHYSICAL (PHY) layer development of communication devices, is certainly the concept of reliable communication operating close to the capacity rate over an Additive White Gaussian Noise (AWGN) channel. To be more specific, the channel codes operating close to the capacity are well known since the first publication of Shannon's work [8], but these codes (denoted as *random codes*) presume unmanageably complex receiver processing. So the fundamental task was rather to find a concept of capacity achieving codes/systems with a reasonably complex receiver processing. We refer our reader to very nice paper [9]. It has been more than a decade when it turned out that the corner stone of the solution is based on the combination of *probabilistic channel codes* (Low-Density Parity-Check (LDPC) codes/ turbo codes or other interleaved and concatenated codes) and *turbo-like decoding principles* (iterative soft message-passing algorithms). These codes perform arbitrary close to the capacity limit so we can say that the powerful scheme with implementable decoder processing is known [10]. In the brief, we would like to mention some other important steps which we believe are leading to why Point-to-Point (P2P) communication is considered as mature today.

### 2.1.4 Besides the Capacity Challenge

Discovery of Trellis Coded Modulation (TCM) was certainly an important step<sup>1</sup> in the development of practical near-the-limit-operating systems. Before TCM discovery, it was widely believed that a good communication system is composed of the constellation with the highest possible minimal Euclidean distance with Gray-like bit-mapping and the channel code with the highest possible minimal Hamming distance. Although this approach works nicely in the case of binary and 4-ary constellations, it worked poorly for higher-cardinality constellations. The problem arises from the fact that Euclidean and Hamming distance are nicely proportional as long as the cardinality is lower or equal to 4. In other cases, a use of powerful channel codes with high minimal Hamming distance does not necessarily imply high minimal Euclidean distance of the overall system. Information theory advises that a system using binary constellations can operate near the capacity only at low Signal-to-Noise Ratio (SNR), therefore, higher cardinality constellations are required for medium-to-high SNR. It was the advent of TCM showing that modulation and channel coding should be designed jointly as a single entity in order to provide the optimal implementable system for medium-to-high SNR.

Apart from the milestone of achieving capacity in AWGN channel for both low and high SNR, we can find similarly fundamental breakthroughs in communication over a *wireless fading channel*. Just to specify some, there are e.g. *space-time coding* in Multiple-Input Multiple-Output (MIMO) systems, adaptive strategies (generally a usage of *feedback*) or modulations and codes tailored for fading channel as a Bit-Interleaved Coded Modulation (BICM). A very nice story of breaking a long standing widely-accepted paradigm is hidden behind the discovery of space-time coding. Before MIMO, it was widely believed that hostile conditions of wireless channel imply some redundancy (denoted as *diversity*) which needs to be provided to ensure certain performance quality. The diversity/redundancy then decreases effective information rate. It was space-time coding to demonstrate that the random fading phenomenon, if appeared uncorrelated at each antenna of MIMO system, could be exploited to not only overcome the hostile fading channel conditions but also to provide additional degrees of freedom which are easy to turn into capacity gains. In other words, space-time coding can provide diversity without sacrificing the rate and potentially the rate can be even boosted (as long as the limit given by diversity-multiplexing gain is fulfilled [11]). We must note, that in the case of random fading channel, a usage of Shannon's type definition of the capacity is not practical. Therefore, information theoreticians introduced a concept of capacity outage and ergodic capacity to effectively capture the random behaviour of the fading channel [12]. BICM modulation in a fading channel can be considered as a counterpart to TCM in an AWGN channel: BICM is a jointly optimised system of modulation, its bit-mapping and channel code in order to a) be robust to harmful effects of wireless channel, b) operate close to the capacity with implementably complex receiver processing. Outside of modulation and coding design, many progresses have

<sup>1</sup>The discovery of TCM as well as Continuous Phase Modulation (CPM) disproved the widely accepted opinion at that time that in order to provide a coding gain some redundancy (e.g. parity bits) which sacrifice bandwidth needs to be provided.

been done e.g. in ISI channel/wideband communication with frequency-selective fading. Here Orthogonal Frequency Division Multiplexing (OFDM) currently seems to be an attractive solution completely converting frequency-selective channel into a set of independent frequency-flat channels with relatively simple equalizer and implementation demands.

### 2.1.5 Point-to-Point Communication is Becoming Mature

It is impossible to mention all key discoveries in communication theory. There are simply too many of them and research is still active in these topics. In addition, they are attractive nowadays due to the current demands and technology, but may not be attractive in the future where maximal data rates might not be as required as e.g. energy consumption or manufacturing costs. By emphasizing some research highlights, we wanted to demonstrate that a lot is known about point-to-point communication (here, we mean one-transceiver-one-receiver communication potentially with multiple antennas) including both information theoretical as well as practical knowledge. We cannot say that research of point-to-point communication is dead, because e.g. there is still a long standing open problem how to match information theory and queuing theory in order to include a notion of *delay*. Some work has been done on delay-constrained channel codes [13], but the theory is rather rudimentary and difficult to deal with. However, delay-constrained communication is desirable and important from the practical point of view since it is closely related<sup>2</sup> to energy-constrained communication. In addition, impact and optimal usage of feedback is widely unexplored even in point-to-point communication (except of singular cases assuming static memoryless channel and time-varying finite-state channel). Besides delay-constraint communication and feedback, there will be always challenging questions of system design with the best performance-to-complexity (manufacturing costs) ratio [14]. Nevertheless, point-to-point communication is becoming a mature technology and many fundamental goals have been already achieved.

## 2.2 Historical Background: Challenging Network Communication

### 2.2.1 Suboptimal Layered Architecture

Current communication networks are designed in a layered manner, i.e. every layer ensures different tasks on which are build the upper-layers, e.g. the PHY layer typically provides modulation, channel coding and synchronisation for the upper Multiple Access Channel (MAC) layer dealing with multiple access coordination and interference. The aim of slicing architecture into layers is to alleviate complex problem of network architecture design into less complex subtasks in the spirit of divide-and-conquer. The layers are optimised separately with the aim that overall performance will be sub-optimally good enough. The PHY layer ensures de facto point-to-point communication whereas the upper MAC layer handles problems specific for network communication. This intuitive architecture division is not only motivated by complexity reduction but also by the fact that network information theory does not provide much insight into it. In fact, current network architectures are rather based on a good knowledge of point-to-point communication theory. We simply do not know the optimal network structure potentially requiring joint optimisation of all the layers at once. The approach of joint optimisation of several layers is denoted as a *cross-layer design*. Although information theory provides only limited advices, we can find singular cases where a cross-layer solution provides great performance gains such as e.g. successive-decoding and interference cancellation or cooperative communication and relaying. It is in contrast e.g. to the source-channel separation theorem for point-to-point communication where the separate optimisation of source coding and channel coding is under ideal conditions jointly optimal. Problems of cross-layer optimisation are typically much more complicated than in the layered model and in practical situations they need to be carried out in decentralised (distributed) manner for which theoretical tools of *convex optimisation* and *game theory* are seen as very attractive today.

<sup>2</sup>This is due to the fact that the delay induced by channel coding is proportional to the codeword length. The overall energy consumption equals to the transmitter's power multiplied by the codeword length, thus it is proportional to the delay.

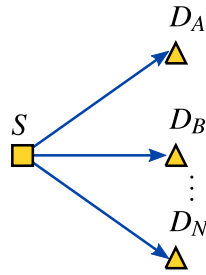


Figure 2.1: Broadcast channel. Source  $S$  transmits distinct data to distinct destinations  $D_A, D_B, \dots, D_N$ .

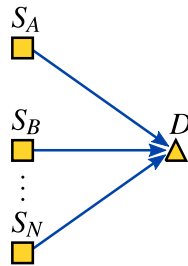


Figure 2.2: Multiple access channel. Each source  $S_A, S_B, \dots, S_N$  transmit distinct data to a common destination  $D$ .

### 2.2.2 Notation Conventions for Network Topologies

Throughout this text, we use the following symbols to denote the following network parts:

■	source node
▲	destination node
●	relay node
◻	both source & destination node
■ — ■	two connected nodes
■ → ▲	information transmission flow

Further, we distinguish the several types of networks:

<i>unicast</i>	network with a single source and a single destination
<i>multiple unicast</i>	network with multiple source-destination pairs
<i>multi-source</i>	network with multiple independent sources
<i>multicast</i>	network with multiple destinations demanding all data from all sources
<i>unidirectional</i>	network with one-way communication
<i>bidirectional</i>	network with two-way communication

### 2.2.3 Troubles of Network Information Theory

Knowledge of fundamental limits and hints how to achieve them is in Multipoint-to-Multipoint (M2M) communication in completely opposite situation as in P2P communication. The majority of network information problems remain unsolved for decades [15]. Current state-of-the-art of network information theory covers knowledge of the capacity region for point-to-multipoint network which is denoted as a Broadcast Channel (BC) depicted in Fig. 2.1. The capacity region of BC is well understood on assumption of static and degraded channel. Also a topology of multipoint-to-point network denoted as a MAC, illustrated in Fig. 2.2, possess known capacity region. Both BC and MAC is well explored assuming

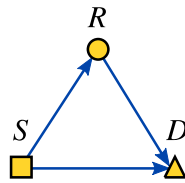


Figure 2.3: Relay channel. Source  $S$  transmits data to destination  $D$  with a help of relay  $R$ .

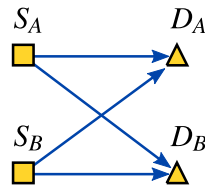


Figure 2.4: Interference channel. Source  $S_A$  transmits to  $D_A$  and source  $S_B$  transmits to  $D_B$ . Both communication pairs introduce interference for each other via cross-talk channels.

AWGN channel, wireless fading channel and recently also MIMO channel. But for instance, just assuming a simple three terminal single relay channel (the simplest M2M network) depicted in Fig. 2.3 or four terminal interference channel (Fig. 2.4), the situation starts to be so complicated that very limited knowledge about the capacity region is available today. Usually only lower- and upper-bounds stated a long time ago are known. There has been a progress in deriving *capacity scaling laws*, which characterize how per-node capacity scales in asymptotically large networks [16]. However, these laws provide just one equal-rate point of the capacity region. Similarly, *interference alignment* can achieve the capacity sum-rate point in a  $K$ -user interference channel (depicted in Fig. 2.5), but it does not achieve the full capacity region [17]. Since the fundamental data rate regions of the simple relay channel or interference channel have eluded researchers for so long, it is unlikely that we can obtain the capacity region for more general networks, especially when practical constraints like network *dynamics* and *feedback* are incorporated.

## 2.2.4 Cooperation and Relaying

Although the fundamental rate regions of multipoint-to-multipoint networks is widely unexplored research area, there are many communication approaches which provide significant gains in compare to current layered communication networks. One of the most important examples is a foundation of *cooperation* and *relaying*, see book [18] and its references. The concept of relaying introduces relay nodes which are solely intended to support communication. Relays may provide additional degrees of freedom or diversity to boost the capacity or outage capacity and considering pathloss in the channel model, the

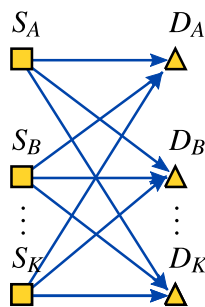


Figure 2.5:  $K$ -user interference channel. Source  $S_A$  transmits to  $D_A$ , source  $S_B$  transmits to  $D_B$  and so on. All communication pairs introduce interference for each other via cross-talk channels.

relay significantly improves effective SNR. Here, we understand cooperation as a collective approach where multiple terminals help each other to jointly accomplish their communication demands. For example, multiple transmitters and/or receivers may cooperate to form a *virtual MIMO* system and jointly obtain diversity-multiplexing gain [11]. Cooperating terminals may also jointly suppress harmful impact of interference e.g. by distributed *beamforming* approach.

### 2.2.5 Network coding and Wireless Network Coding

Besides cooperation and relaying, there is a relatively new and very promising discovery of Network Coding (NC) and its derivatives including Wireless Network Coding (WNC). Our thesis is focused on WNC so the next sections will be devoted to NC and WNC in much greater detail. Here we state only important features relevant to the historical background. The origin of NC as a new scientific field is based on pioneering work [19] showing that routing is not always an optimal approach in the point- (multipoint)-to-multipoint multicast wired network. We use the term multicasting to denote a scenario where every destination require data from all sources of information. Considerable data rate gains are available if intermediate nodes in the network (e.g. relays, routers) perform some form of data compression/coding (denoted as *network coding*) of the data to be further re-transmitted. NC reveals the potential of treating network communication as a whole challenging problem (unlike conventional consideration of a network as a set of P2P links).

WNC strategy performs basically equivalent operations like NC but at the PHY layer which additionally enables to harness carefully handled interference into the capacity gains. On the other side, PHY processing brings several new challenges which needs to be solved/understood e.g. how should network coding like operations be done over non-finite field algebraic structure, impact of *wireless channel parametrisation* and *modulation & code design for WNC* which is considered in this thesis and our work [1, 2, 3, 4, 5, 6]. In current wireless networks is interference induced by shared wireless medium usually eliminated by taking additional orthogonal resources. It presents a considerable amount of resources in dense networks and then the interference is becoming a major issue rather than effects of noise or fading. The term *interference limited networks* is often used. The potential of interference being beneficial would be a similar breakthrough as e.g. that fading can boost the capacity when utilised by MIMO system.

WNC is based on the tree core paradigms:

1. **network coding** (required to reach the max-flow min-cut bound),
2. utilisation of full potential of **wireless broadcast** (not considering wireless medium as a P2P link),
3. interference harnessing **physical-layer processing** (interference on ideal conditions is nothing else than signal superposition and its linear structure can be potentially utilised).

Section 2.3 is devoted to NC and its potential benefits in wireless networks and Sec. 2.4 is devoted to WNC.

### 2.2.6 Other Emerging and Promising Research Areas

Although we cannot guarantee how much promising are individual research fields, we may highlight some of them currently very attractive in the research community. We have already mentioned research areas of still unsolved problems of delay/energy-constrained communication, optimal use of feedback, impact of network/data/channel dynamics, performance-to-complexity trade of in P2P scenario and distributed multi-user cooperation & relaying, NC & WNC, interference mitigation techniques in a M2M scenario. We believe that *network communication problems* possess enormous potential these days which are now under intensive investigation. Even though, network information theory cannot provide desirable fundamental limits in most of the cases, we see a great potential in direction to approximate [20] or find an equivalent problem [21] rather than determine the exact capacity regions of wireless networks. Suitable still-rather-theoretical tools for analysis complex network information theoretical problems are provided

by theory of (nested) *lattice codes* [22], [23]<sup>3</sup>. The lattice codes prove to achieve the capacity in the P2P network but unlike the Shannons' random codes they contain a structure which in certain scenarios with a more complex network topology provides even higher achievable rates than the random codes. The ultimate solution in the search for the optimal network architecture will probably need to joint several theoretical tools like *game theory*, *optimisation theory*, *queuing theory* and *control theory*.

For current state-of-the-art of network information theory we recommend works [14], [15], [25]. An interesting and newly emerging research branch is an application of communication engineering tools now on medical or biological problems like application of information theory on DNA analysis.

---

<sup>3</sup>Although practical lattice codes which achieve the capacity under reasonable complexity constraints have been proposed in [24].

## 2.3 Network Coding

In this section, we briefly focus on basics of NC. The reasons are following:

1. NC shares some essential features of our centre of interest – WNC strategy and
2. much more is known about NC both in the information theoretical way as well as in the practical way (network test-beds based on NC have already been built on which true gains have been successfully measured).

For comprehensive reference literature, we recommend instant primer [26], introductory book [27] and information theoretical analysis summarized in [28] [29]. A very well written historical perspective of NC can be found in [30].

### 2.3.1 Non-optimality of Source-Separation Theorem in Communication Networks

Network coding seems to be *one of the most important discoveries* of communication research in recent times. This shows for example a number of citations of seminal work [19] written by R. Ahlswede, N. Cai, R. Li and R. Yeung in 2000 which exceed 5000 today<sup>4</sup>. NC discovery can be considered as an important milestone in the development of network communication theory because it has disproved a widely believed paradigm of the optimality of a *source-separation theorem* in communication networks [30]. Loosely speaking, it means that if we combine the optimal solution for a single-source single-destination network<sup>5</sup> with the optimal solution for another source-destination pair, it will not be jointly optimal for the network comprising the two sources and the two destinations (i.e. we cannot consider sources separately without losing any performance). As a consequence, it was widely believed that information quantity behaves as a *physical quantity* i.e. as indivisible elementary particles of information. Current networks are based on these principles. The information is *routed* through the network in a *store-and-forward* way, the intermediate nodes (relays, routers) receive and without any change forward the information.

It was the discovery of NC to show that this approach is not optimal and higher information rates are achievable in certain cases if the intermediate nodes perform some form of compression of information to be forwarded. This compression is denoted as *network coding*. Network coded information then represents a mix of information from multiple sources (the sources are not treated independently any more).

### 2.3.2 Network Coding Achieves Max-Flow Min-Cut Bound

Pioneering work [19] shows that network coding solution achieves the mutual information upper-bound given by the *max-flow min-cut bound* in a single-source multicast network. Therefore, it is an optimal solution w.r.t. maximal throughput since higher flow than the max-flow cannot be accommodated. The max-flow min-cut bound determines maximal multicast flow through a single-source *combinational packet network* where the combinational packet network is a network formed by unidirectional error-free bit pipes with the rate 1 [bit/channel use]. Here, multicast communication denotes a situation where each destination requires all data from all sources. The max-flow min-cut bound is derived by application of known results of graph theory on information flows. Given a combinational packet network, we may find the minimal-cut (and thus the-maximal flow) by tools of graph theory such as Ford-Fulkerson algorithm. Here, a cut of a network has a graph theoretical meaning, i.e. it is a cut which separates the network into two parts: into the one containing all sources and the other one containing all destinations. The value of the cut is a number of interrupted vertices (if each is assumed to have a unit data rate). Paper [19] concludes that in single-source multicast network is network coding an optimal solution and it achieves the max-flow min-cut throughput.

<sup>4</sup>Taken from Google Scholar on 9.6.2013

<sup>5</sup> The optimal solution in a network comprising a single source and a single destination is the data routing [27].



### 2.3.3 Linear and Random Linear Network Coding

Discovery of network coding has triggered a tremendous interest of the research community. Soon following work [31] proved that the max-flow min-cut bound in a single-source multicast network is achieved even by *linear network coding*. Linear network coding means that the network coding operations performed by intermediate nodes are a linear combination of all incoming messages performed over some finite field. The output of a network encoder is a packet containing the linear combination and the set of used linear combination coefficients. Every final destination can decode all messages after receiving sufficient number of linearly independent linear combinations and solving the set of linear equations. A polynomial time deterministic algorithm to design linear combination coefficients has been proposed in [26]. Note, that in this case we can talk about a complexity benefits since traditional routing algorithms are NP hard optimisation problems.

After a short period of time, paper [32] introduced a concept of *random linear network coding*, where no deterministic algorithm is used for the coefficient selection. Instead, every node selects the coefficients at random. Providing a finite field size to be sufficiently large, the random linear network coding approach works close to the optimal deterministic solution. It is a great advantage that this approach is completely independent and decentralised. It means that having whatever single-source multicast combinational packet network, we can easily approach the optimal throughput in the desired distributed and decentralised way. This property is interesting especially in wireless mobile ad-hoc networks where we cannot guarantee sufficient robustness and adaptability [33].

### 2.3.4 Non-Linear and Non-Coherent Network Coding

Single-source network coding problems are generally better understood (the maximal rate is given by the max-flow bound and it can be achieved by linear network coding). Considering a general networks with multiple independent sources, the situation turns out not to be a simple extension of the single-source network problems and rather probabilistic tools [28] are available in reaching the optimum such as a *superposition coding* and *non-Shannon-type inequalities* [7], [29]. Paper [34] shows that just leaving a single-source multicast assumption leads to a dramatic change. There exist cases where linear combination of incoming messages is insufficient and more general linear operations using linear transform of a set of messages needs to be used to reach the maximal achievable throughput (a key role also plays the size of the finite field). In some other cases even *non-linear network coding functions* are required to achieve the maximal achievable throughput in general multi-source networks. Giving up the overall optimality, a suboptimal algorithm in linear network coding for multi-source networks has been proposed in [35].

Recently, an approach using random linear network coding without a need to transmit encoding coefficients (without the header containing the coefficients) has been proposed. It is denoted as a *non-coherent network coding* and it removes the redundancy of encoding coefficients in the header of each network coded packet. In non-coherent network coding, we talk about a subspace codeword transmission since the coefficients of linear combinations are unknown. This approach potentially introduces erasures which can be, however, corrected by standard channel codes [27], [33].

### 2.3.5 Gains of Network Coding

Network coding provides primarily data rate/ throughput gains due to the saving of orthogonal resources (e.g. time slots). Theoretically, NC can offer the unlimited throughput gain in the artificial multicast network described by *unidirectional* (i.e. information can flow only in one direction at every link) graphs. Assuming that every link is bidirectional, the offered gain is potentially at most  $2\times$ . However, practical simulations on real test-beds [36] using COPE protocol (an opportunistic architecture for wireless mesh networks using NC) show average throughput gain about  $3-4\times$  when compared to current 802.11 in a wireless 20-node network. The experimental throughput ( $3-4\times$ ) overcome the theoretical gain ( $2\times$ ) because NC also alleviates hot-spots in the network. The alleviated hot-spots experience lower queues and lower rate of dropped packets due to overfull queues [37]. The similar results have been confirmed by CONCERTO protocol in Mobile Ad-hoc NETWORKS (MANETs) [27]. As a consequence of efficient use

of the resources, NC potentially offers high energy savings and small communication delay. In addition, random linear network coding provides an extra possibilities to security issues. Besides throughput gains, NC offers substantial complexity benefits. In case of linear NC, the optimal throughput is achieved by polynomial complexity algorithms. In case of random linear NC, the optimal throughput is achieved even in a distributed and random (potentially unknown) network topology not requiring any routing algorithms (however with redundancy added into the header of every packets).

### 2.3.6 Possible Applications of Network Coding

Possible application scenarios of network coding are very extensive. Basically, NC is always beneficial in dense interference-limited networks with multiple sources and destinations. They range from wired networks which may undergo erasure errors (like in the case of the Internet) to data storages and content sharing services. Promising application scenarios propose also wireless networks in general and relay networks such as e.g. satellite or mobile ad-hoc networks. Especially, the application in wireless networks deserves more attention. In traditional way, a wireless link is allocated for each P2P communication and other possible overheard information at the other unintended nodes are considered as interference. But in case of NC, *wireless broadcast* can be utilised to deliver network coded packet to multiple destinations. Every destination then increases its chance to obtain an additional linearly independent equation (linear combination of packets) which increases its chance for correct decoding.

We must note that the implementation of network coding, even though it stems on very simple and well known algebraic background, is not trivial because it requires to change/modify more layers in the network architecture stack. NC approach is not an evolutionary improvement which can be additively applied to the existing networks without dramatic changes of the architecture. This effect complicates quick and massive deployment as we have seen e.g. in the case of *turbo codes*.

### 2.3.7 Tutorial Examples

Let us demonstrate throughput gains of NC on simple network topologies like a 2-source 2-destination relay channel denoted as a *butterfly network* and a 2-Way Relay Channel (2-WRC). NC is built above some existing PHY layer. It means it operates in a discrete domain of finite fields rather than with real signals. Therefore the simplest models which can demonstrate the gains of NC suffice to assume ideal error-free links. Let each link can accommodate rate 1 symbol (or packet) per-channel-use. Only one terminal can use (i.e. listen or transmit) the link at the same time. The links corresponds to wireless connections so when a node transmits, the same message is delivered to all connected neighbours. In order to better respect hardware constraints, we assume half-duplex bidirectional links (i.e. every terminal is either listening or transmitting but cannot do both at the same time<sup>6</sup>). In such artificial models the gains are shown in the form of saved transmission time slots. In real situation, the channels undergo some imperfectness of wireless communication such as noise, fading, synchronisation errors, etc. and its characterisation is much more complicated. Nevertheless, the gains of NC in more realistic models possess the similar origin that is based on a more efficient use of orthogonal resources.

#### Butterfly Network

First, we demonstrate the gains of NC in a butterfly network<sup>7</sup> shown in Fig. 2.6. Source  $S_A$  wish to transmit the same data to destinations  $D_A$  and  $D_B$  and similarly  $S_B$  transmits to both destinations (i.e. it is a multicast network and it would be a single-source network if we allow an additional source connected to both sources  $S_A$  and  $S_B$ ). Figure 2.7 illustrates standard routing approach in the butterfly network. After

<sup>6</sup>Theoretically, we are able to subtract known transmitted signal and thus receive a signal at the same time but hardware components would require an extraordinary dynamic to perform this cancellation that is not accessible by low-cost hardware components today.

<sup>7</sup>As a butterfly topology is sometimes denoted a topology with additional node which would appear if we separated the relay node into two serially connected relays. Similar properties can be shown in this modified topology. As a butterfly network is also denoted a topology with additional source-node which is connected to sources  $S_A$  and  $S_B$ . The resulting scheme has a single source and multiple destinations, therefore it is a *multicast* network.

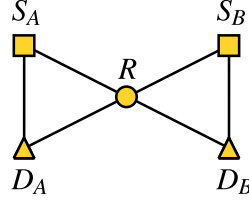


Figure 2.6: Butterfly network. Source  $S_A, S_B$  transmits data to both  $D_A, D_B$  with a help of relay node  $R$ .

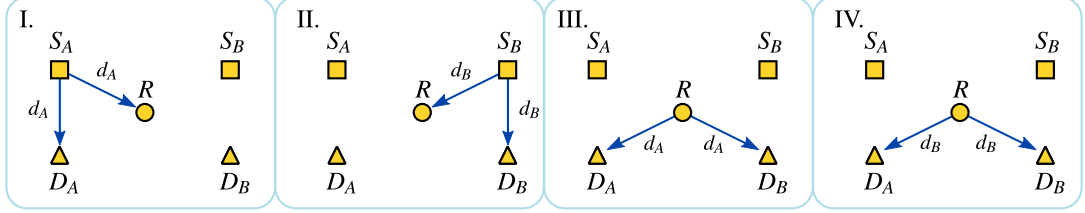


Figure 2.7: Independent communication stages of the standard routing approach in the butterfly network

4 independent stages, both destinations receive data  $d_A$  and  $d_B$ . We denote the first two stages as multiple access stages (two sources transmit towards the relay) and the other two stages as broadcast stages (the relay transmits to both destinations). The NC solution to this multicast problem is depicted in Fig. 2.8. The NC approach differs at the BC stages, where instead of independent transmission (orthogonal in time), the relay compresses information by XORing both symbols into the one network coded symbol

$$d_{AB} = d_A \oplus d_B, \quad (2.1)$$

where symbol  $\oplus$  denotes an eXclusive OR (XOR) operation. This example holds also for the processing per whole packets instead of symbols, in that case symbol  $\oplus$  denotes a bit-wise XOR operation. Note, that XOR is not the only possible network coding function, for instance in case of linear NC the output symbol is

$$d_{AB} = c_A \otimes d_A \oplus c_B \otimes d_B, \quad (2.2)$$

where  $c_A, c_B$  are some non-zero coefficients from finite field  $\mathbb{F}_q$  of size  $q$  and  $\oplus, \otimes$  denote addition and scalar multiplication in  $\mathbb{F}_q$ . The network coded function needs to enable final destination unique decoding. It means that providing already transmitted data, there must be a unique inversion function. This requirement leads to theory of *Latin squares* [38]. The network coded symbol is then broadcast towards both destinations at the same time. The key role is in the final destination processing where every destination interprets the network coded symbol in a different way. Destination  $D_A$  has already received symbol  $d_A$  at stage I. It obtains  $d_B$  from received  $d_{AB}$  symbol and known  $d_A$  by inverse operation to XOR of  $d_{AB}$  as

$$d_B = \mathcal{N}^{-1}(d_{AB}, d_A) = (d_A \oplus d_B) \oplus d_A, \quad (2.3)$$

where an inverse operation of XOR  $\mathcal{N}^{-1}$  is again  $\oplus$ . Destination  $D_B$  has already received  $d_B$  at stage II and thus it obtains desired data symbol  $d_A$  as

$$d_A = \mathcal{N}^{-1}(d_{AB}, d_B) = (d_A \oplus d_B) \oplus d_B. \quad (2.4)$$

## 2-Way Relay Channel

Let us assume a similar scenario as a butterfly network called 2-WRC shown in Fig. 2.9 where the direct channel between  $A$  and  $B$  is not present. In this scenario, terminal  $A$  wish to send data symbol  $d_A$  to terminal  $B$  and vice versa. In the current approach based on data routing, one round of 2-way communication requires 4 independent stages as shows Fig. 2.10.

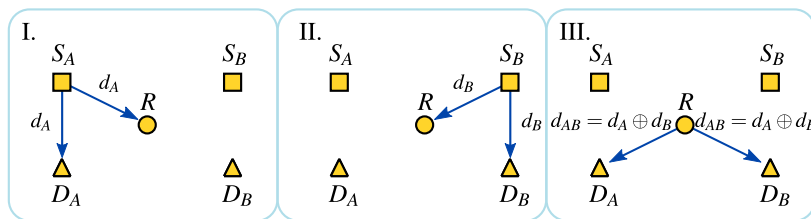


Figure 2.8: Independent communication stages of the NC approach in the butterfly network

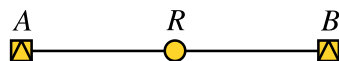


Figure 2.9: 2-way relay channel. Node A bidirectionally communicates with node B.

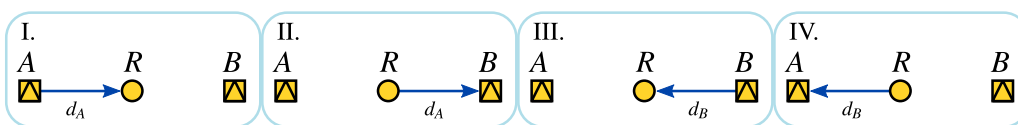


Figure 2.10: One round of 2-way communication in a 2-WRC with the current data routing approach.

Note, that we cannot merge stage I and II together due to the half-duplex constraint. NC solution to 2-WRC is depicted in Fig. 2.11. The final destination processing is the same as for the butterfly network given by (2.3), (2.4). If each link is able to accommodate errorless rate 1bit/channel use, the overall sum-rate (sum of terminal A rate plus terminal B rate) for 2-way communication is  $2/4 = 0.5$  bits/channel use for the routing approach and  $2/3 = 0.\bar{6}$  bits/channel use for the NC approach. Clearly, NC approach provides a higher sum-rate.

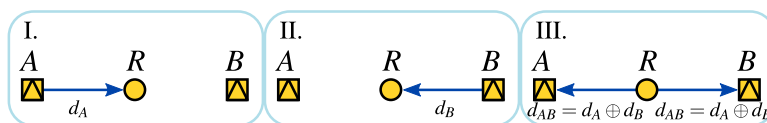


Figure 2.11: One round of 2-way communication in a 2-WRC with the NC strategy.

## 2.4 Wireless (Physical-Layer) Network Coding

WNC is an emerging approach for wireless networking which holds a lot of expectations in the research community today. Its origin dates back to 2006, when parallelly three research groups [39], [40] and [41] introduced the concept of network coding at the physical-layer. WNC originates and shares basic ideas of NC. Particularly, *a) the relaying nodes perform some form of information compression* similarly as does network coding (in wired error-free networks in order to reach a max-flow min-cut capacity bound) and *b) shared wireless medium is utilised as natural broadcast* rather than an interference producing P2P link. The last corner stone of WNC, which is distinct from NC, is *c) a physical-layer processing*. NC has been originally build upon error-free bit-pipes manipulating with data packets and using algebraic operations over finite fields. In WNC, we demand an equivalent operations with real signals at the PHY layer over unreliable wireless channel. This challenging approach (on optimal conditions) allows to exploit interference and turns it into the extra capacity benefits.

For reference and introductory literature, we recommend survey paper [42] with plenty of creditable references, book chapter [43] and tutorials [44] and [45].

### 2.4.1 Discoveries Leading to WNC

Information-theoretical discoveries leading to WNC were elaborating with protocols which require 2 orthogonal stages (one Multiple Access (MA) stage and one BroadCast (BC) stage) in a 2-WRC. Let us consider the example depicted in Fig. 2.11 where 3 stages are employed for one round of 2-way communication. Now, assume not a wired network but a wireless scenario, where instead of data symbols  $d_A$ , modulated signal  $\mathcal{M}(d_A)$  is transmitted;  $\mathcal{M}$  denotes a modulation mapper which maps discrete data symbols/codewords into relevant signals. The first two stages form a MAC channel because both sources wish to send data to the common relay node. In fact, it is a MAC with orthogonally separated sources in temporal domain. Based on network information theory, we can do better by non-orthogonal MAC techniques such as *successive-detection and interference cancellation* where both sources are forced to transmit together at the same time and the receiver decodes the strongest source at first, cancel out and then decode the other one. This approach leads to a 2 stage scheme as shown in Fig. 2.12. We call this scheme as Joint-Decode-and-forward (JDF) relaying strategy, because the relay performs a joint decoding at the MA stage. Note, that JDF scheme is limited by standard MAC capacity region [7].

The other 2-stage scheme which precedes WNC is called Amplify-and-Forward (AF) relaying strategy, where the relay simply amplifies and forwards what it receives at the MA stage. AF processing is much less demanding than JDF, although no AWGN noise is removed at the relay and so AF amplifies apart from the useful signal also the noise which lowers the theoretical information rates. Since AF works in the analogue domain, the term Analogue Network Coding (ANC) is often used [46].

### 2.4.2 Origin of WNC

New and strikingly simple idea of [39], [40] and [41] was that the relay does not need to decode jointly  $[d_A, d_B]$  at the MA stage but rather directly a function of the data which will be broadcast at the BC stage (here, the function of data is an invertible function providing one of the data message e.g. bit-wise XOR  $d_A \oplus d_B$ ). In this text, we denote the invertible function providing one of the data message as a

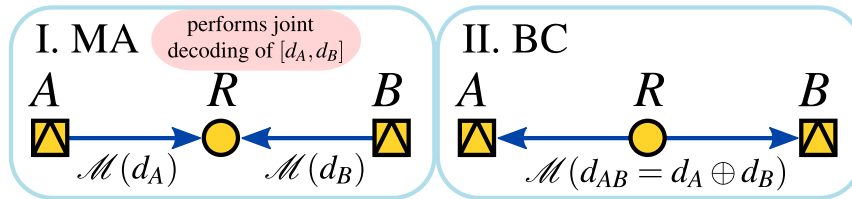


Figure 2.12: One round of 2-way communication in a 2-WRC with non-orthogonally separated MA stages using the NC strategy.

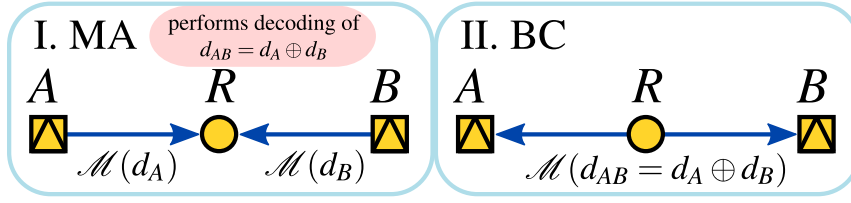


Figure 2.13: One round of 2-way communication in a 2-WRC using the WNC strategy.

*network coding function*, although functions used in the standard NC approach are often considered over finite-field but functions admitted in WNC are more general algebraic structure – Latin squares [38]. The information theoretic rates in case of WNC are not limited by the MAC capacity region. The scheme is briefly depicted in Fig. 2.13. As conjectured in [47], the rectangular capacity region given by the cut-set bound theorem [7] can be potentially achieved. Work [47] compares 2-stage protocols using AF, JDF and the strategy where a function of data is decoded by the relay which is here denoted as De-Noise-and-Forward (DNF). It concludes that the highest achievable rate for symmetric channel links and high SNR provides DNF. In the low SNR region are achievable rates of DNF and JDF asymptotically identical [48].

### 2.4.3 Information Theoretical Considerations of WNC

In current networks, interference is widely understood as a serious obstacle and we usually speak about interference-limited networks. Network coding has a potential to exploit unintended overheard communication (interference) and with combination of WNC it has a potential to eliminate the interference which has direct impact on overall throughput capacity in wireless networks. Information Theoretical analysis [47] proposes WNC as a relaying scheme with the highest achievable rate in 2-WRC. Paper [49] reveals the potential of WNC in wireless ad-hoc networks using *large-scale network analysis*.

Paper [47] shows that WNC based strategy may potentially attain a 2-WRC capacity upper-bound given by the cut-set bound theorem

$$C = \log_2(1 + \gamma) \quad [\text{bits/channel use}], \quad (2.5)$$

where  $\gamma$  symbol denotes a signal-to-noise ratio. Proof that WNC can reliably operate outside of the MAC capacity region was parallelly presented in [48], [50] using theory of *nested lattice codes*. Based on remarkable properties of lattice codes [23], [22], it can be shown that nested lattice codes achieve

$$C = \log_2(1/2 + \gamma) \quad [\text{bits/channel use}]. \quad (2.6)$$

We conclude that WNC using nested-lattice codes reaches the capacity upper-bound within additive  $1/2$  in SNR which is negligible for high SNR conditions.

### 2.4.4 Ambiguous Names Describing WNC

There are multiple labels currently used by the research community which denote the same relaying strategy where *the relay decodes an invertible function of data at the MA stage*. The authors in [39] denote this strategy as DNF, although the name de-noising does not give a true picture of a function decoding and its relation to network coding. For a general name of NC processing at the PHY layer was used the term PNC in [39]. The authors of [41] use the term Compute-and-Forward (CF) which also does not give a true picture similarly as DNF. Recently, the term Physical-Layer Network Coding (PLNC) coined by the authors of [40] is becoming more and more popular. Although it is sometimes used rather for a general name of NC performance at the PHY layer (comprising e.g. also JDF and AF strategies). In [51], the term Hierarchical-Decode-and-Forward (HDF) strategy is used to highlight some differences between network coded data and function of data which are denoted as hierarchical data.

Throughout this thesis, we use the term WNC which is also often used with similar meaning as PLNC. We do not consider its general interpretation, but we use it to denote the relay processing when an invertible function of data is decoded at the MA stage.

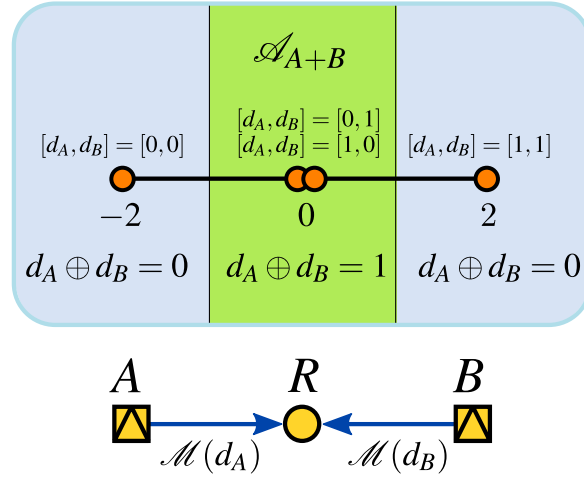


Figure 2.14: Decision regions of  $d_{AB} = d_A \oplus d_B$  decoding at the MA stage of the WNC 2-way relaying.

### 2.4.5 Tutorial Example: WNC in a 2-WRC

Let us consider WNC approach in a 2-WRC as a tutorial example. Although the information theoretical analysis in [47] predicts the highest achievable rates to WNC when terminals use long codewords, we can simply demonstrate the basic principles on per-symbol relaying (which is also practical for real implementation). For the sake of simplicity, assume an ideally time-synchronised scenario with AWGN disturbance<sup>8</sup>. Assuming that both terminals use Binary Phase Shift Keying (BPSK) modulation alphabet  $\mathcal{A}_A = \mathcal{A}_B = \mathcal{A}_{\text{BPSK}} = \{-1, 1\}$ , the received signal at the MA stage is

$$x = s_A + s_B + w, \quad (2.7)$$

where constellation points  $s_A, s_B \in \mathcal{A}_{\text{BPSK}}$  and  $w$  denotes an AWGN noise. We define a one-to-one data-to-signal modulation mapper as

$$\mathcal{M} : d_A = 0 \rightarrow s_A = -1, \quad d_A = 1 \rightarrow s_A = 1. \quad (2.8)$$

Superimposed constellation point  $s_A + s_B$  attains one of the three possible points from  $\mathcal{A}_{A+B} = \{-2, 0, 2\}$ . Notice that constellation points  $-2$  and  $2$  uniquely correspond to data pairs  $[d_A, d_B] = [0, 0]$  and  $[d_A, d_B] = [1, 1]$ , but constellation point  $0$  may correspond to either  $[d_A, d_B] = [0, 1]$  or  $[d_A, d_B] = [1, 0]$  and we cannot decide between them. But this is not a source of errors, because the relay decodes and broadcasts a network coded data symbol  $d_{AB}$  being a bit-wise XOR function

$$d_{AB} = d_A \oplus d_B \quad (2.9)$$

which for both undistinguishable cases  $[0, 1]$  and  $[1, 0]$  yields the same  $d_{AB} = 0 \oplus 1 = 1 \oplus 0 = 1$ , see decision regions for  $d_{AB}$  decoding in Fig. 2.14.

### 2.4.6 Channel Coded WNC

The tutorial example from the preceding section presents an uncoded per-symbol relaying. The per-symbol relaying is practical in the sense that no additional delay is induced at the relay, however it possess much higher error performance as would have with channel coding. There are several ways how to implement channel coding into the WNC 2-way relaying. Theoretically, the scheme with the highest achievable rate requires long codewords used by the terminals at the MA stage. From its superposition is obtained network coded data packet, re-encoded and broadcast to the final destinations. The processing

<sup>8</sup>This could be a baseline model in a static frequency-flat environment with wireless channel cancellation adaptation.

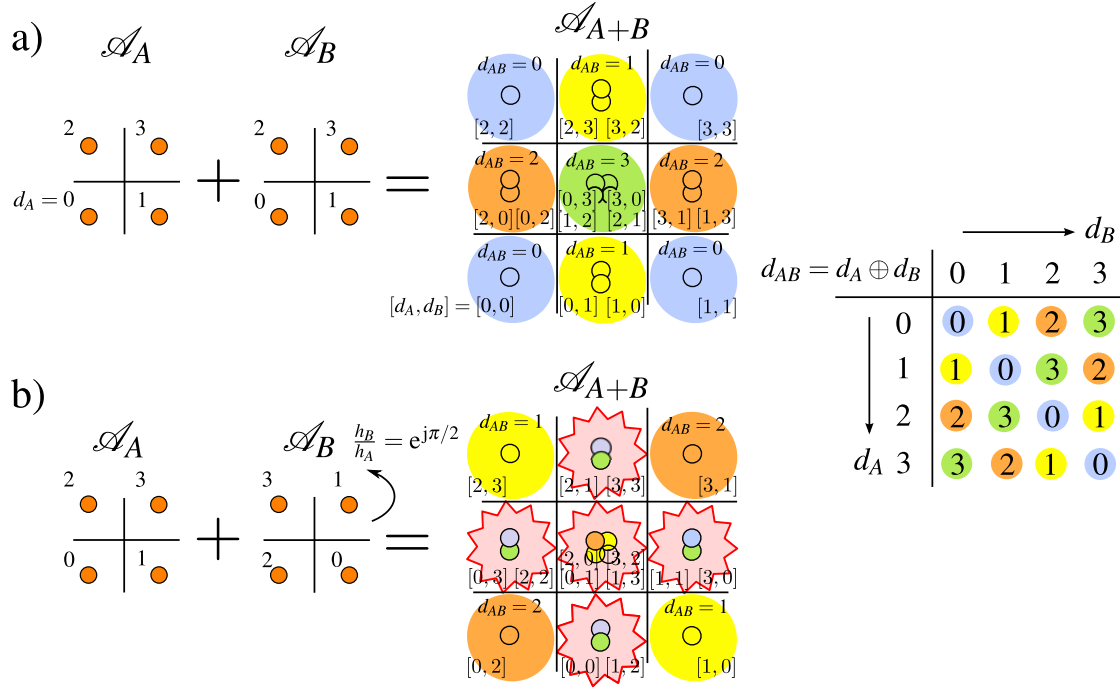


Figure 2.15: Example of the relative-fading at the WNC MA stage using 4QAM constellations and bit-wise XOR decoding. Case a) with  $h_A = h_B = 1$  performs much better than case b) with  $h_A = 1, h_B = e^{j\pi/2}$  although in both cases the magnitude of all channel coefficients are the same.

of channel decoding and network coding should be performed jointly, see its concrete realization using Factor-Graph Sum-Product Algorithm (FG-SPA) with LDPC codes in [52]. A separate processing of these two operations is sub-optimal as claimed in [48] and [53]. The relay processing which uses channel decoding and network coding separately shows approximately 1 dB loss (Bit Error Rate (BER) at  $10^{-4}$  using BPSK constellations and LDPC with interleaver size 1000 and code rate 0.4 at SNR 5 dB [52]) over the optimal processing. Similar performance loss suffers a sub-optimal relaying scheme where network coded symbols are obtained per-symbol and consecutively channel encoded. This approach is denoted as a *layered relay processing* [51]. It requires linearity of the used network coding function, but the processing is less demanding than the previous schemes.

### 2.4.7 Fading Channel Parametrization Effects

#### Relative-Fading of WNC Relay Processing with CSIR

Information theoretical analysis of WNC [47] assumes perfect knowledge of Channel State Information (CSI) at all the nodes which is used for an ideal time, phase and frequency synchronisation and power control. In a real system operating over wireless channel, the amount of feedback required for such a perfect synchronisation would be prohibiting. In order to bring WNC closer to real implementation, work [54] considers only local knowledge of CSI at the receiver side. In this setting, a new form of fading in the WNC relaying appears. We call it a *relative-fading* effect [6], because it happens when a ratio of channel gains is close to certain critical values (denoted as *singularities*) no matter what are the actual channel gain values. So it can happen, that the system performs very poorly even though both channel gains at the MA stage are strong enough. Figure 2.15 presents such a situation when 4QAM constellations are used by the terminals and the relay decodes a bit-wise XOR function. The reason why channel parametrization is still an issue even when perfect Channel State Information at the Receiver side (CSIR) is available (which does not appear in standard P2P communication) is due to the following. The



received signal is

$$x = h_A s_A + h_B s_B + w, \quad (2.10)$$

where  $s_A, s_B$  are constellation space signals,  $h_A, h_B$  are frequency-flat channel coefficients known by the relay and  $w$  denotes a complex AWGN sample with variance  $2N_0$ . The relay may work with an equivalent signal when one of the known coefficients is eliminated e.g. as

$$x' = x/h_A = s_A + h_B/h_A s_B + w' = s_A + \alpha s_B + w', \quad (2.11)$$

where  $w'$  is a sample of AWGN with variance  $2N_0/|h_A|^2$  and  $\alpha$  denotes a channel parameter ratio. We conclude that even with CSIR the superimposed constellation is still parametrized by channel ratio  $\alpha$  which may have a significant impact as shown in Fig. 2.15.

### Adaptive WNC Method Eliminating the Relative-Fading

The authors of [54] proposes an adaptive relay processing where a network coding function decoded by the relay is adaptively chosen according to the actual channel ratio  $\alpha$  in order to maximize minimal Euclidean distance and thus it eliminates the relative-fading. Surprisingly, the proposed network coding adaptation based on 4QAM alphabets requires network coding functions with higher cardinality than 4. Paper [38] analyses the adaptive WNC strategy using theory of Latin squares and proposes a simpler algorithm for the search of suitable network coding functions. Paper [54] also generalises the adaptive WNC strategy for 2-WRC with multiple antennas at the relay. Following works [55], [56] confirm that adaptive WNC strategy provides significant gains in the TCM coded system and in the system using multiple antennas at the relay and destinations. Our latest work [1] advises that there exist better constellations for adaptive WNC than 4QAM such as 4HEX constellation, where the relative-fading is eliminated by adaptive WNC without the use of network coding functions with cardinality higher than 4. The extended (higher than 4) cardinality network codes are undesirable since it introduces redundancy decreasing the data rates at the BC stage.

### Elimination of the Relative-Fading Without any Adaptation

Our works [4], [5] reveal that the relative-fading may not appear for special type of modulation schemes and network coding functions (BPSK and bit-wise XOR being an important example) without any form of adaptation. Such modulations were denoted as Uniformly Most Powerful (UMP) alphabets due to the similarity with UMP parametric detectors which performs the best among all possible detectors for any parameter value. In our case, UMP alphabets are those having maximal (the best) minimal distance among all possible constellations with identical minimal distance of primary alphabet for any channel parameter  $\alpha$  value. Paper [4] identifies some important features of UMP alphabets like a) bit-wise XOR network coding function is necessary but not sufficient condition for UMP alphabets, b) orthogonal and bi-orthogonal signalling is UMP and c) multi-dimensional constellations need to be used to fulfil UMP condition when alphabet cardinality is higher than binary. In the design of multi-dimensional UMP constellations we can beneficially consider naturally multi-dimensional schemes like frequency modulations Frequency Shift Keying (FSK) and CPM [4]. The numerically designed UMP multi-dimensional constellations using non-linear optimisation tools were proposed in [5]. It shows that UMP condition cannot be apparently achieved when constellation spectral efficiency is higher than 1 [bits/complex constellation dimension]. Ignoring the effect of the relative-fading leads to a serious performance degradation and even constellation alphabets which are not UMP but are resistant to the relative channel phase rotation provide considerable gains [5], [57]. According to the extensive performance evaluation in [6], we conclude that the relative-fading has much lower negative impact in a system with a reasonable level of diversity which is a usual assumption in reliable communication systems for wireless channel.

### Non-Coherent WNC 2-Way Relaying

Another method dealing with wireless environment without any adaptation is a non-coherent “blind” approach. It requires no CSI neither on a transmitter nor a receiver side. Paper [58] develops a non-coherent



Figure 2.16: Chain topology. Node  $A$  bidirectionally communicates with node  $B$  via serially concatenated chain of  $n$ -relays.

WNC using orthogonal FSK signalling. The non-coherent WNC relay processing is very different from the canonical P2P non-coherent envelope detector. Another non-coherent WNC scheme using TCM and MIMO 2-way relaying has been recently presented in [59].

### 2.4.8 Constellation Design for WNC in an AWGN 2-WRC

WNC possesses several unique features in comparison to canonical P2P communication. We have already mentioned the effect of relative-fading. As another feature, we present a problem of constellation design optimising minimal Euclidean distance. WNC error performance does not depend only on channel coding & modulation but also on which network coding function is decoded at the relay and what type of symbol indexing is used by the terminals. For instance, 8PSK constellation has minimal distance  $\delta_{\min}^2 = 0.59$ , but when used at WNC MA stage, the minimal distance of bit-wise XOR decoding is only  $\Delta_{\min}^2 = 0.34$ . It can be even shown that there is no network coding function which would result in a higher minimal distance. So, even if the relative-fading is not an issue due to e.g. CSI available at the receiver as well at the transceiver. It is generally not obvious what type of constellation, indexing and network coding function leads to the highest minimal distance. Our paper [2] focuses on this issue. It shows, that constellations taken from a common lattice structure which are indexed in a special way (indices form an arithmetic progression along each lattice dimension; such indexing is denoted as Affine-Indexing (AI)) has a minimal distance equal to the minimal distance in a P2P channel. It works under the condition that modulo-sum network coding function is decoded at the relay. Paper [2] also presents some additional features like that not every lattice-constellation is indexable by AI and it presents a list of constellations with the maximal possible minimal distances. Paper [60] is focused on a joint constellation and network coding function design. It allows unequal channel gains and alphabet cardinalities. The approach considers combination of different canonical constellations like 2-, 4-, 8-QAM etc. finding a combination of constellations, its precoding coefficients and network coding functions leading to the highest minimal distance. This design of network coding functions uses the greedy clustering algorithm trying to cluster the closest superimposed-constellation points (as long as the network coding function is invertible) into the same cluster in order to maximize the minimal distance. The clustering algorithm is the same one introduced in [54].

### 2.4.9 WNC in other than 2-WRC Network Topology

The concept of WNC 2-way relaying is theoretically as well as practically quite well understood for cases with both CSIR & Channel State Information at the Transceiver side (CSIT), CSIR only and no CSI at all, including imperfect time synchronisation [61] and assuming current state-of-art communication approaches such as MIMO, TCM, turbo codes and principles of adaptation. Despite relatively good knowledge of WNC 2-way relaying, the optimal WNC strategy in a more complex network topology is the big unknown. From this point of view is the NC approach at the link-layer much more practical since it scales well into more complex topologies (although it does not provide such capacity gains as WNC). Strategies like the Compress-and-Forward (CF) strategy which designs PHY layer as to match the standard link-layer NC seems to be very promising. So far, WNC has been successfully generalised for a *chain topology* [44] (i.e. a bidirectional network with one source-destination pair and multiple serially connected relays between them depicted in Fig. 2.16) and for a wireless butterfly network [45]. Certainly, we could separate a complex general network topology into several 2-WRCs or other understood topologies, but the resulting scheme would be suboptimal as noticed e.g. in [62], [3]. Paper [62] shows that WNC strategy tailored for a *star topology* (i.e. two source-destination pairs bidirectionally communicating via a relay with reasonably strong cross channel links depicted in Fig. 2.17)) substantially increases achievable

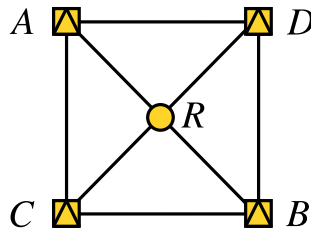


Figure 2.17: Star topology. Node  $A$  bidirectionally communicates with node  $B$  and node  $C$  bidirectionally communicates with node  $D$  with a help of relay  $R$ .

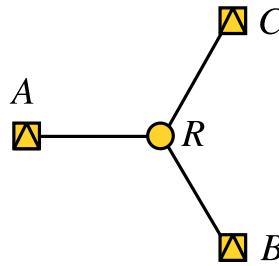


Figure 2.18: 3-terminal 1-relay multicast network. Every node sends data message to all other nodes, i.e. it is a multicast network.

rates over the strategy based on WNC for twice 2-WRC. In a star topology, the cross channel links deliver more information to the final destination, even though the information is not intended to the final destination, it enables higher network coding compression at the BC stage. Similarly as [62], our approach [3] proposes WNC strategy for a *3-terminal 1-relay multicast network* depicted in Fig. 2.18. The gain is obtained w.r.t. the strategy that considers the 3-terminal 1-relay multicast network (3T-1R) as a two 2-WRC. Particularly, paper [3] proposes a joint constellation prerotation & terminal constellation & its indexing & network coding function that allows compression of two orthogonal MA stages (corresponding to  $2 \times$  WNC in a 2-WRC) into the single MA stage where multiple network coded data symbols are decoded at once.

#### 2.4.10 WNC in a General Network Topology

The WNC strategies presented in the preceding subsection are based on an optimisation constrained to a given network topology. So far, no general rule how the optimal solution should look like is known. The generalisation of WNC for a general multi-source multi-destination network is still an open challenge. The situation is very complicated due to a huge number of parameters which influence the optimal solution (e.g. every node may have different form of CSI and level of synchronisation, cooperation and knowledge of the overall network topology, etc.). Development of WNC strategy that is robust to the substantial portion of imperfectness is likely to be more important than the WNC strategy achieving the maximal sum-rates but under unrealistic conditions requiring tremendous data overhead. A WNC design for general wireless network is also challenging due to the lack of information-theoretical knowledge, i.e. there is no paper like [47] for the 2-WRC saying that WNC is the optimal relaying strategy in a general wireless multi-source multi-node network. This fact is demonstrated in unidirectional Multiple Access Relay Channel (MARC) where decoding of a function of the incoming data is not always the best solution [63].

#### 2.4.11 Real Implementation of WNC

There are a few real verifications of WNC gains in a practically implemented system. The reason is a) the same as in case of NC, i.e. the overall network architecture needs to be completely revamped and it

is difficult to simply extend the existing concept by WNC processing, b) several new challenges need to be solved such as an impact of wireless channel and synchronisation issues and generalisation for a general multi-node multi-source network. Recently, paper [64] presents a real implemented solution in a 2-WRC. The authors selected OFDM and Cyclic-Prefix (CP) strategy to combat time asynchronisation and frequency-selective fading. The gain of WNC is confirmed in Ettus Universal Software Radio Peripheral (USRP) scenario based on modification of the 802.11a/g standard. It assumes BPSK terminal constellations, bit-wise XOR network coding function and standard convolutional channel codes. Related work [46] introduced an AF network coding based relying called ANC. Although ANC non-optimally amplifies also AWGN noise, it still provides a SNR gain  $\sim 30\%$  over the NC based solution (implemented in COPE protocol, see Sec. 2.3.5 for more comments about COPE). ANC scheme combats time, phase and frequency asynchronisation by a special signal processing using a non-coherent Minimum-Shift Keying (MSK) modulation implemented in the GNU-radio. We conclude that current state-of-the-art of WNC implementation does not go much further then in the 2-WRC.

## **Part II**

# **Contribution: Modulation Design for Wireless Network Coding**

---

This part is an overview of our contributions related to the WNC research. These works were published mainly in [1, 2, 3, 4, 5, 6]. The publications were usually considerably page-limited. Yet, we have an opportunity to introduce our work with a more space available and in certain cases we may include some parts that were omitted due to the page limitation. We emphasize the impact of our results w.r.t. the other works of the research community. We conclude our work in the last chapter where we discuss potential directions for the future research and possible practical implementations.

We keep individual chapters as a stand alone text each describing a single result. Therefore, the chapters contain some overlaps such as our notation conventions and system model descriptions (when the contributions use the same one). We believe that this is a more easily accessible way how to present our contributions than a single huge chapter with all the contributions mixed together (however without the redundant overlaps). Certainly, we have cleaned up the text to minimize the amount of redundancy and we have synchronised the system descriptions and used notations.

## Chapter 3

# Design of Lattice-Constellations and Constellation-Indexing for WNC 2-Way Relaying using Modulo-Sum Decoding

We consider a wireless (physical-layer) network coding 2-way relaying where both terminals use constellations curved from a common lattice structure and the relay node decodes a modulo-sum function of transmitted data symbols at the multiple-access stage. Performance of such a system with additive white Gaussian noise is strongly determined by the used constellation indexing. For some indexing, the minimal distance of modulo-sum decoding is 0 (some points of superimposed-constellation are equal despite correspondence to unequal modulo-sum of data symbols). It causes a considerable loss in the error performance as well as in the alphabet-constrained capacity.

In this chapter, we show as our contribution that if indices form a modulo-arithmetic progression along each lattice (real) dimension (denoted as Affine Indexing (AI)), the minimal distance of modulo-sum decoding equals to the minimal distance of primary terminal constellations. We also find that some canonical constellation-shapes prevent existence of AI, therefore we propose a greedy-sphere packing algorithm for constellation-shape design which jointly maximizes minimal distance and keeps existence of AI. In certain cases, we have found the constellations with the highest possible minimal distance of a network coding function decoding.

### 3.1 Introduction

#### 3.1.1 Motivation & Related Work

We consider the promising WNC strategy offering potentially the highest achievable throughput in a 2-WRC [47]. WNC encourages relaying nodes to decode an invertible function (denoted as a network coding function) of transmitted data (instead of data itself) at the MA stage. In this work, we assume the invertible function to be described by the modulo-sum operation and terminal constellations to be taken from a common lattice structure (denoted as lattice-constellations), see an illustrative example in Fig. 3.1. We investigate lattice-constellations in the WNC 2-way relaying for the following synergetic reasons:

1. many canonical constellations (including popular QAM) are taken from a lattice [65],
2. many dense lattices are known [23] and implementable in the real system [66],
3. a superposition of lattice-constellations is again a lattice-constellation keeping e.g. the same distance properties,

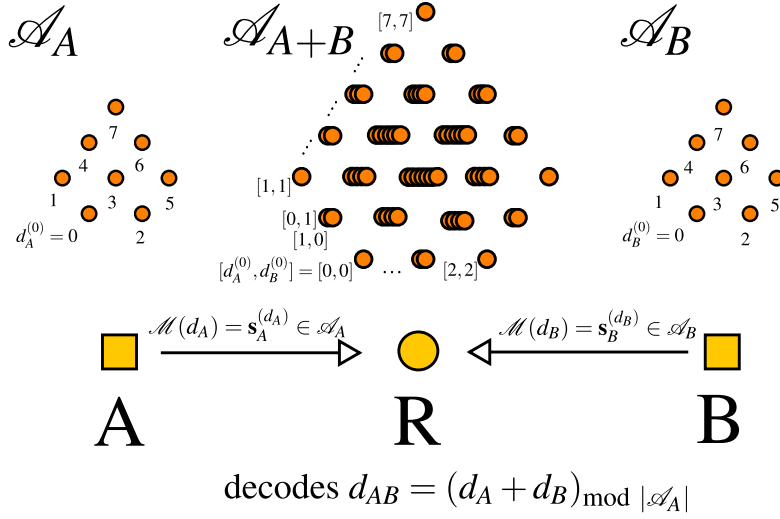


Figure 3.1: Relay  $R$  decodes the modulo-sum function of transmitted data symbols from the superposition of two primary lattice-constellations at the WNC-MA stage.

4. both domains mixed by WNC (the *continuous signal space* of physical-layer and *discrete integer space* of network coding) can be described by common integer algebraic structure for lattice-constellations.

We study an impact of constellation indexing on the overall performance with AWGN (see an example of its impact in Figs. 3.3 and 3.4). Our scenario in comparison to [50], [48] assumes practical finite-dimensional lattices and it does not require a nested lattice structure. WNC performance in an AWGN channel corresponds to the ideally time & phase & power synchronised situation. It may serve also as a performance benchmark for important performance in fading asynchronous channels [54, 4, 5, 67].

## 3.2 System Model

### 3.2.1 2-Way Relay Channel Model

2-WRC comprises terminals A and B bi-directionally communicating via a supporting relay R in a half-duplex manner (each node cannot send and receive at the same time). We assume an ideal time-synchronised scenario with AWGN and a per-symbol low-latency relaying as presented e.g. in [51].

### 3.2.2 Used Notation

We introduce the notation from the perspective of terminal A, since the notation for B is analogical. Let both terminals A and B use the same constellation  $\mathcal{A} = \mathcal{A}_A = \mathcal{A}_B$  including the same constellation-indexing. Alphabet  $\mathcal{A} \subseteq \mathbb{C}^{N_s}$  is assumed to be curved from some  $N_s$ -complex-dimensional lattice  $\Lambda$  with the cardinality  $M = M_A = M_B = |\mathcal{A}|$  to be a power of two. Baseband signal points in the constellation space  $\mathbf{s}_A$  forming the alphabet  $\mathcal{A} = \{\mathbf{s}_A^{(i)}\}_{i=0}^{M-1}$  are assumed to be normalised to the unit mean symbol energy. We use upper-indices when we need to stress a concrete value of given variable. Let data symbol be  $d_A \in \{d_A^{(i)}\}_{i=0}^{M-1} = \mathbb{Z}_M$ , where  $\mathbb{Z}_M = \{0, 1, \dots, (M-1)\}$  denotes non-negative integers with elements lower than  $M$ . We assume constellation mapper  $\mathcal{M} : \mathbb{Z}_M \rightarrow \mathcal{A}$  such that the alphabet indices directly equal to the data symbols  $\mathcal{M}(d_A) = \mathbf{s}_A^{(d_A)}$ . Using lattice-generator matrix  $\mathbf{G}$ , we describe constellations by lattice-coordinate vectors  $\mathbf{a}$  as

$$\mathcal{A} = \left\{ \mathbf{s}_A^{(i)} = \mathbf{G}\mathbf{a}^{(i)} - \bar{\mathbf{m}} : \mathbf{a}^{(i)} \in \mathcal{S} \right\}_{i=0}^{M-1} \quad (3.1)$$



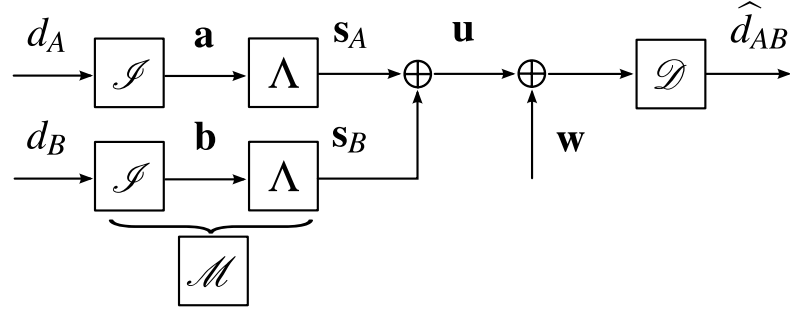


Figure 3.2: Model of the modulo-sum data decoding performed by the relay with AWGN noise at the WNC-MA stage.

where  $\bar{\mathbf{m}} = 1/M \sum_{i=1}^M \mathbf{G}\mathbf{a}^{(i)}$  ensures that  $\mathcal{A}$  is zero-mean. Vector  $\mathbf{a} \in \mathcal{S} \subseteq \mathbb{Z}^{2N_s}$  is  $\mathbf{a} = [a_0, \dots, a_{2N_s-1}]^T$ ,  $a_i \in \mathbb{Z}$ ,  $\forall i \in \mathbb{Z}_{2N_s}$ , where  $\mathcal{S}$  and  $\mathbb{Z} = \{\dots, -1, 0, 1, \dots\}$  denote a set of lattice coordinate vectors (determining constellation shape) and the ring of integers, respectively. The lattice-generator matrix is formed by concatenation of lattice-basis, e.g. rectangular  $Z^2$ , hexagonal  $A_2$ , checkboard  $D_2$ , checkboard  $D_4$  and Gosset  $E_8$  lattice has the following matrices:

$$\begin{aligned}
 \mathbf{G}_{Z^2} &= [1, j], \\
 \mathbf{G}_{A_2} &= [1, 1/2 + j\sqrt{3}/2], \\
 \mathbf{G}_{D_2} &= [\sqrt{2}/2 + j\sqrt{2}/2, -\sqrt{2}/2 + j\sqrt{2}/2], \\
 \mathbf{G}_{D_4} &= \begin{bmatrix} 1 & j & 0 & (1+j)/2 \\ 0 & 0 & 1 & (1+j)/2 \end{bmatrix}, \\
 \mathbf{G}_{E_8} &= \begin{bmatrix} 4 & -2+2j & -2j & 0 & 0 & 0 & 0 & 1+j \\ 0 & 0 & 2 & -2+2j & -2j & 0 & 0 & 1+j \\ 0 & 0 & 0 & 0 & 2 & -2+2j & -2j & 1+j \\ 0 & 0 & 0 & 0 & 0 & 0 & 2 & 1+j \end{bmatrix}. \tag{3.2}
 \end{aligned}$$

We define an indexing mapper and a lattice-modulation mapper as

$$\mathcal{I} : \mathbb{Z}_M \mapsto \mathcal{S}, \mathcal{I}(d_A) = \mathbf{a}^{(d_A)}, \tag{3.3}$$

$$\Lambda : \mathcal{S} \mapsto \mathcal{A}, \Lambda(\mathbf{a}) = \mathbf{G}\mathbf{a} - \bar{\mathbf{m}} = \mathbf{s}_A, \tag{3.4}$$

respectively. The lattice-constellation modulation mapper is

$$\mathcal{M}(d_A) = \Lambda(\mathcal{I}(d_A)) = \mathbf{s}_A. \tag{3.5}$$

### 3.2.3 Wireless Network Coding in a 2-Way Relay Channel

The WNC 2-way relaying consists of a MA stage when both terminals transmit simultaneously to the relay with modulo-sum data decoding and a BC stage when the relay broadcasts the modulo-sum network coded data symbol. Final destinations perform successful detection exploiting knowledge of its own data via an invertibility of modulo-sum operation (similarly as in the network coding approach). Here, we focus on the MA stage since its performance is more challenging than at the BC stage due to the additional multiple-access interference.

#### MA stage

The relay receives a superposition of signals from terminal A and B (the scheme is depicted in Fig. 3.2)

$$\mathbf{x} = \mathbf{u} + \mathbf{w} = \mathbf{s}_A + \mathbf{s}_B + \mathbf{w}, \tag{3.6}$$

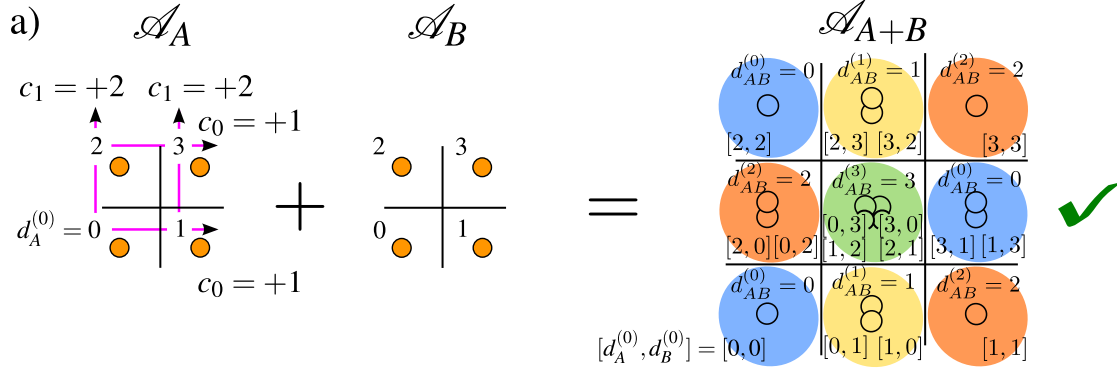


Figure 3.3: Minimal distance of the modulo-sum decoding with constellation indexing a) equals to the minimal distance of primary constellations since all identical superimposed-constellation points lie in the decoding region with the identical modulo-sum data symbol  $d_{AB}$  (marked by distinct colours according to the associated multiplicative table) depicted in Fig. (3.5). Symbols  $c_0$  and  $c_1$  denotes index-increments of an arithmetic progression along each dimension as will be discussed in Sec. 3.3.2.

where  $\mathbf{w}$  is a complex  $N_s$ -dimensional AWGN vector with variance  $2N_0$  per-complex dimension and  $\mathbf{u}$  is a superimposed-constellation point  $\mathbf{u} \in \mathcal{A}_{A+B} \subseteq \mathbb{C}^{N_s}$  where

$$\mathcal{A}_{A+B} = \left\{ \mathbf{u}^{(i,j)} = \mathbf{s}_A^{(i)} + \mathbf{s}_B^{(j)} : \mathbf{s}_A^{(i)}, \mathbf{s}_B^{(j)} \in \mathcal{A} \right\}_{i=0, j=0}^{M-1, M-1}. \quad (3.7)$$

The standard maximum likelihood decoding of a modulo-sum data symbol

$$\hat{d}_{AB} = \arg \max_{d_{AB}} p(\mathbf{x}|d_{AB}), \quad (3.8)$$

uses the following likelihood function

$$p(\mathbf{x}|d_{AB}) = \frac{1}{M_{AB}} \sum_{(d_A, d_B)_{\text{mod } M_{AB}} = d_{AB}} p_w(\mathbf{x} - \mathcal{M}(d_A) - \mathcal{M}(d_B)), \quad (3.9)$$

where the summation runs over all  $[d_A, d_B]$  such that  $(d_A + d_B)_{\text{mod } M_{AB}} = d_{AB} \in \mathbb{Z}_{M_{AB}}$  and the cardinality of modulo-sum data symbols is  $M_{AB}$ . Since modulo-sum is a minimum-cardinality network coding function  $M_{AB} = M$ . The noise probability density function equals to

$$p_w(\mathbf{w}) = \frac{1}{(2\pi N_0)^{N_s}} e^{-\|\mathbf{w}\|^2 / 2N_0}. \quad (3.10)$$

### 3.3 Affine Indexing for Modulo-Sum Decoding

#### 3.3.1 Impact of indexing

Figures 3.3 and 3.4 demonstrates the impact of the constellation indexing on the performance of modulo-sum (Fig. 3.5) decoding at the WNC-MA stage with 4-QAM constellations and indexing a) and b) (index '2' switched with '3'). Unlike for indexing a), the modulo-sum decoding using indexing b) contains some superimposed-constellation points (e.g.  $[0, 2]$  and  $[1, 3]$ ) which are equal despite the correspondence to unequal modulo-sum data symbols (i.e. the minimal distance of modulo-sum decoding is 0) which causes a considerable loss of the capacity as can be seen in Fig. 3.11 (dashed line).

#### 3.3.2 Suitability of Affine Indexing

The following lemma explains why the errorless modulo-sum decoding using indexing a) in Fig. 3.3 was not accidental.

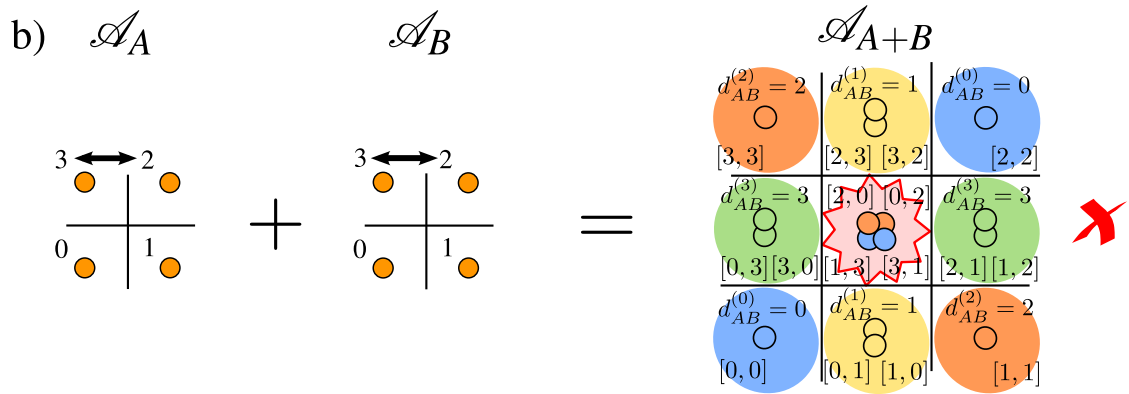


Figure 3.4: Indexing b) implies that some superimposed points of modulo-sum decoding will be decoded erroneously.

		→ $d_A$			
	$d_{AB}$	0	1	2	3
0	0	0	1	2	3
1	1	1	2	3	0
2	2	2	3	0	1
3	3	3	0	1	2

Figure 3.5: Modulo-sum operation  $d_{AB} = (d_A + d_B)_{\text{mod}4}$  where  $d_A, d_B \in \mathbb{Z}_4$ .

**Lemma 1.** *Lattice-constellation indices forming a modulo-arithmetic progression along each lattice (real) dimension (i.e. inverse indexing function  $\mathcal{I}^{-1}$  (3.3) is modulo-affine (denoted (AI)) imply that all equal superimposed-constellation points correspond to the same modulo-sum data symbol.*

*Proof.* Let two superimposed-constellation points  $\mathbf{u}^{(d_A, d_B)}, \mathbf{u}'^{(d'_A, d'_B)} \in \mathcal{A}_{A+B}$  correspond to distinct data symbol pairs  $[d_A, d_B] \neq [d'_A, d'_B]$  and fall to the same constellation point:

$$\mathbf{u}^{(d_A, d_B)} = \mathbf{u}'^{(d'_A, d'_B)}. \quad (3.11)$$

Assuming primary constellations to be taken from a common lattice, we may use (3.1) and (3.7) to expand (3.11) as

$$\mathbf{G}(\mathbf{a} + \mathbf{b}) - 2\overline{\mathbf{m}} = \mathbf{G}(\mathbf{a}' + \mathbf{b}') - 2\overline{\mathbf{m}} \quad (3.12)$$

and thus  $\mathbf{a} + \mathbf{b} = \mathbf{a}' + \mathbf{b}'$  must hold which expanded per-dimension yields

$$a_i + b_i = a'_i + b'_i, \forall i \in \mathbb{Z}_{2N_s}. \quad (3.13)$$

The superimposed point  $\mathbf{u}$  (resp.  $\mathbf{u}'$ ) matches modulo-sum data symbol  $d_{AB} = (d_A + d_B)_{\text{mod } M}$  (resp.  $d'_{AB}$ ). Let us further expand  $d_{AB}$  and  $d'_{AB}$  utilising that index mapping function  $\mathcal{I}(d_A) = \mathbf{a}$  is bijective and so the existence of inversion function  $\mathcal{I}^{-1}(\mathbf{a}) = d_A$  is ensured. Exclusive symbols simplify to

$$\begin{aligned} d_{AB} &= (d_A + d_B)_{\text{mod } M} = (\mathcal{I}^{-1}(\mathbf{a}) + \mathcal{I}^{-1}(\mathbf{b}))_{\text{mod } M}, \\ d'_{AB} &= (d'_A + d'_B)_{\text{mod } M} = (\mathcal{I}^{-1}(\mathbf{a}') + \mathcal{I}^{-1}(\mathbf{b}'))_{\text{mod } M}. \end{aligned} \quad (3.14)$$

The precondition of the lemma is  $\mathcal{I}^{-1}$  to be a modulo-affine function and so it can be expressed as

$$\mathcal{I}^{-1}(\mathbf{a}) = \left( \sum_{i=0}^{2N_s-1} c_i a_i + z \right)_{\text{mod } M}, \quad (3.15)$$

where  $c_i \in \mathbb{Z}$  denotes a common increment of a modulo-arithmetic progression in the  $i$ th lattice (real) dimension. Integer  $z \in \mathbb{Z}$  is an integer constant which represents a cyclic-shift of the indices. Using (3.15), we expand (3.14) as

$$\begin{aligned} d_{AB} &= (d_A + d_B)_{\text{mod } M} = (\mathcal{I}^{-1}(\mathbf{a}) + \mathcal{I}^{-1}(\mathbf{b}))_{\text{mod } M} = \left( \left( \sum_{i=0}^{2N_s-1} c_i a_i + z \right)_{\text{mod } M} + \left( \sum_{i=0}^{2N_s-1} c_i b_i + z \right)_{\text{mod } M} \right)_{\text{mod } M} \stackrel{\diamond}{=} \\ &\stackrel{\diamond}{=} \left( \sum_{i=0}^{2N_s-1} c_i a_i + z + \sum_{i=0}^{2N_s-1} c_i b_i + z \right)_{\text{mod } M} = \left( \sum_{i=0}^{2N_s-1} c_i (a_i + b_i) + 2z \right)_{\text{mod } M} \end{aligned} \quad (3.16)$$

where in  $\diamond$  step, we use the modulo-arithmetic rule

$$(x + y)_{\text{mod } M} = (x_{\text{mod } M} + y_{\text{mod } M})_{\text{mod } M}. \quad (3.17)$$

By the same manipulations, we obtain

$$d'_{AB} = \left( \sum_{i=0}^{2N_s-1} c_i (a'_i + b'_i) + 2z \right)_{\text{mod } M}. \quad (3.18)$$

Comparing (3.16) with (3.18), we conclude that if superimposed-constellation points are equal ((3.13) holds), then  $d_{AB} = d'_{AB}$  which proves the lemma.  $\square$

**Example 1.** Note, the indices of indexing a) (Fig. 3.3) in the first horizontal dimension are '0' and '1', and '2' and '3' both with common horizontal index-increment  $c_0 = +1$ ; similarly the index-increment in the vertical dimension is  $c_1 = +2$  (indices '0' and '2', and '1' and '3'). Therefore indexing a) is AI, unlike to indexing b) where e.g. the common increment for the first horizontal index pair '0', '1' is +1, but for the second pair '3', '2' is  $-1$  which does not allow AI.

**Corollary 1.** *It can be easily shown that all superimposed-constellation points lie in the same lattice as primary lattice-constellation points. Obviously, if all equal superimposed-constellation points correspond to the same modulo-sum data symbol (according to Lemma 1), then the minimal distance of modulo-sum decoding [54]*

$$\Delta_{\min} = \min_{(d_A+d_B) \bmod M \neq (d'_A+d'_B) \bmod M} \left\| \mathbf{u}^{(d_A, d_B)} - \mathbf{u}^{(d'_A, d'_B)} \right\|, \quad (3.19)$$

*equals to the minimal distance of primary lattice-constellation  $\Delta_{\min} = \delta_{\min}$ , where minimal distance of  $\mathcal{A}_A$  is defined as*

$$\delta_{\min} = \min_{d_A \neq d'_A} \left\| \mathbf{s}_A^{(d_A)} - \mathbf{s}_A^{(d'_A)} \right\|. \quad (3.20)$$

The error performance of uncoded modulo-sum decoding for high signal-to-noise ratio in AWGN is well determined by  $\Delta_{\min}$  (3.19). A design of the system with the maximal  $\Delta_{\min}$  is not an obvious task because instead of modulo-sum operation, generally every invertible function (e.g. bit-wise XOR) is admissible and thus we face a joint optimisation problem (over constellations and invertible functions). The number of all possible invertible functions is related to the number of distinct Latin squares which increases w.r.t. cardinality very quickly (see [4] Tab.1) and the problem starts to be numerically unmanageable. However, utilising Lemma 1 and Corollary 1, we may fix the invertible function to be the modulo-sum function and we search over the lattice-constellations with the maximal  $\delta_{\min}$  which can be indexed by AI. We concern on the existence of AI in the following section.

### 3.3.3 Existence of AI for Canonical Lattice-Constellations

#### Existence verification algorithm

We use a brute-force approach to investigate whether canonical lattice-constellations can be indexed by AI: we try all combinations of  $c_i$  which we take from the following set

$$c_i \in \mathcal{A}_c = \{1, 2, \dots, (M-1)\} = \mathbb{Z}_M \setminus \{0\}, \forall i \in \mathbb{Z}_{2N_s} \quad (3.21)$$

and check whether indexing function  $\mathcal{I}$  is bijective. By the restriction  $c_i$  to be taken only from set  $\mathcal{A}_c$ , we cover all possibilities because the arithmetic progression of AI needs to be taken modulo  $M$ .

#### Considered lattices

Although Lemma 1 holds for arbitrary dimensional lattice-constellations, we focus on single complex-dimensional ones ( $N_s = 1$ ) since they are often implemented and easy to be shown with their indexing. Particularly, we restrict on the rectangular  $Z^2$ , checkboard  $D_2$  and hexagonal  $A_2$  lattice with generator matrices (3.2).

#### Results

Table 3.1 summarizes existence of AI for several canonical constellations. Symbol  $[c_0, c_1]$  denotes a possible pair of common increments of AI and symbol  $\times$  labels the cases which cannot be indexed by any  $[c_0, c_1]$  (no AI exists). We have found that constellations with rectangular-type of shape in the rectangular  $Z^2$  lattice as well as square shape in the checkboard  $D_2$  lattice can be indexed by AI. Unfortunately, some constellation shapes that cannot be indexed by AI are often used in technical practise e.g. cross-shapes in the rectangular  $Z^2$  lattice with odd bit-cardinalities  $M = 32, 128$  and also those with high-cardinality sphere-like shapes.

Table 3.1: List of canonical constellations and its possible affine indexing described by  $[c_0, c_1]$

$\Lambda$	$M_d$	shape	$\mathcal{A}$	$\delta_{\min}^2$	$[c_0, c_1]$
$Z^2$	2	rectangular		4	[1, 0]
	4	rectangular		0.8	[1, 0]
	4	square		2	[1, 2]
	8	rectangular		0.67	[1, 4]
	8	sphere		0.82	[1, 3]
	16	square		0.4	[1, 4]
	16	cross		0.4	×
	32	rectangular		0.15	[1, 8]
	32	cross		0.2	×
	64	square		0.095	[1, 8]
	128	rectangular		0.038	[1, 16]
	128	cross		0.048	×
	128	sphere		0.049	×
	$D_2$	8	square		0.8
32		square		0.19	[1, 7]
128		square		0.047	[1, 15]
$A_2$	8	sphere		0.93	[1, 3]
	16	sphere		0.46	×
	32	sphere		0.23	×

**Algorithm 3.1** Greedy-Sphere Packing Design of Constellation-Shapes Ensuring Affine-Indexing.

1. Choose  $N_s$ -dimensional lattice (a generator matrix  $\mathbf{G}$ ) from which we want to construct  $M$ -ary constellation.
2. Choose index-increments of AI  $[c_0, c_1, \dots] \in \mathcal{A}_c^{2N_s}$  where  $\mathcal{A}_c = \{1, 2, \dots, (M-1)\}$ .
3. **Initiation:** set of lattice-coordinates includes the zero-coordinate vector  $\mathcal{S} := \{\mathbf{a}_0 = \mathbf{0}\}$ ; the current centroid is  $\bar{\mathbf{m}} := \mathbf{0}$  and the set of indices includes 0 index  $\mathcal{A}_d := \{0\}$ .
4. **Repeat**
  - (a) Create a set of all hypothetical coordinate candidates  $\mathcal{S}_x$  which are in the neighbourhood to all points in  $\mathcal{S}$  but are not included in  $\mathcal{S}$ . (Coordinate vector  $\mathbf{a}_x \in \mathbb{Z}^{2N_s}$  is in the neighbourhood of coordinate vector  $\mathbf{a}_y$  if  $\|\mathbf{a}_x - \mathbf{a}_y\| = 1$ , i.e.  $\mathbf{a}_x$  differs from  $\mathbf{a}_y$  in only one dimension by  $\pm 1$ .)
  - (b) Exclude all hypothetical coordinates  $\mathbf{a}_y \in \mathcal{S}_x$  with the index  $d_y = \mathcal{S}^{-1}(\mathbf{a}_y) = \left(\sum_{i=0}^{2N_s-1} c_i a_i^{(y)} + z\right)_{\text{mod } M}$  already included in the set of indices  $d_y \in \mathcal{A}_d$ .
  - (c) Choose the one  $\mathbf{a}_* \in \mathcal{S}_x$  with the signal point closest to the actual centroid  $\mathbf{a}_* = \arg \min_{\mathbf{a} \in \mathcal{S}_x} \|\mathbf{G}\mathbf{a} - \bar{\mathbf{m}}\|$ .
  - (d) **Update:** include coordinate vector  $\mathbf{a}_*$  into  $\mathcal{S} := \mathcal{S} \cup \{\mathbf{a}_*\}$ , include index  $d_* := \mathcal{S}^{-1}(\mathbf{a}_*) = \left(\sum_{i=0}^{2N_s-1} c_i a_{*,i}\right)_{\text{mod } M}$  into  $\mathcal{A}_d := \mathcal{A}_d \cup \{d_*\}$  and set a new centroid  $\bar{\mathbf{m}} := 1/|\mathcal{S}| \sum_{i=1}^{|\mathcal{S}|} \mathbf{G}\mathbf{a}_i$  where  $|\mathcal{S}|$  denotes the cardinality of  $|\mathcal{S}|$ .
5. **Until**  $|\mathcal{S}| = M$
6. **Minimal Distance Maximisation:** running step 2) through 5) for all distinct  $[c_0, c_1, \dots] \in \mathcal{A}_c^{2N_s}$  in step 2), we find the constellation with the maximal minimal distance denoted as  $\delta_{\min, \text{AI}}$  for corresponding optimal  $[c_0, c_1, \dots]_{\text{AI}}$ . (We assume cyclic-shift of indices  $z$  to be 0 in step 4b), since the maximal minimal distance is not influenced by  $z$ .)

**3.3.4 Greedy-Sphere Packing for Constellation Shape Design which Ensures AI**

Results from the preceding section indicate that sphere-like lattice-constellation shapes for high-cardinalities apparently prevent existence of AI. However, sphere-like constellation shapes possess the maximal shaping gain [65],[68]. So, the question is: can we design sphere-like lattice-constellation shapes for high-cardinalities and ensure existence of AI? We propose the following simple optimisation algorithm to answer this question.




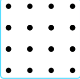
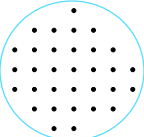
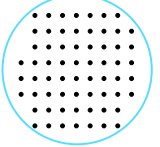



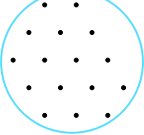
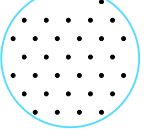
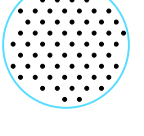
**Optimisation algorithm**

Finding the optimal constellation shape for a general lattice structure requires high complexity optimisation especially in high-dimensional and high-cardinality alphabet case. Paper [66] suggests heuristic low-complexity greedy-sphere packing algorithm for a constellation-shape design. It cannot always bring the optimum, nevertheless, it may yield a near-optimal solution with a good performance. The algorithm initially starts from the lattice origin and iteratively includes constellation points which are nearest to the actual centroid until  $M$  points are selected. We modify this algorithm to additionally ensure existence of AI (we select only the lattice point which is nearest to the actual centroid from the set of neighbouring lattice-points with not already included AI-indices). The proposed algorithm is summarized in Alg. 3.1.

**Results**

The found constellations (restricting on  $Z^2$  and  $A_2$  lattices) with the maximal minimal distance which can be indexed by AI are summarized in Table 3.2. Symbol  $[c_0, c_1]_{\text{AI}}$  denotes the common increments for which Alg. 3.1 converges to the highest minimal distance  $\delta_{\min, \text{AI}}$ . Symbol  $\delta_{\min}$  denotes the minimal distance of alphabets obtained by Alg. 3.1 irrespectively of existence of AI (without step 4b)). Parameter  $10 \log_{10} \left( \frac{\delta_{\min, \text{AI}}^2}{\delta_{\min}^2} \right)$  measures de-facto a price we pay for constellations being able to be indexed by AI.

Table 3.2: List of constellations designed by Algorithm 3.1.

$\Lambda$	$M_d$	$\mathcal{A}$	$[c_0, c_1]_{AI}$	$\delta_{\min, AI}^2$	$\delta_{\min}^2$	$10 \log_{10} \left( \frac{\delta_{\min, AI}^2}{\delta_{\min}^2} \right)$
$Z^2$	2		[1, 0]	4	4	0
	4		[1, 2]	2	2	0
	8		[1, 3]	0.82	0.82	0
	16		[1, 4]	0.4	0.4	0
	32		[1, 7]	0.193	0.2	-0.15
	64		[1, 24]	0.097	0.098	-0.04
$A_2$	2		[1, 0]	4	4	0
	4		[1, 2]	2	2	0
	8		[1, 3]	0.93	0.93	0
	16		[1, 7]	0.453	0.457	-0.04
	32		[1, 6]	0.224	0.227	-0.06
	64		[1, 8]	0.112	0.113	-0.04



### 3.3.5 Generalisation for $N_A$ –terminal WNC MA stage

It can be shown that Lemma 1 holds in a general network with  $N_A$ –terminals where  $N_A \geq 2$ . We assume that modulo-sum of all data symbols from all  $N_A$  terminals is to be decoded at the relay, i.e. the relay decodes

$$d_{A_0 A_1 \dots A_{N_A-1}} = \left( \sum_{i=0}^{N_A-1} d_{A_i} \right)_{\text{mod } M}, \quad (3.22)$$

where  $A_i$  denotes the  $i$ th terminal.

*Proof.* The proof has identical structure as the proof of Lemma 1. Two interfering superimposed-constellation points mean

$$\sum_{j=0}^{N_A-1} \mathbf{a}_j = \sum_{j=0}^{N_A-1} \mathbf{a}'_j. \quad (3.23)$$

It yields (per-dimension)

$$\sum_{j=0}^{N_A-1} a_{i,j} = \sum_{j=0}^{N_A-1} a'_{i,j}, \forall i \in \mathbb{Z}_{2N_s}. \quad (3.24)$$

Now, the modulo-sum network coded symbol corresponding to superimposed-constellation point  $\mathbf{u}$  equals to

$$\begin{aligned} d_{A_0 A_1 \dots A_{N_A-1}} &= \left( \sum_{j=0}^{N_A-1} d_{A_j} \right)_{\text{mod } M} = \left( \sum_{j=0}^{N_A-1} \mathcal{I}^{-1}(\mathbf{a}_j) \right)_{\text{mod } M} = \\ &= \left( \sum_{j=0}^{N_A-1} \left( \sum_{i=0}^{2N_s-1} c_i a_{i,j} + z \right) \right)_{\text{mod } M} = \left( \sum_{i=0}^{2N_s-1} c_i \left( \sum_{j=0}^{N_A-1} a_{i,j} \right) + N_A z \right)_{\text{mod } M} \end{aligned} \quad (3.25)$$

and similarly for  $\mathbf{u}'$

$$d'_{A_0 A_1 \dots A_{N_A-1}} = \left( \sum_{i=0}^{2N_s-1} c_i \left( \sum_{j=0}^{N_A-1} a'_{i,j} \right) + N_A z \right)_{\text{mod } M}. \quad (3.26)$$

Equation (3.25) equals to (3.26) for interfering points (3.24) which proves the modified lemma.  $\square$

### 3.3.6 Generalisation for Asymmetric Alphabet Cardinalities

Let us assume that the channel gains between relay  $R$  and terminals  $A$  and  $B$  are unequal. Surely, we can achieve the higher two-way sum-rate when we use suitable unequal constellation cardinalities  $M_A \neq M_B$ . Therefore, let us consider the case  $\mathcal{A}_A \neq \mathcal{A}_B$ .

It can be shown that Lemma 1 still holds if both constellations are curved from the same lattice ( $\mathbf{G}_A = \mathbf{G}_B$ ) with *identical common increments*  $c_{i,A} = c_{i,B}, \forall i \in \mathbb{Z}_{2N_s}$ . The last condition make an additional restriction on which constellations can be used together, see an example with 4-QAM and 8-QAM in Fig. 3.6 and 3.7.

## 3.4 Error Performance Evaluation

### 3.4.1 Analytical Symbol Pair-wise Error Approximation

Figure 3.9 shows the uncoded symbol error performance of several canonical constellations from Table 3.1 and optimised constellations from Table 3.2. Figure 3.10 then supports our derivations by performance of multi-dimensional lattice-constellations taken from the 4-real-dimensional  $D_4$  checkboard lattice and the 8-real-dimensional  $E_8$  Gosset lattice [69]. The performance curves are supported by the following analytical uncoded symbol error performance *pair-wise error* approximation (tight for high SNR)

$$P_{se} \sim N_{\min} Q \sqrt{\Delta_{\min}^2 \gamma / 2}, \quad (3.27)$$

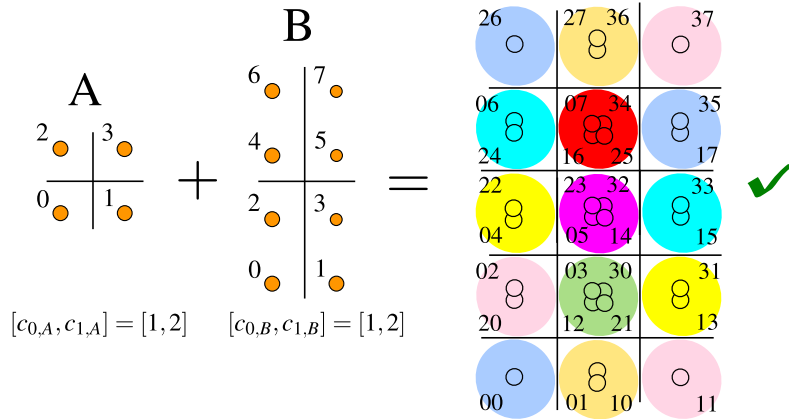


Figure 3.6: Terminal A uses 4-QAM constellation indexed by affine-indexing with  $[c_{0,A}, c_{1,A}] = [1, 2]$  and terminal B uses rectangular-shape 8-QAM constellation with  $[c_{0,B}, c_{1,B}] = [1, 2]$ . The modulo-sum decoding (described by the Latin square in Fig. 3.8) in a noiseless channel is errorless since  $c_{i,A} = c_{i,B}$ ,  $\forall i \in \mathbb{Z}_{2N_s}$ .

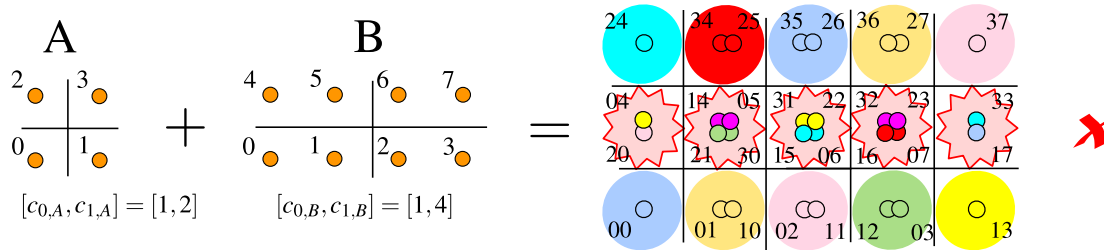


Figure 3.7: Terminal A uses 4-QAM constellation indexed by affine-indexing with  $[c_{0,A}, c_{1,A}] = [1, 2]$  and terminal B uses rectangular-shape 8-QAM constellation with  $[c_{0,B}, c_{1,B}] = [1, 4]$ . The modulo-sum decoding (shown in Fig. 3.8) in a noiseless channel is erroneous since  $c_{1,A} = 2 \neq c_{1,B} = 4$ .

$d_A \backslash d_B$	0	1	2	3	4	5	6	7
0	0	1	2	3	4	5	6	7
1	1	2	3	4	5	6	7	0
2	2	3	4	5	6	7	0	1
3	3	4	5	6	7	0	1	2

Figure 3.8: Modulo-sum operation  $(d_A + d_B)_{\text{mod}8}$  where  $d_A \in \mathbb{Z}_4$  and  $d_B \in \mathbb{Z}_8$ .

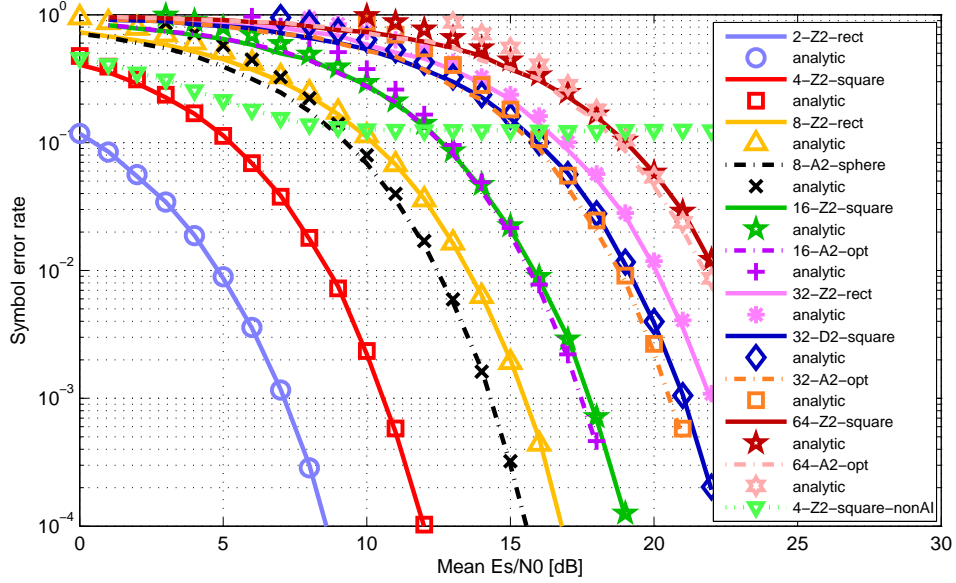


Figure 3.9: Uncoded symbol error performance curves of several canonical constellations from Table 3.1 and optimised constellations from Table 3.2. The light-green line with triangular markers denotes 4-QAM performance. It shows the impact of the erroneous modulo-sum decoding caused by *non-AI* indexed constellations (demonstrated in Fig. 3.4). The dash-dotted curves denoted as 'analytic' are the pair-wise symbol performance bounds (3.27).

where  $P_{se}$  denotes a symbol error probability,  $N_{\min}$  is a multiplicative constant corresponding to the average number of nearest neighbours,  $Q$  is a  $Q$ -function,  $\Delta_{\min}$  is defined in (3.19) and  $\gamma$  is a per-symbol SNR,

$$\gamma = \bar{\mathcal{E}}_s / \sigma^2 = \bar{\mathcal{E}}_s / (2N_0) = 1 / (2N_0), \quad (3.28)$$

where we suppose the unit mean symbol energy constellations  $\bar{\mathcal{E}}_s = 1$  and  $\sigma^2$  denotes the variance of complex AWGN sample which equals to  $\sigma^2 = 2N_0$ .





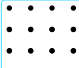
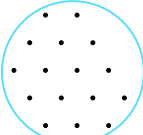

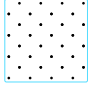
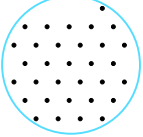

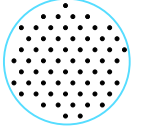


### 3.4.2 Average Number of Nearest Neighbours for WNC Method

It is interesting that in the case of WNC function decoding at the MA stage, the average number of nearest neighbours  $N_{\min}$  does not count numbers of constellation points but a number of nearest decision regions with different modulo-sum data symbols. Let us explain a computation of  $N_{\min}$  for plain BPSK constellation. Its superimposed constellation is depicted in our illustrative example in Fig. 2.14. Superimposed constellation point  $-2$  has the one nearest  $d_{AB} = 1$  decision region (containing point 0) and point 2 has also the single nearest  $d_{AB} = 1$  decision region. Next, there are two points which fall to the same signal space point 0, both have exactly the two nearest neighbour decision regions corresponding to different  $d_{AB}$  symbol. Summing up and dividing by 4 (we compute an average per-superimposed constellation point), it yields

$$N_{\min} = 1/4 + 1/4 + 2/4 + 2/4 = 1.5. \quad (3.29)$$

Note, that in the P2P AWGN channel, the average number of nearest neighbours of BPSK constellation is a *different* value  $N_{\min} = 1/2 + 1/2 = 1$ . Table 3.3 summarizes  $\Delta_{\min}^2$  and  $N_{\min}$  for the considered constellations used in Fig. 3.9 and 3.10.

Table 3.3: List of constellations and its  $\Delta_{\min}^2$  and  $N_{\min}$  used in Fig. 3.9 and 3.10.

$\Lambda$	$M_d$	$\mathcal{A}$	$\Delta_{\min}^2$	$N_{\min}$
$Z^2$	2		4	1.5
$Z^2$	4		2	3
$Z^2$	8		0.67	3.375
$A_2$	8		0.93	5.125
$Z^2$	16		0.4	3.75
$A_2$	16		0.45	5.625
$Z^2$	32		0.15	3.84
$D_2$	32		0.19	3.873
$A_2$	32		0.22	5.845
$Z^2$	64		0.095	4
$A_2$	64		0.11	6
$Z^2$	2		4	1.5
$D_4$	4	result of Alg. 3.1	5.33	5.25
$E_8$	16	result of Alg. 3.1	7.26	30.19
$D_4$	8	result of Alg. 3.1	4	12
$Z^2$	4		2	3
$D_4$	16	result of Alg. 3.1	2.33	15.11

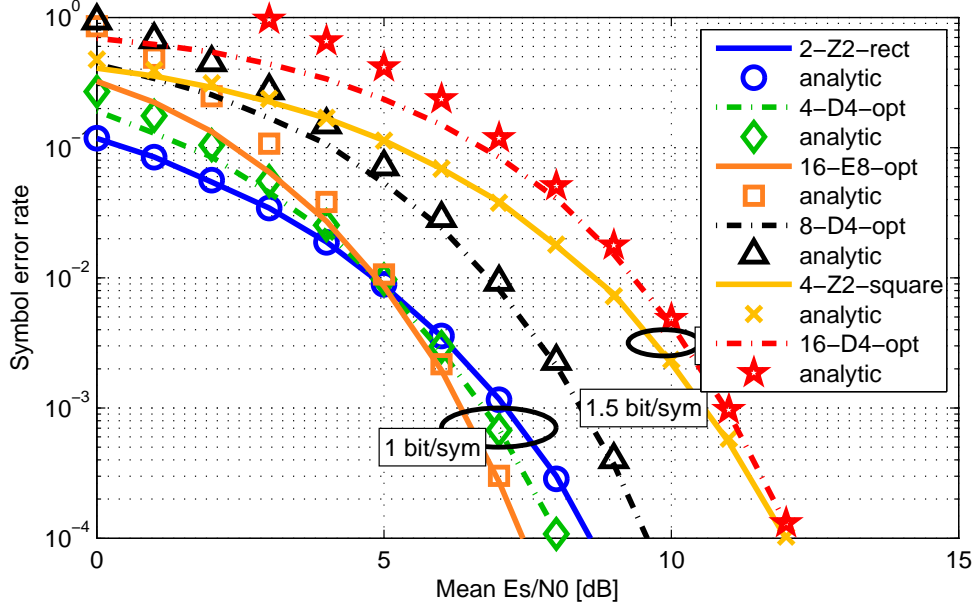


Figure 3.10: Uncoded symbol error performance of multi-dimensional lattice-constellations taken from 4-real-dimensional  $D_4$  checkboard lattice and 8-real-dimensional  $E_8$  Gosset lattice. The curves corresponding to the identical bit-rate are grouped together. The dash-dotted curves denoted as 'analytic' are the pair-wise symbol performance bounds (3.27).

### 3.5 Alphabet-Constrained Capacity Evaluation

In the previous sections, we have considered the minimal distance measure as a performance measure, although performance of channel coded system using the ideal capacity-approaching codes are more practical. For that reason, we evaluate Alphabet-Constrained Capacity (ACC). ACC is a mutual information between discrete-valued uniformly-distributed input (determined by particular constellation) and unconstrained-output. It represents the maximal possible achievable rate using given constellation. System with concatenated linear capacity-approaching channel code is expected to perform close to these curves [51]. The ACC curves of WNC in a 2WRC can be easily numerically evaluated by

$$C^* = \log_2 M + \frac{1}{M} \int_{\mathbf{x} \in \mathbb{C}^{N_s}} \sum_{d_{AB}=1}^M p(\mathbf{x}|d_{AB}) \log_2 \frac{p(\mathbf{x}|d_{AB})}{\sum_{d'_{AB}=1}^M p(\mathbf{x}|d'_{AB})} d\mathbf{x}. \quad (3.30)$$

where  $p(\mathbf{x}|d_{AB})$  equals to (3.9), for the derivation and more detailed discussion see [51].

Figure 3.11 presents ACC curves for several considered constellations and indexing (all uses AI except of the one from the example in Fig. 3.4). Curves described by 'maxmin-shape' denote the cases with the shape maximised by Alg. 3.1. The results show that AI lattice-constellations with modulo-sum relay decoding is a viable approach in an AWGN 2-WRC.

### 3.6 Conclusion

In this chapter, we have studied impact of constellation indexing on the performance of relay processing at the multiple-access stage of WNC in a 2-way relay channel. We consider the scenario where both terminals use constellations curved from a common lattice (denoted as lattice-constellations) and the relay decodes modulo-sum operation of transmitted data symbols. The proposed constellation-indexing (denoted as Affine-Indexing (AI)) implies the minimal distance of modulo-sum decoding to be equal to

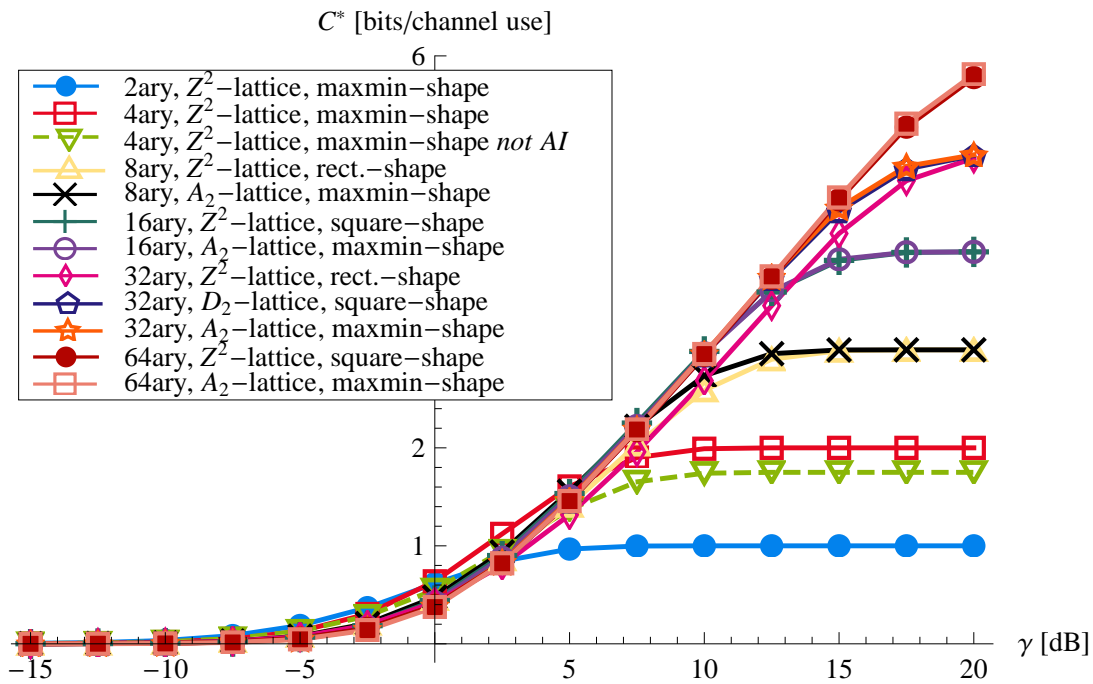


Figure 3.11: Alphabet-constrained capacities of several canonical constellations from Table 3.1 and optimised constellations from Table 3.2. The dashed-line curve with 4-QAM constellation shows the impact of erroneous modulo-sum decoding caused by a constellation-indexing which is *not* AI (the example in Fig. 3.4). Figure 3.4 shows that 4 out of 16 superimposed-constellation points are erroneously interfering (with 50% probability of error). It yields  $4/16 = 1/4$  of interfering points and  $1/4 \cdot 50\% = 1/8$  are erroneous which equals to  $\log_2 4/8 = 0.25$  of erroneous bits. The loss of 0.25 over AI case (solid-red-square line) bits for high SNR is well seen on the dashed-line curve.

the minimal distance of primary terminal constellation (for some non-AI indexing the minimal distance is 0). We have found that not every lattice-constellation shape can be indexed by AI. Unfortunately, sphere-like shapes cannot be indexed by AI, therefore we have proposed a greedy-sphere packing algorithm for the constellation shape design maximizing the minimal distance while keeping the existence of AI. The proposed AI lattice-constellations not only possess good minimal distance properties (if taken from a dense lattice), but also perform well in the measure of alphabet-constrained capacity.

We see a great potential of the WNC strategy using AI lattice-constellations with modulo-sum relay decoding also in a general multi-source multi-destination network. Especially the connection of WNC with lattice-constellations is interesting since a superposition of any number of interfering terminals (using alphabets taken from an identical lattice) lay again in the same lattice and all the lattice-constellation points can be described by integer coefficients. It means that the domains mixed by WNC (the *continuous signal space* of physical-layer and *discrete integer space* of network coding) can be described by a common integer algebraic structure. Based on our results, the invertible modulo-sum network coding function with AI indexed lattice-constellations seems to naturally correspond to the additive property of interfering electromagnetic waves at the WNC MA stage.

## Chapter 4

# Design of Constellations for Adaptive Minimum-Cardinality WNC utilising Hexagonal Lattice

We focus on a constellation design for adaptive WNC strategy in a wireless 2-way relay channel. It is well known that 4QAM constellation requires extended-cardinality network coding adaptation to avoid all singular channel parameters at the MA stage. The cardinality extension is undesirable since it introduces the redundancy decreasing the data rates at the broadcast stage.

In this chapter, we target a constellation design removing all the singularities without the cardinality extension. We show that such a constellation is a 4-ary constellation taken from hexagonal lattice (4HEX) which we present as a main contribution. Adaptive WNC using 4HEX (illustrated in Fig. 4.1) keeps comparable error performance at the MA stage as popular 4QAM, however without the cardinality extension. The similar properties has been found also by unconventional 3HEX and 7HEX constellations.

### 4.1 Introduction

#### 4.1.1 Motivation & Related Work

WNC theoretically offers the highest achievable throughput in a wireless 2-WRC assuming perfect CSI at all the nodes [47]. Considering more practical situation with CSI at the receivers, WNC performance emerges a new type of fading phenomenon. This fading (denoted as Relative-Fading (RF)) appears when a ratio of channel coefficients equals to certain critical values (denoted as singularities) when typical constellations are used by the terminals. The singularities force a minimal distance of network coding relay decoding to 0, regardless of magnitudes of the channel coefficients. Even if the channel parameters are Rayleigh/Rice distributed, the average performance is remarkably degraded due to this phenomenon. The authors in [54] propose an adaptive WNC strategy eliminating this performance degradation. It adapts network coding function according to the actual channel parameter ratio so as to maximize the minimal distance (it is equivalent to removing all the singularities). The authors in [5] designed multi-dimensional constellations which avoid the singularities even without network coding adaptation, however its spectral efficiency seems to be upper-limited by 1 bit-per-complex-dimension. Existence of singularities for constellations with higher spectral efficiency is without the adaptation apparently inevitable. Paper [38] presents a simplified search for network coding functions based on the theory of Latin squares. Both [54] and [38] conclude that 4QAM requires extended-cardinality network coding adaptation to avoid all the singularities. The cardinality extension is undesirable since it introduces the redundancy decreasing the data rates at the BC stage.



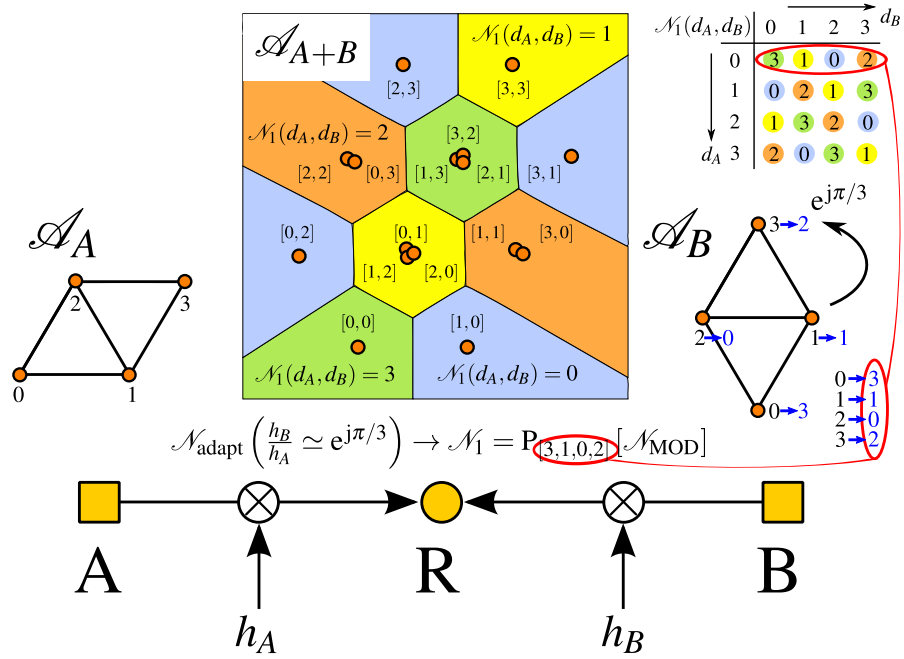


Figure 4.1: Multiple-access stage of WNC in a 2-WRC using adaptive network coding  $\mathcal{N}_{\text{adapt}}(h_B/h_A)$  and 4-ary hexagonal constellations.

## 4.2 System Model

### 4.2.1 Signal Space Model and Used Notation

Let both terminals A and B use the same constellation (including the same constellation-indexing)  $\mathcal{A}_A = \mathcal{A}_B = \mathcal{A}$  which is assumed to be linear ( $\mathcal{A} \subseteq \mathbb{C}$ ) and curved from a common lattice. The notation from the perspective of terminal A is following. Baseband signal points in the constellation space  $s_A$  forming the alphabet  $\mathcal{A} = \{s_A^{(i)}\}_{i=0}^{M-1}$  are assumed to be normalised to the unit mean symbol energy, where  $M$  is a constellation cardinality  $M = |\mathcal{A}|$ . The upper-indices  $\star^{(i)}$  are used when a concrete value of the variable is to be stressed, otherwise they are omitted. We define a constellation mapper  $\mathcal{M} : \mathbb{Z}_M \rightarrow \mathcal{A}$  such that the alphabet indices directly correspond to data symbols  $\mathcal{M}(d_A) = s_A^{(d_A)}$ , where data symbols are  $d_A \in \mathbb{Z}_M$  and  $\mathbb{Z}_M = \{0, 1, \dots, (M-1)\}$  denotes the set of non-negative integers lower than  $M$ . Using lattice-generator matrix  $\mathbf{G}$ , we unambiguously describe constellation signals by lattice-coordinate vectors  $\mathbf{a}$  as

$$s_A^{(i)} = \mathbf{G}\mathbf{a}^{(i)} - \bar{\mathbf{m}}, \forall i \in \mathbb{Z}_M, \quad (4.1)$$

where  $\bar{\mathbf{m}} = 1/M \sum_{i=0}^{M-1} \mathbf{G}\mathbf{a}^{(i)}$  ensures that  $\mathcal{A}$  has a zero-mean. Vector  $\mathbf{a} = [a_0, a_1]^T \in \mathcal{S} \subseteq \mathbb{Z}^2$  is taken from a set of lattice coordinates  $\mathcal{S}$  (determining the constellation shape), where  $\mathbb{Z} = \{\dots, -1, 0, 1, \dots\}$  denotes the ring of integers. Generator matrices of the rectangular  $\mathbb{Z}^2$  and the hexagonal  $A_2$  lattice are  $\mathbf{G}_{\mathbb{Z}^2} = [1, j]$  and  $\mathbf{G}_{A_2} = [1, 1/2 + j\sqrt{3}/2]$ . A one-to-one indexing mapper between the constellation-indices and the lattice-coordinates is defined as

$$\mathcal{I} : \mathbb{Z}_{M_d} \mapsto \mathcal{S}, \mathcal{I}(d_A) = \mathbf{a}^{(d_A)}. \quad (4.2)$$

### 4.2.2 2-Way Relay Channel and Model Assumptions

A 2-WRC consists of two terminals A and B bi-directionally communicating via supporting relay R in a half-duplex manner (each node cannot send and receive at the same time). We assume an idealised

time-synchronised scenario and Rayleigh/Rice flat fading with CSI at the receivers. We analyse an uncoded per-symbol WNC relaying and we expect similar performance trends as with concatenated channel coding, see [52], [51] for more details about the receiver processing of such a concatenation.

### 4.2.3 Adaptive WNC in a wireless 2-WRC

The WNC 2-way relaying consists of a MA stage and a BC stage. At the first MA stage, both terminals transmit simultaneously to the relay which receives a signal superposition

$$x = h_A s_A + h_B s_B + w = u + w, \quad (4.3)$$

where  $u \in \mathcal{A}_{A+B}$  denotes a superimposed signal

$$u^{(d_A, d_B)} = h_A s_A^{(d_A)} + h_B s_B^{(d_B)}, \forall d_A, d_B \in \mathbb{Z}_M, \quad (4.4)$$

where  $w$  is a complex AWGN noise with variance  $2N_0$  and  $h_A, h_B$  are fading channel coefficients. The relay decodes a network coded data symbol  $d_{AB}$  as

$$\hat{d}_{AB} = \arg \max_{d_{AB}} p(x|d_{AB}), \quad (4.5)$$

where the likelihood function is

$$p(x|d_{AB}) = \frac{1}{M_{AB}} \sum_{\mathcal{N}(d_A, d_B)=d_{AB}} \frac{1}{2\pi N_0} e^{-\frac{|x-u^{(d_A, d_B)}|^2}{2N_0}}. \quad (4.6)$$

The summation in (4.6) runs over all  $[d_A, d_B] \in \mathbb{Z}_M^2$  such that  $\mathcal{N}(d_A, d_B) = d_{AB}$ . The network coding function  $\mathcal{N}$  fulfils an exclusive law of network coding [54]

$$\begin{aligned} \mathcal{N}(d_A, d_B) &\neq \mathcal{N}(d'_A, d_B), & d_A &\neq d'_A, \\ \mathcal{N}(d_A, d_B) &\neq \mathcal{N}(d_A, d'_B), & d_B &\neq d'_B \end{aligned} \quad (4.7)$$

in order to ensure decodability at the destinations when one of the terminal data symbols is provided. We denote the cardinality of network coded symbols as  $M_{AB}$  ( $d_{AB} \in \mathbb{Z}_{M_{AB}}$ ). It is generally  $M_{AB} \geq M$ , when  $M_{AB} = M$  (resp.  $M_{AB} > M$ ), we denote such  $\mathcal{N}$  as a *minimum-* (resp. *extended-*) cardinality one. The maximal capacity gain due to the network coding-based information compression is achieved when cardinality  $M_{AB}$  is minimal. Function  $\mathcal{N}$  is uniquely specified by its Latin square [38] which we denote as a matrix  $\mathbf{N}$ , where  $\mathcal{N}(d_A, d_B) = [\mathbf{N}]_{d_A, d_B}$ . We will use modulo-sum  $\mathcal{N}_{\text{MOD}}(d_A, d_B) = (d_A + d_B)_{\text{mod}M}$  and bit-wise XOR  $\mathcal{N}_{\text{XOR}}(d_A, d_B) = d_A \oplus d_B$  minimum-cardinality network coding functions which possess the following Latin squares (for  $M = 4$ )

$$\mathbf{N}_{\text{XOR}} = \begin{bmatrix} 0 & 1 & 2 & 3 \\ 1 & 0 & 3 & 2 \\ 2 & 3 & 0 & 1 \\ 3 & 2 & 1 & 0 \end{bmatrix}, \quad \mathbf{N}_{\text{MOD}} = \begin{bmatrix} 0 & 1 & 2 & 3 \\ 1 & 2 & 3 & 0 \\ 2 & 3 & 0 & 1 \\ 3 & 0 & 1 & 2 \end{bmatrix}. \quad (4.8)$$

In the adaptive WNC strategy [54], the relay adaptively selects network coding function  $\mathcal{N}_{\text{adapt}}$  according to instantaneous CSI (channel ratio  $\alpha = h_B/h_A$ ) in order to maximize the minimal distance of the relay processing. It can be shown that the minimal distance is maximized if all so-called singular channel parameters are *avoided* [38].

**Definition 1.** A *singular* channel parameter  $\alpha = h_B/h_A$  is such a channel ratio for which  $h_A, h_B \neq 0$  and

$$s_A^{(d_A)} + \alpha s_B^{(d_B)} = s_A^{(d'_A)} + \alpha s_B^{(d'_B)}, [d_A, d_B] \neq [d'_A, d'_B]. \quad (4.9)$$

A function  $\mathcal{N}$  *avoids a singularity*  $\alpha$  when (4.9) holds and  $\mathcal{N}(d_A, d_B) = \mathcal{N}(d'_A, d'_B)$  and thus situation (4.9) is not a source of errors in network coded data decoding (4.5).

At the second BC stage, the relay broadcasts network coded data symbol  $d_{AB}$  and the final destinations subsequently perform successful detection exploiting the knowledge of its own data symbols and (4.7).

### 4.3 Analysis of 4QAM Singularities

We analyse the singularities of 4QAM with a help of Theorems 1, 2, 3. More details about Theorem 1 are in [2].

**Theorem 1.** *Assume a superposition of two constellations taken from a common lattice. If both constellation-indices form a modulo-arithmetic progression along each lattice dimension (inversion of (4.2)  $\mathcal{S}^{-1}$  is modulo-affine (denoted as Affine Indexing (AI)), then all equal superimposed-constellation points correspond to an identical modulo-sum data symbol.*

*Proof.* The proof and more discussions are presented in Sec. 3.3.2.  $\square$

Theorem 1 shows that singularity  $\alpha = 1$  ( $h_A = h_B = 1$ ) can be avoided by minimum-cardinality modulo-sum function  $\mathcal{N}_{\text{MOD}}$  providing AI indexed constellations. 4QAM can be indexed by AI [2] with  $\mathbf{c} = [1, 2]$  (where  $c_i \in \mathbb{Z}$  denotes a common increment of a modulo-arithmetic progression in the  $i$ th dimension) as shown in Fig. 4.2.

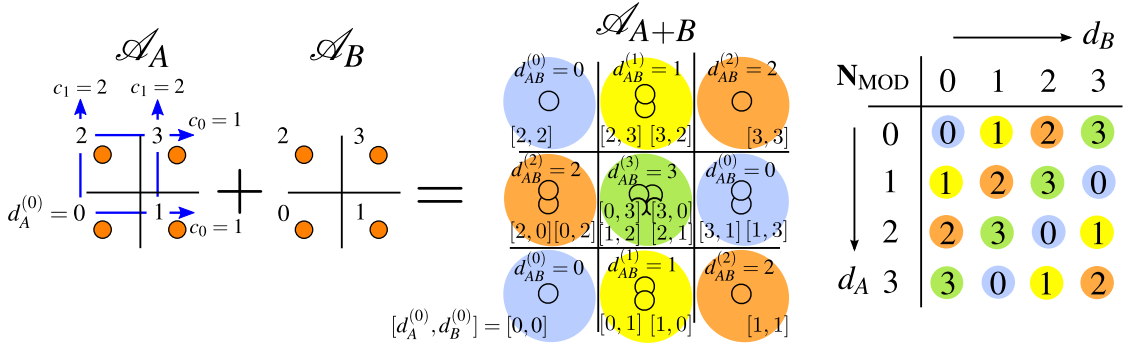


Figure 4.2: Modulo-sum function avoids singularity  $\alpha = 1$  if both constellations are indexed by affine-indexing.

**Definition 2.** A vector permutation  $P[\star]$  which maps vector  $\mathbf{n} = [0, 1, \dots, (M-1)]$  on a vector

$$\mathbf{p} = [p_0, p_1, \dots, p_{(M-1)}] \quad (4.10)$$

is denoted as  $P_{\mathbf{p}}[\mathbf{n}] = \mathbf{p}$ . In a similar way, we define a column matrix permutation as

$$P_{\mathbf{p}}[\mathbf{N}] = [\mathbf{N}_{\star p_0}, \mathbf{N}_{\star p_1}, \dots, \mathbf{N}_{\star p_{(M-1)}}], \quad (4.11)$$

where  $\mathbf{N}_{\star i}$  denotes the  $i$ th column of matrix  $\mathbf{N}$ . We describe a row permutation as  $P_{\mathbf{p}^T}[\mathbf{N}] = P_{\mathbf{p}}[\mathbf{N}^T]^T$  and the exponent of the permutation as  $P_{\mathbf{p}}^2[\mathbf{N}] = P_{\mathbf{p}}[P_{\mathbf{p}}[\mathbf{N}]]$  where  $P^0$  is an identity.

**Theorem 2.** *Let network coding function  $\mathcal{N}$  with Latin square  $\mathbf{N}$  avoid a singularity  $\alpha$  using constellations  $\mathcal{A}_A, \mathcal{A}_B$ . Now, if we re-index constellation  $\mathcal{A}_A$  (resp.  $\mathcal{A}_B$ ) according to some permutation  $P$ , then the same singularity  $\alpha$  is avoided by the network coding function with the Latin square permuted by the permutation  $P$  on rows (resp. columns) of  $\mathbf{N}$ .*

Theorem 2 is obvious and instead of the proof we rather clearly demonstrate the principle on the example in Fig. 4.3. Here, the channel parameters  $h_A = 1$  and  $h_B = e^{j\pi/2}$  ( $\alpha = e^{j\pi/2}$ ) cause  $90^\circ$  rotation of the constellation  $\mathcal{A}_B$ . The rotation effectively means only a constellation re-indexing due to the symmetry of 4QAM constellation shape and rectangular lattice. Now, if we find some new indices (denoted by blue colour in Fig. 4.3) forming AI jointly with indexing of  $\mathcal{A}_A$ , then the singularity is avoided by modulo-sum function. There always exists a permutation which maps old indices to the new AI indices  $P_{\mathbf{p}}[\star]$  and according to Theorem 2 the removing singularity network coding function has Latin square  $P_{\mathbf{p}}[\mathbf{N}_{\text{MOD}}]$ . Similar principle is depicted also in Fig. 4.1.

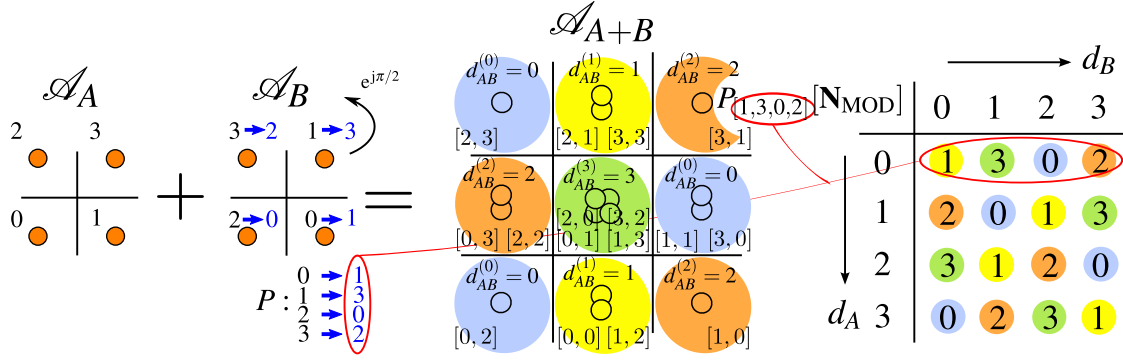


Figure 4.3: Column permutation (that re-index  $\mathcal{A}_B$  to be jointly AI with indexing  $\mathcal{A}_A$ ) of modulo-sum function which avoids singularity  $\alpha = e^{j\pi/2}$ .

**Theorem 3.** *If network coding function  $\mathcal{N}$  avoids a singularity  $\alpha$ ,  $\alpha \neq 0$ , then the same  $\mathcal{N}$  avoids also  $1/\alpha$ .*

*Proof.* We obtain the theorem simply, when we multiply both sides of (4.9) by  $1/\alpha$  on condition that  $s_A, s_B$  are from the same alphabet  $\mathcal{A}$ .  $\square$

Let summarize analysis of 4QAM singularities. According to Theorem 2 and 3, once we avoid singularities taken modulo  $90^\circ$  rotation and with  $|\alpha| \leq 1$ , then we avoid all of them. Particularly, they are  $\{1, (1+i)/2\}$ . According to Theorem 1 we avoid singularity 1 by the minimum-cardinality modulo-sum function or according to [54] by the bit-wise XOR function. Unfortunately, works [54], [38] show that removal of singularity  $(1+i)/2$  requires *extended-cardinality* Latin square

$$\mathbf{N}_2 = \begin{bmatrix} 0 & 1 & 2 & 3 \\ 2 & 3 & 1 & 4 \\ 3 & 0 & 4 & 2 \\ 4 & 2 & 0 & 1 \end{bmatrix}. \quad (4.12)$$

Figure 4.4 presents the normalised parametric minimal distance defined as

$$\Delta_{\min}^2(\alpha) = \min_{\mathcal{N}_{\text{adapt}}(d_A, d_B) \neq \mathcal{N}_{\text{adapt}}(d'_A, d'_B)} \left\| \Delta s_A^{(d_A, d'_A)} + \alpha \Delta s_B^{(d_B, d'_B)} \right\|^2,$$

where  $\Delta s_A^{(d_A, d'_A)} = s_A^{(d_A)} - s_A^{(d'_A)}$ ,  $\Delta s_B^{(d_B, d'_B)} = s_B^{(d_B)} - s_B^{(d'_B)}$ . It verifies that all singularities have been avoided (i.e.  $\Delta_{\min}^2(\alpha)$  is non-zero for any non-zero  $\alpha$ ). The relay adaptively selects  $\mathcal{N}_i$  according to adaptive network coding function  $\mathcal{N}_{\text{adapt}}(\alpha)$  shown in Fig. 4.5 where  $\mathbf{N}_2$  is defined by (4.12) and

$$\begin{aligned} \mathbf{N}_0 &= \mathbf{N}_{\text{XOR}}, & \mathbf{N}_1 &= P_{[1,3,0,2]}[\mathbf{N}_0], & \mathbf{N}_3 &= P_{[1,3,0,2]}[\mathbf{N}_2], \\ \mathbf{N}_4 &= P_{[1,3,0,2]}^2[\mathbf{N}_2], & \mathbf{N}_5 &= P_{[1,3,0,2]}^3[\mathbf{N}_2]. \end{aligned} \quad (4.13)$$

## 4.4 Proposed Hexagonal Constellations

### 4.4.1 4-ary HEX Constellation

In the preceding section, we have found that all unit-length singularities  $|\alpha| = 1$  of 4QAM can be avoided by *minimum-cardinality* network coding functions. Particularly, there are four unit-length singularities  $\{e^{j2\pi k/4}\}_{k=0}^3$  due to the  $90^\circ$  symmetry of the rectangular lattice. This motivates us to consider constellations taken from the hexagonal lattice since there are possibly six unit-length singularities  $\{e^{j2\pi k/6}\}_{k=0}^5$

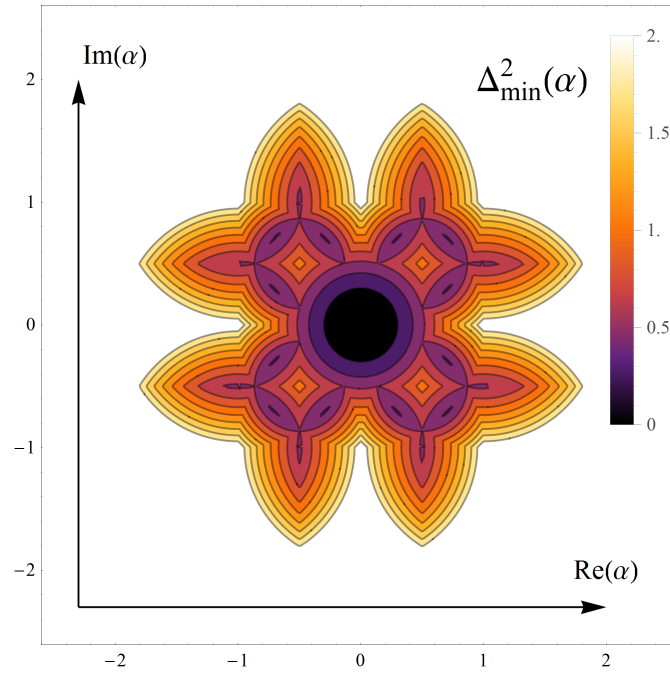


Figure 4.4: Parametric minimal distance  $\Delta_{\min}^2(\alpha)$  of 4QAM constellation.

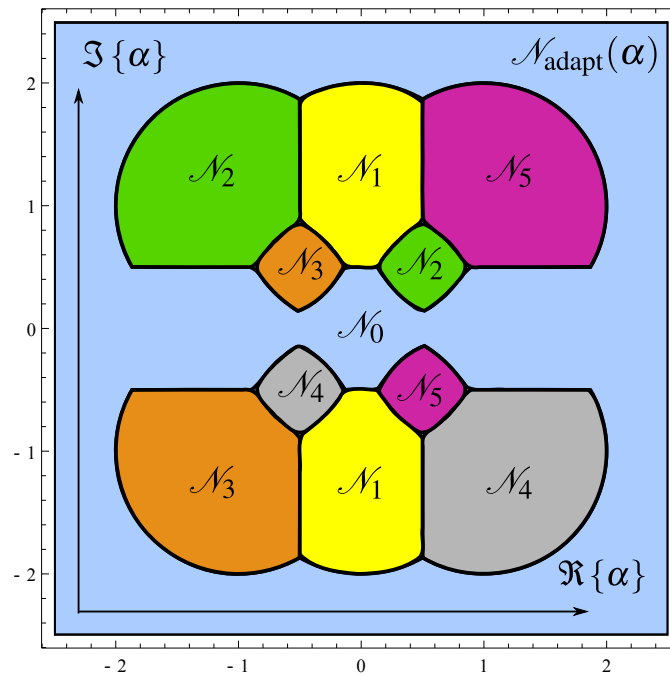


Figure 4.5: Adaptive network coding function  $\mathcal{N}_{\text{adapt}}(\alpha)$  of 4QAM constellation.

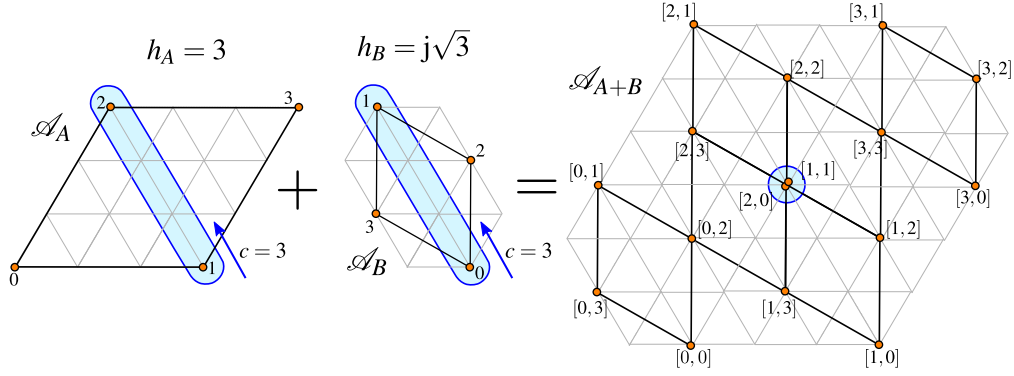


Figure 4.6: Singularity  $\alpha = j\sqrt{3}/3$  is avoided by the modulo-sum network coding function if all indices in the critical lattice-dimension (emphasized) are indexed by affine-indexing (here with coefficient  $c = 3$ ).

due to its  $60^\circ$  symmetry. The number of singularities is limited and depends only on the alphabet cardinality so we may hope that if we avoid more singularities by minimum-cardinality functions we could conceivably avoid all of them. Let us analyse the singularities of 4ary hexagonal constellation (4HEX)

$$\mathcal{A}_{4\text{HEX}} = \sqrt{2}/4 \left\{ -3 - j\sqrt{3}, 1 - j\sqrt{3}, -1 + j\sqrt{3}, 3 + j\sqrt{3} \right\}, \quad (4.14)$$

depicted in Fig. 4.1. The shape of 4HEX is symmetric to  $180^\circ$  rotation. Therefore we suffice to analyse singularities taken modulo  $180^\circ$  rotation and with  $|\alpha| \leq 1$ . They are

$$\left\{ 1, e^{j\pi/3}, e^{j2\pi/3}, \sqrt{3}/3 e^{j\pi/6}, j\sqrt{3}/3, \sqrt{3}/3 e^{j5\pi/6} \right\}. \quad (4.15)$$

We avoid unit-length singularities  $\{1, e^{j\pi/3}, e^{j2\pi/3}\}$  by the same procedure as in the case of 4QAM: we search for such a new indexing of  $\mathcal{A}_A$  and  $\mathcal{A}_B$  that would be jointly AI and then the permuted modulo-sum function avoid these singularities. However, there does not exist an indexing that would be jointly AI for

$$\left\{ \sqrt{3}/3 e^{j\pi/6}, j\sqrt{3}/3, \sqrt{3}/3 e^{j5\pi/6} \right\}. \quad (4.16)$$

But a more detailed analysis shows that two super-imposed points which fall to the same position are composed of the signal points taken from a single lattice dimension. Thus, if the constellation-indices are jointly AI in this critical dimension, than the singularity is avoided by modulo-sum as shown e.g. in Fig. 4.6. All singularities of 4HEX can be avoided by the following *minimum-cardinality* modulo-sum based adaptation  $\mathcal{N}_{\text{adapt}}^{\text{MOD}}(\alpha)$  using the functions

$$\begin{aligned} \mathbf{N}_0 &= \mathbf{N}_{\text{MOD}}, \mathbf{N}_1 = P_{[3,1,0,2]}[\mathbf{N}_0], \mathbf{N}_2 = P_{[0,2,1,3]}^T [P_{[2,1,0,3]}[\mathbf{N}_0]], \\ \mathbf{N}_3 &= P_{[3,2,1,0]}[\mathbf{N}_0], \mathbf{N}_4 = P_{[3,2,1,0]}[\mathbf{N}_1], \mathbf{N}_5 = P_{[3,2,1,0]}[\mathbf{N}_2]. \end{aligned} \quad (4.17)$$

There is a numerically manageable number (4 in the standard form) of all 4ary minimum-cardinality Latin squares (unlike for 8-ary cardinality where there is  $\sim 10^{12}$  Latin squares). Based on a brute-force search, we found that bit-wise XOR based network coding adaptation requires an adaptation to only 3 functions  $\mathbf{N}_i = P_{[0,2,3,1]}^i[\mathbf{N}_{\text{XOR}}]$ ,  $i \in \mathbb{Z}_3$  and thus it is more practical for real implementation. See Figures 4.5, 4.8 and 4.9 summarizing the 4HEX adaptation.

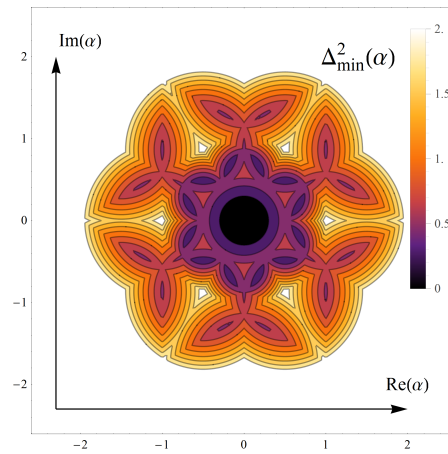


Figure 4.7: Parametric minimal distance of the adaptive WNC strategy using 4HEX.

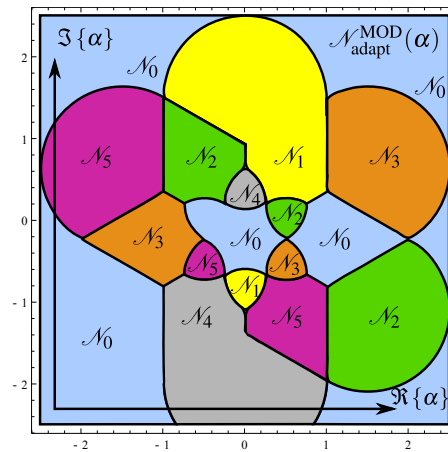


Figure 4.8: Adaptive network coding  $\mathcal{N}_{\text{adapt}}^{\text{MOD}}(\alpha)$  based on the modulo-sum function for 4HEX.

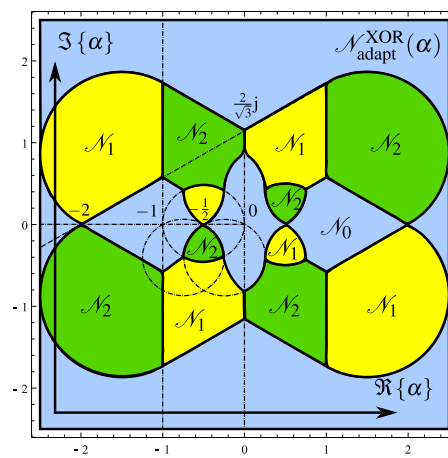


Figure 4.9: Adaptive network coding  $\mathcal{N}_{\text{adapt}}^{\text{XOR}}(\alpha)$  based on the bit-wise XOR function for 4HEX.

#### 4.4.2 Unconventional 3-ary and 7-ary HEX Constellations

In the similar way, we analyse

$$\mathcal{A}_{3\text{HEX}} = \left\{ e^{-j5\pi/6}, e^{-j\pi/6}, j \right\} \quad (4.18)$$

and

$$\mathcal{A}_{7\text{HEX}} = \sqrt{7/6} \left\{ e^{-j2\pi/3}, e^{-j\pi/3}, -1, 0, 1, e^{j2\pi/3}, e^{j\pi/3} \right\} \quad (4.19)$$

constellations with  $60^\circ$  rotationally symmetric shapes. The singularities taken modulo  $60^\circ$  and  $|\alpha| \leq 1$  are  $\{1\}$  and  $\{1/2, 1, 1/\sqrt{3}e^{j\pi/6}, 2/\sqrt{3}e^{j\pi/6}\}$ , respectively. All the singularities are avoided by the *minimum-cardinality* network coding adaptation depicted in Fig. 4.10 and 4.11, 4.12 and 4.13 where

$$\mathbf{N}_i = P_{[0,2,1]}^i[\mathbf{N}_{\text{MOD}}], i \in \mathbb{Z}_2 \quad (4.20)$$

and

$$\mathbf{N}_i = P_{[1,4,0,3,6,2,5]}^i[\mathbf{N}_{\text{MOD}}], i \in \mathbb{Z}_6, \quad (4.21)$$

respectively.

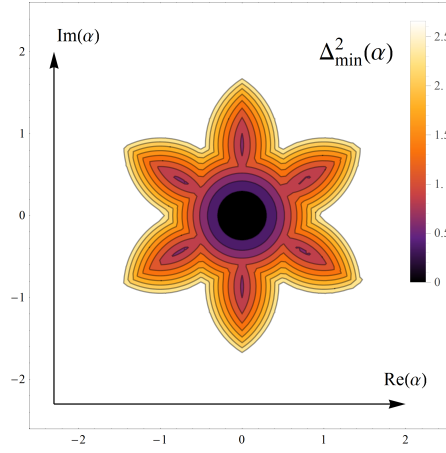


Figure 4.10: Parametric minimal distance  $\Delta_{\min}^2(\alpha)$  of the adaptive WNC strategy using 3HEX constellation.

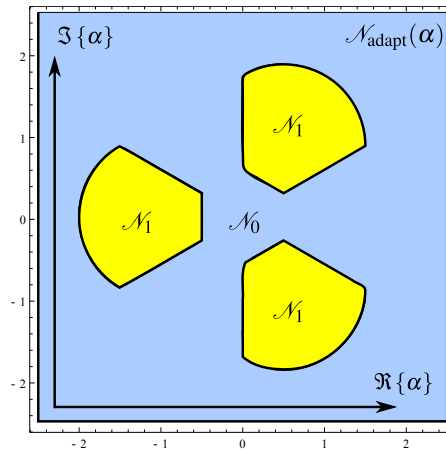


Figure 4.11: Adaptive network coding function  $\mathcal{N}_{\text{adapt}}(\alpha)$  for 3HEX constellation.



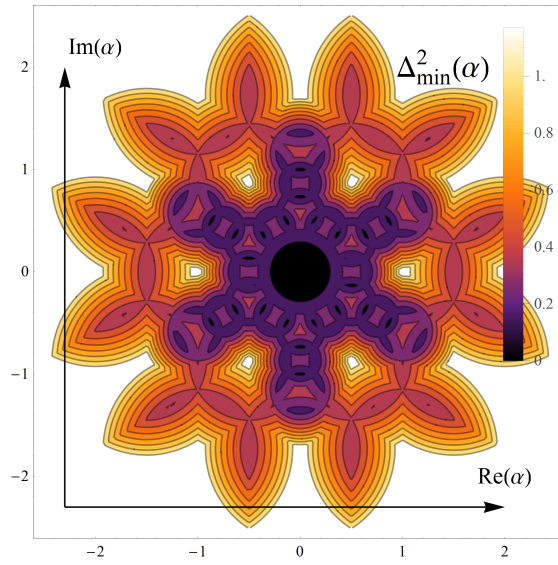


Figure 4.12: Parametric minimal distance  $\Delta_{\min}^2(\alpha)$  of the adaptive WNC strategy using 7HEX constellation.

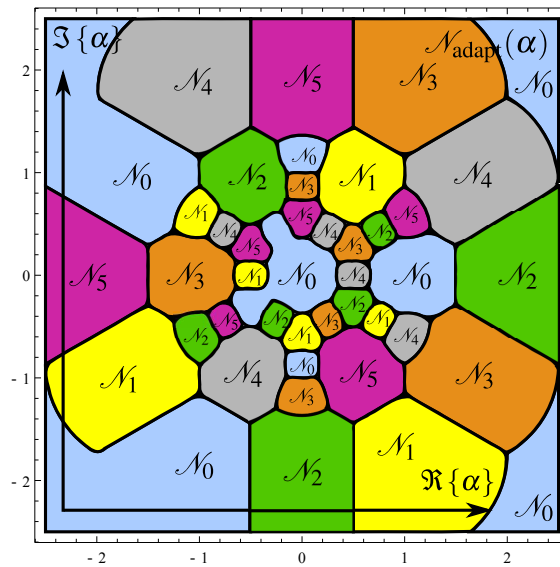


Figure 4.13: Adaptive network coding function  $\mathcal{N}_{\text{adapt}}(\alpha)$  for 7HEX constellation.

### 4.5 Performance Evaluation

The performance of the uncoded network coded symbol decoding at the MA stage (4.5) is depicted in Fig.4.14. We conclude that the performance of the minimum-cardinality network coding adaptation using 4HEX is considerable better than the minimum-cardinality adaptation using 4QAM (because the singularity  $(1+j)/2$  cannot be avoided.) and it is comparable to the extended-cardinality adaptation using 4QAM.

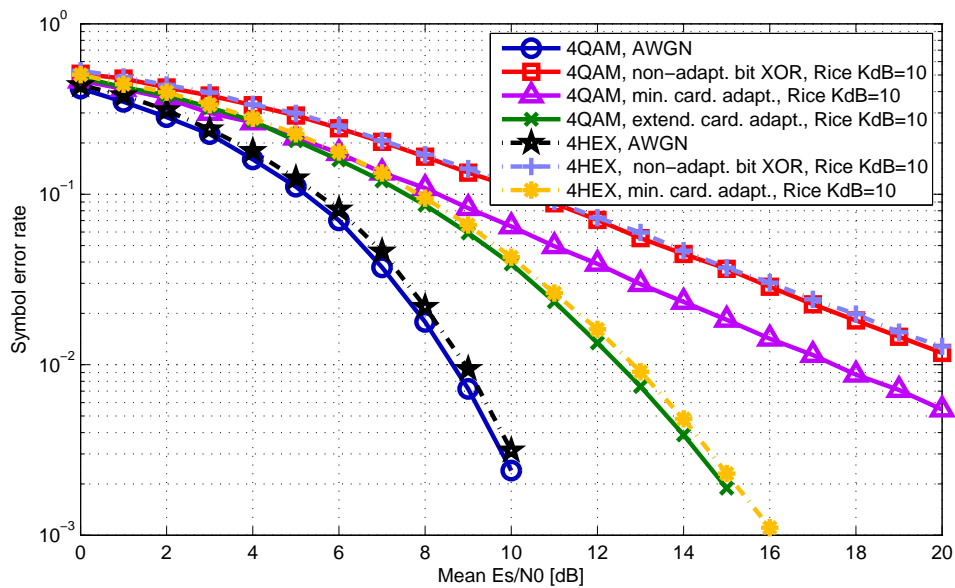


Figure 4.14: Network coded symbol error rate at the MA stage of the adaptive WNC strategy in Rician  $K = 10$  dB channel using 4QAM and 4HEX constellations.

## 4.6 Conclusion

We present 3HEX, 4HEX and 7HEX constellations which avoid all singularities in the adaptive WNC 2-way relaying without the network coding cardinality extension which increases the redundancy at the BC stage (as in the case of 4QAM). The proposed 4HEX constellation clearly outperforms 4QAM in the considered scenario. In addition, 4HEX uses the adaptation using bit-wise XOR permutations which enables a simple channel coding concatenation implementation [51]. Based on these properties, we conclude that the adaptive WNC with 4HEX is very convenient for practical implementation.

## Chapter 5

# Design of UMP Alphabets employing Multi-Dimensional Frequency Modulations

WNC is a promising 2-way relaying strategy due to its potential to operate outside of the classical MAC capacity region. Assuming a practical scenario with Channel State Information at the Receiver side (CSIR) and *no channel adaptation*, there exist modulations and network coding functions for which even non-zero channel parameters (denoted as singular) cause zero minimal distance – significantly degrading its performance.

In this chapter, we show that non-binary linear alphabets cannot avoid these singular parameters. Moreover, some network coding functions even imply its existence. We show that such a function is not a bit-wise XOR. We define the robust alphabets avoiding all singularities and achieving the minimal distance upper-bound for all parameter values. We denote these alphabets as Uniformly Most Powerful (UMP). We find that any binary, any non-binary orthogonal and any bi-orthogonal modulation is always UMP when combined with the bit-wise XOR function. Apparently, non-binary UMP alphabets are multi-dimensional and so we optimize naturally multi-dimensional modulations such as Frequency Shift Keying (FSK) and full-response Continuous Phase Modulation (CPM) to yield UMP alphabets. In case of FSK, we optimise its modulation index and in case of full-response CPM, we optimise its frequency pulse shape. UMP alphabets provide considerable error performance gains, although they require always more bandwidth than in the P2P case. The extended-bandwidth alphabets may still have comparable benefits when we demand e.g. alphabets with the constant envelope property.

## 5.1 Introduction

### 5.1.1 Motivation & Related Work

The direct estimation of network coded data from the signal interference at the MA stage of the WNC 2-way relaying is very promising due to its ability to operate outside of the classical MAC capacity region [47]. WNC performance with CSIR is in contrast to traditional P2P communication strongly channel parameter dependent. Surprisingly, there are modulation alphabets (e.g. popular QPSK) for which even non-zero channel parameters (denoted as singular) cause 0 minimal distance of the network coded symbol decoding (which significantly degrades its performance). Adaptive extended-cardinality network coding [54] and adaptive precoding technique [60] were proposed to suppress this phenomenon which we denote as a relative-fading. However, both techniques require some form of adaptation that might be problematic. The papers [58], [70] are also related, but assumes a different setting – non-coherent (no CSIR) WNC using the complex-orthogonal FSK modulation.

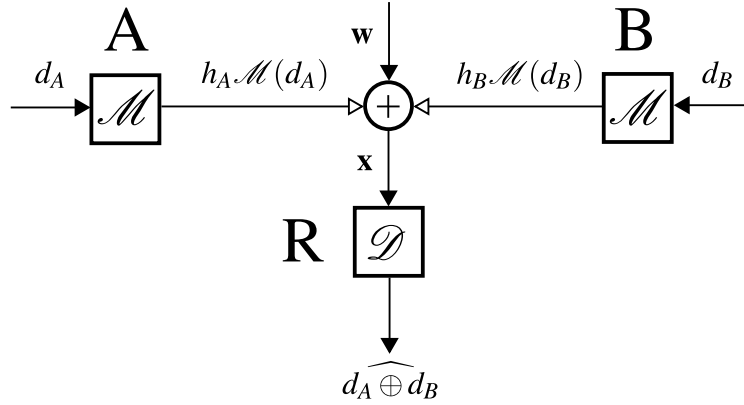


Figure 5.1: Model of the WNC MA stage.

## 5.2 System Model

### 5.2.1 Constellation Space Model and Used Notation

Let both terminals  $A$  and  $B$  in a 2-WRC use the same modulation alphabet  $\mathcal{A}_A = \mathcal{A}_B = \mathcal{A}$  with cardinality  $|\mathcal{A}| = M$  to be strictly a power of two. We suppose that the alphabet is formed by complex arbitrary-dimensional baseband signals in the constellation space  $\mathcal{A} = \{\mathbf{s}_T^{(d_T)}\}_{d_T=0}^{M-1} \subseteq \mathbb{C}^{N_s}$ , where symbol  $d_T \in \mathbb{Z}_M = \{0, 1, \dots, M-1\}$  denotes a data symbol transmitted by terminal  $T \in \{A, B\}$  and  $N_s$  denotes the signal space dimensionality. Linear modulations (e.g. PSK, QAM) have a single complex dimension, i.e.  $N_s = 1$  and their constellation vectors are complex scalars  $s_T \in \mathbb{C}$ . Later in this chapter, we consider non-linear frequency modulations FSK and full-response CPM which have multi-dimensional waveform and its dimensionality is  $N_s = M$ . The constellation space vectors are consequently  $\mathbf{s}_T \in \mathbb{C}^{N_s}$ . Without loss of generality, we assume a memoryless constellation mapper  $\mathcal{M}$  such that it directly corresponds to the signal indexation,  $\mathbf{s}_T^{(d_T)} = \mathcal{M}(d_T)$ . When we do not need to distinguish whether a signal correspond to terminal  $A$  or  $B$ , we omit a lower index  $T \in \{A, B\}$ . We can do this because  $\mathcal{A}_A = \mathcal{A}_B = \mathcal{A}$ .

### 5.2.2 Model Assumptions

We assume a time-synchronized scenario with full CSIR which is obtained e.g. by preceding tracking of pilot signals. The synchronization issues are beyond the scope of this chapter and the interested reader may see e.g. [71], [72] for further details. We restrict ourselves that adaptive techniques are not available either due to e.g. missing feedback channel, increased system complexity, or infeasible channel dynamics. We consider per-symbol relaying (avoiding delay induced at the relay) and no channel coding which, however, can be additionally concatenated to this model [51].

### 5.2.3 WNC Strategy

The WNC strategy in a 2-WRC consists of two stages. At the first MA stage, both terminals  $A$  and  $B$  transmit simultaneously to the relay in the interfering manner, see Fig 5.1. The received composite (interfering) signal is

$$\mathbf{x} = h_A \mathbf{s}_A + h_B \mathbf{s}_B + \mathbf{w}, \quad (5.1)$$

where  $\mathbf{w}$  is a complex AWGN with variance  $2N_0$  per complex dimension, and the channel parameters  $h_A$  and  $h_B$  are frequency-flat complex Gaussian random variables with unit variance and Rayleigh/Rician distributed envelope. The Rician factor  $K$  is defined as a power ratio between stationary and scattered components. We assume that the channel parameters  $h_A, h_B$  are known to  $R$ . Subsequently, the relay decodes a network coding function of data symbols  $d_{AB} = \mathcal{N}(d_A, d_B)$ . Operation  $\mathcal{N}$  is an invertible

Table 5.1: Number of minimal-cardinality network coding functions in the standard notation

$M$	2	4	8
Number of distinct <b>NC</b> Latin squares	1	24	$\sim 10^{16}$

operation which incorporates data from multiple sources via a principle of exclusivity, see Sec. 5.2.4 for more details. We assume a minimal-cardinality operation, i.e. the cardinality of  $d_{AB}$  alphabet is  $M_{AB} = M$  [73]. We suppose an approximated *nearest neighbour* two-step decoding [45]: an estimate of network coded data symbol  $d_{AB}$  is obtained by the joint maximum likelihood decoding

$$[\hat{d}_A, \hat{d}_B] = \arg \min_{[d_A, d_B]} \|\mathbf{x} - h_A \mathbf{s}_A^{(d_A)} - h_B \mathbf{s}_B^{(d_B)}\|^2 \quad (5.2)$$

followed by the network coding function  $\hat{d}_{AB} = \mathcal{N}(\hat{d}_A, \hat{d}_B)$ . At the BC stage, the relay broadcasts network coded symbol  $d_{AB}$  which is sufficient for successful decoding. Particularly, terminal A obtains desired data symbol  $d_B$  with knowledge of  $d_{AB}$  and its own data  $d_A$  as  $d_B = \mathcal{N}^{-1}(d_{AB}, d_A)$ , where  $\mathcal{N}^{-1}$  denotes an inverse function to  $\mathcal{N}$ . In this chapter, we entirely focus on the MA stage which dominates the error performance rather than BC stage due to the additional multiple access interference [45].

## 5.2.4 Network Coding Operation

We are aware that the term *network coding* may evoke a link-layer processing using finite field algebra. However, WNC strategy requires only the existence of an inversion providing one of the source data symbols. Moreover, the network coding function is regarded as an operation not necessarily commutative. This algebraic structure (when minimal-cardinality is assumed) is defined as a *Latin square*. We denote the Latin square by a matrix **NC**, where  $d_{AB} = \mathcal{N}(d_A, d_B) = [\mathbf{NC}]_{d_A, d_B}$ . For example, matrices

$$\mathbf{NC}_{\text{XOR}} = \begin{bmatrix} 0 & 1 \\ 1 & 0 \end{bmatrix}, \quad \mathbf{NC}_{\text{MOD}} = \begin{bmatrix} 0 & 1 & 2 & 3 \\ 1 & 2 & 3 & 0 \\ 2 & 3 & 0 & 1 \\ 3 & 0 & 1 & 2 \end{bmatrix}, \quad \mathbf{NC}_{\text{XOR}} = \begin{bmatrix} 0 & 1 & 2 & 3 \\ 1 & 0 & 3 & 2 \\ 2 & 3 & 0 & 1 \\ 3 & 2 & 1 & 0 \end{bmatrix}, \quad (5.3)$$

define binary XOR, quaternary modulo-sum and quaternary bit-wise XOR operation, respectively. We use an abbreviation 'XOR' to denote the bit-wise XOR network coding function. We assume **NC** matrices to be in the standard form (i.e. the first row is in increasing order starting from 0). We restrict ourselves on the minimal-cardinality **NC** (i.e.  $d_{AB} \in \mathbb{Z}_M$ ) in order to minimise the redundancy at the BC stage. It is interesting that the number of all distinct Latin squares grows very fast with the alphabet size [74] as depicted in Tab. 5.1. This fact forbids a brute-force method in a network coding function optimisation for large cardinalities.

## 5.2.5 Parametric Superimposed Constellation

Since the relay knows CSIR, we will conveniently introduce the model of superimposed constellation which uses instead of  $h_A, h_B$  only one complex parameter  $\alpha$  always  $|\alpha| \leq 1$ . The useful received signal (5.1) can be normalize by  $h_A$

$$\mathbf{x}' = \mathbf{x}/h_A = \mathbf{s}_A + \alpha \mathbf{s}_B + \mathbf{w}', \quad (5.4)$$

where  $\alpha = h_B/h_A \in \mathbb{C}$  and  $E[\|\mathbf{w}'\|^2] = 2N_0N_s/|h_A|^2$  or by  $h_B$

$$\mathbf{x}'' = \mathbf{x}/h_B = 1/\alpha \mathbf{s}_A + \mathbf{s}_B + \mathbf{w}'', \quad (5.5)$$

with  $E[\|\mathbf{w}''\|^2] = 2N_0N_s/|h_B|^2$  where operator  $E[\star]$  denotes a statistical expectation. By the adaptive switching between (5.4) and (5.5), we ensure that  $|\alpha|$  or  $|1/\alpha|$  is always lower or equal to 1. The decoding processing (5.2) remains the same for both cases, therefore the switching has only a theoretical meaning

that we need to focus on the system performance only for  $|\alpha| \leq 1$ . A useful composite signal is defined as  $\mathbf{u}^{(d_A, d_B)}(\alpha) = \mathbf{s}_A^{(d_A)} + \alpha \mathbf{s}_B^{(d_B)}$  or  $\mathbf{u}^{(d_A, d_B)}(\alpha) = \alpha \mathbf{s}_A^{(d_A)} + \mathbf{s}_B^{(d_B)}$  according to  $|\alpha|$ . For both cases when  $\mathcal{A}_A = \mathcal{A}_B$ , the useful parametric signal at the relay is

$$\mathbf{u}^{(d_A, d_B)}(\alpha) = \mathbf{s}_A^{(d_A)} + \alpha \mathbf{s}_B^{(d_B)}, \quad |\alpha| \leq 1. \quad (5.6)$$

## 5.3 Minimal Distance as a Performance Measure and the Impact of Singular Channel Parameters

### 5.3.1 Minimal Distance

Let us focus on the error performance at the MA stage. Defining a symbol error  $\hat{d}_{AB} \neq d_{AB}$ , the symbol error probability is well approximated by the sum of weighted pairwise error probabilities. The pairwise error probability is a function of the distance between signals corresponding to  $d_{AB} \neq d'_{AB}$  and the pairwise error probability dominating the performance for high SNR is a function of the minimal distance. In our case, the minimal distance is a minimal distance between superimposed signals  $\mathbf{u}^{(d_A, d_B)}$  and  $\mathbf{u}^{(d'_A, d'_B)}$  with different network coded symbols

$$\Delta_{\min}^2(\alpha) = \min_{\mathcal{N}(d_A, d_B) \neq \mathcal{N}(d'_A, d'_B)} \left\| \mathbf{u}^{(d_A, d_B)}(\alpha) - \mathbf{u}^{(d'_A, d'_B)}(\alpha) \right\|^2 \quad (5.7)$$

and we call it a *minimal distance of the network coding decoding*, when it is clear we omit the attribute 'of network coding decoding'.

Note, that the minimal distance is given not only by the modulation alphabet, but also by  $\mathcal{N}$  operation. In general, the minimal distance is parametrized by  $\alpha$  and so is the error performance.

*Remark 1.* Facing the fact, that the superimposed constellation is randomly parametrized, we start investigation with the simplification that the error performance is given solely by the minimal distance. We are aware that this is a rough approximation, since the minimal distance is a relevant performance metric only asymptotically (as  $\text{SNR} \rightarrow \infty$ ) and the error curves are linearly proportional also to the number of signal pairs having the minimal distance  $N_{\min}$ .

### 5.3.2 Singular Channel Parameters

The WNC-MA stage with CSIR has the minimal distance as well as the asymptotic performance parametrised by the channel parameter ratio. For some modulation alphabets and network coding function, there exist such non-zero parameters (called singular) which yield even 0 minimal distance. This problem is well demonstrated e.g. by QPSK and complex-orthonormal QFSK (modulation index  $\kappa = 1$ ) modulation with XOR function (5.3). The minimal distance of QPSK is depicted in Fig. 5.2 indicating several singular parameters e.g.  $\alpha = j$ . On the contrary, the numerical evaluation of QFSK with  $\kappa = 1$  (Fig. 5.3) seems to have the minimal distance parabolically dependent on  $|\alpha|$  as

$$\Delta_{\min}^2(\alpha) = 2|\alpha|^2. \quad (5.8)$$

It has no singular parameters and therefore it is robust to the parametrization. Zero distance for  $\alpha = 0$  is expected because it means that one of the channel is relatively zero. This part of the work focuses on the design of alphabets and  $\mathcal{N}$  like this. Figure 5.4 with QFSK  $\kappa = 1$  and modulo-sum NC (5.3) demonstrates that not only a modulation alphabet, but also a network coding function influence the parameter robustness.

**Definition 3** (Singular parameters). A singular parameter is such a non-zero parameter  $\alpha$  that forces two superimposed signals corresponding to different  $d_{AB}$  symbols to the same point (equivalently, it implies zero minimal distance). It means, for some  $\alpha \neq 0$ , there exists  $\mathcal{N}(d_A, d_B) \neq \mathcal{N}(d'_A, d'_B)$  that

$$\left\| \mathbf{u}^{(d_A, d_B)}(\alpha) - \mathbf{u}^{(d'_A, d'_B)}(\alpha) \right\|^2 = 0. \quad (5.9)$$

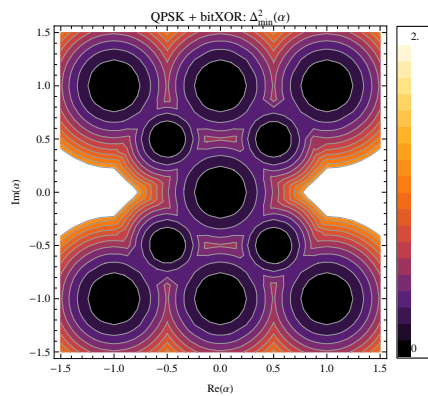


Figure 5.2: Parametric minimal distance of QPSK and bit-wise XOR. For some non-zero singular parameters (e.g.  $\alpha = j$ ), we expect poor performance.

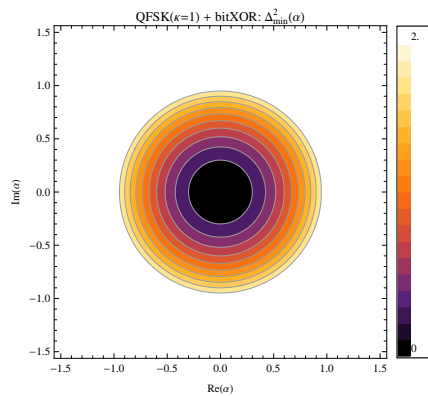


Figure 5.3: Parametric minimal distance of QFSK with  $\kappa = 1$  and bit-wise XOR. The scheme is robust to the relative-fading and moreover it is UMP

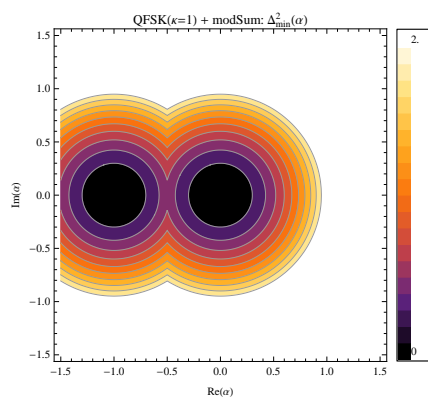


Figure 5.4: Parametric minimal distance of QFSK with  $\kappa = 1$  and the modulo-sum network coding function. The scheme is not UMP due to the zero minimal distance for singular parameter  $\alpha = -1$ .

### 5.3.3 Network Coding Function Not Implying Singularities

We will show that  $\mathcal{N}$  must fulfil certain conditions not to imply singular parameters, regardless of the assumed modulation alphabet. These conditions reduce the number of  $\mathcal{N}$ , see Tab. 5.1, involved in the search for the schemes robust to the relative-fading.

**Theorem 4.** *Latin square NC with different symbols on the main diagonal implies singularity  $\alpha = -1$ . A Latin square NC which is not symmetric over the main diagonal has singularity  $\alpha = 1$  regardless of the used modulation.*

*Proof.* Let two superimposed signals  $\mathbf{u}^{(d_A, d_B)}, \mathbf{u}^{(d'_A, d'_B)}$ ,  $d_A \neq d'_A$  correspond to  $d_A = d_B, d'_A = d'_B$  (i.e. the NC Latin square main diagonal) and their  $d_{AB}$  symbols are different  $\mathcal{N}(d_A, d_B) \neq \mathcal{N}(d'_A, d'_B)$ . Equation (5.9) simplifies to

$$\left\| \mathbf{s}^{(d_A)} - \mathbf{s}^{(d'_A)} + \alpha \left( \mathbf{s}^{(d_A)} - \mathbf{s}^{(d'_A)} \right) \right\|^2 = |1 + \alpha|^2 \left\| \mathbf{s}^{(d_A)} - \mathbf{s}^{(d'_A)} \right\|^2 \quad (5.10)$$

which yields singularity  $\alpha = -1$ . Similarly, let us assume a non-symmetric NC Latin square. Assume  $\mathbf{u}^{(d_A, d_B)}, \mathbf{u}^{(d'_B, d'_A)}$  with  $\mathcal{N}(d_A, d_B) \neq \mathcal{N}(d'_B, d'_A)$ , equation (5.9) expands to

$$\left\| \mathbf{s}^{(d_A)} - \mathbf{s}^{(d'_A)} + \alpha \left( \mathbf{s}^{(d'_A)} - \mathbf{s}^{(d_A)} \right) \right\|^2 = |1 - \alpha|^2 \left\| \mathbf{s}^{(d_A)} - \mathbf{s}^{(d'_A)} \right\|^2 \quad (5.11)$$

and the singularity channel parameter is  $\alpha = 1$ . We conclude that the NC Latin square should be symmetric with the same symbols on its main diagonal in order to avoid singularities  $\{1, -1\}$ .  $\square$

*Remark 2.* Bit-wise XOR fulfils the above conditions and it is the only solution for the binary and quaternary alphabet cardinality (unfortunately it is not the only choice for e.g. octal alphabet cardinality) [74]. Once we fix NC Latin square (at least for the binary and quaternary case), the last thing that determines the parameter robustness is a modulation alphabet. Therefore, from now on, we assume

$$\mathcal{N}(d_A, d_B) = d_A \oplus d_B \quad (5.12)$$

to be a bit-wise XOR function and we relate the parametrization robustness to particular modulation alphabets.

### 5.3.4 Non-Binary Linear Modulations are never UMP

**Lemma 2.** *Non-binary linear modulations unavoidably possess singular parameters.*

*Proof.* Linear modulations like QAM, PSK have dimensionality  $N_s = 1$ . Let us consider superimposed signals  $u^{(d_A, d_B)}, u^{(d'_A, d'_B)}$  with  $\mathcal{N}(d_A, d_B) \neq \mathcal{N}(d'_A, d'_B)$  and symbols  $d_A \neq d'_A, d_B \neq d'_B$  (i.e. not being in the same row and column of NC Latin square). There exists such a channel parameter ratio that

$$\begin{aligned} u^{(d_A, d_B)}(\alpha') &= u^{(d'_A, d'_B)}(\alpha'), \\ s^{(d_A)} + \alpha' s^{(d_B)} &= s^{(d'_A)} + \alpha' s^{(d'_B)}, \end{aligned} \quad (5.13)$$

this parameter equals to  $\alpha' = (s^{(d'_A)} - s^{(d_A)}) / (s^{(d_B)} - s^{(d'_B)})$ . Binary alphabets are excluded from this consideration because its different superimposed signals always lie in the same row or column of the NC Latin square.

Since we assume channel model switching, it would be a singular parameter if it was  $|\alpha'| \leq 1$ , but as we have discussed in the previous section, the NC Latin square should be symmetric and so, also for symmetric signals  $u^{(d_B, d_A)}, u^{(d'_B, d'_A)}$  there exist a parameter  $\alpha''$  such

$$\begin{aligned} u^{(d_B, d_A)}(\alpha'') &= u^{(d'_B, d'_A)}(\alpha''), \\ s^{(d_B)} + \alpha'' s^{(d_A)} &= s^{(d'_B)} + \alpha'' s^{(d'_A)}, \end{aligned} \quad (5.14)$$

$\alpha'' = 1/\alpha'$ . Hence, the singular parameter equals to  $\alpha'$  or  $\alpha''$ , whether its absolute value is lower or equal to one.  $\square$



## 5.4 Uniformly Most Powerful Alphabet

We define a class of alphabets with the minimal distance of the form like in (5.8), avoiding all singular parameters and being robust to the channel parametrization. We will show that the form (5.8) corresponds to the alphabets reaching the minimal distance upper-bound for all parameter values.

### 5.4.1 Minimal Distance Upper-bound

**Lemma 3.** *The minimal distance of any alphabet is upper-bounded by*

$$\Delta_{\min}^2(\alpha) \leq |\alpha|^2 \delta_{\min}^2, \quad (5.15)$$

where  $\delta_{\min}^2$  is the minimal distance of a primary modulation alphabet  $\mathcal{A}$ ,

$$\delta_{\min}^2 = \min_{d_A \neq d'_A} \left\| \mathbf{s}^{(d_A)} - \mathbf{s}^{(d'_A)} \right\|^2 \quad (5.16)$$

and  $d_A, d'_A \in \mathbb{Z}_M$ .

*Proof.* We obtain the upper-bound by evaluating minimum operator along the superimposed signals corresponding to a single row of **NC** Latin square (i.e. for  $d_A = d'_A$ ),

$$\Delta_{\min}^2(\alpha) \leq \min_{d_B \neq d'_B} \left\| \mathbf{u}^{(d_A, d_B)} - \mathbf{u}^{(d'_A, d'_B)} \right\|^2 = \min_{d_B \neq d'_B} |\alpha|^2 \left\| \mathbf{s}^{(d_B)} - \mathbf{s}^{(d'_B)} \right\|^2. \quad (5.17)$$

Since we do not evaluate the minimum operator along the all possible superimposed signal differences, we must use an inequality. The minimum evaluation along a single column of **NC** Latin square ( $c_B = c'_B$  in (5.7)) yields

$$\min_{d_A \neq d'_A} \left\| \mathbf{u}^{(d_A, d_B)} - \mathbf{u}^{(d'_A, d'_B)} \right\|^2 = \min_{d_A \neq d'_A} \left\| \mathbf{s}^{(d_A)} - \mathbf{s}^{(d'_A)} \right\|^2 = \delta_{\min}^2. \quad (5.18)$$

As we are considering  $|\alpha| \leq 1$ , we conclude that the bound (5.15) is more tight than (5.18).  $\square$

### 5.4.2 UMP Alphabet Definition

**Definition 4.** Uniformly most powerful (UMP) alphabets have the minimal distance reaching the upper-bound (5.15) for all parameter values

$$\Delta_{\min}^2(\alpha) = |\alpha|^2 \delta_{\min}^2, \forall \alpha \in \mathbb{C}, |\alpha| \leq 1, \quad (5.19)$$

where  $\delta_{\min}^2$  is defined in (5.16) and  $d_A, d'_A \in \mathbb{Z}_M$ . We restrict on  $|\alpha| \leq 1$  due to the adaptive switching strategy described in Sec. 5.2.5.

### 5.4.3 UMP Alphabet Properties

*Remark 3.* It is important to stress that UMP alphabets do not have any singular  $\alpha_{cat}$  and according to Lemma 2 and Remark 2, non-binary linear modulations are never UMP and all UMP alphabets are using XOR function.

*Remark 4.* Extended-cardinality  $\mathcal{N}$  as well as minimal-cardinality  $\mathcal{N}$  have different symbols in each row of **NC** Latin square (Sudoku principle) and thus the bound holds for extended-cardinality  $\mathcal{N}$  as well. Particularly, for the systems using adaptive network coding [54]. In the other words, the performance of the adaptive WNC system cannot be better than of UMP alphabet if both are using alphabets with the same  $\delta_{\min}^2$ .

*Remark 5.* Two properties influence a good WNC performance, a) being UMP and b) having a large minimal distance of individual constellations  $\delta_{\min}^2$ . These properties can be interpreted as follows. The property b) is proportional to robustness to AWGN. Condition a) (considering the upper-bound (5.15)) presents the best possible type of inevitable parametrization by  $\alpha$ .

*Remark 6* (A parallel with the UMP statistical tests). If we match error performance with the minimal distance for the sake of simplicity (Remark 1), then among all alphabets with identical  $\delta_{\min}^2$ , the UMP alphabets have the best performance  $\forall \alpha \in \mathbb{C}$ . Based on this observation, we use the term UMP originally used in statistical detection theory due to the common principle. Composite hypothesis tests have parametric PDFs and the UMP detector, if exists, yields the best performance for all parameter values [75]. It resembles exactly our case, the likelihood function of joint  $[d_A, d_B]$  detection is also parametrized (by  $h_A, h_B$ ) and assuming CSIR the optimal detector of UMP alphabets has the best performance for all parameter values.

#### 5.4.4 Binary Modulation is UMP

Evaluating formula (5.7) with respect to the binary NC Latin square (5.3), we straightforwardly obtain

$$\Delta_{\min}^2(\alpha) = |\alpha|^2 \delta_{\min}^2, \quad (5.20)$$

where  $\delta_{\min}^2 = \left\| \mathbf{s}^{(0)} - \mathbf{s}^{(1)} \right\|^2$ . It means that binary alphabets are always UMP regardless of the particular alphabet. Considering Remark 5, the optimal binary UMP alphabet is BPSK having the maximal possible  $\delta_{\min}^2$ .

#### 5.4.5 Non-Binary Orthonormal Modulation is UMP

We have seen in Fig. 5.3 that complex-orthonormal QFSK is UMP. This holds for a general alphabet-cardinality which describes the following lemma.

**Lemma 4.** *Complex-orthonormal<sup>1</sup> modulation is UMP.*

*Remark 7.* Before we prove the Lemma 4, it is convenient to introduce a simplified UMP condition easier to verify. The UMP condition (5.19) implies that the minimum distance is formed by the superimposed signal differences corresponding to the rows of NC Latin square, see e.g. the proof of Lemma 3. Therefore, if the norm of superimposed signal differences with indices not being in the same row of NC Latin square is always larger or equal than the bound,

$$\left\| \mathbf{u}^{(d_A, d_B)} - \mathbf{u}^{(d'_A, d'_B)} \right\|^2 \geq |\alpha|^2 \delta_{\min}^2, \quad (5.21)$$

for  $\forall d_A \neq d'_A, d_B \neq d'_B, \mathcal{N}(d_A, d_B) \neq \mathcal{N}(d'_A, d'_B)$  and  $\forall \alpha \in \mathbb{C}, |\alpha| \leq 1$ , then (5.19) is fulfilled. Let us expand the left side of (5.21) as

$$\left\| \mathbf{s}^{(d_A)} - \mathbf{s}^{(d'_A)} \right\|^2 + |\alpha|^2 \left\| \mathbf{s}^{(d_B)} - \mathbf{s}^{(d'_B)} \right\|^2 + 2\Re \left\{ \alpha^* \left\langle \mathbf{s}^{(d_A)} - \mathbf{s}^{(d'_A)}, \mathbf{s}^{(d_B)} - \mathbf{s}^{(d'_B)} \right\rangle \right\}, \quad (5.22)$$

where  $\langle \star, \star \rangle$  denotes an inner product. Since inequality (5.22) must hold for all  $\varphi = \arg \alpha$ , it must hold for the worst case  $\varphi_c$ , where the part with the inner product is minimal and (5.22) becomes

$$\left\| \mathbf{s}^{(d_A)} - \mathbf{s}^{(d'_A)} \right\|^2 + |\alpha|^2 \left\| \mathbf{s}^{(d_B)} - \mathbf{s}^{(d'_B)} \right\|^2 + 2|\alpha| \left| \left\langle \mathbf{s}^{(d_A)} - \mathbf{s}^{(d'_A)}, \mathbf{s}^{(d_B)} - \mathbf{s}^{(d'_B)} \right\rangle \right|. \quad (5.23)$$

This form of invariance condition is easier to verify due to the presence of only one real variable  $|\alpha|$ .

<sup>1</sup>For the sake of notation simplicity, we assume orthonormal modulations rather than orthogonal with constant symbol energy. The results here shown for orthonormal modulations are true also in orthogonal case with the constant symbol energy.

*Proof.* Orthonormal modulations have all distances (as well as the minimal one) for  $d_A \neq d'_A, d_B \neq d'_B$  equal to 2, then (5.23) simplifies to

$$2 + 2|\alpha|^2 - 2|\alpha| \left| \left\langle \mathbf{s}^{(d_A)} - \mathbf{s}^{(d'_A)}, \mathbf{s}^{(d_B)} - \mathbf{s}^{(d'_B)} \right\rangle \right| \geq 2|\alpha|^2 \quad (5.24)$$

which further adjusts to

$$1 \geq |\alpha| \left| \left\langle \mathbf{s}^{(d_A)} - \mathbf{s}^{(d'_A)}, \mathbf{s}^{(d_B)} - \mathbf{s}^{(d'_B)} \right\rangle \right|. \quad (5.25)$$

While (5.25) must hold for any  $|\alpha| \leq 1$  it requires to hold for critical  $|\alpha| = 1$ . Here, a critical parameter is such a parameter that if the condition is fulfilled for the critical one then it is fulfilled for all other parameter values. Condition (5.25) with critical  $|\alpha| = 1$  is then

$$1 \geq \left| \left\langle \mathbf{s}^{(d_A)} - \mathbf{s}^{(d'_A)}, \mathbf{s}^{(d_B)} - \mathbf{s}^{(d'_B)} \right\rangle \right| = \left| \left\langle \mathbf{s}^{(d_A)}, \mathbf{s}^{(d_B)} \right\rangle + \left\langle \mathbf{s}^{(d'_A)}, \mathbf{s}^{(d'_B)} \right\rangle - \left\langle \mathbf{s}^{(d_A)}, \mathbf{s}^{(d'_B)} \right\rangle - \left\langle \mathbf{s}^{(d'_A)}, \mathbf{s}^{(d_B)} \right\rangle \right|. \quad (5.26)$$

We prove the validity of (5.26) considering that any inner product of orthonormal modulation is either 0 or 1. Equation (5.26) is fulfilled except of the case where the r.h.s. equals to 2. It happens when  $\left\langle \mathbf{s}^{(d_A)}, \mathbf{s}^{(d_B)} \right\rangle = 1$  &  $\left\langle \mathbf{s}^{(d'_A)}, \mathbf{s}^{(d'_B)} \right\rangle = 1$  &  $\left\langle \mathbf{s}^{(d_A)}, \mathbf{s}^{(d'_B)} \right\rangle = 0$  &  $\left\langle \mathbf{s}^{(d'_A)}, \mathbf{s}^{(d_B)} \right\rangle = 0$  and when  $\left\langle \mathbf{s}^{(d_A)}, \mathbf{s}^{(d_B)} \right\rangle = 0$  &  $\left\langle \mathbf{s}^{(d'_A)}, \mathbf{s}^{(d'_B)} \right\rangle = 0$  &  $\left\langle \mathbf{s}^{(d_A)}, \mathbf{s}^{(d'_B)} \right\rangle = 1$  &  $\left\langle \mathbf{s}^{(d'_A)}, \mathbf{s}^{(d_B)} \right\rangle = 1$ . Let us consider the first case,  $\left\langle \mathbf{s}^{(d_A)}, \mathbf{s}^{(d_B)} \right\rangle = 1$  &  $\left\langle \mathbf{s}^{(d'_A)}, \mathbf{s}^{(d'_B)} \right\rangle = 1$  entails that  $\mathbf{s}^{(d_A)} = \mathbf{s}^{(d_B)}$  &  $\mathbf{s}^{(d'_A)} = \mathbf{s}^{(d'_B)}$  thus  $d_A = d_B$  &  $d'_A = d'_B$  which corresponds to the signals taken from the main diagonal of the NC Latin square. Thus, using the  $\mathcal{N}$  function suitable for UMP this case is excluded (Remark 2). Similarly, the second condition  $\left\langle \mathbf{s}^{(d_A)}, \mathbf{s}^{(d'_B)} \right\rangle = 1$  &  $\left\langle \mathbf{s}^{(d'_A)}, \mathbf{s}^{(d_B)} \right\rangle = 1$  implies  $d_A = d'_B$  &  $d_B = d'_A$  and is excluded by  $\mathcal{N}$  with symmetrical NC Latin square, again solved by the bit-wise XOR function.  $\square$

## 5.5 Design of UMP Frequency Modulations

In this section, we consider non-linear frequency modulations which naturally possess multi-dimensional alphabets required to avoid singular parameters (according to Lemma 2). We will conclude that the considered frequency modulations avoid singular parameters and are close to meet the UMP condition. We propose and use a simple scalar parametrization easy to adjust the UMP condition. Based on the error simulations, we will find that existence of singular parameters is much more detrimental than not being UMP. In the case of frequency modulations (without singular parameters), UMP alphabets are important since they form a performance benchmark (according to Remark 6).

### 5.5.1 Design of UMP Frequency Shift Keying Modulation

#### FSK Definition and Basic Properties

We assume the following unit-energy FSK signals of one symbol duration

$$s^{(d)}(t) = e^{j2\pi\kappa d \frac{t}{T_s}}, \quad (5.27)$$

where  $t \in [0, T_s)$  is a temporal variable,  $T_s$  is a symbol duration and  $d \in \mathbb{Z}_M$  denotes a data symbol. Its constellation space alphabet is  $N_s$ -dimensional  $\mathcal{A} = \{\mathbf{s}^{(d)}\}_{d=0}^{M-1} \subset \mathbb{C}^{N_s}$ , where  $N_s = M$ . Its signal correlation as well as minimal distance is determined by modulation index  $\kappa$  which also roughly corresponds to the occupied bandwidth [69]. It is well-known fact that FSK is complex-orthonormal for integer modulation index  $\kappa \in \mathbb{N}$  and with minimal  $\kappa = 1$  is often used in the non-coherent envelope detection. In coherent detection (with CSIR), it has the minimal distance  $\delta_{\min}^2 = 2$  for  $\kappa = 1/2$ . In this case, it is often denoted as minimum shift.

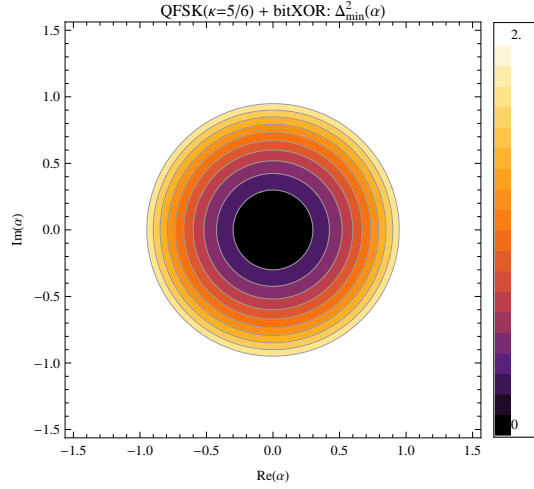


Figure 5.5: Parametric minimal distance of UMP- QFSK with optimized  $\kappa = 5/6$ .

### Design of UMP-QFSK Modulation by Modulation-Index Optimization

According to Lemma 4, FSK  $\kappa = 1$  is UMP. Yet, we try to answer the question whether a full complex-orthogonality is required to meet UMP and whether a less bandwidth UMP alphabet exists. To investigate the non-orthogonal case, we assume  $\kappa < 1$  which also means a modulation roughly with narrower bandwidth (see more detailed discussion of bandwidth requirements in Sec. 5.6.3).

Let us assume quaternary  $M = 4$  (binary is UMP regardless of alphabet, Sec. 5.4.4) FSK (QFSK) to consider this question. Let optimize modulation index  $\kappa$  to meet the UMP condition.

**Lemma 5.** *QFSK  $\kappa = 5/6$  is UMP, see Fig. 5.5. The same approach may be used for any alphabet cardinality – the results for octal UMP-FSK require  $\kappa = 13/14$  which leads to a conjecture that  $\kappa(M) = 2^{M-3}/2^{M-2}$  is sufficient.*

*Proof.* We have seen in Sec. 5.4.5 that the condition implying UMP property (5.23) is

$$\left\| \mathbf{s}^{(d_A)} - \mathbf{s}^{(d'_A)} \right\|^2 + |\alpha|^2 \left\| \mathbf{s}^{(d_B)} - \mathbf{s}^{(d'_B)} \right\|^2 - 2|\alpha| \left| \left\langle \mathbf{s}^{(d_A)} - \mathbf{s}^{(d'_A)}, \mathbf{s}^{(d_B)} - \mathbf{s}^{(d'_B)} \right\rangle \right| \geq |\alpha|^2 \delta_{\min}^2, \quad (5.28)$$

which must hold for  $d_A \neq d'_A, d_B \neq d'_B, \mathcal{N}(d_A, d_B) \neq \mathcal{N}(d'_A, d'_B)$  and  $\forall \alpha \in \mathbb{C}, |\alpha| \leq 1$ . The following steps further adjust (5.28) to a suitable 2nd order polynomial form

$$|\alpha|^2 \left( \left\| \mathbf{s}^{(d_B)} - \mathbf{s}^{(d'_B)} \right\|^2 - \delta_{\min}^2 \right) - 2|\alpha| \left| \left\langle \mathbf{s}^{(d_A)} - \mathbf{s}^{(d'_A)}, \mathbf{s}^{(d_B)} - \mathbf{s}^{(d'_B)} \right\rangle \right| + \left\| \mathbf{s}^{(d_A)} - \mathbf{s}^{(d'_A)} \right\|^2 \geq 0, \quad (5.29)$$

$$|\alpha|^2 - 2|\alpha| \frac{\left| \left\langle \mathbf{s}^{(d_A)} - \mathbf{s}^{(d'_A)}, \mathbf{s}^{(d_B)} - \mathbf{s}^{(d'_B)} \right\rangle \right|}{\left\| \mathbf{s}^{(d_B)} - \mathbf{s}^{(d'_B)} \right\|^2 - \delta_{\min}^2} + \frac{\left\| \mathbf{s}^{(d_A)} - \mathbf{s}^{(d'_A)} \right\|^2}{\left\| \mathbf{s}^{(d_B)} - \mathbf{s}^{(d'_B)} \right\|^2 - \delta_{\min}^2} \geq 0, \quad (5.30)$$

$$(|\alpha| - b)^2 + c \geq 0, \quad (5.31)$$

where auxiliary constants

$$b = \frac{\left| \left\langle \mathbf{s}^{(d_A)} - \mathbf{s}^{(d'_A)}, \mathbf{s}^{(d_B)} - \mathbf{s}^{(d'_B)} \right\rangle \right|}{\left\| \mathbf{s}^{(d_B)} - \mathbf{s}^{(d'_B)} \right\|^2 - \delta_{\min}^2}, \quad b \geq 0 \quad (5.32)$$

and

$$c = -b^2 + \frac{\left\| \mathbf{s}^{(d_A)} - \mathbf{s}^{(d'_A)} \right\|^2}{\left\| \mathbf{s}^{(d_B)} - \mathbf{s}^{(d'_B)} \right\|^2 - \delta_{\min}^2} \quad (5.33)$$

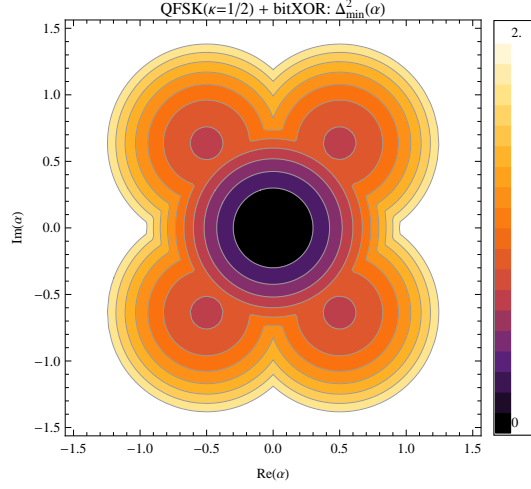


Figure 5.6: QFSK  $\kappa = 1/2$  demonstrates that the real-orthogonality does not suffice to meet UMP property. However, its minimal distance is not so poor as in case of QPSK and no singularities are present.

are not functions of  $|\alpha|$ . Thus, the condition (5.28) has a critical  $|\alpha|$  which equals to either  $b$  if  $b \leq 1$  or to limiting value 1 if  $b \geq 1$ . In Fig. 5.7, we plot the constant  $b$  for all indices  $d_A \neq d'_A, d_B \neq d'_B, \mathcal{N}(d_A, d_B) \neq \mathcal{N}(d'_A, d'_B)$  for QFSK and bit-wise XOR function. We conclude that constant  $b$  is always greater than 1 for roughly  $\kappa \gtrsim 0.3$ . For practical purposes, we restrict on  $\kappa \geq 1/2$  because than minimal distance  $\delta_{\min}^2$  is reasonably high. The restriction implies that constant  $b \geq 1$  and so the critical  $|\alpha| = 1$ . The l.h.s of (5.28) for critical  $|\alpha| = 1$  are depicted in Fig. 5.8 by the thin light blue curves. In the same figure, we chart their minimum (thick blue)  $\Delta_{\min}^2$  and minimal distance  $\delta_{\min}^2$  (thick green). The lowest modulation index leading to UMP-QFSK is  $\kappa = 5/6$ .  $\square$

## 5.5.2 Bi-Orthonormal Modulation is UMP

According to the results from the preceding section, we see that the UMP property does not require an accurate complex orthonormal alphabet. We have a conjecture that any bi-orthonormal modulation is UMP. The Appendix proves the following lemma.

**Lemma 6.** *Bi-orthonormal modulation is always UMP.*

*Remark 8.* Interestingly, the symmetrical NC Latin square with the same main diagonal is not sufficient in this case and an extra kind of symmetry, which obeys XOR as well, is required.

## 5.5.3 Design of UMP Continuous Phase Modulation

### CPM Basic Properties

CPM is a constant envelope modulation (suitable e.g. for satellite communication) with more compact spectrum in comparison to the traditional linear modulations with constant envelope (i.e. using the rectangular (REC) modulation pulse). CPM has a multidimensional alphabet and better spectral properties than FSK (no Dirac pulses in the spectrum and faster asymptotic spectrum attenuation due to the continuous phase). The bandwidth requirements of the considered schemes are investigated in Sec. 5.6.3. CPM includes memory [76] and its modulator consists of the discrete part including memory and the non-linear memoryless part [77]. Denominator of CPM modulation index  $\kappa$  is proportional to the number of modulator states described by its trellis and the optimal decoder may use the popular Viterbi decoding algorithm. CPM possess several degrees of freedom, for simplicity, we restrict on the full-response variant (i.e. the frequency pulse is of the one symbol length) and the minimum shift  $\kappa = 1/2$  case for which constellation space alphabet is  $N_s = M$  dimensional.

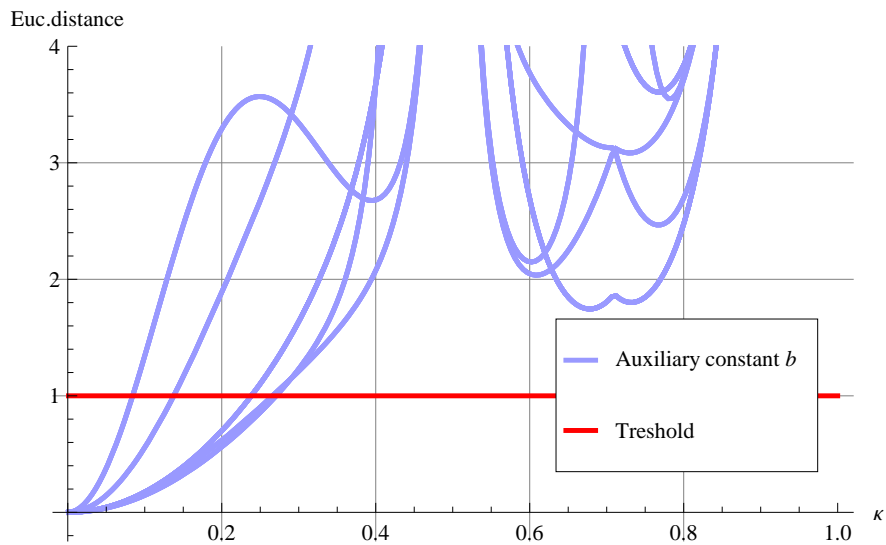


Figure 5.7: Auxiliary constant  $b$  (5.32) as a function of modulation index  $\kappa$  for QFSK. Note that  $b$  is always greater than one for the schemes of interest where  $\kappa \geq 1/2$ .

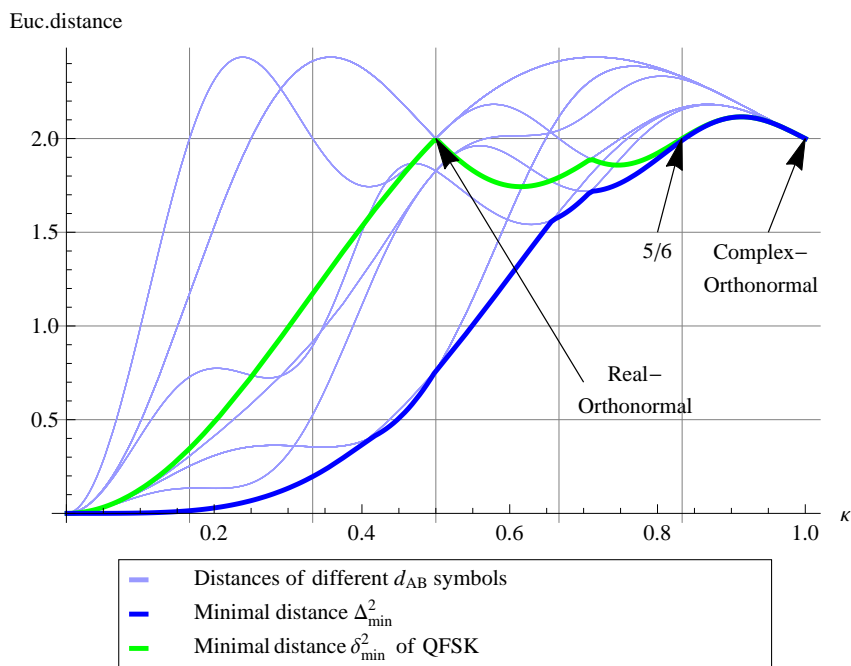


Figure 5.8: Distances of the superimposed symbols corresponding to different  $d_{AB}$  symbols for QFSK. The minimal value of modulation index fulfilling the UMP condition (i.e. the green thick line meets the blue thick line) is  $\kappa = 5/6$ .

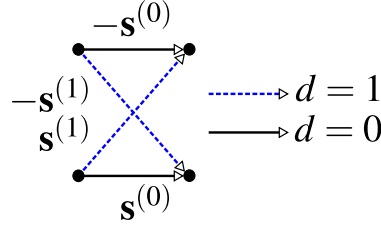


Figure 5.9: Binary full-response  $\kappa = 1/2$  CPM trellis. Note, if signal space vectors  $\mathbf{s}^{(0)}$  and  $\mathbf{s}^{(1)}$  are orthonormal, then the resulting alphabet is bi-orthonormal.

### Design of Full-Response $\kappa = 1/2$ UMP-CPM by Pulse Shape Optimization

In the same way we have excluded channel coding from a design of UMP alphabet, we do not need to consider modulation memory of CPM. In our case, only the non-linear memoryless part is determining. The assumed full-response  $\kappa = 1/2$  CPM has the modulation trellis with only two states. The non-linear memoryless alphabet consists of  $2M$  signals where the first half (starting from the first state) has the opposite sign than the other half (starting from the latter state), see the trellis of binary scheme in Fig 5.9.

Our design is based on Lemma 6, utilizing the above mentioned symmetries, we design a bi-orthonormal UMP modulation simply by keeping the signals starting from the first state orthonormal.

### CPM Signals Notation

Let us denote a positive-sign alphabet (signals starting from the zero state) as  $\mathcal{A}^+$  and negative-sign alphabet  $\mathcal{A}^- = -\mathcal{A}^+$ . The overall alphabet (non-linear memoryless part) is  $\mathcal{A} = \mathcal{A}^+ \cup \mathcal{A}^-$ . Assuming the unit energy signals, the full-response  $h = 1/2$  CPM has

$$\mathcal{A}^+ = \left\{ s^{(i)}(t) \right\}_{i=0}^{M-1} = \left\{ e^{j\pi\left(\frac{1}{2}(M-1)+d\beta(t)\right)} \right\}, \quad (5.34)$$

where data symbol  $d \in \{-(M-1), -(M-3), \dots, (M-1)\}$ ,  $t$  is normalized to the one symbol duration  $t \in [0, 1)$  and  $\beta(t)$  is a phase pulse.

### Proposed Pulse Parametrization

The remaining degree of freedom which we exploit to set the signal correlation is a phase pulse shape. We introduce a simple shaping form obtained as a linear parametrization of Raised Cosine (RC) pulse which we denote as a Scaled RC (SRC) pulse. The proposed parametric SRC phase pulse is

$$\beta(t, p) = \frac{1}{2} \left( t - p \frac{\sin 2\pi t}{2\pi} \right), \quad (5.35)$$

where  $p$  is a real parameter. The phase pulse correspond to REC pulse for  $p = 0$  and to RC pulse for  $p = 1$ , see Fig. 5.10. This parametrization has number of advantages, it does not influence the number of modulator states/signal alphabet cardinality and it has a known analytical formula for bandwidth [78].

### Design of Binary UMP-CPM

**Lemma 7.** Binary full-response CPM with  $\kappa = 1/2$  and SRC pulse (5.35) with  $p \simeq 2.35$  is UMP.

*Proof.* Let us consider a binary case, the positive-sign alphabet is

$$\mathcal{A}^+ = \left\{ s^{(0)}(t), s^{(1)}(t) \right\} = \left\{ e^{j\pi\left(\frac{1}{2}+\beta(p,t)\right)}, e^{j\pi\left(\frac{1}{2}-\beta(p,t)\right)} \right\}. \quad (5.36)$$

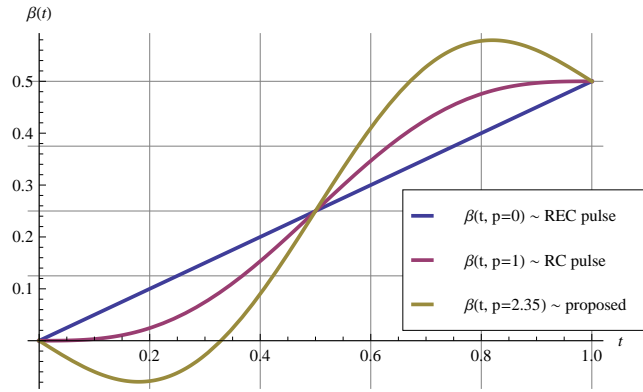


Figure 5.10: Proposed parametric SRC pulse linearly scale its cosine part.

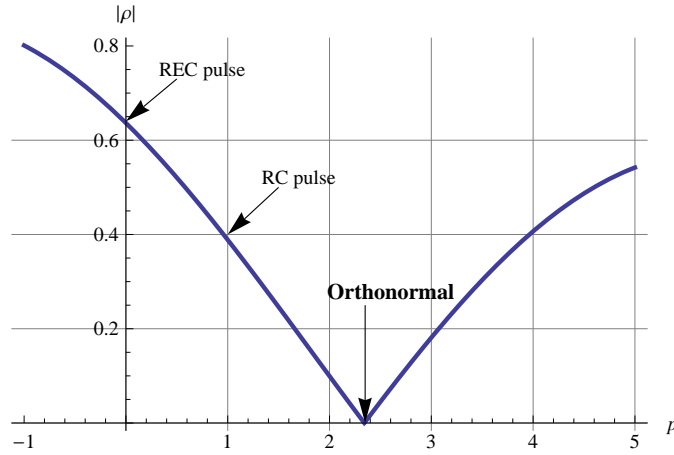


Figure 5.11: Absolute value of correlation coefficient between two signals of binary full-response CPM with  $\kappa = 1/2$  and parametric SRC pulse. The parameter value forming orthonormal alphabet is  $p \simeq 2.35$ .

The correlation coefficient  $\rho = \langle s^{(0)}(t), s^{(1)}(t) \rangle = \int_0^1 s^{(0)}(t) s^{(1)*}(t) dt$  has an analytic expression in the case of SRC pulse. The expression consists of generalized hyper-geometric functions with a zero real part, see  $|\rho|$  in Fig. 5.11. We conclude that  $p \simeq 2.35$  leads to the orthonormal signals.  $\square$

*Remark 9.* The proposed pulse parametrization has an extra advantage that the squared norm of the signal difference of binary alphabet is always 2 for any  $p$ . The reason is simply given by the zero real part of  $\rho$  for any  $p$ , as has been mentioned in the proof above, then  $\|s^{(0)}(t) - s^{(1)}(t)\|^2 = 2(1 - \Re\{\rho\}) = 2$ . Hence, we can adjust the among of correlation required for UMP condition without affecting overall minimal distance  $\delta_{\min}^2$ .

We evaluate the parametric minimal distance in Figs. 5.12, 5.13, 5.14 to confirm the UMP property of the proposed scheme. We conclude that the minimal distance of non-UMP schemes with REC and RC are close to be UMP. In the last section with numerical results, we see that the error performance of these schemes are practically identical. However, in the case of quaternary/higher order alphabet the differences are more significant.

### Design of Quaternary UMP-CPM

**Lemma 8.** *Quaternary full-response CPM with  $\kappa = 1/2$  and SRC pulse (5.35) with  $p \simeq -7$  or  $p \simeq 10.2$  is UMP.*



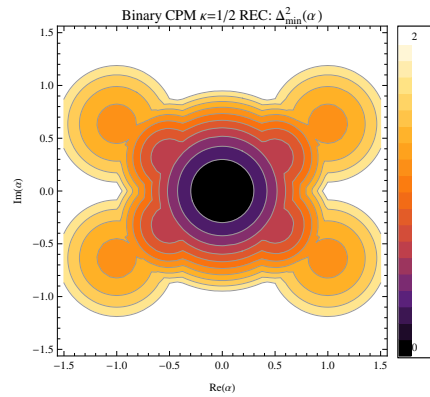


Figure 5.12: Parametric minimal distance of binary full-response CPM with  $\kappa = 1/2$  and REC pulse  $p = 0$ .

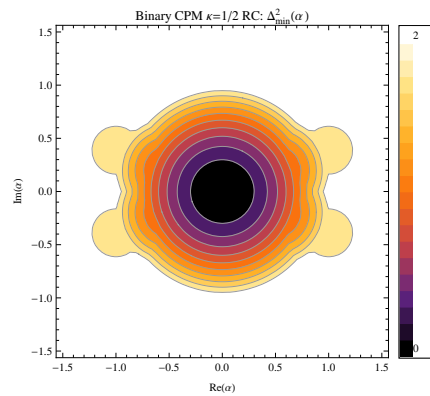


Figure 5.13: Parametric minimal distance of binary full-response CPM with  $\kappa = 1/2$  and RC pulse  $p = 1$ .

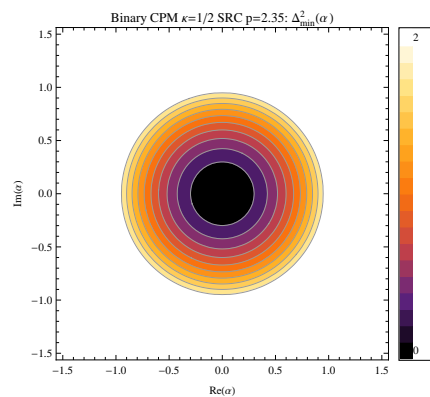


Figure 5.14: Parametric minimal distance of binary full-response CPM with  $\kappa = 1/2$  and UMP SRC pulse with  $p \simeq 2.35$ .

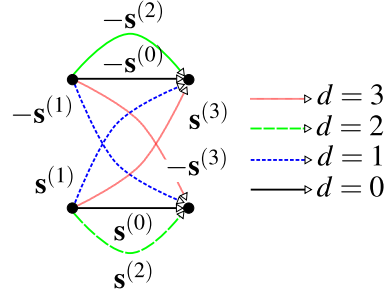


Figure 5.15: Trellis of quaternary full-response CPM with modulation index  $\kappa = 1/2$ . Again, orthonormality of  $\{s_i\}_{i=0}^3$  implies bi-orthonormality of the overall alphabet.

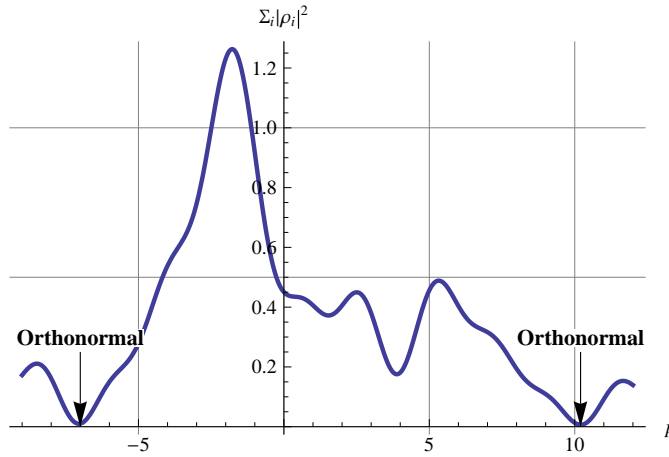


Figure 5.16: Sum of the squared absolute values of individual correlation coefficients of quaternary full-response CPM with  $\kappa = 1/2$  and SRC pulse. The parameter values forming orthonormal alphabet are  $p \in \{-7, 10.2\}$ .

*Proof.* The preceding derivation for binary alphabet can be generalized for any alphabet cardinality, for simplicity we focus on the quaternary case. Let us consider 4-ary full-response CPM  $\kappa = 1/2$  and SRC pulse, the modulation trellis has the same number of states, see Fig. 5.15. The positive sign alphabet is

$$\mathcal{A}^+ = \left\{ e^{j\pi\left(\frac{3}{2}t + d\beta(t,p)\right)} \right\}, \quad (5.37)$$

where  $d \in \{-3, -1, 1, 3\}$ . Our target is to make set  $\mathcal{A}^+$  orthonormal by variation of parameter  $p$ . There are 4 signals in the set, thus there are six different signal pairs that must be mutually orthonormal. Let us assume a sum of squared absolute values of individual correlation coefficients (of every signal pairs from  $\mathcal{A}^+$ )  $\sum_i |\rho_i|^2$  as an auxiliary indication function. This indication function is zero only for the orthogonal alphabet. In Fig. 5.16, we depict the indicating function against parameter  $p$  concluding that orthonormal set is obtained e.g. for  $p \in \{-7, 10.2\}$  which proves the lemma.  $\square$

To demonstrate the UMP property of the proposed scheme, we evaluate the parametric minimal distance with REC, RC and proposed SRC pulse, see Figs. 5.17, 5.18, 5.19.

Contrary to the binary case, the minimal distance of non-UMP schemes with REC and RC are far to be UMP. The scheme with RC pulse has even lower  $\delta_{\min}^2 = 1$  which is in correspondence with the following error simulations.

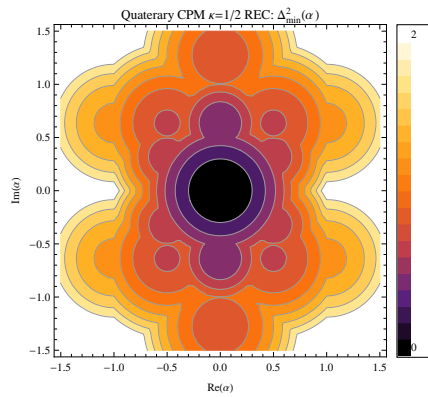


Figure 5.17: Parametric minimal distance of quaternary full-response CPM with  $\kappa = 1/2$  and REC pulse  $p = 0$ .

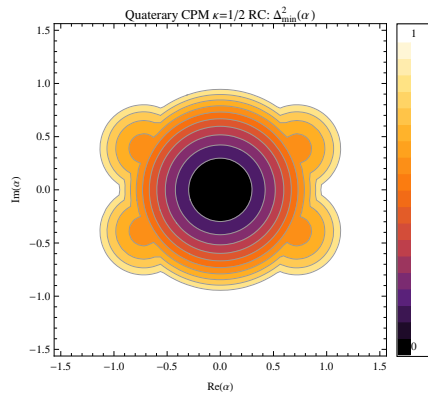


Figure 5.18: Parametric minimal distance of quaternary full-response CPM with  $\kappa = 1/2$  and RC pulse  $p = 1$ .

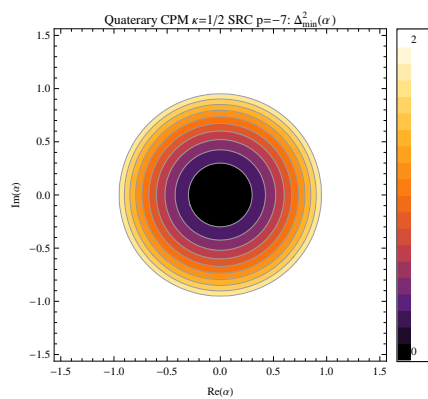


Figure 5.19: Parametric minimal distance of UMP quaternary full-response CPM with  $\kappa = 1/2$  and SRC pulse with  $p \simeq -7$ .

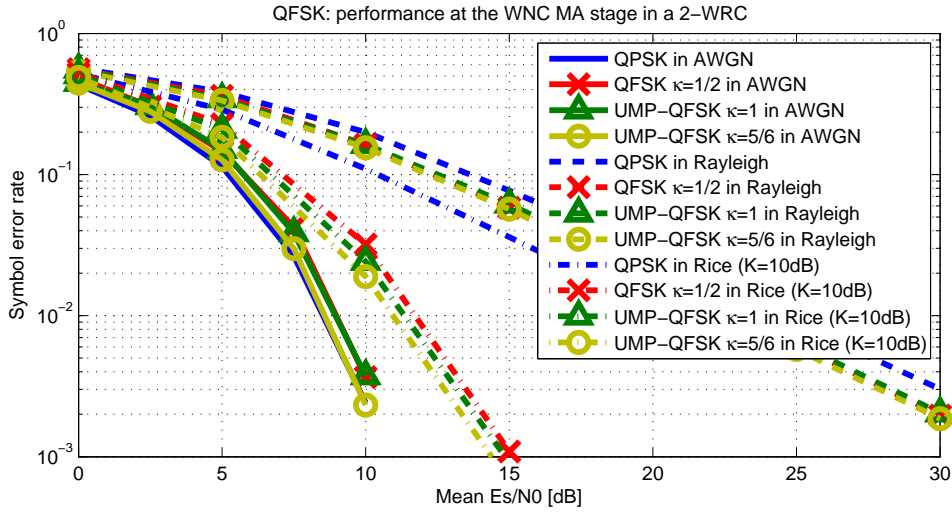


Figure 5.20: SER at the MA stage assuming uncoded detection with CSIR in AWGN, Rayleigh and Rice  $K = 10$ dB fading channel for memoryless modulations: QPSK, QFSK  $\kappa = 1/2$ , UMP-QFSK  $\kappa = 1$  and UMP-QFSK  $\kappa = 5/6$

## 5.6 Numerical Results

### 5.6.1 Error Performance of Memoryless Modulations

Let us numerically evaluate SER at the WNC MA stage for several considered alphabets. We assume a simple AWGN channel and a frequency-flat uncorrelated Rayleigh/Rice (with Rician factor  $K = 10$ dB) fading channel. As we have discussed in Sec. 5.2.2, we assume an uncoded system and perfect CSIR. Figure 5.20 depicts the following memoryless modulations using the bit-wise XOR function: non-UMP QPSK, QFSK  $\kappa = 1/2$ , UMP-QFSK  $\kappa = 1$  and the proposed UMP-QFSK  $\kappa = 5/6$ . All modulation alphabets have the same minimal distance of scalar modulation  $\delta_{\min}^2 = 2$ , therefore the performance in the AWGN channel is asymptotically the same. The advantage of UMP alphabets is more evident in the fading channels. Particularly, non-UMP QPSK has roughly  $\sim 2$  dB penalty in Rayleigh fading and even about  $\sim 10$  dB penalty in Rice  $K = 10$  dB over the UMP alphabets. It is interesting that the non-UMP QFSK  $\kappa = 1/2$  is also well robust to the channel parametrization. Therefore, we may expect that non-linear modulations avoiding all singular parameters are generally more robust to the channel parametrization than the linear one. We support the error simulations by related end-to-end throughput simulations including the BC stage. We evaluate the throughputs as a relative number of bits of correctly detected 256-bit long packets, see Fig. 5.21.

### 5.6.2 Error Performance of Full-response CPM

Here, SER at the MA stage of non-linear full-response CPM  $\kappa = 1/2$  with the optimized modulation pulses are shown. We have seen that the presence of discrete memory does not influence the UMP property, although it can not be ignored at the receiver side. We use a joint  $[\hat{d}_A, \hat{d}_B]$  decoding algorithm based on the vector Viterbi algorithm [55] describing the structure of receiving signals by a super-trellis with super-states. Each super-state is a vector of the states connecting together the actual state at node A with the state at node B. Then, the joint estimate of  $[\hat{d}_A, \hat{d}_B]$  is obtained by the sequence Viterbi algorithm over the super-trellis. Thereafter, the network coded data symbols are obtained as  $\hat{d}_{AB} = \hat{d}_A \oplus \hat{d}_B$ .

In Fig. 5.22, it is depicted SER of binary full-response CPM  $\kappa = 1/2$  with REC, RC and the proposed SRC pulse and also UMP-BPSK modulation as a reference. We describe binary full-response CPM  $\kappa = 1/2$  as a Minimum Shift Keying (MSK) modulation to shorten the notation, though MSK strictly use the REC pulse. We conclude that the non-UMP schemes with different pulses have almost the same

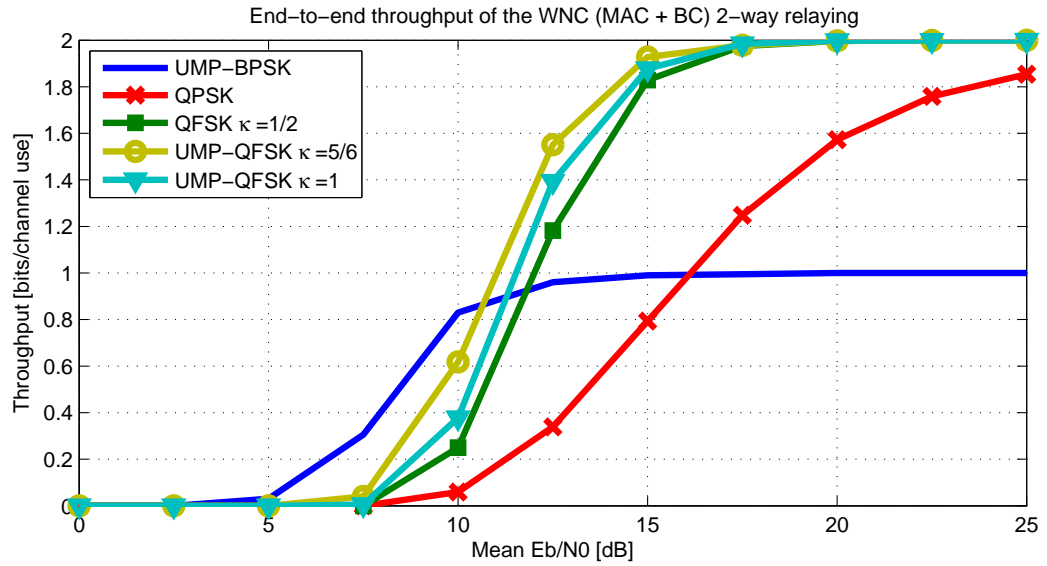


Figure 5.21: End-to-end throughput of the WNC strategy (including MA and BC stage) assuming uncoded detection with CSIR in Rice  $K = 10$ dB fading channel for memoryless modulations: UMP-BPSK, QPSK, QFSK  $\kappa = 1/2$ , UMP-QFSK  $\kappa = 1$  and UMP-QFSK  $\kappa = 5/6$ .

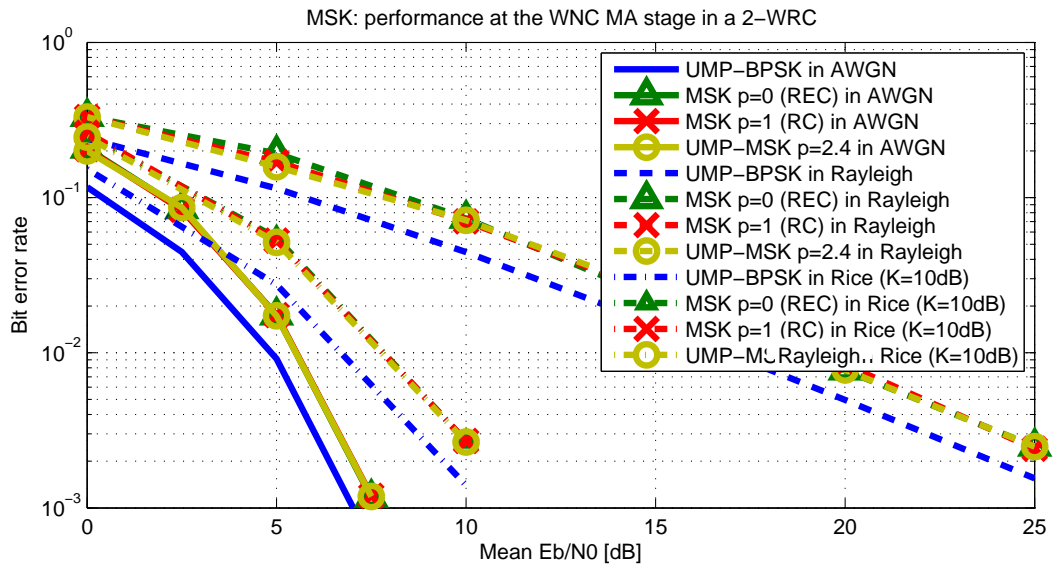


Figure 5.22: SER at the MA stage assuming uncoded detection with CSIR in AWGN, Rayleigh and Rice  $K = 10$ dB fading channel of binary full-response CPM  $\kappa = 1/2$  (MSK) with REC, RC and the proposed SRC pulse. Additionally, we depict UMP-BPSK as a reference.

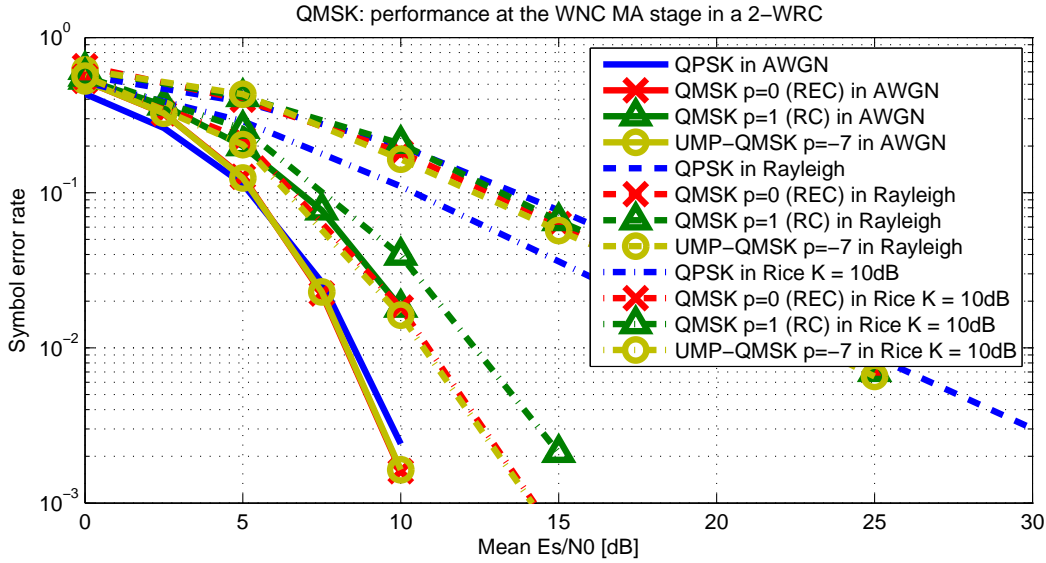


Figure 5.23: SER at the MA stage assuming uncoded detection with CSIR in AWGN, Rayleigh and Rice  $K = 10$ dB fading channel of quaternary full-response CPM  $\kappa = 1/2$  (QMSK) with REC, RC and the proposed SRC pulse. Additionally, we depict non-UMP QPSK as a reference.

performance, as we expected from Figs. 5.12, 5.13, 5.14. Therefore choosing a pulse with the narrowest spectra (REC) is appropriate. In this case, the proposed SRC pulse has only a theoretical value as a performance benchmark.

The proposed SRC pulse is more advantageous for quaternary alphabet, see Fig. 5.23. We shortly denote quaternary full-response CPM  $\kappa = 1/2$  as a QMSK modulation. We observe that the performance with REC pulse is close to the UMP alphabet performance, but contra-intuitively the performance with RC pulse is by several dBs worse even in the AWGN channel. The REC pulse, in this case, is a practical choice because the proposed SRC pulse requires more bandwidth, see the bandwidth comparison in the following section.

### 5.6.3 Bandwidth Comparison

The bandwidth requirement of the considered modulations is presented in Tab. 5.2. The first part of the table describes the bandwidth of linear memoryless alphabets (denoted shortly as 'Linear  $\mathcal{L}$ ') which is solely given by the used pulse function [69]. We present the well-known Root Raised Cosine (RRC) pulse parametrized by roll-off factor  $\lambda$  whose compact and finite bandwidth is  $W = (1+\lambda)/2T_s$ . Due to the finiteness of the bandwidth, the ideal RRC has the infinite time duration. Vice versa, the REC pulse finite in the temporal domain has the infinite bandwidth. We use the fractional power-containment bandwidth definition where  $W_{99\%}$  is a bandwidth containing 99% of the total signal power. In this work, all linear modulations (with one complex dimension including BPSK) use the same bandwidth. Note the significant difference of error performance between BPSK and QPSK in Fig. 5.20 and 5.22. BPSK is UMP only if it uses a single entire complex dimension (entire bandwidth), thus it needs one real dimension more than in the point-to-point communication.

The other part of the table is dedicated to non-linear modulations. We denote full-response CPM  $\kappa = 1/2$  with SRC pulse by acronym 'MSK'. Its fractional bandwidth (analytically described in [78]) shows that bi-orthogonal case require more bandwidth than e.g. the case with  $p = 0$ . The similar trend has also bandwidth of QMSK which we obtained according to [76], see the average power spectral densities in Fig. 5.24.

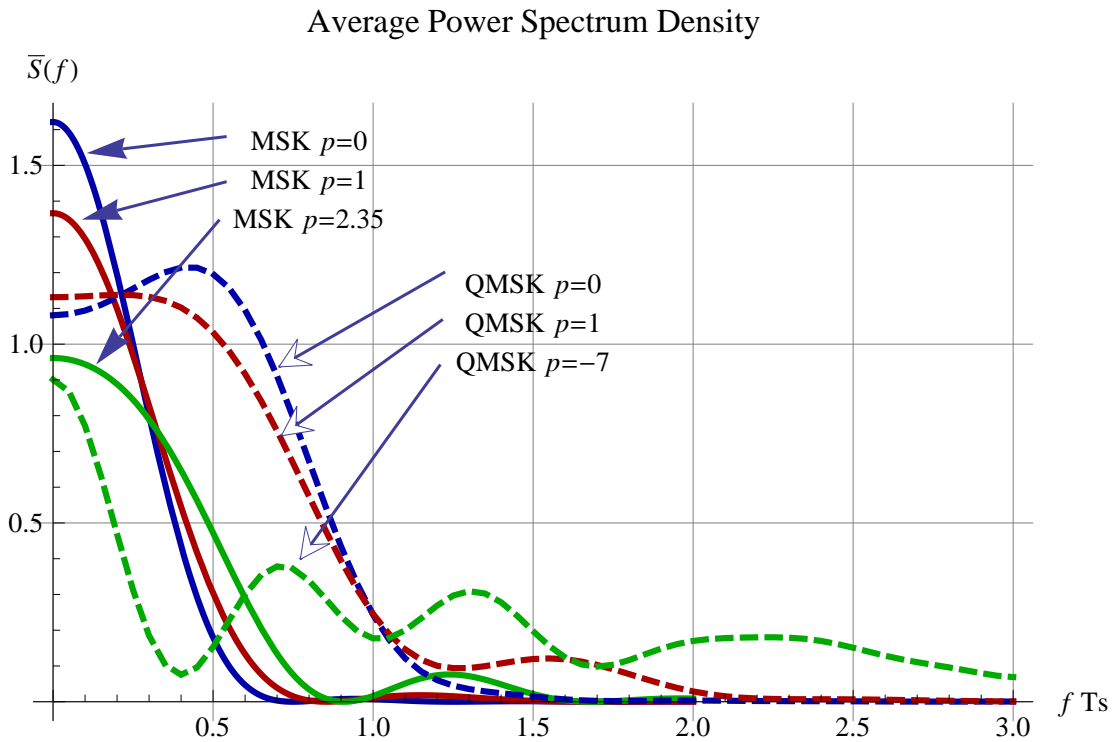


Figure 5.24: Average power spectral densities of binary and quaternary full-response CPM  $\kappa = 1/2$  (MSK and QMSK) for several different values of parameter  $p$ .

Table 5.2: Bandwidth comparison

◇ Linear $\mathcal{A}$	RRC $\lambda = 0$	RRC $\lambda = 1$	REC
$WT_s$	0.5	1	10.3
◇ QFSK	$\kappa = 1/2$	$\kappa = 5/6$	$\kappa = 1$
$W_{99\%} T_s$	10.9	15	21
◇ MSK	$p = 0$	$p = 1$	$p = 2.35$
$W_{99\%} T_s$	0.6	1.1	1.5
◇ QMSK	$p = 0$	$p = 1$	$p = -7$
$W_{99\%} T_s$	1.4	1.8	5.9

Table 5.3: Summary of the proposed alphabets

Alphabet	UMP relation	Notes
BPSK	UMP	optimal binary alphabet
QFSK $\kappa = 1/2$	close to UMP	not optimal spectra
QFSK $\kappa = 5/6$	UMP	more bandwidth than QFSK $\kappa = 1/2$
MSK $p = 0$	close to UMP	better spectrum than FSK; include memory
QMSK $p = 0$	close to UMP	better spectrum than FSK; include memory
MSK $p \simeq 2.35$	UMP	more bandwidth than MSK $p = 0$
QMSK $p \simeq -7$	UMP	more bandwidth than QMSK $p = 0$

## 5.7 Conclusion and Discussions

In this chapter, we have investigated modulations and network coding functions robust to the relative-fading of WNC not requiring any channel adaptation techniques. We have found that such a modulation is BPSK. Definitely the other linear modulations (PSK, QAM, ...) with higher cardinality than 2 are not robust to the relative-fading, because they possess so-called singular parameters. The singular parameter is such a non-zero channel parameter which causes zero minimal distance (it strongly degrades the overall average performance). It is interesting that the minimum-cardinality network coding function  $\mathcal{N}$  should have symmetrical NC Latin square with the same diagonal not to imply singular parameters. These conditions fulfils bit-wise XOR which is the unique choice for binary and quaternary alphabet. It has been shown that to avoid the singular parameters, the modulations with more than a single complex dimension have to be considered. This inspired us to assume non-linear frequency modulations naturally having a multi-dimensional wave-forming alphabet. We have precisely defined UMP alphabets which not only obviate all singular parameters but also reach the minimal distance upper-bound for all parameter values. UMP can be interpreted as the most suitable type of unavoidable channel parametrization and among all alphabets with the identical minimal distance of the primary terminal alphabet, the UMP alphabets have the best performance serving as a performance benchmark. It has been proven that any binary, non-binary complex-orthogonal and non-binary complex- bi-orthogonal alphabets are UMP.

We have found that the considered FSK and full-response  $\kappa = 1/2$  CPM avoid singular parameters and we have optimized their parameters (modulation index for FSK and phase pulse shape for CPM) to meet the UMP condition. Based on the numerical simulations, we conclude that the existence of singular parameters is much more detrimental than the violation of UMP condition. The proposed alphabets are summarized in Tab. 5.3.

We have analysed error and bandwidth performance of the used modulations in Sec. 5.6. However, the optimal modulation choice depends besides of error-bandwidth performance also on the other properties such as complexity or hardware requirements. For instance, BPSK with RRC pulse and MSK  $p = 0$  have comparable error-bandwidth performance, but MSK possesses the constant envelope (which allows more efficient power amplifier) at the price of more complex decoding processing (i.e. it includes the Viterbi algorithm). If we insist on the constant envelope property than MSK  $p = 0$  needs to be compared with BPSK with REC which requires much more bandwidth. BPSK with REC pulse and two times shorter pulse duration (to deliver 2 bits per channel use) have similar error performance but two times wider bandwidth than QFSK  $\kappa = 1/2$ . On the other hand, QFSK receiver consists of parallel bank of matched filters (number of filters equals to the dimensionality) while BPSK receiver has only one filter. QMSK  $p = 0$  is more preferable than QFSK  $\kappa = 1/2$  since it owns narrower bandwidth, if we can afford slightly more complex decoding processing.



## Appendix

*Proof (Bi-orthonormal modulation is UMP).* Let us consider modified condition (5.28) which we have used in the UMP-FSK derivation. It states that UMP alphabet modulation fulfils

$$\left\| \mathbf{s}^{(d_A)} - \mathbf{s}^{(d'_A)} \right\|^2 + |\alpha|^2 \left\| \mathbf{s}^{(d_B)} - \mathbf{s}^{(d'_B)} \right\|^2 - 2|\alpha| \left| \left\langle \mathbf{s}^{(d_A)} - \mathbf{s}^{(d'_A)}, \mathbf{s}^{(d_B)} - \mathbf{s}^{(d'_B)} \right\rangle \right| \geq |\alpha|^2 \delta_{\min}^2, \quad (5.38)$$

for  $d_A \neq d'_A, d_B \neq d'_B, d_A \oplus d_B \neq d'_A \oplus d'_B$ , where  $d_A, d_B, d'_A, d'_B \in \mathbb{Z}_M$  and  $\forall \alpha \in \mathbb{C}, |\alpha| \leq 1$ . Assume a bi-orthonormal modulation for which two bi-orthonormal signals have one of the three possible mutual relations. They are orthonormal (described by symbol  $\perp$ ), or the same  $\Leftarrow$  or have the opposite sign  $\Leftarrow$ . According to the mutual relation, its inner product and squared norm of its difference is

$$\left\langle \mathbf{s}^{(d_A)}, \mathbf{s}^{(d_B)} \right\rangle = \begin{cases} 0, & \perp \\ 1, & \Leftarrow \\ -1, & \Leftarrow \end{cases} \quad \left\| \mathbf{s}^{(d_A)} - \mathbf{s}^{(d_B)} \right\|^2 = \begin{cases} 2, & \perp \\ 0, & \Leftarrow \\ 4, & \Leftarrow \end{cases}. \quad (5.39)$$

In the first step, we analyse all possible values of the inner product term

$$\begin{aligned} z &= \left| \left\langle \mathbf{s}^{(d_A)} - \mathbf{s}^{(d'_A)}, \mathbf{s}^{(d_B)} - \mathbf{s}^{(d'_B)} \right\rangle \right| \\ &= \left| \left\langle \mathbf{s}^{(d_A)}, \mathbf{s}^{(d_B)} \right\rangle + \left\langle \mathbf{s}^{(d'_A)}, \mathbf{s}^{(d'_B)} \right\rangle - \left\langle \mathbf{s}^{(d_A)}, \mathbf{s}^{(d'_B)} \right\rangle - \left\langle \mathbf{s}^{(d'_A)}, \mathbf{s}^{(d_B)} \right\rangle \right|. \end{aligned} \quad (5.40)$$

Without taking into account the restrictions  $d_A \neq d'_A, d_B \neq d'_B$  and  $d_A \oplus d_B \neq d'_A \oplus d'_B$ , the term  $z \in \{0, 1, 2, 3, 4\}$ . Note, if the term  $z = 0$ , then the inequality (5.38) is fulfilled because by definition

$$\left\| \mathbf{s}^{(d_B)} - \mathbf{s}^{(d'_B)} \right\|^2 \geq \delta_{\min}^2. \quad (5.41)$$

There are four inner products in (5.40) that can take three different geometrical arrangements ( $\perp, \Leftarrow, \Leftarrow$ ) altogether there is  $3^4 = 81$  combinations. We will show by exhaustive listing of all cases where  $z \neq 0$  that such a case

**a)** cannot happen because the inner products give such results that geometrically this situation cannot exist (e.g. two vectors cannot be orthonormal and perpendicular at the same time) or

**b)** the inequality (5.38) is still fulfilled or

**c)** this situation is excluded the symmetries of the bit-wise XOR function

concluding that always  $z = 0$ , which proves the lemma.

In the second step, we show that  $z \neq 1$  because always the case **a)** happen. Due to the space limitation we will not list all the cases considering geometrical properties. It is sufficient to list only those schemes which have different geometrical arrangement. Let us denote the geometrical arrangement by a vector of inner products. The ordered configurations leading to  $z = 1$  are

$$\begin{aligned} &(0, 0, 0, 1), (0, 0, 0, -1), (0, 1, 1, 1), \\ &(0, 1, 1, -1), (0, 1, -1, -1), (0, -1, -1, -1). \end{aligned} \quad (5.42)$$

For example, let us assume the situation where

$$\left( \left\langle \mathbf{s}^{(d_A)}, \mathbf{s}^{(d_B)} \right\rangle, \left\langle \mathbf{s}^{(d'_A)}, \mathbf{s}^{(d'_B)} \right\rangle, \left\langle \mathbf{s}^{(d_A)}, \mathbf{s}^{(d'_B)} \right\rangle, \left\langle \mathbf{s}^{(d'_A)}, \mathbf{s}^{(d_B)} \right\rangle \right) = (0, 0, 0, 1). \quad (5.43)$$

In Fig. 5.25 we draw all possible configurations corresponding to the first three inner products

$$\left( \left\langle \mathbf{s}^{(d_A)}, \mathbf{s}^{(d_B)} \right\rangle, \left\langle \mathbf{s}^{(d'_A)}, \mathbf{s}^{(d'_B)} \right\rangle, \left\langle \mathbf{s}^{(d_A)}, \mathbf{s}^{(d'_B)} \right\rangle \right) = (0, 0, 0), \quad (5.44)$$

which implies that the last term is  $\left\langle \mathbf{s}^{(d'_A)}, \mathbf{s}^{(d_B)} \right\rangle = 0$ . In this case, it is not true, hence this situation never occur. Therefore, the situations with any permutation of the inner products  $(0, 0, 1, 0), (0, 1, 0, 0),$

$$\left( \langle \mathbf{s}^{(d_A)}, \mathbf{s}^{(d_B)} \rangle, \langle \mathbf{s}^{(d'_A)}, \mathbf{s}^{(d'_B)} \rangle, \langle \mathbf{s}^{(d_A)}, \mathbf{s}^{(d'_B)} \rangle \right) = (0, 0, 0)$$

$$\Rightarrow \langle \mathbf{s}^{(d'_A)}, \mathbf{s}^{(d_B)} \rangle = 0$$

Figure 5.25: Possible geometrical configurations  $\left( \langle \mathbf{s}^{(d_A)}, \mathbf{s}^{(d_B)} \rangle, \langle \mathbf{s}^{(d'_A)}, \mathbf{s}^{(d'_B)} \rangle, \langle \mathbf{s}^{(d_A)}, \mathbf{s}^{(d'_B)} \rangle \right) = (0, 0, 0)$  imply  $\langle \mathbf{s}^{(d'_A)}, \mathbf{s}^{(d_B)} \rangle = 0$ .

$$\left( \langle \mathbf{s}^{(d_A)}, \mathbf{s}^{(d_B)} \rangle, \langle \mathbf{s}^{(d'_A)}, \mathbf{s}^{(d'_B)} \rangle, \langle \mathbf{s}^{(d_A)}, \mathbf{s}^{(d'_B)} \rangle \right) = (1, 1, 1)$$

$$\Rightarrow \langle \mathbf{s}^{(d'_A)}, \mathbf{s}^{(d_B)} \rangle = 1$$

Figure 5.26: Possible geometrical configurations  $\left( \langle \mathbf{s}^{(d_A)}, \mathbf{s}^{(d_B)} \rangle, \langle \mathbf{s}^{(d'_A)}, \mathbf{s}^{(d'_B)} \rangle, \langle \mathbf{s}^{(d_A)}, \mathbf{s}^{(d'_B)} \rangle \right) = (1, 1, 1)$  imply  $\langle \mathbf{s}^{(d'_A)}, \mathbf{s}^{(d_B)} \rangle = 1$ .

$$\left( \langle \mathbf{s}^{(d_A)}, \mathbf{s}^{(d_B)} \rangle, \langle \mathbf{s}^{(d'_A)}, \mathbf{s}^{(d'_B)} \rangle, \langle \mathbf{s}^{(d_A)}, \mathbf{s}^{(d'_B)} \rangle \right) = (-1, -1, -1)$$

$$\Rightarrow \langle \mathbf{s}^{(d'_A)}, \mathbf{s}^{(d_B)} \rangle = -1$$

Figure 5.27: Possible geometrical configurations  $\left( \langle \mathbf{s}^{(d_A)}, \mathbf{s}^{(d_B)} \rangle, \langle \mathbf{s}^{(d'_A)}, \mathbf{s}^{(d'_B)} \rangle, \langle \mathbf{s}^{(d_A)}, \mathbf{s}^{(d'_B)} \rangle \right) = (-1, -1, -1)$  imply  $\langle \mathbf{s}^{(d'_A)}, \mathbf{s}^{(d_B)} \rangle = -1$ .

$$\left( \langle \mathbf{s}^{(d_A)}, \mathbf{s}^{(d_B)} \rangle, \langle \mathbf{s}^{(d'_A)}, \mathbf{s}^{(d'_B)} \rangle, \langle \mathbf{s}^{(d_A)}, \mathbf{s}^{(d'_B)} \rangle \right) = (1, 1, -1)$$

$$\Rightarrow \langle \mathbf{s}^{(d'_A)}, \mathbf{s}^{(d_B)} \rangle = -1$$

Figure 5.28: Possible geometrical configurations  $\left( \langle \mathbf{s}^{(d_A)}, \mathbf{s}^{(d_B)} \rangle, \langle \mathbf{s}^{(d'_A)}, \mathbf{s}^{(d'_B)} \rangle, \langle \mathbf{s}^{(d_A)}, \mathbf{s}^{(d'_B)} \rangle \right) = (1, 1, -1)$  imply  $\langle \mathbf{s}^{(d'_A)}, \mathbf{s}^{(d_B)} \rangle = -1$ .

$$\left( \langle \mathbf{s}^{(d_A)}, \mathbf{s}^{(d_B)} \rangle, \langle \mathbf{s}^{(d'_A)}, \mathbf{s}^{(d'_B)} \rangle, \langle \mathbf{s}^{(d_A)}, \mathbf{s}^{(d'_B)} \rangle \right) = (1, -1, -1)$$

$$\Rightarrow \langle \mathbf{s}^{(d'_A)}, \mathbf{s}^{(d_B)} \rangle = 1$$

Figure 5.29: Possible geometrical configurations  $\left( \langle \mathbf{s}^{(d_A)}, \mathbf{s}^{(d_B)} \rangle, \langle \mathbf{s}^{(d'_A)}, \mathbf{s}^{(d'_B)} \rangle, \langle \mathbf{s}^{(d_A)}, \mathbf{s}^{(d'_B)} \rangle \right) = (1, -1, -1)$  imply  $\langle \mathbf{s}^{(d'_A)}, \mathbf{s}^{(d_B)} \rangle = 1$ .

$$\left( \left\langle \mathbf{s}^{(d_A)}, \mathbf{s}^{(d_B)} \right\rangle, \left\langle \mathbf{s}^{(d'_A)}, \mathbf{s}^{(d'_B)} \right\rangle, \left\langle \mathbf{s}^{(d_A)}, \mathbf{s}^{(d'_B)} \right\rangle, \left\langle \mathbf{s}^{(d'_A)}, \mathbf{s}^{(d_B)} \right\rangle \right) = (0, 0, -1, -1)$$

Figure 5.30: One possible geometrical configuration of  $\left( \left\langle \mathbf{s}^{(d_A)}, \mathbf{s}^{(d_B)} \right\rangle, \left\langle \mathbf{s}^{(d'_A)}, \mathbf{s}^{(d'_B)} \right\rangle, \left\langle \mathbf{s}^{(d_A)}, \mathbf{s}^{(d'_B)} \right\rangle, \left\langle \mathbf{s}^{(d'_A)}, \mathbf{s}^{(d_B)} \right\rangle \right) = (0, 0, -1, -1)$

etc. are also excluded. In Fig. 5.26 and 5.27, we similarly show that configuration  $(1, 1, 1) \Rightarrow 1$  and  $(-1, -1, -1) \Rightarrow -1$ . We denote these three situations above as a  $(x, x, x) \Rightarrow x$  law. The last remaining configurations of  $z = 1$ , (5.42), which are not excluded by the  $(x, x, x) \Rightarrow x$  law, are  $(0, 1, 1, -1)$  and  $(0, 1, -1, -1)$ . They are again excluded by **a**), see Fig. 5.28 and 5.29. Since we excluded all situations where  $z = 1$  then  $z \neq 1$ .

In the last third step, we will conclude that  $|\alpha| = 1$  is critical and check all the remaining situations/configurations where  $z \in \{2, 3, 4\}$ . We will see that either **a**) or **c**) happen and thus always  $z = 0$ . We have seen in the Sec. 5.5.1 that  $|\alpha| = 1$  is critical if the term  $b = \left| \left\langle \mathbf{s}^{(d_A)} - \mathbf{s}^{(d'_A)}, \mathbf{s}^{(d_B)} - \mathbf{s}^{(d'_B)} \right\rangle \right| / \left\| \mathbf{s}^{(d_B)} - \mathbf{s}^{(d'_B)} \right\|^2 - \delta_{\min}^2$  is  $b \geq 1$ . In our case,  $b = z/2$  and assuming  $z \in \{2, 3, 4\}$  always  $b \geq 1$  and so a critical parameter is  $|\alpha| = 1$ .

The configurations corresponding to the case  $z = 2$  are

$$(0, 0, 1, 1), (0, 0, -1, -1), (0, 1, -1, 0), (1, 1, 1, -1). \quad (5.45)$$

The configuration  $(0, 0, 1, 1)$  entails that  $\mathbf{s}^{(d_A)} = \mathbf{s}^{(d'_B)}$  &  $\mathbf{s}^{(d'_A)} = \mathbf{s}^{(d_B)}$  thus implies  $d_A = d'_B$  &  $d'_A = d_B$  and is excluded by symmetrical **NC** Latin square which we already assume. The configuration  $(0, 0, -1, -1)$  is rather problematic, see its configuration in Fig. 5.30. Without deep analysis, we conclude that whatever mapping between waveforms  $\mathbf{s}^{(d_A)}$  and data symbols  $d_A$  we use, the bit-wise XOR function will always exclude this situation. In other words, the superimposed signals of this situation have always the same  $d_{AB}$  symbol. The configuration  $(0, 1, -1, 0)$  falls into case **b**), where the situation is geometrically possible, but it implies that  $\|\mathbf{s}^{(d_A)} - \mathbf{s}^{(d'_A)}\|^2 = 4$  and the condition (5.38) is automatically fulfilled. The similar situation occurs for the configurations

$$(0, 1, 0, -1), (0, -1, 0, 1), (0, -1, 1, 0), \\ (1, 0, 0, -1), (1, 0, -1, 0), (-1, 0, 0, 1), (-1, 0, 1, 0). \quad (5.46)$$

The case of  $z = 3$  are excluded in a similar way as for  $z = 1$ . The last case  $z = 4$  have possible configurations

$$(1, 1, -1, -1), (-1, -1, 1, 1). \quad (5.47)$$

The former case means  $\mathbf{s}^{(d_A)} = \mathbf{s}^{(d_B)}$  &  $\mathbf{s}^{(d'_A)} = \mathbf{s}^{(d'_B)}$  thus  $d_A = d_B$  &  $d'_A = d'_B$  which corresponds to superimposed signals from the main diagonal of **NC** Latin square. This is excluded, because such a condition we already assume. The latter case implies  $d_A = d_B$  &  $d'_A = d'_B$  and is again excluded by symmetrical **NC** Latin square.

By the above three steps, we have proven  $z = 0$ , which proves the lemma.  $\square$

## Chapter 6

# Design of General UMP Alphabets by Non-linear Optimization Tools

Wireless network coding is a promising 2-way relay strategy due to its potential to operate outside of the classical MAC capacity region. We consider a practical scenario assuming CSIR and no channel-adaptation, where WNC performance is unavoidably parametrized by channel fading coefficients. While some modulations have the minimal distance reaching its upper-bound for all parameter values (e.g. BPSK), some other modulations have the minimal distance much lower (e.g. QPSK), which appears as it undergoes additional fading (denoted as a relative-fading). The design of modulations with performance similar to BPSK (denoted as Uniformly Most Powerful (UMP)) have been introduced in the preceding chapter.

In this chapter, we formulate a UMP alphabet design as a bi-quadratically-constrained linear optimisation problem on which the standard non-linear optimization methods are applied. We design a list of UMP multi-dimensional modulations for several alphabet cardinalities and dimensions. It seems that the every found UMP alphabet has the rate-per-dimension upper-bounded by 1 bit/complex dimension (the rate of standard UMP BPSK alphabet). Therefore, we propose a different type of alphabets called weak UMP alphabets which have unlimited rate-per-dimension but fulfil the UMP condition only for parameter ratios  $|\alpha| = 1$  which implies robustness to the phase rotation and the Rician-type of fading. As expected, weak UMP alphabets perform several dB gain over canonical alphabets in the Rice channel.

## 6.1 Introduction

### 6.1.1 Motivation & Related Work

Performance of the WNC 2-way relying at the MA stage with CSIR is unavoidably parametric. There are some modulation alphabets (e.g. QPSK) for which even non-zero channel parameters cause dramatic performance degradation. In contrast, the modulations robust to this effect (e.g. BPSK) are denoted as UMP [4] since their asymptotic performance depends on the parameters in the utmost way – its minimal distance reaches the upper-bound for all channel parameter values. Non-binary UMP alphabets require more than one complex dimension which may provide non-linear multi-dimensional frequency modulations [4]. Adaptive extended-cardinality network coding [54] and adaptive precoding technique [60] were proposed to suppress the problem with channel parametrization. However, both techniques require some form of adaptation that might not be always available.

This chapter proceeds development of UMP alphabets [4]. We formulate its design as an optimization problem with given number of degrees of freedom on which non-linear constrained optimization methods are applied. In contrast to [4], we are not restricted on frequency modulations where precise required bandwidth is difficult to set. The found linear (with one complex dimension) weak UMP alphabets perform several dB gain over the canonical linear alphabets (PSK, QAM, ASK). The optimized multi-dimensional UMP alphabets do not significantly overcome BPSK.

## 6.2 System Model

### 6.2.1 Constellation Space Model and Used Notation

Let terminal  $T \in \{A, B\}$  in a 2-WRC use modulation alphabet  $\mathcal{A}_T$  with cardinality  $|\mathcal{A}_T| = M$  to be strictly a power of two. We suppose that the alphabet is formed by complex arbitrary-dimensional baseband signals in the constellation space,  $\mathcal{A}_T = \{\mathbf{s}_T^{(d_T)}\}_{d_T=0}^{M-1} \subset \mathbb{C}^{N_s}$ , where symbol  $d_T \in \mathbb{Z}_M = \{0, 1, \dots, M-1\}$  denotes a data symbol transmitted by terminal  $T \in \{A, B\}$  and  $N_s$  denotes the signal dimensionality. The extra dimensions are assumed to be taken from any independent resource of dimensions e.g. time- or frequency-slots. Further, we assume memoryless constellation mapper  $\mathcal{M}_T$  such that it directly corresponds to the signal indexation,  $\mathbf{s}_T^{(d_T)} = \mathcal{M}_T(d_T)$ . We distinguish between two cases: (a) both terminals use identical alphabets  $\mathcal{A}_A = \mathcal{A}_B$  implying  $\mathcal{M}_A = \mathcal{M}_B$ , in this case index  $T \in \{A, B\}$  is omitted. Case (b) assumes that both terminals use general alphabets  $\mathcal{A}_A \neq \mathcal{A}_B$  with the same cardinality.

### 6.2.2 Model Assumptions

We assume a time-synchronized scenario with full CSIR which are obtained e.g. by preceding tracking of pilot signals. The synchronization issues are beyond the scope of this chapter and interested reader may see e.g. [71] for further details. We restrict ourselves that adaptive techniques are not available either due to the missing feedback channel, or the increased system complexity, or the channel dynamics and its estimation errors are making this approach infeasible. We consider a per-symbol relaying (avoiding delay induced at the relay) and no channel coding which however can be additionally concatenated with our scheme [51].

### 6.2.3 Wireless Network Coding Two-Way Relaying

The WNC strategy in a 2-WRC consists of two stages. At the first MA stage, both terminals A and B transmit simultaneously to the relay in the interfering manner. The received signal is

$$\mathbf{x} = h_A \mathbf{s}_A + h_B \mathbf{s}_B + \mathbf{w}, \quad (6.1)$$

where  $\mathbf{w}$  is complex AWGN with variance  $2N_0$  per complex dimension, and the channel parameters  $h_A$  and  $h_B$  are frequency-flat complex Gaussian random variables with unit variance and Rayleigh/Rician distributed envelope. The Rician factor  $K$  is defined as a power ratio between stationary and scattered components.

Subsequently, the relay makes the Maximum Likelihood (ML) decoding of network coded data symbol  $d_{AB} = \mathcal{N}(d_A, d_B)$  from interfering signal (6.1). Operation  $\mathcal{N}$  is a network coding function which incorporates data from multiple sources via the principle of exclusivity [51] see (4.7). We assume a minimal-cardinality  $\mathcal{N}$  function, i.e. the cardinality of  $d_{AB}$  alphabet is  $M$  [73]. The ML decoding at the relay

$$\widehat{d}_{AB} = \arg \max_{d_{AB}} p(\mathbf{x}|d_{AB}), \quad (6.2)$$

uses the following likelihood function of  $d_{AB}$  [51]

$$p(\mathbf{x}|d_{AB}) = \frac{1}{M} \sum_{d_A, d_B: \mathcal{N}(d_A, d_B) = d_{AB}} p(\mathbf{x}|d_A, d_B), \quad (6.3)$$

where likelihood of joint  $[d_A, d_B]$  is

$$p(\mathbf{x}|d_A, d_B) = \frac{1}{(2N_0\pi)^{N_s}} \exp\left(-\frac{1}{2N_0} \|\mathbf{x} - h_A \mathbf{s}_A^{(d_A)} - h_B \mathbf{s}_B^{(d_B)}\|^2\right), \quad (6.4)$$

by  $\|\star\|^2$  we denote the squared vector norm. At the BC stage,  $R$  broadcasts network coded symbol  $d_{AB}$  which is sufficient for the successful decoding. Particularly, the terminal A obtains desired data  $d_B$  with

knowledge of  $d_{AB}$  and its own data  $d_A$  as  $d_B = \mathcal{N}^{-1}(d_{AB}, d_A)$  and vice versa for  $B$ . In this chapter, we entirely focus on the MA stage which dominates the error performance due to the additional multiple access interference.

## 6.3 Error Performance at the MA Stage

### 6.3.1 Nearest Neighbour Approximation of ML Metric

The relay needs to evaluate a sum of Gaussian exponential functions (6.3) to obtain a network coded data estimate (even requiring the knowledge of  $N_0$ ). However, for sufficiently high SNR, always one of the exponential functions significantly outweighs the others and receiver metric (6.3) can be well approximated by the largest one as

$$\sum_{d_A, d_B: \mathcal{N}(d_A, d_B) = d_{AB}} p(\mathbf{x}|d_A, d_B) \simeq \max_{d_A, d_B: \mathcal{N}(d_A, d_B) = d_{AB}} p(\mathbf{x}|d_A, d_B). \quad (6.5)$$

Inserting (6.5) into (6.3) and (6.2), we obtain the approximate ML decoding

$$\widehat{d_{AB}} \simeq \arg \max_{d_A, d_B: \mathcal{N}(d_A, d_B) = d_{AB}} p(\mathbf{x}|d_A, d_B) \quad (6.6)$$

which is equivalent to the nearest neighbour joint decoding

$$[\hat{d}_A, \hat{d}_B] = \arg \max_{d_A, d_B} p(\mathbf{x}|d_A, d_B) \quad (6.7)$$

followed by network coding  $\widehat{d_{AB}} = \mathcal{N}(\hat{d}_A, \hat{d}_B)$ . Here,  $N_0$  is not needed and thus the latter method seems to be more practical (at least for high SNR regime).

### 6.3.2 Pairwise Error Union-Bound and Its Parametrization

The error performance of the relay processing using the approximate metric can be well upper-bounded by the pairwise error union-bound. Let  $P_e = \Pr\{\widehat{d_{AB}} \neq d_{AB}\}$  be a probability of a wrong decision, then the union-bound is

$$P_e \leq \frac{1}{M} \sum_{d_{AB}} \sum_{d'_{AB} \neq d_{AB}} P_{2e}, \quad (6.8)$$

where  $P_{2e}$  is the pairwise error probability of decoding  $d'_{AB}$  when  $d_{AB}$  was transmitted. If we define the squared Euclidean distance of a function decoding as

$$\Delta_{A,B}^2 = \left\| h_A \left( \mathbf{s}_A^{(d_A)} - \mathbf{s}_A^{(d'_A)} \right) + h_B \left( \mathbf{s}_B^{(d_B)} - \mathbf{s}_B^{(d'_B)} \right) \right\|^2, \quad (6.9)$$

where  $\mathcal{N}(d_A, d_B) \neq \mathcal{N}(d'_A, d'_B)$ , then the pairwise error is  $P_{2e} = Q\left(\sqrt{\Delta_{A,B}^2/4N_0}\right)$ , where

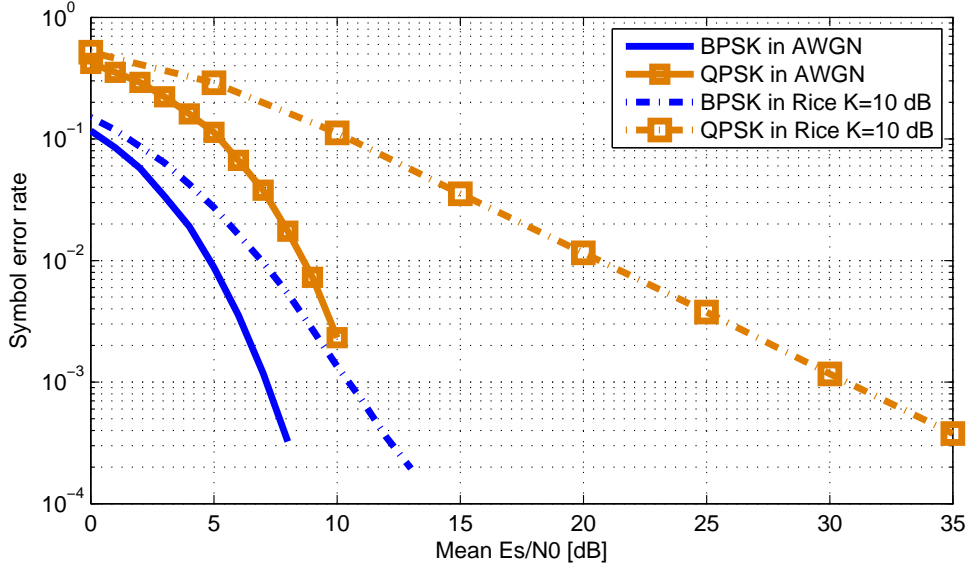
$$Q(x) = 1/\sqrt{2\pi} \int_x^\infty \exp(-u^2/2) du. \quad (6.10)$$

For high SNR, the union-bound is proportional mostly to the highest  $P_{m2e} = Q\left(\sqrt{\Delta_{\min}^2/4N_0}\right)$ , where the minimal distance is defined as

$$\Delta_{\min}^2 = \min_{\mathcal{N}(d_A, d_B) \neq \mathcal{N}(d'_A, d'_B)} \left\| h_A \left( \mathbf{s}_A^{(d_A)} - \mathbf{s}_A^{(d'_A)} \right) + h_B \left( \mathbf{s}_B^{(d_B)} - \mathbf{s}_B^{(d'_B)} \right) \right\|^2. \quad (6.11)$$

Conveniently, since the relay knows both channel parameters, we may put either  $h_A$  or  $h_B$  out of the squared norm and assume the normalized minimal distances

$$|h_A|^2 \Delta_{\min}^2 = |h_B|^2 \Delta_{\min}^2 = \Delta_{\min}^2. \quad (6.12)$$

Figure 6.1: Symbol error rate of BPSK and QPSK in AWGN and Rice  $K = 10$  dB channel.

Supposing  $\alpha = h_B/h_A$ , the normalized distances are

$$\begin{aligned}\Delta_{\min}^{\prime 2}(\alpha) &= \min_{\mathcal{N}(d_A, d_B) \neq \mathcal{N}(d'_A, d'_B)} \left\| \left( \mathbf{s}_A^{(d_A)} - \mathbf{s}_A^{(d'_A)} \right) + \alpha \left( \mathbf{s}_B^{(d_B)} - \mathbf{s}_B^{(d'_B)} \right) \right\|^2, \\ \Delta_{\min}^{\prime\prime 2}(\alpha) &= \min_{\mathcal{N}(d_A, d_B) \neq \mathcal{N}(d'_A, d'_B)} \left\| 1/\alpha \left( \mathbf{s}_A^{(d_A)} - \mathbf{s}_A^{(d'_A)} \right) + \left( \mathbf{s}_B^{(d_B)} - \mathbf{s}_B^{(d'_B)} \right) \right\|^2.\end{aligned}\quad (6.13)$$

Since, we can use either  $\Delta_{\min}^{\prime 2}$  or  $\Delta_{\min}^{\prime\prime 2}$  so that  $|\alpha|$  or  $|1/\alpha|$  is lower or equal to 1, than from now, we assume that  $|\alpha| \leq 1$ .

It is important to see that minimal distance (6.11) as well as the performance bound are functions of channel parameters  $h_A, h_B$ . The average error performance bound, which is of the scope, is then

$$\bar{P}_{m2e} \simeq N_{\min} E_{h_A, h_B} \left[ Q \left( \sqrt{\Delta_{\min}^2(h_A, h_B)/4N_0} \right) \right], \quad (6.14)$$

where  $E_{h_A, h_B}[\star]$  is an average operator over  $h_A, h_B$  distributions and  $N_{\min}$  denotes a multiplicative factor which equals to the average number of nearest neighbours, see more details in Sec. 3.4.2.

## 6.4 Uniformly Most Powerful Alphabet

### 6.4.1 Problem of Parametric Performance at the MA stage

Asymptotic performance measure (6.11) is parametric and the way of parameter dependence is given solely by the used network coding function and alphabet. The performance of BPSK and QPSK for case (a)  $\mathcal{A}_A = \mathcal{A}_B$  well demonstrates that some modulations are more parameter robust than some other modulations, see Fig. 6.1. Although the performance in AWGN agree with 3 dB shift between their minimal distances of its primary alphabet defined as

$$\delta_{\min}^2 = \min_{i \neq j} \left\| \mathbf{s}^{(i)} - \mathbf{s}^{(j)} \right\|^2, \quad \mathbf{s}^{(i)}, \mathbf{s}^{(j)} \in \mathcal{A}, \quad (6.15)$$

the performance in Rice  $K = 10$  dB shows a fundamental difference. QPSK appears as it undergoes much stronger fading than BPSK. The reason of the QPSK performance loss in comparison to BPSK

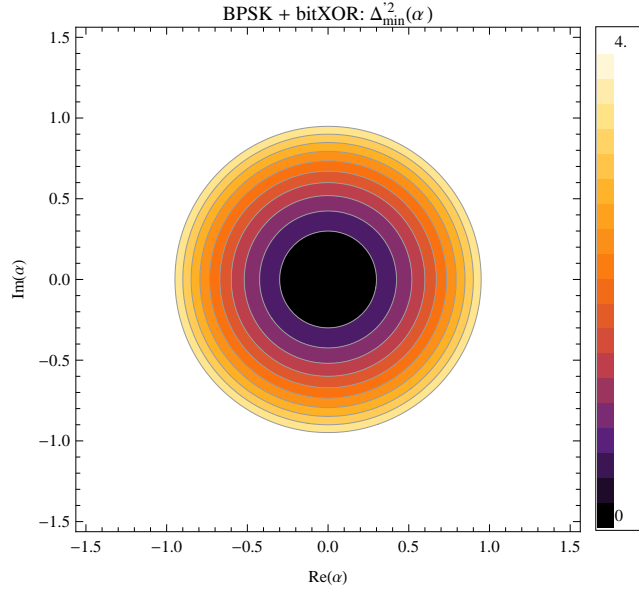


Figure 6.2: Minimal distance  $\Delta_{\min}^{\prime 2}(\alpha)$  of BPSK showing no singularities.

is well shown by their normalized parametric minimal distances  $\Delta_{\min}^{\prime 2}$  (6.13) shown in Fig. 6.2 and 6.3.

The BPSK minimal distance has a parabolic type of parametrization, while QPSK indicates even zero distances for some non-zero parameter ratios  $\alpha$  which we call *singular parameters*. They effectively present additional deep fading which appears as a diversity-loss in the error curves.

## 6.4.2 UMP Definition and Properties

We define a class of modulations with parabolic type of parametrization as has BPSK, in order to avoid all singular parameters.

**Definition 5.** Uniformly Most Powerful (UMP) alphabet has the normalized minimal distance equal to

$$\Delta_{\min}^{\prime 2}(\alpha) = |\alpha|^2 \delta_{\min}^2, \quad \forall \alpha \in \mathbb{C}, |\alpha| \leq 1, \quad (6.16)$$

where the minimal distance of primary alphabets  $\delta_{\min}^2$  is

$$\delta_{\min}^2 = \delta_{T,\min}^2 = \min_{d_T \neq d'_T} \left\| \mathbf{s}_T^{(d_T)} - \mathbf{s}_T^{(d'_T)} \right\|^2, \quad \forall d_T, d'_T \in \mathbb{Z}_M, T \in \{A, B\}, \quad (6.17)$$

$$\delta_{\min}^2 = \min_{T \in \{A, B\}} \{ \delta_{T,\min}^2 \} \quad (6.18)$$

for case (a)  $\mathcal{A}_A = \mathcal{A}_B$  and case (b)  $\mathcal{A}_A \neq \mathcal{A}_B$ , respectively.

Yet, we state several important lemmas; the proofs and further discussion can be found in chapter 5.

**Remark 10.** The term  $|\alpha|^2 \delta_{\min}^2$  in (6.16) is an upper-bound on the distance  $\Delta_{\min}^{\prime 2}(\alpha)$  for any alphabet and  $\mathcal{N}$  function including the extended-cardinality one used e.g. in [54].

**Lemma 9.** Network coding functions meet the following conditions to allow UMP condition (6.16):

1.  $\mathcal{N}(d, d) = \mathcal{N}(d', d')$ ,  $\forall d, d' \in \mathbb{Z}_M$ ,
2.  $\mathcal{N}(d, d') = \mathcal{N}(d', d)$ ,  $\forall d, d' \in \mathbb{Z}_M$ .



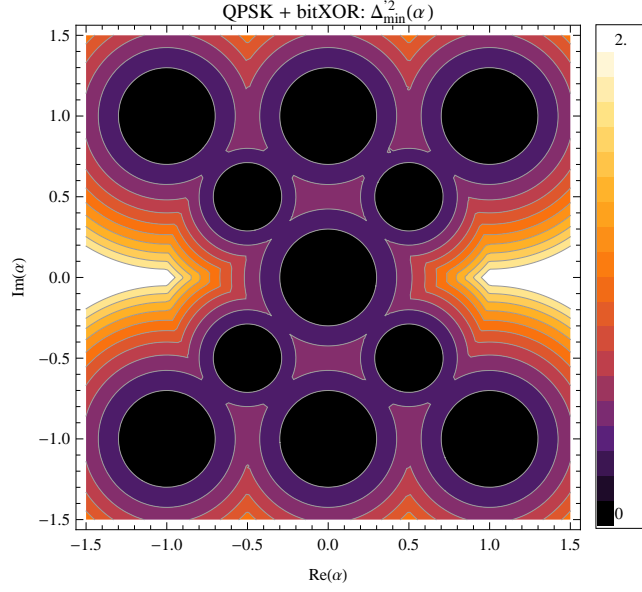


Figure 6.3: Minimal distance  $\Delta_{\min}^2(\alpha)$  of QPSK showing singular parameters  $\{\pm j, \pm 1 \pm j, \pm 1/2 \pm j/2\}$ .

These conditions are fulfilled by the bit-wise XOR operation and it is the unique solution for binary and quaternary case.

**Lemma 10.** All non-binary single-dimensional alphabets ( $N_s = 1$ , e.g. PSK, ASK, QAM) have some singularity  $\alpha$  and thus are never UMP. Non-binary UMP alphabets require extra dimensions, e.g. bi-orthogonal alphabets are UMP.

**Lemma 11.** The UMP condition (6.16) is equivalent to the following two conditions (not using parameter  $\alpha$ )

$$\left\| \mathbf{s}_A^{(d_A)} - \mathbf{s}_A^{(d'_A)} \right\|^2 + \left\| \mathbf{s}_B^{(d_B)} - \mathbf{s}_B^{(d'_B)} \right\|^2 - 2 \left| \left\langle \mathbf{s}_A^{(d_A)} - \mathbf{s}_A^{(d'_A)}, \mathbf{s}_B^{(d_B)} - \mathbf{s}_B^{(d'_B)} \right\rangle \right| \geq \delta_{\min}^2, \quad (6.19)$$

$$- \left| \left\langle \mathbf{s}_A^{(d_A)} - \mathbf{s}_A^{(d'_A)}, \mathbf{s}_B^{(d_B)} - \mathbf{s}_B^{(d'_B)} \right\rangle \right| + \left\| \mathbf{s}_B^{(d_B)} - \mathbf{s}_B^{(d'_B)} \right\|^2 \leq \delta_{\min}^2 \quad (6.20)$$

valid for all  $d_A \neq d'_A, d_B \neq d'_B$  such that  $\mathcal{N}(d_A, d_B) \neq \mathcal{N}(d'_A, d'_B)$ ; symbol  $\langle \star, \star \rangle$  denotes an inner product. The first condition (6.19) corresponds to the UMP condition for  $|\alpha| = 1$  and the latter (6.20) must be satisfied to keep the property also for  $|\alpha| < 1$ .

*Remark 11.* Setting (6.16) into (6.12) yields  $\Delta_{\min}^2 = |h_A|^2 |\alpha|^2 \delta_{\min}^2 = |h_B|^2 \delta_{\min}^2$ . Therefore, considering average performance bound (6.14), we conclude that the UMP alphabets have the asymptotic performance proportional to the performance of point-to-point communication,

$$\bar{P}_{m2e} \simeq N_{\min} E_{h_B} \left[ Q \left( \sqrt{|h_B|^2 \delta_{\min}^2 / 4N_0} \right) \right]. \quad (6.21)$$

## 6.5 UMP Alphabets Designed by Non-linear Optimization Tools

### 6.5.1 Optimization Goal

The aim of this chapter is to design UMP modulations for arbitrary modulation cardinality  $M$  and dimensionality  $N_s$ . We distinguish between two cases (a) the same alphabets  $\mathcal{A}_A = \mathcal{A}_B$  and (b) the unequal alphabets  $\mathcal{A}_A \neq \mathcal{A}_B$  and based on Lemma 9 we consider bit-wise XOR operation. As an optimization problem, we consider the maximization of  $\delta_{\min}^2$  (6.17) subject to UMP condition (6.16) resp. (6.19, 6.20).

## 6.5.2 Energy Conditions

For a fair energy comparison, we add obvious energy conditions, assuming that the mean symbol energy per dimension is one (resp. two), i.e.

$$\frac{1}{MN_s} \sum_{d=0}^{M-1} \|\mathbf{s}^{(d)}\|^2 = 1, \quad (6.22)$$

$$\frac{1}{MN_s} \sum_{d=0}^{M-1} \left( \|\mathbf{s}_A^{(d)}\|^2 + \|\mathbf{s}_B^{(d)}\|^2 \right) = 2 \quad (6.23)$$

for case (a)  $\mathcal{A}_A = \mathcal{A}_B$  and (b)  $\mathcal{A}_A \neq \mathcal{A}_B$ , respectively. We assume equalities, since if we find UMP alphabets that have average energy lower than one, than we could scale the alphabets enlarging  $\delta_{\min}^2$ . We interpret condition (6.23) as that one terminal can transmit more power at the expense of the other one. The energy dis-balance could be consequently balanced by periodic switching of the roles which terminal has higher power.

## 6.5.3 Optimization Problem

Let us summarize the previous conditions, the optimization is:

$$\text{maximize } \delta_{\min}^2 \quad (6.24)$$

s.t.: UMP (6.19, 6.20) and energy (6.22) resp. (6.23) condition.

In the optimization design, we must carefully consider cases when  $N_s = 1$  and  $N_s > 1$ , since according to Lemma 10, the non-binary alphabets never meet the UMP condition for  $N_s = 1$ . In this case, we soften the UMP condition to be satisfied only for  $|\alpha| = 1$ , i.e. instead of (6.19, 6.20) we require (6.19) only. Such modulations will be denoted as *weak UMP*. The motivation is that it can be shown [57] that by increasing Rician factor  $K$ , the probability distribution of  $\alpha$  concentrates more around  $|\alpha| = 1$ .

## 6.5.4 Problem Classification

The optimization problem (6.24) is a standard minimax problem [79] which is conveniently reformulated denoting  $\delta_{\min}^2 = t$  as

$$\text{maximize } t \quad (6.25)$$

subject to the additional minimal distance condition

$$t \leq \left\| \mathbf{s}^{(d)} - \mathbf{s}^{(d')} \right\|^2, \forall d, d' \in \mathbb{Z}_M : d \neq d'. \quad (6.26)$$

Objective function (6.25) is now linear. Let us examine the form of the constraints (6.19, 6.20), (6.22) and (6.26). They are made by squared vector norms, squared norms of vector differences and absolute values of inner product of vector differences. The norm of vectors and vector differences are quadratic, unfortunately, the absolute value term incorporates a root of the sum of squares in the same way as  $|z| = \sqrt{\Re^2\{z\} + \Im^2\{z\}}, z \in \mathbb{C}$ , thus the overall constraints are not quadratic. Taking the square of the re-ordered conditions with absolute values, we obtain equivalent conditions of the 4th order, e.g. equivalent condition to (6.20) is

$$\left( \left\| \mathbf{s}_B^{(d_B)} - \mathbf{s}_B^{(d'_B)} \right\|^2 - \delta_{\min}^2 \right)^2 \leq \left| \left\langle \mathbf{s}_A^{(d_A)} - \mathbf{s}_A^{(d'_A)}, \mathbf{s}_B^{(d_B)} - \mathbf{s}_B^{(d'_B)} \right\rangle \right|^2 \quad (6.27)$$

which possess after some simplifications e.g. term  $\left\| \mathbf{s}_B^{(d_B)} - \mathbf{s}_B^{(d'_B)} \right\|^4$ .

Table 6.1: Numerically designed UMP alphabets

$M$	$N_s$	$\log_2 M/N_s$	(a) $\delta_{\min}^2, \mathcal{A}_A = \mathcal{A}_B$	(b) $\delta_{\min}^2, \mathcal{A}_A \neq \mathcal{A}_B$	(c) $\delta_{\min}^2$ , not UMP
2	1	1	4	4	4
4	1	2	0.4 <sup>†</sup>	0.68 <sup>†</sup>	2
4	2	1	4	4.35	5.3
4	3	2/3	8	8	8
8	1	3	0.044 <sup>†</sup>	0.088 <sup>†</sup>	0.93
8	2	3/2	1 <sup>†</sup>	1.86	4
8	3	1	4.36	4.83	6.54
8	4	3/4	8	8	9.16

Therefore, our optimization problem is order-4 polynomially (a.k.a. bi-quadratically) constrained linear program. Apparently, this is at least the NP-hard problem, since it includes NP-hard quadratic problems. Bi-quadratic conditions also make hard to determine whether the problem is convex or not which would considerably simplify the choice of solving methods [79].

### 6.5.5 Problem Settings

We have  $M$  vectors with  $N_s$ -complex dimensions to determine. Without loss in generality, we assume the first vector lying in the first coordinate,  $\mathbf{s}^{(0)} = (s_{00}^{\Re} + j0, 0, \dots, 0)$ ,  $s_{00}^{\Re} \in \mathbb{R}$ . The number of real optimization variables is  $2MN_s - M - 1$ . The number of conditions (6.19, 6.20) is proportional to the number of all  $d_A, d_B, d'_A, d'_B \in \mathbb{Z}_M$ ,  $d_A \neq d'_A$ ,  $d_B \neq d'_B$  such that  $\mathcal{N}(d_A, d_B) \neq \mathcal{N}(d'_A, d'_B)$  which equals to

$$1/2M^2(M-1)(M-2) \quad (6.28)$$

and it grows proportionally to  $M^4$ . According to the energy constraints (6.22), we may coarsely restrict all variables to be within  $|s_{kl}^{\Re}| \leq \sqrt{MN_s}$ ,  $|s_{kl}^{\Im}| \leq \sqrt{MN_s}$ , where  $s_{kl}^{\Re}, s_{kl}^{\Im}$  denote real and imaginary part of the  $k$ th vector in the  $l$ th dimension.

### 6.5.6 Non-linear Optimization Methods

Since all conditions are twice differentiable, we apply the commonly used non-linear global optimization method based on the Nelder-Mead algorithm [80]. This approach works fine up-to  $M = 4$ , then the large number of conditions (see Sec. 6.5.5) and apparently large number of local optimums make it infeasible – unlikely finding the global optima. To confirm our solutions more reliably, we started the Nelder-Mead algorithm with several different points of its random number generator utilizing an extensive parallel multi-core computing implementation. For  $M > 4$ , we use the local optimization method based on the interior points algorithm [79]. We start it for several randomly chosen initial points to increase the chance that local method finds the global optimum. Finally, all solutions are confirmed by the numerical evaluation of the parametric minimal distance (6.13).

## 6.6 Numerical Results

The results are presented in Table 6.1. We show minimal distances  $\delta_{\min}^2$  (6.17) as a function of alphabet cardinality  $M$  and signal dimensionality  $N_s$ , supplemented by spectral efficiency per dimension  $\log_2 M/N_s$ . We distinguish three cases, (a) the UMP alphabets assuming  $\mathcal{A}_A = \mathcal{A}_B$ , (b) the UMP alphabets assuming not equal alphabets  $\mathcal{A}_A \neq \mathcal{A}_B$  and (c) the alphabets constrained by energy condition (6.22) only (not UMP). Case (c) serves as an upper-bound on  $\delta_{\min}^2$  of case (a) and (b) since it involves fewer constraints. For brevity, we denote dimensionality as D.

According to the discussion from Sec. 6.5.3, 4-ary and 8-ary 1-D alphabets are only weak UMP (denoted by †). Their parametric minimal distance  $\Delta_{\min}^2(\alpha)$  for case (a) are depicted in Figs. 6.4 and 6.5.

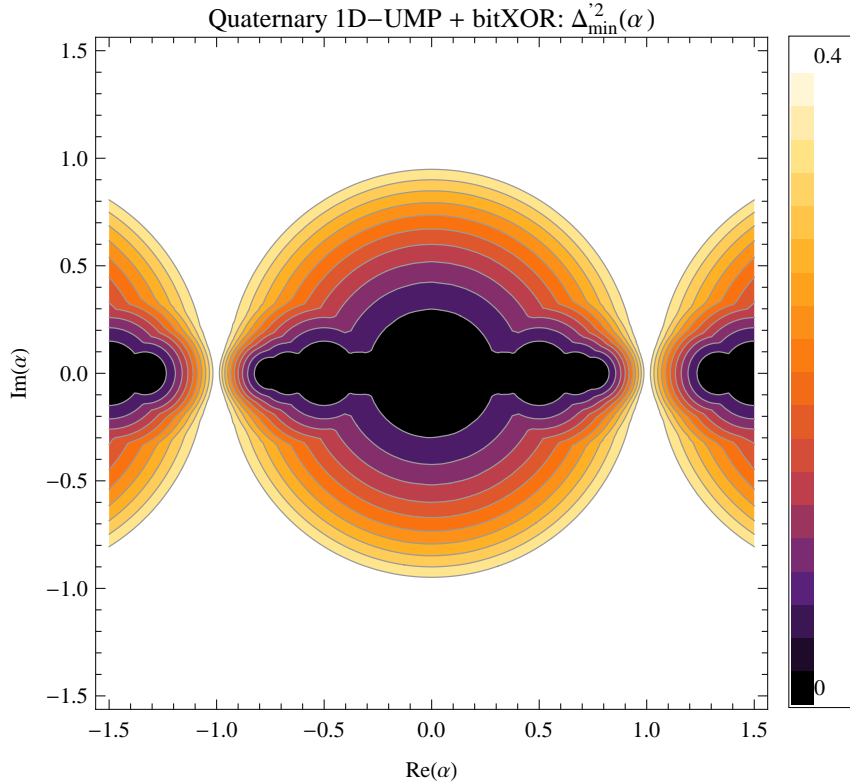


Figure 6.4: Minimal distance  $\Delta_{\min}^2$  of 4-ary 1-D weak UMP alphabet.

The found weak UMP alphabets are real (lie in one real dimension), though we have searched over the complex dimensional space. They are symmetrically distributed around zero (antipodal) and in contrast to ASK, they are not uniformly distributed, see Fig. 6.6. Particularly,

$$\mathcal{A} = \sqrt{2/5}\{-2, -1, 1, 2\} \quad (6.29)$$

and

$$\mathcal{A} = \sqrt{1/91}\{-13, -11, -7, -5, 5, 7, 11, 13\} \quad (6.30)$$

is 4-ary and 8-ary weak UMP alphabet, respectively.

Let us consider case (a) and the unit per-symbol-efficiency alphabets. We conclude that BPSK is UMP and has maximal  $\delta_{\min}^2$  in 2-ary 1-D case. The same  $\delta_{\min}^2$  has 4-ary 2-D alphabet

$$\mathcal{A} = \{(1, 1), (1, -1), (-1, 1), (-1, -1)\} \quad (6.31)$$

which was suggested also in [81]. We obtain a bit larger  $\delta_{\min}^2$  in 8-ary 3-D case, see its minimal distance  $\Delta_{\min}^2$  in Fig. 6.8. In spite of larger  $\delta_{\min}^2$ , 8-ary 3-D alphabet does not overcome BPSK (see the bit-error-rate curves in Fig. 6.7) since it possess larger minimal distance multiplicity  $N_{\min}$  and infeasible efficient bit-mapping (some pair-wise errors with  $\delta_{\min}^2$  cause more than one bit error), where the bit-mapping was chosen to minimize the bit errors of the pair-wise error event with  $\delta_{\min}^2$ .

Considering case (b), we may increase  $\delta_{\min}^2$  of UMP alphabets in compare to case (a), at the expense of the power switching between terminals, see discussion in Sec. 6.5.2. Remarkable are the weak UMP 4-ary 1-D alphabets  $\mathcal{A}_A \neq \mathcal{A}_B$  which resemble a scaled version of canonical QPSK alphabets (see Fig. 6.9) which have been proposed in [57]. For completeness, we depict parametric minimal distance  $\Delta_{\min}^2(\alpha)$  for the 4-ary 2-D UMP alphabets in Figs. 6.10 and 6.11.

In Fig. 6.12, we evaluate symbol error rate of 4-ary and 8-ary 1-D Weak UMP alphabets with traditional PSK and ASK modulations. For high SNR, weak alphabets provide several dB gain in comparison

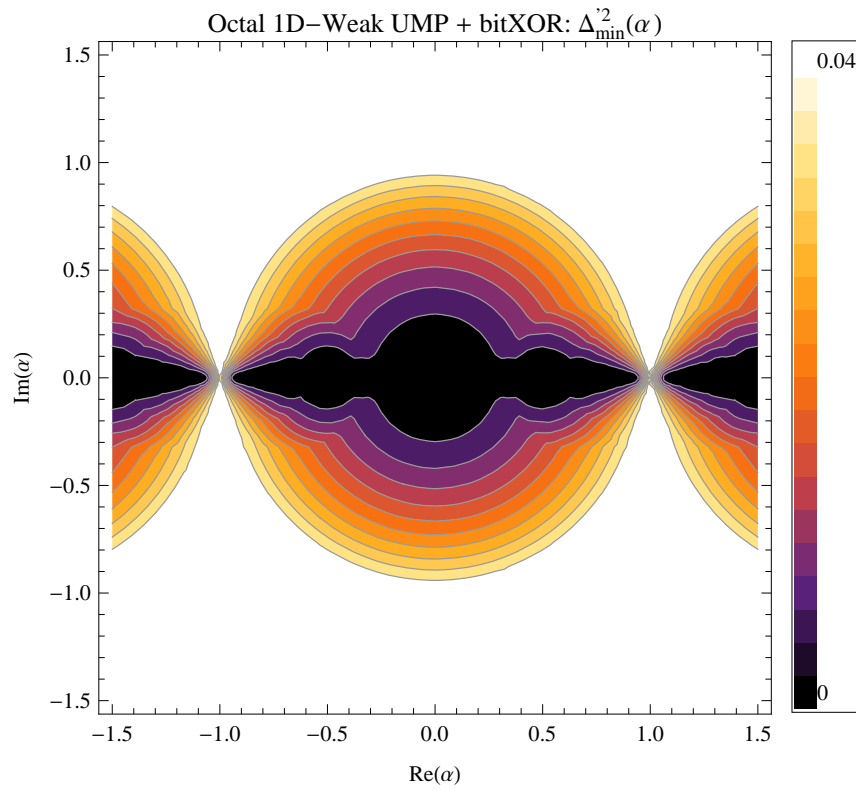


Figure 6.5: Minimal distance  $\Delta_{\min}^2$  of 8-ary 1-D weak UMP alphabet.

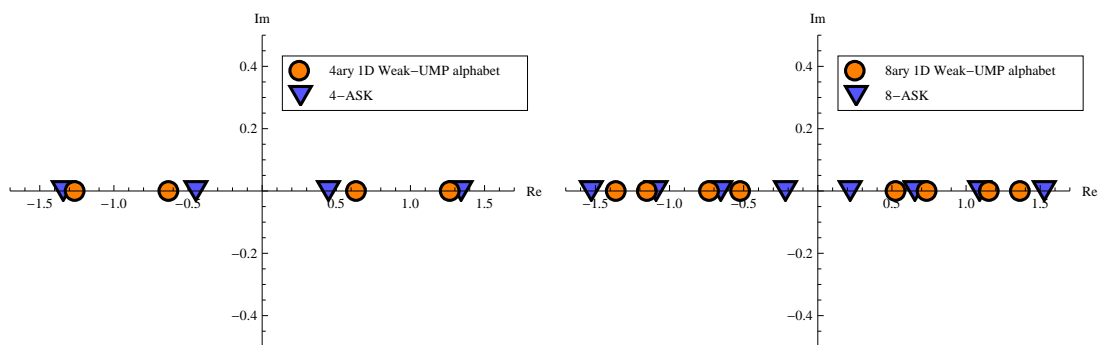


Figure 6.6: 4- and 8-ary 1-D Weak UMP alphabets.

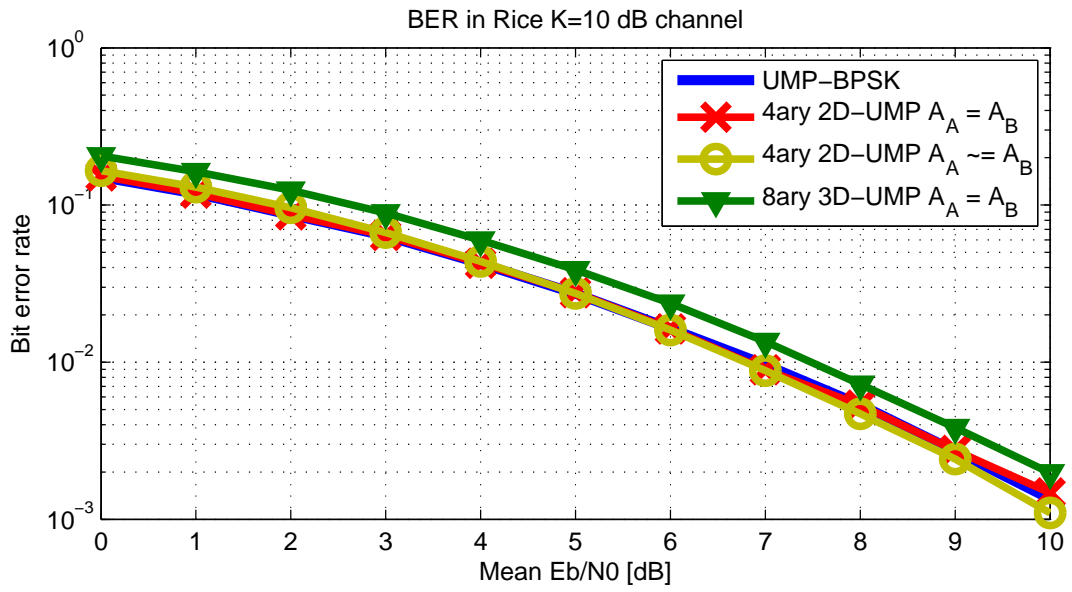


Figure 6.7: Bit error rate of the unit per-symbol-efficiency UMP alphabets in Rice  $K = 10$  dB channel.

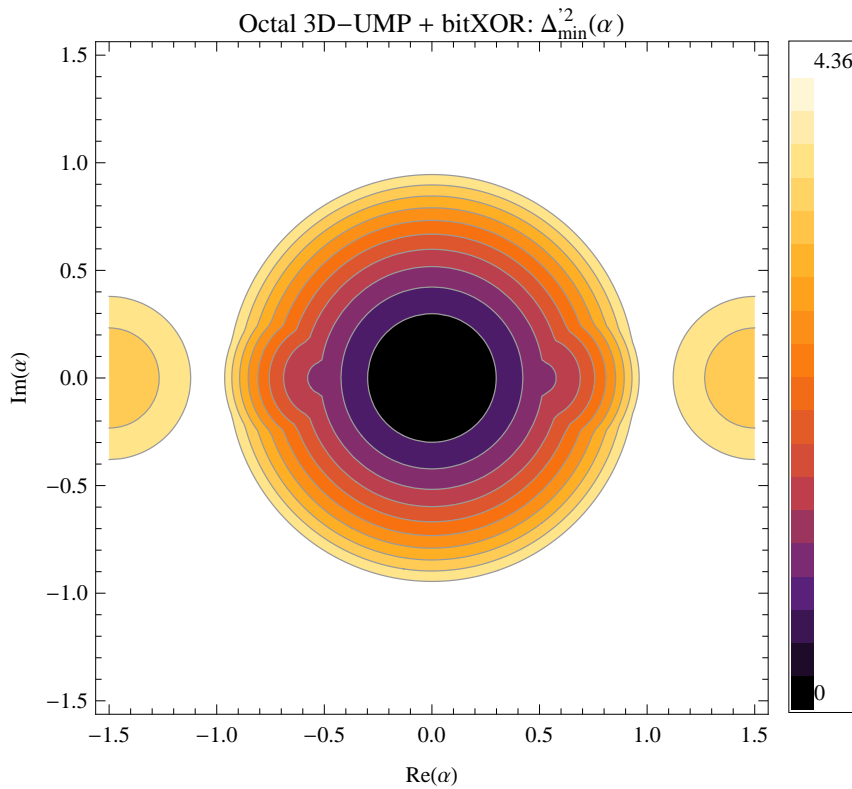


Figure 6.8: Minimal distance  $\Delta_{\min}^2$  of 8-ary 3-D UMP alphabet.

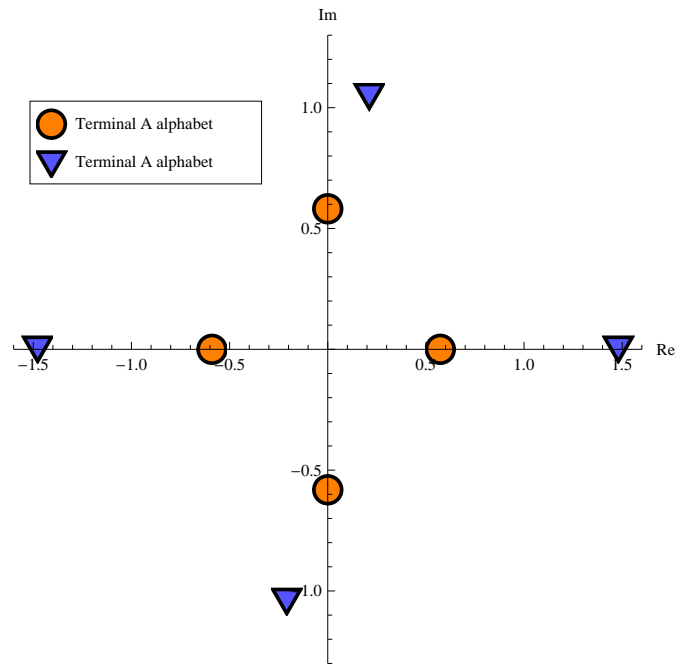


Figure 6.9: 4-ary 1-D weak UMP alphabets  $\mathcal{A}_A \neq \mathcal{A}_B$  resembles scaled QPSK.

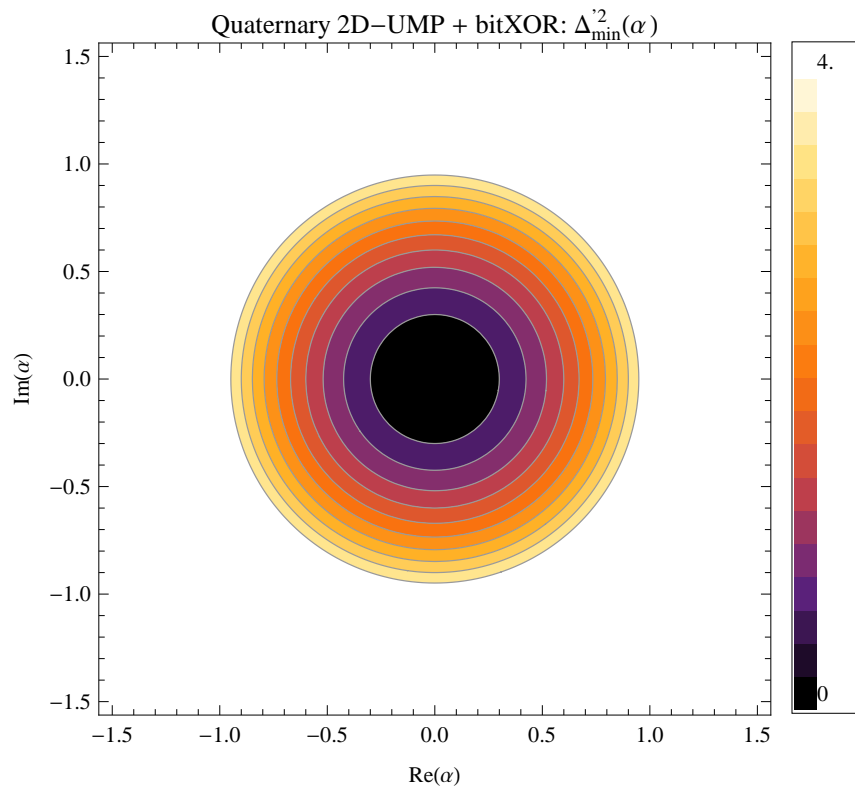


Figure 6.10: Minimal distance  $\Delta_{\min}^2$  of 4-ary 2-D UMP alphabet for case  $\mathcal{A}_A = \mathcal{A}_B$ .

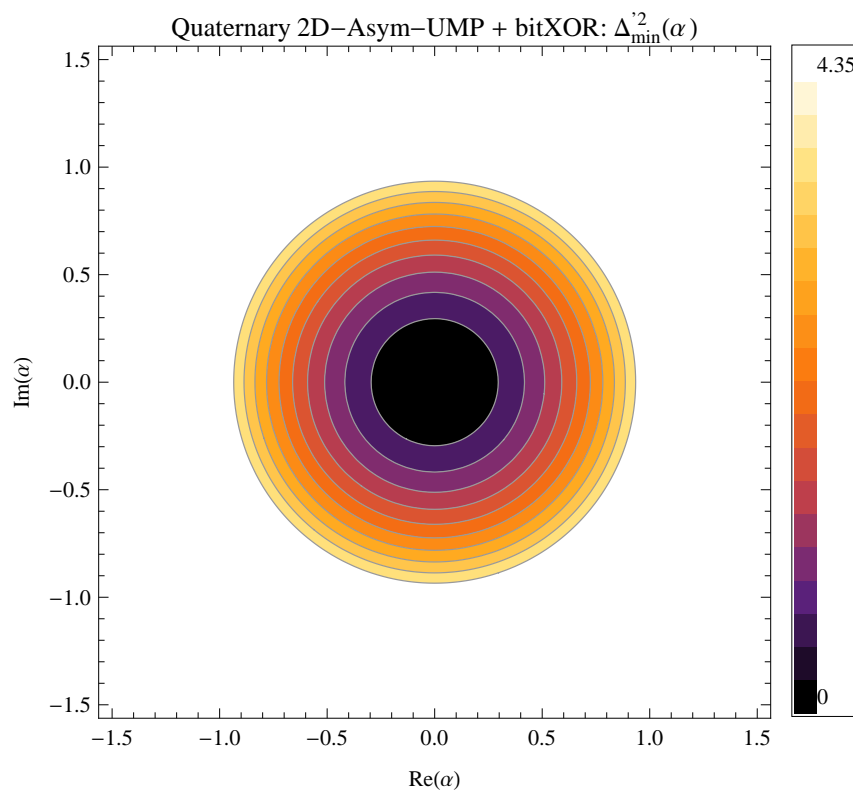


Figure 6.11: Minimal distance  $\Delta_{\min}^{\prime 2}$  of 4-ary 2-D UMP alphabet for case  $\mathcal{A}_A \neq \mathcal{A}_B$ .



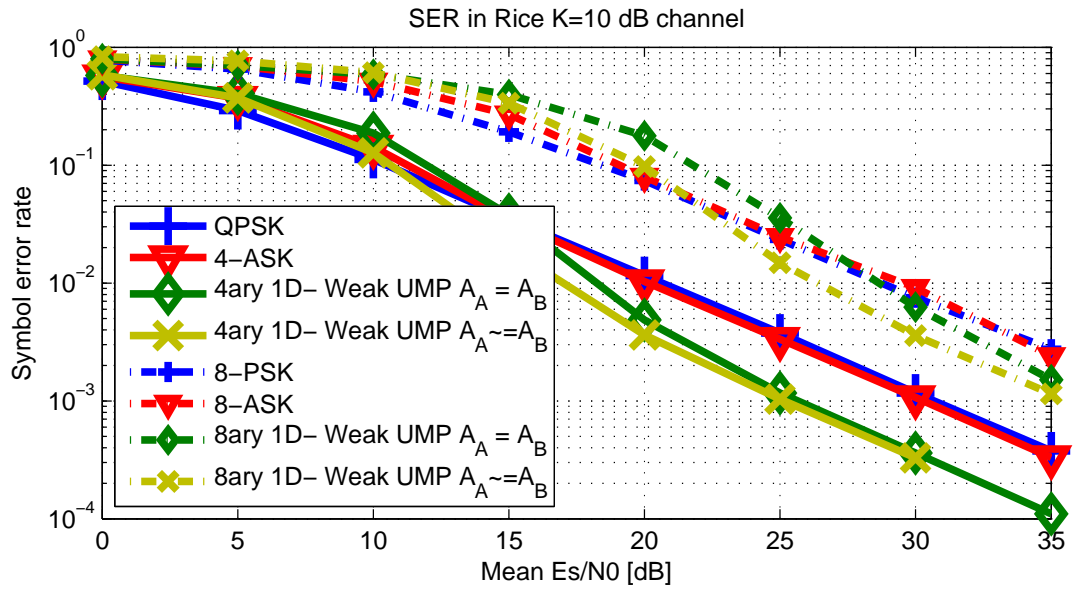


Figure 6.12: Symbol error rate of 4-ary and 8-ary Weak UMP alphabets in Rice  $K = 10$  dB channel.

to w.r.t. PSK/ASK, however they have identical slope of the error curves (diversity). The same slope of the error curves is due to the fact that the weak UMP alphabets possess the singular channel parameters.

## 6.7 Conclusion

We conclude that the numerically optimized non-binary linear alphabets (denoted as weak UMP) perform several dB gain over canonical linear alphabets for HDF 2-way relying with CSIR in Rice fading channels. However, they fulfil only weak UMP condition and thus possess so called singular parameters which still significantly corrupts the performance. We found that the optimized UMP alphabets do not significantly overcome BPSK and their spectral efficiency is limited by 1 bit/complex dimension.

## Chapter 7

# Impact of Relative-Fading in WNC 2-Way Relaying with Diversity Reception

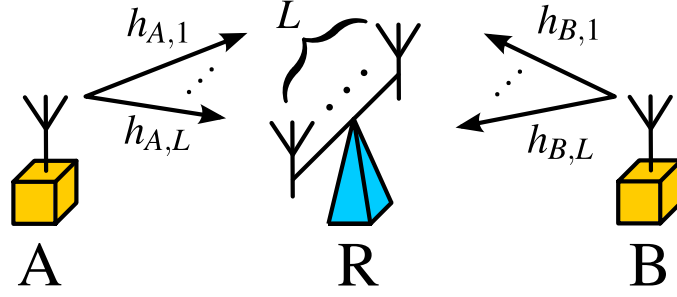
We identify two distinct sources of fading significantly degrading the performance of the WNC 2-way relaying with CSIR: Absolute-Fading (AF) and Relative-Fading (RF). AF corresponds to a standard small-scale fading of a wireless point-to-point channel when absolute values of the channel parameters are insufficiently strong. RF is a unique paradigm of WNC occurring when certain critical data symbols are transmitted and a ratio of channel parameters is close to certain critical values. In this chapter, we show that the diversity reception techniques (essential to restrain AF) significantly suppresses RF as well. We measure the impact of RF on the uncoded error performance and ergodic alphabet-constrained capacity of representative QPSK alphabet in a wireless Rayleigh/Rice channel. We conclude that RF is sufficiently suppressed by systems with a reasonable level of diversity which is typically assumed if only AF is present.

### 7.1 Introduction

#### 7.1.1 Motivation & Related Work

We focus on the WNC scheme with perfect CSIR. Two distinct sources of fading at the MA stage are identified: AF and RF. AF corresponds to a standard small-scale fading of a wireless point-to-point channel when absolute values of channel parameters are insufficiently strong. RF is a unique paradigm of WNC occurring when certain critical data symbols are transmitted and a ratio of channel parameters is close to certain critical singular values regardless of its absolute values.

In this chapter, we study the impact of RF in a diversity reception 2-WRC. We consider diversity reception since it provides an effective way to eliminate fading [11] even if only AF is present. Although we assume a simple Single-Input Multiple-Output (SIMO) scenario, our results hold with other sources of diversity (e.g. in time or frequency). Combination of the spatial diversity systems with WNC have been considered in recent works [82, 83, 84, 59] focusing on beam-forming optimisation, diversity evaluation, transmit diversity and non-coherent approach, respectively. To measure the impact of RF separately from AF, we study behaviour of representative QPSK alphabet in the phase-synchronised scenario and in the scenario with random channel phase difference. QPSK attains the upper-bound on minimal distance (the UMP upper-bound, introduced in chapter 5) and moreover RF is not present if phase synchronisation is provided. We compare the impact of RF on the uncoded error performance and ergodic Alphabet-Constrained Capacity (ACC) (mutual information). We conclude that RF is less significant for systems with reasonable level of diversity which is needed anyway in order to suppress the ubiquitous AF. The major finding of this chapter is to demonstrate that the gain of demanding RF suppressing strategies

Figure 7.1:  $L$ -branch diversity SIMO bidirectional relaying.

[4, 5, 57, 60, 54] in diversity systems is not significant especially with modern near capacity-operating channel codes.

## 7.2 WNC in Diversity SIMO 2-WRC

### 7.2.1 Model Assumptions

We consider a wireless 2-WRC shown in Fig. 7.1 comprising terminals A and B bi-directionally communicating via a supporting relay R in a half-duplex manner (each node cannot send and receive at the same time). The relay is equipped with  $L$  antennas for SIMO diversity reception. We assume a time-synchronised scenario with perfect CSIR. We avoid adaptive techniques [60], [54] due to the increase of system complexity or insufficiently reliable channel estimations [85]. We assume a practical per-symbol low-latency relaying which can be additionally concatenated with linear channel codes according to the network-channel coding separation theorem [51].

### 7.2.2 Signal Space Model

Terminals A and B use a common alphabet  $\mathcal{A}_A = \mathcal{A}_B = \mathcal{A}$  which is assumed to be a canonical linear scheme with the alphabet cardinality  $M = |\mathcal{A}|$  to be a power of two. The baseband signals in the constellation space  $s_T^{(d_T)} \in \mathbb{C}$  forming the alphabet  $\mathcal{A} = \{s_T^{(d_T)}\}_{d_T=0}^{M-1}$  are normalised to unit mean symbol energy. Let  $d_T \in \mathbb{Z}_M = \{0, 1, \dots, (M-1)\}$  be a data symbol transmitted by terminal  $T \in \{A, B\}$ . We assume a memoryless constellation mapper  $\mathcal{M} : \mathbb{Z}_M \rightarrow \mathcal{A}$  such that  $s_T^{(d_T)} = \mathcal{M}(d_T)$ .

### 7.2.3 Bidirectional Relaying based on WNC

Bidirectional relaying based on WNC consists of a MA stage when both terminals transmit simultaneously to the relay with network coded data decoding and a BC stage when the relay broadcasts the previously decoded network coded data symbol. Final destinations perform successful detection exploiting the knowledge of its own data, similarly as in the network coding approach.

#### XOR Operation

Network coded data symbol (denoted as  $d_{AB}$ ) incorporates data from multiple sources via an invertible network coding operation  $\mathcal{N}$  [51]. Throughout this chapter, we consider a *bit-wise XOR* operation  $d_{AB} = \mathcal{N}(d_A, d_B) = d_A \oplus d_B$  since the other invertible operations e.g. *modulo-sum* function does not fulfil certain symmetries (the same symbols on the main diagonal of symmetric Latin square [4]) implying existence of singular parameters and RF.

### MA Stage

Received signal at the  $L$ -antenna relay is

$$\mathbf{x} = \mathbf{h}_A s_A + \mathbf{h}_B s_B + \mathbf{w}, \quad (7.1)$$

where  $\mathbf{w}$  is a complex AWGN with variance  $2N_0$  per-complex dimension, and vector of channel parameters  $\mathbf{h}_T = (h_{T,1}, \dots, h_{T,L})$ ,  $T \in \{A, B\}$  is formed by frequency-flat complex Gaussian uncorrelated random variables with the unit variance and a Rayleigh/Rician distributed envelope. We use Rician factor  $K$  defined as a power ratio between stationary and scattered components. The maximum likelihood decoding of  $d_{AB}$  at the relay

$$\widehat{d}_{AB} = \arg \max_{d_{AB}} p(\mathbf{x}|d_{AB}), \quad (7.2)$$

uses the likelihood function derived in [51]

$$p(\mathbf{x}|d_{AB}) = \frac{1}{M} \sum_{d_A, d_B: d_A \oplus d_B = d_{AB}} p_w(\mathbf{x} - \mathbf{h}_A s_{d_A} - \mathbf{h}_B s_{d_B}), \quad (7.3)$$

where the noise PDF equals to

$$p_w(\mathbf{w}) = \frac{1}{(2\pi N_0)^L} e^{-\|\mathbf{w}\|^2/2N_0}. \quad (7.4)$$

### BC Stage

$R$  broadcasts the network-coded symbol  $d_{AB}$  obtained at the preceding MA stage. Thereafter, final destination  $A$  obtains desired data symbol  $d_B$  with knowledge of  $d_{AB}$  and its own data  $d_A$  as  $d_B = d_{AB} \oplus d_A$  and vice versa for terminal  $B$ .

### Performance Bottleneck

We focus on the challenging MA stage, since it apparently dominates the overall error performance due to the additional multiple access interference.

## 7.3 Minimal Distance Analysis

This section concerns with a performance analysis of WNC based on a minimal distance. The minimal distance analysis is attractive due to the simple mathematical tractability which enables an intuitive description in a simple geometric model, e.g. in which we define AF and RF and observe several important properties. However, the analysis sufficiently describes only the performance of uncoded systems for high SNR. The performance of systems using modern near-capacity operating channel codes (e.g. LDPC, turbo-codes) is influenced by the whole codeword distance spectrum including its multiplicity where the minimal distance description is insufficient [86]. For that reason, we analyse also the ACC curves in Section 7.4.

### 7.3.1 Minimal Distance of WNC

The network-coded symbol decoding error probability at the MA stage is well approximated by a sum of weighted pairwise error probabilities. The pairwise error probability dominating the performance of uncoded system for high SNR is a function of the minimal distance [5].

**Definition 6.** Let the minimal distance respecting bit-wise XOR decoding is defined as

$$\Delta_{\min}^2(\mathbf{h}_A, \mathbf{h}_B) = \min_{d_A \oplus d_B \neq d'_A \oplus d'_B} \|\Delta \mathbf{u}(\mathbf{h}_A, \mathbf{h}_B)\|^2 \quad (7.5)$$

where

$$\Delta \mathbf{u}(\mathbf{h}_A, \mathbf{h}_B) = (\Delta u_1(h_{A,1}, h_{B,1}), \dots, \Delta u_L(h_{A,L}, h_{B,L})) \quad (7.6)$$

is a vector of differences of superimposed constellation space signals  $\Delta u_i(h_{A,i}, h_{B,i}) = h_{A,i}\Delta s_A + h_{B,i}\Delta s_B$ , at the  $i$ th antenna  $i \in \mathbb{Z}_L$  and  $\Delta s_T = s_T^{(d_T)} - s_T^{(d'_T)}$ , denotes the signal difference of terminal  $T \in \{A, B\}$ .

Throughout this chapter, we use the term *minimal distance* to denote minimal distance (7.5). Besides, we use the term *primary minimal distance* to denote the standard minimal distance of terminal alphabet  $\mathcal{A}$  defined as

$$\delta_{\min}^2 = \min_{i \neq j} |s^{(i)} - s^{(j)}|^2, \quad s^{(i)}, s^{(j)} \in \mathcal{A}. \quad (7.7)$$

### 7.3.2 Absolute-Fading and Relative-Fading

Minimal distance (7.5) is parametrised by channel coefficients  $\mathbf{h}_A, \mathbf{h}_B$ . We define a *fading* w.r.t. symbol decoding when the minimal distance drops near-to-zero for some channel realisations as

$$\Delta_{\min}^2(\mathbf{h}_A, \mathbf{h}_B) < \varepsilon \quad (7.8)$$

where  $\varepsilon$  is sufficiently small. Following order-of-magnitude approximation in [11], sufficiently small roughly means  $\varepsilon$  to be inversely proportional to SNR,  $\varepsilon \sim 1/\text{SNR}$ . Notation  $\star < \varepsilon$  denotes  $\star$  being near-to-zero w.r.t. SNR and symbol  $\sim$  means proportionally in order-of-magnitude approximation.

**Definition 7.** *Absolute-Fading (AF)* we define as fading (7.8) providing that  $\|\mathbf{h}_A\| < \varepsilon'$  or  $\|\mathbf{h}_B\| < \varepsilon'$ . In other words, whenever absolute value of any channel is near-to-zero (seriously weak), there will be a high probability of error symbol decision regardless what data symbols were transmitted.

**Definition 8.** *Relative-Fading (RF)* is a non-absolute fading. It is a fading when  $\|\mathbf{h}_A\| > \varepsilon'$  and  $\|\mathbf{h}_B\| > \varepsilon'$ . Non-zero norm channel parameters forcing minimal distance to zero (and so causing RF) which we denoted as singular. Since minimal distance (7.5) compares all possible data symbols, RF fulfilling (7.8) represents error symbol detection only for some critical data symbols pairs. In contrast to AF, the RF phenomenon depends on what data symbols are being transmitted.

**Example 2.** RF can be clearly visualised in a single antenna case  $L = 1$ . The minimal distance is parametrised by scalar values  $h_A, h_B$ . Since we assume CSIR, we may introduce a normalised minimal distance

$$\Delta_{\min}^{\prime 2}(\alpha) = \Delta_{\min}^2(h_A, h_B)/|h_A| = \min_{d_A \oplus d_B \neq d'_A \oplus d'_B} \|\Delta s_A + \alpha \Delta s_B\|^2 \quad (7.9)$$

where channel ratio  $\alpha = h_B/h_A$ . RF can be equivalently described using (7.9) as if  $\Delta_{\min}^{\prime 2}(\alpha) < \varepsilon$  for some  $\alpha$  and  $|h_A| > \varepsilon', |h_B| > \varepsilon'$ . We denote channel parameter ratio  $\alpha = h_B/h_A$  forcing  $\Delta_{\min}^{\prime 2}(\alpha) = 0$  as *singular*. For example, QPSK alphabet and XOR function possess singularities  $\{\pm j, \pm 1 \pm j, \pm 1/2 \pm j/2\}$  as shows Fig. 7.2.

### 7.3.3 Minimal Distance Upper-Bound Suppressing Relative-Fading

**Lemma 12.** *Minimal distance (7.5) is upper-bounded as*

$$\Delta_{\min}^2 \leq \delta_{\min}^2 \min \left\{ \|\mathbf{h}_A\|^2, \|\mathbf{h}_B\|^2 \right\} \quad (7.10)$$

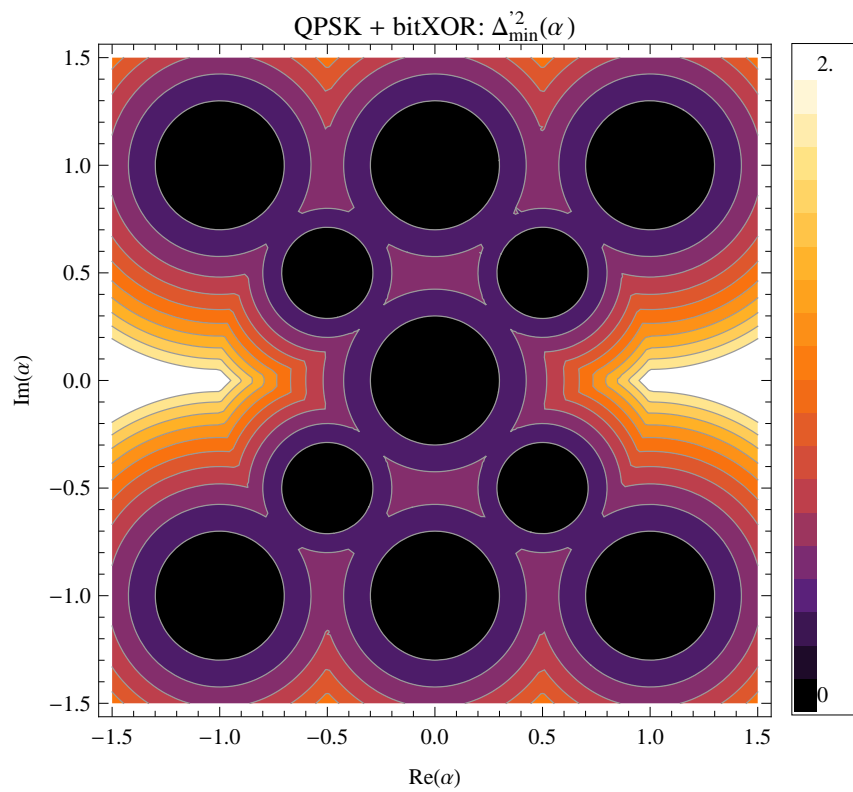
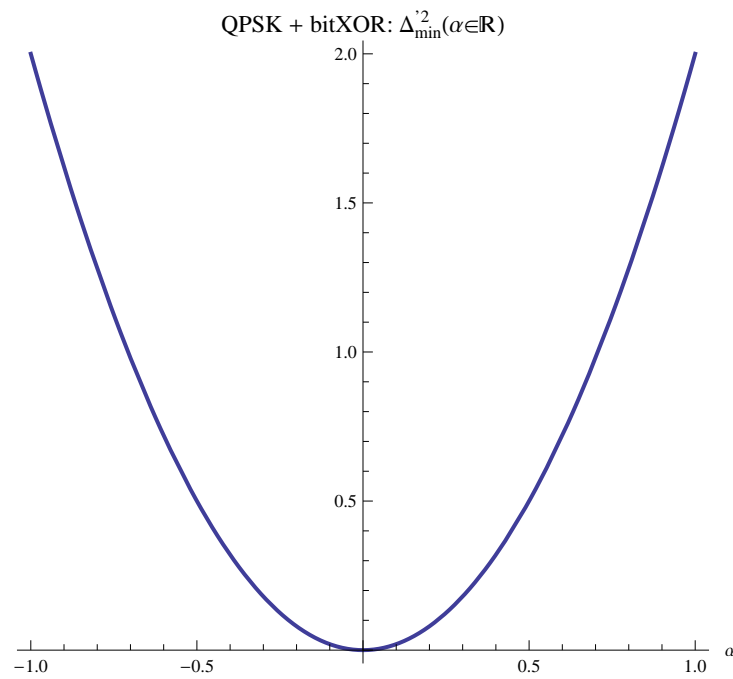
where  $\delta_{\min}^2$  stands for primary minimal distance (7.7).

*Proof.* Bound (7.10) is derived simply by evaluating minimum operation in (7.5) for cases a)  $d_A = d'_A$  and b)  $d_B = d'_B$ . Since we do not evaluate the minimum for all data symbol pairs such that  $d_A \oplus d_B \neq d'_A \oplus d'_B$ , we obtain the inequality. Assuming case a) (resp. b)), (7.5) simplifies to

$$\min_{d_A \oplus d_B \neq d'_A \oplus d'_B, d_A = d'_A} \|\Delta \mathbf{u}\|^2 = \min_{d_B \neq d'_B} \|\mathbf{h}_B \Delta s_B\|^2 = \delta_{\min}^2 \|\mathbf{h}_B\|^2, \quad (7.11)$$

$$\min_{d_A \oplus d_B \neq d'_A \oplus d'_B, d_B = d'_B} \|\Delta \mathbf{u}\|^2 = \min_{d_A \neq d'_A} \|\mathbf{h}_A \Delta s_A\|^2 = \delta_{\min}^2 \|\mathbf{h}_A\|^2, \quad (7.12)$$

respectively. Taking (7.11), (7.12) together gives us the bound (7.10).  $\square$

Figure 7.2:  $\alpha = |\alpha|e^{j\Delta\theta} \in \mathbb{C}$ .Figure 7.3: Cut over real axis  $\alpha \in \mathbb{R}$ ,  $\Delta\theta = 0$ .

*Claim 1.* The alphabets reaching bound (7.10) for all possible channel realisations (denoted as UMP) do not possess any singular channel parameters. It is because the r.h.s. of (7.10) is near-to-zero only if one of the channel norm is near-to-zero. Hence, RF is not present (regardless of transmitted data symbols). As shown in [4], such an alphabet is e.g. BPSK. In contrast, QPSK has several catastrophic parameters (see Fig. 7.2) and does not reach the bound. Surprisingly, it reaches the bound for real channel parameter ratio  $\alpha \in \mathbb{R}$  as shown in Fig. 7.3. *This is a key founding which enables us to independently study the impact of absolute-fading and relative-fading on representative QPSK performance.* AF and RF is present for general complex channel parameters but only AF is present for the real channel parameters (i.e. zero channel phase difference  $\Delta\theta_i = \arg h_{B,i} - \arg h_{A,i} = 0, i \in \mathbb{Z}_L$ ).

*Remark 12.* Since the extended-cardinality network coding mapper cannot cluster data symbols corresponding to  $d_A = d'_A$  or  $d_B = d'_B$  together due to the principle of exclusivity, bound (7.10) holds also for extended-cardinality adaptive network coding approach [54].

## 7.4 Alphabet-Constrained Capacity Analysis

ACC is a mutual information between a discrete-valued uniformly-distributed input (given by the particular modulation alphabet) and an unconstrained-output. It is an information-theoretical tool representing an achievable rate using particular alphabet with the ideal capacity-achieving channel codes [51].

### 7.4.1 Parametric ACC

ACC in WNC SIMO bidirectional relaying is expressed by likelihood functions of network coded symbol decoding (7.3) as

$$C^* = \log_2 M + \frac{1}{M} \int_{\mathbf{x} \in \mathbb{C}^L} \sum_{d_{AB}=1}^M p(\mathbf{x}|d_{AB}) \log_2 \frac{p(\mathbf{x}|d_{AB})}{\sum_{d'_{AB}=1}^M p(\mathbf{x}|d'_{AB})} d\mathbf{x}. \quad (7.13)$$

which is parametrised by channel parameters  $\mathbf{h}_A, \mathbf{h}_B$ .

### 7.4.2 Ergodic ACC

Providing an ergodic observation, ACC averaged over channel parameters  $\mathbf{h}_A, \mathbf{h}_B$  is expressed as

$$\overline{C^*} = \int_{\mathbf{h}_A \in \mathbb{C}^L, \mathbf{h}_B \in \mathbb{C}^L} C^* p(\mathbf{h}_A) p(\mathbf{h}_B) d\mathbf{h}_A d\mathbf{h}_B. \quad (7.14)$$

where  $p(\mathbf{h})$  is PDF of particular channel model. As an illustrative example, let us consider  $L = 1$  for which ergodic  $\overline{C^*}$  in the polar coordinates is

$$\overline{C^*} = \frac{1}{(2\pi)^2} \iiint_{[0, 2\pi]^2 \times [0, \infty]^2} C^*(\rho_A e^{j\theta_A}, \rho_B e^{j\theta_B}) p(\rho_A) p(\rho_B) d\theta_A d\theta_B d\rho_A d\rho_B \quad (7.15)$$

where  $p(\rho)$  is a relevant Rayleigh/Rice distribution. We may save one phase-averaging, supposing

$$|\rho_A e^{j\theta_A} \Delta s_A + \rho_B e^{j\theta_B} \Delta s_B + w| = |\rho_A \Delta s_A + \rho_B e^{j\Delta\theta} \Delta s_B + w'|, \quad (7.16)$$

where the channel phase difference is  $\Delta\theta = \theta_B - \theta_A$  and  $w' = e^{-j\theta_A} w$  is circularly symmetric AWGN with the same statistic as  $w$  and so

$$\overline{C^*} = \frac{1}{2\pi} \iint_{[0, 2\pi] \times [0, \infty]^2} C^*(\rho_A, \rho_B e^{j\Delta\theta}) p(\rho_A) p(\rho_B) d\Delta\theta d\rho_A d\rho_B. \quad (7.17)$$

Similarly, we compute the ergodic ACC for  $L$  higher than 1.

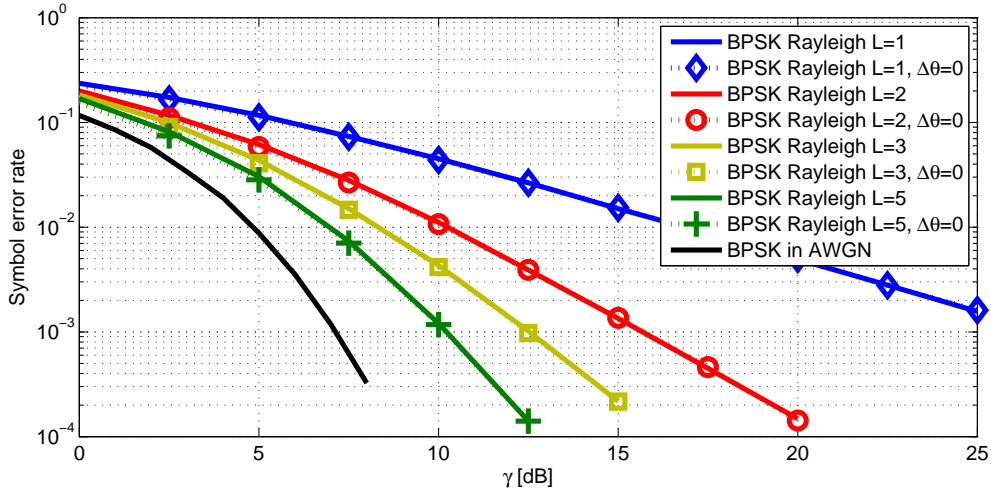


Figure 7.4: SER of BPSK in a SIMO Rayleigh channel.

Table 7.1: The losses of uncoded QPSK error performance (i.e. a gap between performance with  $\Delta\theta$  random and  $\Delta\theta = 0$ ) caused by the relative-fading and the absolute-fading (in dB at SER $10^{-4}$ )

Diversity order $L$	1	2	3	5
RF loss in Rayleigh	2	0.6	0.15	0.1
AF loss in Rayleigh	30.5	13	7.5	4
RF loss in Rice $K = 10$ dB	22.7	8.6	3.8	0.7
AF loss in Rice $K = 10$ dB	6	2.2	1.5	0.7

## 7.5 Numerical Results

Now, we show the uncoded symbol error performance and ergodic ACC of WNC at the MA stage. We assume Rayleigh/Rice  $K = 10$  dB flat fully-interleaved fading channel coefficients to be perfectly known at receivers. The message consists of a sequence of  $N_d = 256$  symbols. The antenna array gain of SIMO is removed from SNR in order to clearly observe the effects of diversity on the performance i.e. SNR is defined as  $\gamma = 1/2N_0L$ . We assume diversity order  $L$  not higher than 2 for ergodic ACC analysis and occasionally we restrict on most interesting SNR range  $[0, 15]$  dB due to the substantial numerical demands. For the sake of numerical stability, we use the Gaussian approximation of Rician PDF in ACC evaluation (7.17) described in [87, p.126].

We consider BPSK and QPSK alphabets and two type of channels: A) real channels with zero phase channel difference  $\Delta\theta = 0$  and B) realistic uniformly distributed  $\Delta\theta$ . BPSK reaches UMP bound (7.10) for all channel parameter values and therefore it performs in the same way for A)  $\Delta\theta = 0$  as well as for B) random  $\Delta\theta$  as confirm SER curves in Fig. 7.4, 7.5 and ACC plots in Fig. 7.8, 7.9.

In contrast to BPSK, QPSK possesses several singular parameters for B) random  $\Delta\theta$  and no singular parameter for A)  $\Delta\theta = 0$  (see Fig. 7.2, 7.3). Tables 7.1, 7.2 present impact of AF and RF on the QPSK performance. We observe in Fig. 7.6 that the impact of RF on the uncoded performance w.r.t. to AF in the Rayleigh channel is negligible. Rician factor  $K$  increases the impact of RF w.r.t. AF as shown in Fig. 7.7. The same trend is observed at ACC in Fig. 7.10, 7.11. The impact of RF on the performance in uncoded case is much higher than in the channel coded case with modern channel codes (described by ACC). Diversity  $L = 5$  (resp.  $L = 2$ ) suppresses the loss of RF under 1 dB for both considered channels in uncoded (resp. ACC) case.



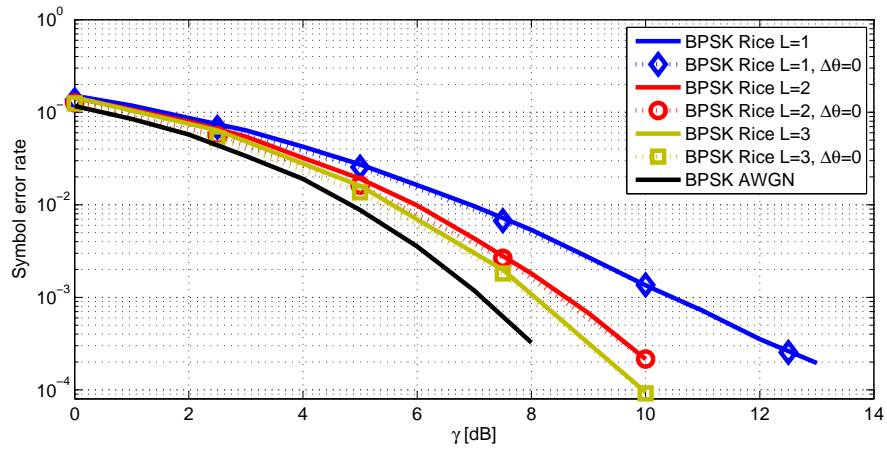


Figure 7.5: SER of BPSK in a SIMO Rice channel.

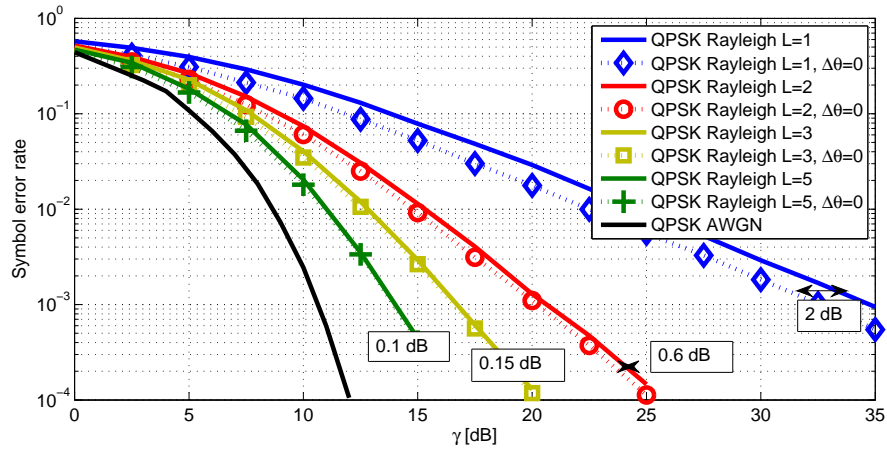


Figure 7.6: SER of QPSK in a SIMO Rayleigh.

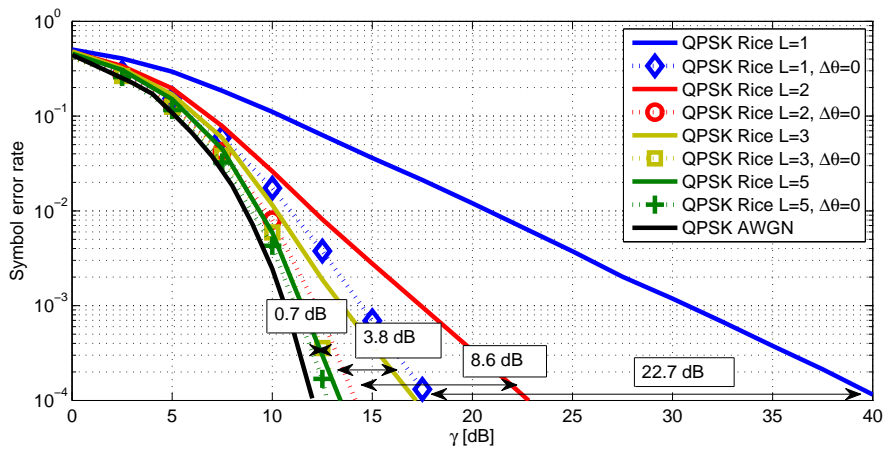


Figure 7.7: SER of QPSK in a SIMO Rice channel.

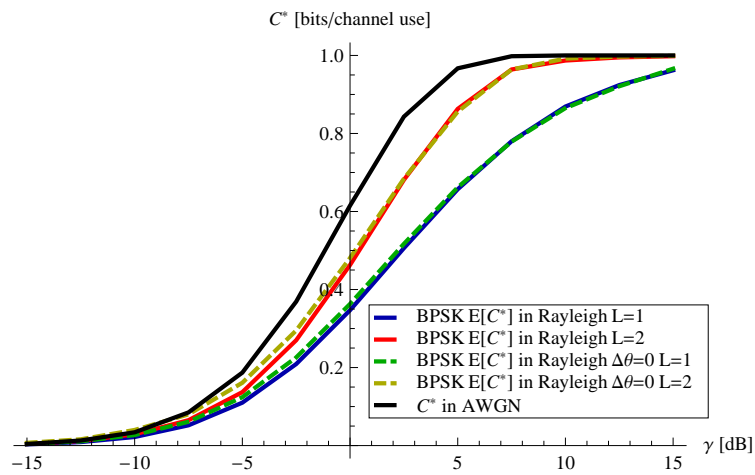


Figure 7.8: ACC of BPSK in a SIMO Rayleigh channel.

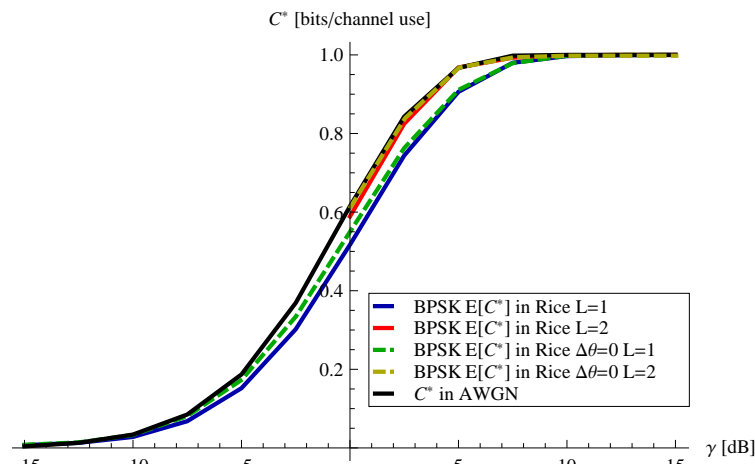


Figure 7.9: ACC of BPSK in a SIMO Rice channel.

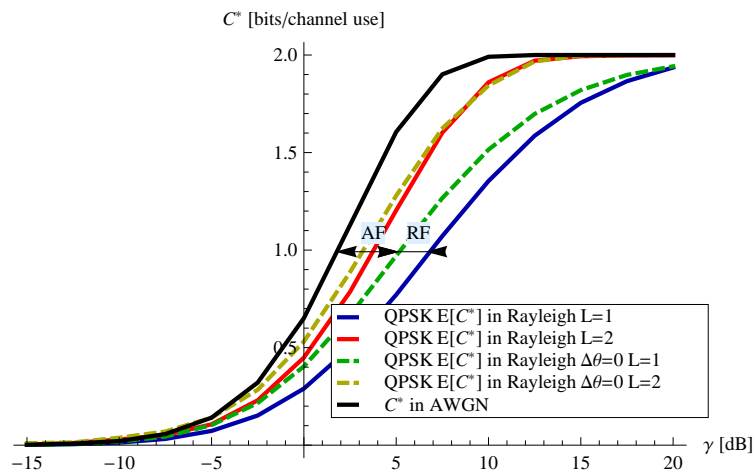


Figure 7.10: ACC of QPSK in a SIMO Rayleigh channel.

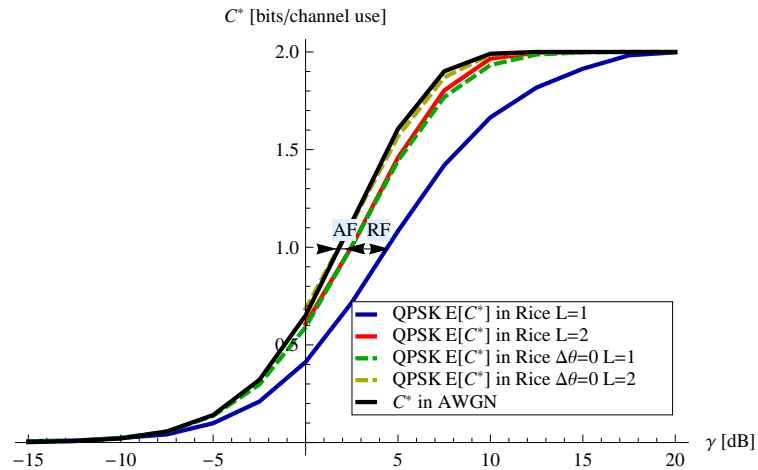


Figure 7.11: ACC of QPSK in a SIMO Rice channel.

Table 7.2: Losses of  $C^*$  of QPSK caused by the relative-fading and the absolute-fading (in dB at rate 1 [bits/channel use]).

Diversity order $L$	1	2
RF loss in Rayleigh	1.75	0.5
AF loss in Rayleigh	3.5	1.5
RF loss in Rice $K = 10$ dB	2	0.75
AF loss in Rice $K = 10$ dB	0.75	0

## 7.6 Conclusion

In this chapter, we have analysed the impact of the relative-fading and the absolute-fading of representative QPSK alphabet in a diversity single-input multiple-output 2-way relay channel with WNC and CSIR. It has been found that the impact of RF w.r.t. AF is more significant in strong line-of-sight (Rician) channels and less significant in Rayleigh channels. The minimal distance analysis as well as uncoded error performance shows that RF is significantly suppressed if diversity order is increased. For example, the losses caused by RF drop under 1 dB or are much lower than AF losses for moderate diversity order  $L = 5$ . The alphabet-constrained capacity analysis, representing the system performance with modern near capacity-operating channel codes, show that the losses caused by RF are much lower than in the uncoded case (below 1 dB even for only diversity  $L = 2$ ). We conclude that demanding RF suppressing approaches [4, 5, 57, 60, 54] do not provide large gains if combined with diversity reception techniques and modern state-of-the-art channel codes.

## Chapter 8

# Optimised Constellation-Prerotation for WNC Relaying in 3-Terminal 1-Relay Network

WNC method is an interference harnessing physical-layer concept combining network coding principles and broadcast nature of the wireless medium. Significant capacity gains of WNC were shown in a wireless 2-WRC. The extension of WNC to more complicated network topologies potentially offers even larger gains than in the 2-WRC. However, such an extension is generally non-trivial.

In this chapter, we show that it is feasible to achieve additional considerable capacity gains in compare to bidirectional relaying approach in a 3-Terminal 1-Relay (3T-1R) network. We focus on the constellation design for its uplink MA stage. The throughput maximisation is achieved by an optimised prerotation of carefully selected source constellations and corresponding network coding functions, effectively reducing the number of required MA stages. We propose ASK and modulo sum operation with  $\pi/3$  prerotation which seems to be a favourable choice for 3T-1R since it keeps the same minimal distance as in the point-to-point case.

## 8.1 Introduction

### 8.1.1 Motivation & Related Work

Extension of WNC to more complicated network topologies has been investigated so far only sparsely. The extension is generally non-trivial, but it offers even larger gains than in the 2-WRC. WNC has been successfully generalised for a “chain” multi-hop and “butterfly” topology [73] and for a “star” topology with multiple bidirectionally communicating pairs sharing the same relay [62]. Concept [62] exploits the overheard conversation between neighbouring terminals providing additional information links. These additional links increase the amount of side-information at the final destinations which allow a stronger compression of information to be broadcast (the number of required BC stages). The compression is covered by the network coding approach respecting the amount of available side-information.

In this chapter, we introduce a novel WNC paradigm which offers higher achievable rates in complex multi-source networks based on a carefully handled multi-source MA stage when the relay decodes a network coded data symbols. Our proposed approach optimises a precoding (prerotation) of source constellations which allows an effective reduction of the number of required MA stages. This approach is demonstrated in a 3T-1R network (see Fig. 8.1). Our proposed approach is applicable to a more general setting especially in combination with the utilization of additional overheard information links [62]. The 3T-1R topology is considered e.g. also in recent related works [88], [89] and [90]. Work [88] optimises resource management of the 3T-1R network considered as two separated 2-WRCs. This scenario serves us as a benchmark model for our proposed method.

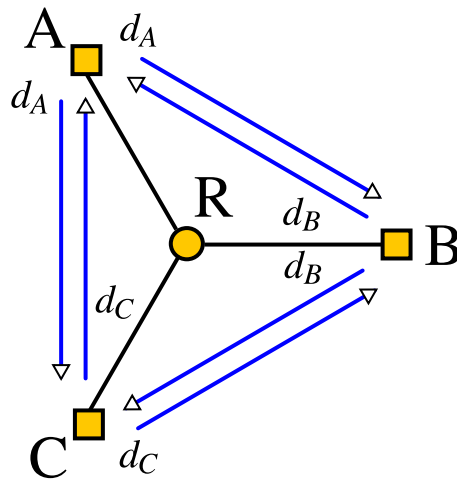


Figure 8.1: Wireless 3T-1R network.

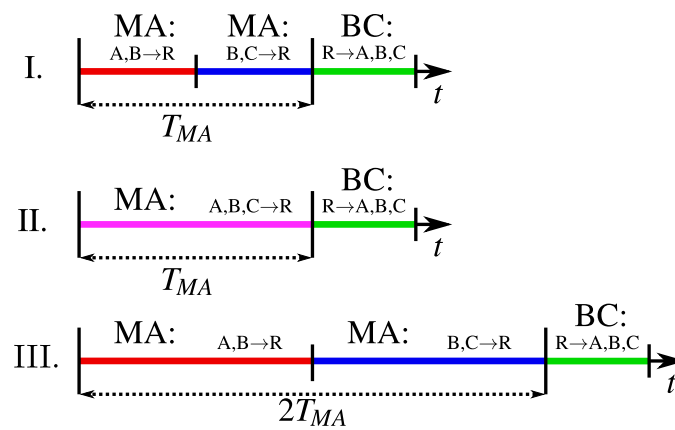


Figure 8.2: I. 2-Stage MA strategy, II. 1-Stage MA strategy and III. 2-Stage MA strategy transmitting the same amount of information as II.

## 8.2 System Model

### 8.2.1 3-Terminal 1-Relay Network

Let us consider the 3T-1R network comprising three terminals  $A, B, C$  communicating in a half-duplex manner via relay  $R$ . Every terminal wishes to send its message to all other terminals; the data-flows, denoted by oriented blue lines in Fig. 8.1, represent e.g. “video-conference” – the nodes are exchanging its common status information. Nonetheless, the aim of our scenario is to simply demonstrate benefits of the WNC-based multi-source (esp. more than 2-source) MA strategy. Unlike in [62], we do not assume a presence of direct links among terminals. Our scenario assumes a time-synchronised low-mobility environment allowing adaptive-precoding strategy [60] inverting the wireless channel fading coefficients and arbitrary setting the constellation prerotation. Further, we assume a per-symbol relaying and we do not consider channel coding which can be additionally concatenated to our scheme [51].

### 8.2.2 Constellation Space Model and Used Notation

The terminals use a common primary alphabet  $\mathcal{A}_A = \mathcal{A}_B = \mathcal{A}_C = \mathcal{A}$  which is assumed to be a canonical linear scheme (ASK, PSK, QAM) with the cardinality of the alphabet  $|\mathcal{A}| = M$  to be a power of two. The baseband signals in the constellation space forming the alphabet  $\mathcal{A} = \{s_T^{(d_T)}\}_{d_T=0}^{M-1}$ , where  $s_T^{(d_T)} \in \mathbb{C}$  are normalised to the unit mean symbol energy. Let  $d_T \in \mathbb{Z}_M = \{0, 1, \dots, (M-1)\}$  be a data symbol transmitted by terminal  $T \in \{A, B, C\}$  to all other terminals. We also assume a memoryless constellation mapper  $\mathcal{M}$  such that  $s_T^{(d_T)} = \mathcal{M}(d_T)$ .

### 8.2.3 Considered MA strategies

We consider two major MA strategies, see Fig. 8.2: I. 2-stage MA strategy and II. 1-stage MA strategy, described later in Sec. 8.3.1 and Sec. 8.3.2, respectively. Since we assume the same symbol duration case I has half the rate than II due to the orthogonal separation of MA stages. Case III is introduced for comparison purposes as it possess the same rate as II, however requiring additional time resources.

## 8.3 WNC Strategy in a 3T-1R Network

Final destinations using WNC in the 3T-1R network (as well as in the 2-WRC) can successfully decode messages from other terminals with knowledge of its own data and network coded data, similarly as in the link-layer network coding approach. Network coded data incorporate data from multiple sources via an invertible network coding function  $\mathcal{N}$  [45]. The typical minimum-cardinality  $\mathcal{N}$  operations are bit-wise XOR

$$d_{AB} = d_A \oplus d_B, \quad (8.1)$$

and modulo- $M$  addition

$$d_{AB} = (d_A + d_B)_{\text{mod}M}. \quad (8.2)$$

The broadcast of network coded data is desirable since it reduces the required amount of information to be broadcast without a loss of performance.

In the 3T-1R, broadcast of  $d_{AB}$  and  $d_{BC}$  is sufficient because the terminal  $A$  obtains desired data  $d_B$  and  $d_C$  with a help of its own data  $d_A$  by the following steps: at first

$$d_B = \mathcal{N}^{-1}(d_{AB}, d_A), \quad (8.3)$$

is decoded followed by

$$d_C = \mathcal{N}^{-1}(d_{BC}, d_B), \quad (8.4)$$

where  $\mathcal{N}^{-1}$  is the inversion of  $\mathcal{N}$ . In a similar way,  $B$  obtains  $d_A = \mathcal{N}^{-1}(d_{AB}, d_B)$  and  $d_C = \mathcal{N}^{-1}(d_{BC}, d_B)$ , and  $C$  obtains  $d_B = \mathcal{N}^{-1}(d_{BC}, d_C)$  and  $d_A = \mathcal{N}^{-1}(d_{AB}, d_B)$ . In this chapter, we focus on the MA strategies where the relay decodes network coded data  $[d_{AB}, d_{BC}]$ .

### 8.3.1 Two-stage MA strategy

The natural extension of WNC for a 3T-1R network would be to separate the 3T-1R network into two separate 2-WRCs i.e. the MA stage would be divided into the two independent stages as appeared e.g. in [88]. At the first stage,  $A$  and  $B$  (resp. at the latter stage  $B$  and  $C$ ) are simultaneously transmitting and  $\hat{d}_{AB}$  (resp.  $\hat{d}_{BC}$ ) are decoded as follows. The adaptive-precoding strategy [60] inverts the channel fading coefficients  $h_A, h_B$  by setting the precoding coefficients to  $p_A = 1/h_A, p_B = 1/h_B$ . The received signal at the relay is

$$x = h_A p_A s_A^{(d_A)} + h_B p_B s_B^{(d_B)} + w = s_A^{(d_A)} + s_B^{(d_B)} + w, \quad (8.5)$$

where  $w$  is a complex AWGN noise with variance  $2N_0$  and frequency-flat coefficients  $h_A$  and  $h_B$  follow appropriate distributions. We suppose an easy-to-implement variant with two-step decoding processing [45]: an estimate of network coded data  $\hat{d}_{AB}$  (and similarly for  $\hat{d}_{BC}$ ) is obtained by 1) the Joint Maximum Likelihood (JML) decoding

$$[\hat{d}_A, \hat{d}_B] = \arg \min_{[d_A, d_B]} \left| x - s_A^{(d_A)} - s_B^{(d_B)} \right|^2 \quad (8.6)$$

followed by 2) the network coding operation  $\hat{d}_{AB} = \mathcal{N}(\hat{d}_A, \hat{d}_B)$ . Note, that by JML we are not able to distinguish e.g.  $[s_A^{(d_A)}, s_B^{(d_B)}] = [1, -1]$  from  $[s_A^{(d_A)}, s_B^{(d_B)}] = [-1, 1]$  when BPSK alphabet is considered. However, it is not a source of errors, since we are interested in decoding of  $\hat{d}_{AB}$  which is in both cases identical and equals to  $\hat{d}_{AB} = 1$ .

### 8.3.2 One-stage MA strategy

In addition to invert the wireless channel coefficients, the adaptive-precoding technique [60] enables prerotation of individual constellations to the desired position as seen at the relay which permits a joint detection of both network coded data symbols  $[d_{AB}, d_{BC}]$  at the single MA stage. Let

$$p_A = 1/h_A, \quad p_B = 1/h_B \exp(j\varphi_1), \quad p_C = 1/h_C \exp(j\varphi_2) \quad (8.7)$$

be the adaptive precoding coefficients together with the proposed constellation prerotations where the alphabet of terminal  $A$  remains fixed and  $B$  alphabet (resp.  $C$ ) is rotated by angle  $\varphi_1$  (resp.  $\varphi_2$ ). The received composite signal is

$$x = s_A^{(d_A)} + s_B^{(d_B)} e^{j\varphi_1} + s_C^{(d_C)} e^{j\varphi_2} + w, \quad (8.8)$$

where  $w$  is a complex AWGN noise with variance  $2N_0$  and  $h_A, h_B, h_C$  are frequency-flat coefficients. The WNC-based network coded data decoding resembles the preceding two-stage case; initial JML yields

$$[\hat{d}_A, \hat{d}_B, \hat{d}_C] = \arg \min_{[d_A, d_B, d_C]} \left| x - s_A^{(d_A)} - s_B^{(d_B)} e^{j\varphi_1} - s_C^{(d_C)} e^{j\varphi_2} \right|^2 \quad (8.9)$$

which is followed by the network coded data encoding

$$[\hat{d}_{AB}, \hat{d}_{BC}] = [\mathcal{N}(\hat{d}_A, \hat{d}_B), \mathcal{N}(\hat{d}_B, \hat{d}_C)]. \quad (8.10)$$

Similarly, an erroneous joint detection (8.9) is error-free as long as it produces correct network coded pair  $[d_{AB}, d_{BC}] = [\hat{d}_{AB}, \hat{d}_{BC}]$ .

### 8.3.3 Optimised Constellation Prerotation for the 1-stage MA Strategy

The prerotation angles  $[\varphi_1, \varphi_2]$  are chosen to maximise the squared minimal Euclidean distance between important signal points of a superimposed (composite) constellation which mostly influences the system error performance for sufficiently high SNR [54]. We define the minimal distance as

$$\Delta_{\min}^2(\varphi_1, \varphi_2) = \min_{[d_{AB}, d_{BC}] \neq [d'_{AB}, d'_{BC}]} \left| u(\varphi_1, \varphi_2) - u'(\varphi_1, \varphi_2) \right|^2 \quad (8.11)$$

Table 8.1: Minimal distances  $\Delta_{\min}^2$  of composite constellations with optimised constellation prerotation  $\hat{\varphi}_1$  for different primary alphabets  $\mathcal{A}$  and network coding function  $\mathcal{N}$ 

$\mathcal{A}$	$\delta_{\min}^2$	$\mathcal{N}$	$\hat{\varphi}_1$	$\Delta_{\min}^2$	$10\log_{10}\left(\frac{\Delta_{\min}^2}{\delta_{\min}^2}\right)$
BPSK	4	XOR	$\pi/3$	4	0
4-ASK	0.8	MOD	$\pi/3$	0.8	0
4-ASK	0.8	XOR	$0.19\pi$	0.088	-9.6
QPSK	2	MOD	$0.097\pi$	0.19	-10.2
QPSK	2	XOR	$0.097\pi$	0.19	-10.2
8-ASK	0.19	MOD	$\pi/3$	0.19	0
8-ASK	0.19	XOR	$0.19\pi$	0.0076	-14
8-PSK	0.56	MOD	$1.21\pi$	0.0089	-18
8-PSK	0.56	XOR	$1.21\pi$	0.0089	-18

to properly respect  $[d_{AB}, d_{BC}]$  decoding from the superimposed constellation, where composite signal is

$$u(\varphi_1, \varphi_2) = s_A^{(d_A)} + s_B^{(d_B)} e^{j\varphi_1} + s_C^{(d_C)} e^{j\varphi_2}, \quad (8.12)$$

and similarly

$$u'(\varphi_1, \varphi_2) = s_A^{(d'_A)} + s_B^{(d'_B)} e^{j\varphi_1} + s_C^{(d'_C)} e^{j\varphi_2}. \quad (8.13)$$

The prerotation angles are set to maximise the minimal distance,

$$[\hat{\varphi}_1, \hat{\varphi}_2] = \arg \max_{[\varphi_1, \varphi_2]} \Delta_{\min}^2(\varphi_1, \varphi_2). \quad (8.14)$$

The numerically obtained results for several alphabets and network coding functions are summarised in Table 8.1. Apparently due to the symmetry of our problem, there are multiple optimal solutions but all of them have the second optimal angle  $\hat{\varphi}_2 = 2\hat{\varphi}_1$ . Acronyms 'XOR' and 'MOD' refer to bit-wise XOR and modulo- $M$  function, respectively. Note that by evaluating of the minimum in (8.11) with fixed  $d_A$  and  $d_B$  and variable  $d_C$ , we obtain the minimal distance of primary alphabet

$$\delta_{\min}^2 = \min_{i \neq j} |s^{(i)} - s^{(j)}|^2. \quad (8.15)$$

Therefore,  $\Delta_{\min}^2$  is naturally upper-bounded by  $\delta_{\min}^2$ . In our notation,  $\delta_{\min}^2$  refers to the minimal distance of primary alphabet  $\mathcal{A}$  while  $\Delta_{\min}^2$  is a minimal distance of the composite alphabet (superposition of three prerotated  $\mathcal{A}$ ) and affected also by the chosen  $\mathcal{N}$ .

The results show that  $M$ -ary  $M$ -ASK, modulo sum operation and  $\pi/3$  prerotation forms the compact hexagonal structure, see Figs. 8.3, 8.4, 8.5, which is favourable since it keeps the same minimal distance as in the point-to-point case  $\Delta_{\min}^2(\hat{\varphi}_1, \hat{\varphi}_2) = \delta_{\min}^2$ .

### 8.3.4 Generalisation for a multi-source network

The extension to multi-source  $N$ -Terminal 1-Relay (NT-1R) network is trivial in the sense that we can always optimise the mutual prerotation of alphabets w.r.t. network coded data decoding. However, we cannot always expect the optimality possessed by the solution in the 3T-1R network ( $\pi/3$  prerotated  $M$ -ASK and modulo sum operation) where by optimality, we mean that minimal distance  $\Delta_{\min}^2$  equals to its upper-bounding minimal distance of primary alphabet  $\delta_{\min}^2$ . The design of the alphabets similarly optimal in an NT-1R network is challenging and apparently it requires a joint design of  $N$  distinct alphabets. Based on this work, we may conjecture that the optimal composite constellation would form some dense lattice-constellation (apparently multi-dimensional) with  $N$ -axis of symmetry, since in 3T-1R the result is the dense hexagonal lattice with 3 axis of symmetry (marked in Fig 8.3 by the dashed lines).



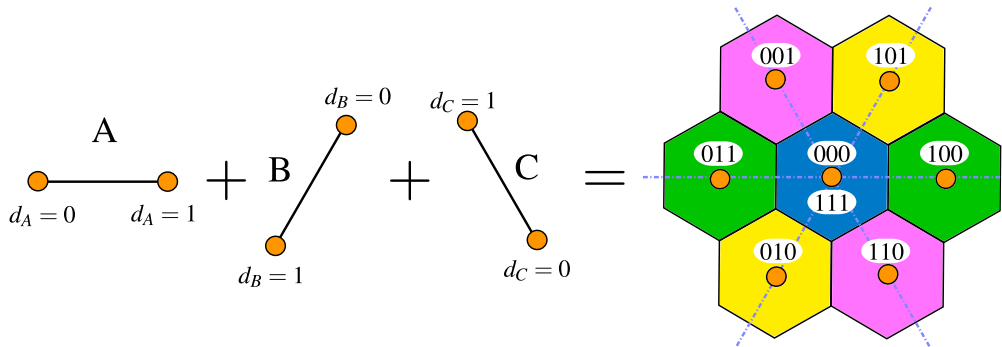


Figure 8.3: Composite constellation of three mutually  $\pi/3$  prerotated BPSK modulations. The interfering signals at the point 0 in the signal space correspond to  $[d_A, d_B, d_C] = [0, 0, 0]$  and  $[1, 1, 1]$ . Since these points lie in the region with identical  $[d_{AB}, d_{BC}]$  (identical colour), it is not a source of errors.

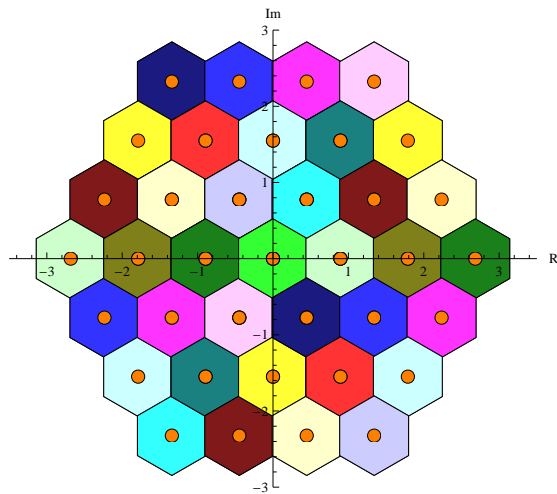


Figure 8.4: Superimposed-constellation of  $\pi/3$  prerotated 4-ASK. Interfering points are not a source of errors because they are clustered in the same coloured region  $[d_{AB}, d_{BC}]$ ; similarly as in Fig. 8.3.

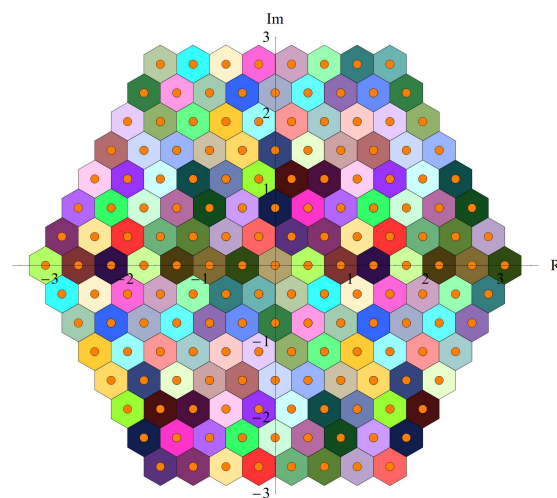


Figure 8.5: Superimposed-constellation of  $\pi/3$  prerotated 8-ASK. Interfering points are not a source of errors because they are clustered in the same coloured region  $[d_{AB}, d_{BC}]$ ; similarly as in Fig. 8.3.

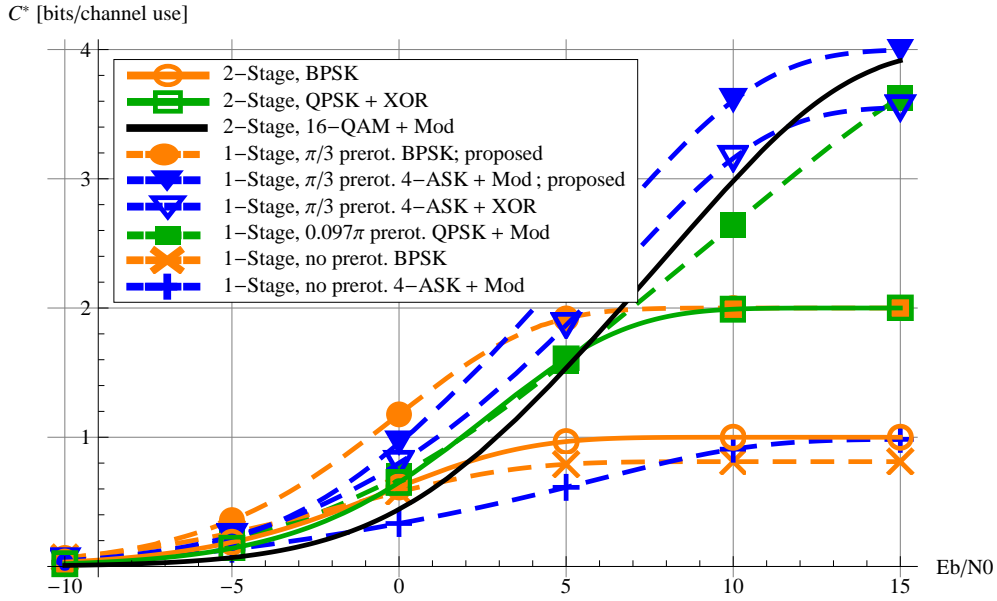


Figure 8.6: Alphabet-constrained capacity curves for several alphabets, network coding operations and mutual prerotations.

## 8.4 Performance Evaluation

In Fig. 8.6, we compare different alphabets in the 1-stage (dashed lines) and the 2-stage (solid lines) MA strategies by its Alphabet-Constrained Capacities (ACC)  $C^*$ . ACC is the information theoretical channel capacity respecting the practical constraints given by the particular alphabet i.e. the capacity with a discrete-valued uniformly-distributed input and an unconstrained output. We numerically evaluate  $C^*$  as the mutual information between uniformly distributed  $[d_{AB}, d_{BC}]$  and the received signal (8.5) for the 2-stage MA strategy and between received signal (8.8) for the 1-stage MA strategy. More detailed description of  $C^*$  evaluation is e.g. in [51]. All wireless links are assumed to have the same SNR for the sake of simplicity. The depicted 2-stage strategies correspond to case I in Fig. 8.2 and attain asymptotically ( $\text{SNR} \rightarrow \infty$ ) only half  $C^*$  of the 1-stage strategy (case II) due to the orthogonal separation of the MA stages (it requires two channel uses to deliver the same amount of information). Reference case III is not depicted in Fig. 8.6, since its capacity is simply the case I capacity multiplied by 2, however, requiring two times more of the temporal-resources. We confirm that the 1-stage MA strategy with optimally prerotated ASK modulations and modulo sum operation performs the highest constrained capacity for given SNR among the other considered strategies.

## 8.5 Conclusion

This work proposes an optimised constellation-prerotation for carefully selected constellations and network coding functions for the WNC-based strategy in the 3T-1R network. It effectively reduces the number of MA stages resulting in the considerable capacity gains. We believe that the proposed paradigm is applicable in general settings attractive especially in combination with the utilization of additional overhead information links as pointed out in [62]. Our proposed approach exploits the knowledge of network topology, data-flows and channel adaptation technique.

## Chapter 9

# Conclusion

This thesis is concerned with a modulation design for the emerging wireless network architecture denoted as Wireless Network Coding (WNC). The modulation design topic is challenging even in the simplest possible network scenario – a 2-Way Relay Channel (2-WRC) which is our most assumed scenario. The reason is that unlike in the standard point-to-point communication, the WNC method works with a signal superposition where a crucial impact on the overall performance possess also a network coding function used by the relay (relay processing in general). Moreover, there are considerably more possibilities of mutual distributed synchronisation among the nodes including the quality of Channel State Information (CSI). Generally, there is a larger amount of parameters significantly influencing the system performance than in the point-to-point communication.

We see a great potential of our work considering the affine-indexed lattice-constellations with modulo-sum relay decoding [2]. This contribution is rather theoretical one, but due to its simple analytical results, it provides a very useful theoretical tool. As far as we know, the modulations and network coding functions have been so far designed only numerically, particularly, by suboptimal greedy clustering algorithm [54] or by the algorithm filling a partially-filled Latin squares [38] (it is an NP hard algorithm very similar to the algorithm solving a Sudoku game). It can provide a solution only for reasonably large constellation alphabets. In our approach, we are always sure that the modulo-sum function is decodable at the relay as long as all lattice-constellations are affine-indexed. We believe that the lattice-constellations are naturally suitable for the modulo-sum decoding also in a general network topology because a superposition of any number of constellations taken from the same lattice is again a point in that lattice. It is very convenient that we can describe both domains mixed by WNC (i.e. the continuous signal space of physical-layer and the discrete integer space of network coding) by a common algebraic structure (by lattice-coordinate integer vectors).

We have successfully utilised the discovered properties of the affine-indexed lattice-constellations with modulo-sum relay decoding and based on them we find a 4HEX constellation suitable for adaptive WNC strategy [1]. Our proposed 4HEX constellation is probably the most practical contribution suitable for real implementation. In addition, the adaptive WNC with 4HEX uses the bit-wise XOR function which enables a simplified relay processing (requiring a linear network coding function).

The considerable part of our work studies the negative impact of the relative-fading. We have found the frequency multi-dimensional modulations robust to the relative-fading [4]. These modulations are beneficial especially when also the constant envelope property is demanded (e.g. in low-cost receivers or satellite communication). Our analysis of a general design of Uniformly Most Powerful (UMP) alphabets reveals that we cannot entirely eliminate the relative-fading by a suitable alphabet design when a spectral-efficiency is higher than 1 bit/dimension [5]. In that case, we can find alphabets (denoted as weak UMP) with better performance than standard QAM, PSK but still the proposed modulations perform considerably worst than the utmost UMP scheme. The obstacle of the relative-fading seems to be practically solved when some level of diversity is assumed [6]. Either the environment is so static that we can effort some form of adaptation eliminating the relative-fading or the environment is so dynamic that a rich source of temporal or frequency diversity is available. Our analysis shows that the relative-fading has significantly lower negative impact when enough diversity is provided (diversity is employed anyway

if only standard absolute-fading is present).

WNC in a 2-WRC is both theoretically as well as practically quite well understood but the generalisation of WNC into a more complex network topology is still an open problem. We have identified another potential source of gains based on the optimisation of the multiple-access stage in [3]. The future direction of the WNC research must contain an issue of WNC generalisation in order to provide a complete network architecture based on WNC. So far, the generalisation is strongly dependent on the assumed topology and there is no general concept how to scale WNC into a whatever network size. Certainly, the most important question is whether WNC can still provide the best performance in such a general wireless network as it can provide in a 2-WRC. This essential problem needs to be addressed and answered also by means of measured gains in the real scenario simulation which includes e.g. overall overheads due to the distributed synchronisation assumptions. The future steps should focus on a mutual time asynchronisation which forbid the constellation space model (widely assumed in our work). We believe that also a deeper analysis deserves paper [63] which states that in some cases (like unidirectional relay multiple access channel) the WNC strategy does not have to provide the best throughput so the future work should definitely aim at a more careful analysis of Complex-Field Network Coding (CFNC) w.r.t. the WNC strategy.

# Bibliography

- [1] M. Hekrdla and J. Sykora, “Hexagonal constellations for adaptive physical-layer network coding 2-way relaying,” *under resubmission to Communications Letters, IEEE*.
- [2] —, “On indexing of lattice-constellations for wireless network coding with modulo-sum decoding,” in *Proc. IEEE Vehicular Technology Conf. (VTC)*, 2013. [Online]. Available: [http://radio.feld.cvut.cz/~sykora/publications/papers/Hekrdla-Sykora\\_2013-VTC-S.pdf](http://radio.feld.cvut.cz/~sykora/publications/papers/Hekrdla-Sykora_2013-VTC-S.pdf)
- [3] —, “Optimised constellation prerotation for 3-terminal 1-relay network with wireless network coding,” *Communications Letters, IEEE*, vol. 16, no. 8, pp. 1200–1203, august 2012. [Online]. Available: [http://radio.feld.cvut.cz/~sykora/publications/papers/Hekrdla-Sykora\\_2012-IEEE-L-COM.pdf](http://radio.feld.cvut.cz/~sykora/publications/papers/Hekrdla-Sykora_2012-IEEE-L-COM.pdf)
- [4] —, “Design of uniformly most powerful alphabets for HDF 2-way relaying employing non-linear frequency modulations,” *EURASIP J. on Wireless Comm. and Netw.*, vol. 128, pp. 1–18, October 2011. [Online]. Available: [http://radio.feld.cvut.cz/~sykora/publications/papers/Hekrdla-Sykora\\_2011-EURASIP-J-WCN.pdf](http://radio.feld.cvut.cz/~sykora/publications/papers/Hekrdla-Sykora_2011-EURASIP-J-WCN.pdf)
- [5] —, “Uniformly most powerful alphabet for HDF two-way relaying designed by non-linear optimization tools,” in *Wireless Communication Systems (ISWCS), 2011 8th International Symposium on*, nov. 2011, pp. 594–598.
- [6] —, “Suppression of relative-fading by diversity reception in wireless network coding 2-way relaying,” in *COST IC1004 MCM*, Lyon, France, May 2012, pp. 1–8, TD-12-04033.
- [7] T. M. Cover and J. A. Thomas, *Elements of Information Theory*, 2nd ed. John Wiley & Sons, 1991.
- [8] C. E. Shannon, “A mathematical theory of communication,” *The Bell System Technical Journal*, vol. 27, pp. 379–423, 623–, july, october 1948.
- [9] G. Forney and D. Costello, “Channel coding: The road to channel capacity,” *Proc. IEEE*, vol. 95, no. 6, pp. 1150–1177, june 2007.
- [10] A. Burr, “Turbo-codes: The ultimate error control codes?” *Electronics and Communications Engineering Journal*, vol. 13, no. 4, pp. 155–165, 2001.
- [11] D. Tse and P. Viswanath, *Fundamentals of wireless communication*. New York, NY, USA: Cambridge University Press, 2005.
- [12] E. Biglieri, J. Proakis, and S. S. (Shitz), “Fading channels: Information-theoretic and communications aspects,” *IEEE Trans. Inf. Theory*, vol. IT-44, no. 6, pp. 2619–2692, Oct. 1998.
- [13] Y. Polyanskiy, H. Poor, and S. Verdú, “Channel coding rate in the finite blocklength regime,” *IEEE Trans. Inf. Theory*, vol. 56, no. 5, pp. 2307–2359, may 2010.
- [14] M. Dohler, R. Heath, A. Lozano, C. Papadias, and R. Valenzuela, “Is the PHY layer dead?” *IEEE Commun. Mag.*, vol. 49, no. 4, pp. 159–165, april 2011.

- [15] A. Goldsmith, M. Effros, R. Koetter, M. Medard, A. Ozdaglar, and L. Zheng, “Beyond Shannon: The quest for fundamental performance limits of wireless ad hoc networks,” *IEEE Commun. Mag.*, vol. 49, no. 5, pp. 195–205, may 2011.
- [16] F. Xue and P. R. Kumar, “Scaling laws for ad hoc wireless networks: An information theoretic approach,” in *Foundations and Trends in Networking*. Now Publishers, 2006, pp. 16–47.
- [17] V. Cadambe and S. Jafar, “Interference alignment and degrees of freedom of the K-user interference channel,” *IEEE Trans. Inf. Theory*, vol. 54, no. 8, pp. 3425–3441, aug. 2008.
- [18] M. Dohler and Y. Li, *Cooperative communications: Hardware, channel and PHY*. John Wiley & Sons, 2010.
- [19] R. Ahlswede, N. Cai, S.-Y. R. Li, and R. W. Yeung, “Network information flow,” *IEEE Trans. Inf. Theory*, vol. 46, no. 4, pp. 1204–1216, Jul. 2000.
- [20] D. Tse, “It is easier to approximate,” in *Proc. IEEE Internat. Symp. on Inf. Theory (ISIT), 2009, plenary talk*, march 2010.
- [21] R. Koetter, M. Effros, and M. Medard, “A theory of network equivalence part I: Point-to-point channels,” *IEEE Trans. Inf. Theory*, vol. 57, no. 2, pp. 972–995, feb. 2011.
- [22] R. Zamir, “Lattices are everywhere,” in *Inf. Theory and App. Workshop (ITA), San Diego*, 2009.
- [23] J. Conway, N. Sloane, and E. Bannai, *Sphere packings, lattices, and groups*. Springer, 1999.
- [24] N. Sommer, M. Feder, and O. Shalvi, “Low-density lattice codes,” *Information Theory, IEEE Transactions on*, vol. 54, no. 4, pp. 1561–1585, 2008.
- [25] J. Andrews, S. Shakkottai, R. Heath, N. Jindal, M. Haenggi, R. Berry, D. Guo, M. Neely, S. Weber, S. Jafar, and A. Yener, “Rethinking information theory for mobile ad hoc networks,” *IEEE Commun. Mag.*, vol. 46, no. 12, pp. 94–101, december 2008.
- [26] C. Fragouli, J.-Y. Le Boudec, and J. Widmer, “Network coding: An instant primer,” *Proc. ACM Signal Commun. (SIGCOMM)*, vol. 36, no. 1, pp. 63–68, Jan. 2006.
- [27] M. Medard and A. Sprintson, *Network Coding: Fundamentals and Applications*. Academic Press, 2011.
- [28] R. W. Yeung, S.-Y. R. Li, N. Cai, and Z. Zhang, *Network Coding Theory*. now Publishers, 2006.
- [29] R. W. Yeung, *Information Theory and Network Coding*. Springer, 2008.
- [30] R. Yeung, “Network coding: A historical perspective,” *Proc. IEEE*, vol. 99, no. 3, pp. 366–371, march 2011.
- [31] S.-Y. Li, R. Yeung, and N. Cai, “Linear network coding,” *IEEE Trans. Inf. Theory*, vol. 49, no. 2, pp. 371–381, feb. 2003.
- [32] T. Ho, M. Medard, R. Koetter, D. Karger, M. Effros, J. Shi, and B. Leong, “A random linear network coding approach to multicast,” *IEEE Trans. Inf. Theory*, vol. 52, no. 10, pp. 4413–4430, oct. 2006.
- [33] C. Fragouli, “Network coding: Beyond throughput benefits,” *Proc. IEEE*, vol. 99, no. 3, pp. 461–475, march 2011.
- [34] R. Dougherty, C. Freiling, and K. Zeger, “Insufficiency of linear coding in network information flow,” *IEEE Trans. Inf. Theory*, vol. 51, no. 8, pp. 2745–2759, aug. 2005.
- [35] R. Koetter and M. Medard, “An algebraic approach to network coding,” *IEEE Trans. Networking*, vol. 11, no. 5, pp. 782–795, oct. 2003.

- [36] S. Katti, H. Rahul, W. Hu, D. Katabi, M. Medard, and J. Crowcroft, “XORs in the air: Practical wireless network coding,” *IEEE Trans. Networking*, vol. 16, pp. 497 – 510, June 2008.
- [37] C. Fragouli, D. Katabi, A. Markopoulou, M. Medard, and H. Rahul, “Wireless network coding: Opportunities and challenges,” in *Proc. IEEE Military Communications Conference (MILCOM)*, oct. 2007, pp. 1 – 8.
- [38] V. Namboodiri, V. Muralidharan, and B. Rajan, “Wireless bidirectional relaying and latin squares,” in *Proc. IEEE Wireless Commun. Network. Conf. (WCNC)*, april 2012, pp. 1404 –1409.
- [39] P. Popovski and H. Yomo, “The anti-packets can increase the achievable throughput of a wireless multi-hop network,” in *Proc. IEEE Internat. Conf. on Commun. (ICC)*, vol. 9, jun. 2006, pp. 3885 – 3890.
- [40] S. Zhang, S. Liew, and P. Lam, “Hot topic: Physical layer network coding,” in *ACM MOBICOM*, Los Angeles, sept 2006.
- [41] B. Nazer and M. Gastpar, “Computing over multiple-access channels with connections to wireless network coding,” in *Proceedings of the 2006 International Symposium on Information Theory (ISIT 2006)*, Seattle, WA, July 2006.
- [42] —, “Reliable physical layer network coding,” *Proc. IEEE*, vol. 99, no. 3, pp. 438 –460, march 2011.
- [43] P. Popovski and T. Koike-Akino, “Coded bidirectional relaying in wireless networks,” in *Advances in Wireless Communications*, V. Tarokh, Ed. Springer, 2009.
- [44] S. C. Liew, S. Zhang, and L. Lu, “Physical-layer network coding: Tutorial, survey, and beyond,” *in press, Physical Communication*, 2012. [Online]. Available: <http://arxiv.org/ftp/arxiv/papers/1105/1105.4261.pdf>
- [45] J. Sykora and A. Burr, “Wireless network coding: Network coded modulation in the network aware PHY layer,” in *Proc. IEEE Wireless Commun. Network. Conf. (WCNC)*, Cancun, Mexico, March 2011, tutorial.
- [46] S. Katti, S. Gollakota, and D. Katabi, “Embracing wireless interference: Analog network coding,” in *Proc. ACM Signal Commun. (SIGCOMM)*, 2007.
- [47] P. Popovski and H. Yomo, “Physical network coding in two-way wireless relay channels,” in *Proc. IEEE Internat. Conf. on Commun. (ICC)*, june 2007.
- [48] M. Wilson, K. Narayanan, H. Pfister, and A. Sprintson, “Joint physical layer coding and network coding for bidirectional relaying,” *IEEE Trans. Inf. Theory*, vol. 56, no. 11, pp. 5641 –5654, nov. 2010.
- [49] K. Lu, S. Fu, Y. Qian, and H.-H. Chen, “On capacity of random wireless networks with physical-layer network coding,” *IEEE J. Sel. Areas Commun.*, vol. 27, no. 5, pp. 763 –772, june 2009.
- [50] B. Nazer and M. Gastpar, “Compute-and-forward: Harnessing interference through structured codes,” *IEEE Trans. Inf. Theory*, vol. 57, no. 10, pp. 6463 –6486, oct. 2011.
- [51] J. Sykora and A. Burr, “Layered design of hierarchical exclusive codebook and its capacity regions for HDF strategy in parametric wireless 2-WRC,” *IEEE Trans. Veh. Technol.*, vol. 60, no. 7, pp. 3241–3252, Sep. 2011.
- [52] D. Wübben and Y. Lang, “Generalized sum-product algorithm for joint channel decoding and physical-layer network coding in two-way relay systems,” in *Proc. IEEE Global Telecommun. Conf. (GlobeCom)*, 2010, pp. 1–5.

- [53] S. Zhang and S.-C. Liew, "Channel coding and decoding in a relay system operated with physical-layer network coding," *IEEE J. Sel. Areas Commun.*, vol. 27, no. 5, pp. 788–796, jun. 2009.
- [54] T. Koike-Akino, P. Popovski, and V. Tarokh, "Optimized constellations for two-way wireless relaying with physical network coding," *IEEE J. Sel. Areas Commun.*, vol. 27, no. 5, pp. 773–787, Jun. 2009.
- [55] —, "Denoising strategy for convolutionally-coded bidirectional relaying," in *Proc. IEEE Internat. Conf. on Commun. (ICC)*, 2009.
- [56] T. Koike-Akino, "Adaptive network coding in two-way relaying MIMO systems," in *Proc. IEEE Global Telecommun. Conf. (GlobeCom)*, Miami, USA, Dec. 2010.
- [57] T. Uricar and J. Sykora, "Non-uniform 2-slot constellations for bidirectional relaying in fading channels," *Communications Letters, IEEE*, vol. 15, no. 8, pp. 795–797, august 2011. [Online]. Available: [http://radio.feld.cvut.cz/~sykora/publications/papers/Uricar-Sykora\\_2011-IEEE-L-COM.pdf](http://radio.feld.cvut.cz/~sykora/publications/papers/Uricar-Sykora_2011-IEEE-L-COM.pdf)
- [58] J. Sørensen, R. Krigslund, P. Popovski, T. Akino, and T. Larsen, "Physical layer network coding for FSK systems," *IEEE Commun. Lett.*, vol. 13, no. 8, pp. 597–599, august 2009.
- [59] T. Koike-Akino and P. Orlik, "Non-coherent grassmann TCM design for physical-layer network coding in bidirectional MIMO relaying systems," in *Proc. IEEE Internat. Conf. on Commun. (ICC)*, june 2011, pp. 1–5.
- [60] T. Koike-Akino, P. Popovski, and V. Tarokh, "Adaptive modulation and network coding with optimized precoding in two-way relaying," *Proc. IEEE Global Telecommun. Conf. (GlobeCom)*, pp. 1–6, nov. 2009.
- [61] L. Lu, S. C. Liew, and S. Zhang, "Optimal decoding algorithm for asynchronous physical-layer network coding," in *Proc. IEEE Internat. Conf. on Commun. (ICC)*, june 2011, pp. 1–6.
- [62] J. H. Sørensen, R. Krigslund, P. Popovski, T. Akino-Koike, and T. Larsen, "Scalable DeNoise-and-Forward in bidirectional relay networks," *Computer Networks*, vol. 54, pp. 1607–1614, July 2010.
- [63] T. Wang and G. Giannakis, "Complex field network coding for multiuser cooperative communications," *IEEE J. Sel. Areas Commun.*, vol. 26, no. 3, pp. 561–571, april 2008.
- [64] L. Lu, T. Wang, S. C. Liew, and S. Zhang, "Implementation of physical-layer network coding," in *Proc. IEEE Internat. Conf. on Commun. (ICC)*, june 2012, pp. 4734–4740.
- [65] J. Forney, G., R. Gallager, G. Lang, F. Longstaff, and S. Qureshi, "Efficient modulation for band-limited channels," *IEEE J. Sel. Areas Commun.*, vol. 2, no. 5, pp. 632–647, sep 1984.
- [66] T. Koike-Akino and V. Tarokh, "Sphere packing optimization and EXIT chart analysis for multi-dimensional QAM signaling," in *Proc. IEEE Internat. Conf. on Commun. (ICC)*, june 2009, pp. 1–5.
- [67] L. Lu and S. C. Liew, "Asynchronous physical-layer network coding," *IEEE Trans. Wireless Commun.*, vol. 11, no. 2, pp. 819–831, february 2012.
- [68] J. Forney, G.D. and G. Ungerboeck, "Modulation and coding for linear gaussian channels," *IEEE Trans. Inf. Theory*, vol. 44, no. 6, pp. 2384–2415, oct 1998.
- [69] S. Benedetto and E. Biglieri, *Principles of digital transmission with wireless applications*. New York, NY, USA: Kluwer Academic Publishers, 2002.
- [70] M. Valenti, D. Torrieri, and T. Ferrett, "Noncoherent physical-layer network coding using binary CPFSK modulation," in *Proc. IEEE Military Communications Conference (MILCOM)*, oct. 2009, pp. 1–7.



- [71] O. Simeone, U. Spagnolini, Y. Bar-Ness, and S. Strogatz, "Distributed synchronization in wireless networks," *IEEE Signal Process. Mag.*, vol. 25, no. 5, pp. 81 – 97, sep. 2008.
- [72] S. Zhang, S. C. Liew, and H. Wang, "Synchronization analysis in physical layer network coding," *CoRR*, vol. abs/1001.0069, 2010. [Online]. Available: <http://arxiv.org/ftp/arxiv/papers/1001/1001.0069.pdf>
- [73] J. Sykora and A. Burr, "Network coded modulation with partial side-information and hierarchical decode and forward relay sharing in multi-source wireless network," in *Proc. European Wireless Conf. (EW)*, Lucca, Italy, April 2010, pp. 639 –645.
- [74] B. D. McKay and I. M. Wanless, "On the number of latin squares," *Ann. Combin.*, vol. 9, pp. 335–344, 2005.
- [75] S. M. Kay, *Fundamentals of Statistical Signal Processing: Detection Theory*. Prentice-Hall, 1998.
- [76] J. Anderson, C.-E. Sundberg, and T. Aulin, *Digital Phase Modulation*. Springer, 1986.
- [77] B. E. Rimoldi, "A decomposition approach to CPM," *IEEE Trans. Inf. Theory*, vol. 34, no. 2, pp. 260–270, Mar. 1988.
- [78] F. Amoroso, "Pulse and spectrum manipulation in the minimum (frequency) shift keying (msk) format," *IEEE Trans. Commun.*, vol. 24, no. 3, pp. 381 – 384, Mar. 1976.
- [79] S. Boyd and L. Vandenberghe, *Convex Optimization*. New York, NY, USA: Cambridge University Press.
- [80] M. Avriel, *Nonlinear Programming*. New York, NY, USA: Dover Publications, 2003.
- [81] T. Uricar and J. Sykora, "Design criteria for hierarchical exclusive code with parameter-invariant decision regions for wireless 2-way relay channel," *EURASIP Journal on Wireless Communications and Networking*, vol. 2010, pp. 1–13, 2010, article ID 921427.
- [82] J. Sykora and E. A. Jorswieck, "Network coded modulation with HDF strategy and optimized beamforming in 2-source 2-relay network," in *Proc. IEEE Vehicular Technology Conf. (VTC)*, San Francisco, USA, Sept. 2011, pp. 1–6.
- [83] H. Gao, X. Su, and T. Lv, "Combined MRC-like reception and transmit diversity for physical-layer network coding with multiple-antenna relay," in *Proc. Internat. Conference on Telecommun. (ICT)*, may 2011, pp. 304 –308.
- [84] A. Khina, Y. Kochman, and U. Erez, "Physical-layer MIMO relaying," in *Proc. IEEE Internat. Symp. on Inf. Theory (ISIT)*, 31 2011-aug. 5 2011, pp. 2437 –2441.
- [85] K. Yasami, A. Razi, and A. Abedi, "Analysis of channel estimation error in physical layer network coding," *IEEE Commun. Lett.*, vol. 15, no. 10, pp. 1029 –1031, october 2011.
- [86] E. Biglieri, *Coding for wireless channels*. Springer, 2005.
- [87] G. Durgin, *Space-Time Wireless Channels*. NJ, USA: Prentice-Hall, 2002.
- [88] Y. Jeon, Y.-T. Kim, M. Park, and I. Lee, "Opportunistic scheduling for three-way relay systems with physical layer network coding," in *Proc. IEEE Vehicular Technology Conf. (VTC)*, may 2011, pp. 1 –5.
- [89] K. Anwar and T. Matsumoto, "Iterative spatial demapping for simultaneous full data exchange in three-way relaying channels," in *COST IC1004 MCM*, Barcelona, Spain, May 2012, tD(12)03073.
- [90] T. Cui, T. Ho, and J. Kliewer, "Space-time communication protocols for n-way relay networks," in *Proc. IEEE Global Telecommun. Conf. (GlobeCom)*, dec. 2008, pp. 1 –5.

# Curriculum Vitae

I was born in 1983 in Prague, the Czech Republic.

## Current Position:

- PhD Associate at Czech Technical University in Prague, Czech Republic.

## Research interests:

- wireless communication, signal processing, mathematics.

## Education:

- M.S. (2009) at Czech Technical University in Prague, Czech Republic. *Thesis topic: Receiver Signal Processing for Space-Time Coded CPM in MIMO System.*
  - Erasmus at Rheinisch-Westfälische Technische Hochschule (RWTH) in Aachen, Germany, Spring Semester 2008.
- B.S. (2006) at Czech Technical University in Prague, Czech Republic. *Thesis topic: GPS Receiver Signal Processing.*

## Publications:

URL: <http://scholar.google.com/citations?user=ChZ6TI4AAAAJ>

- Journal Articles
  - M. Hekrdla and J. Sykora. Hexagonal Constellations for Adaptive Physical-Layer Network Coding 2-Way Relaying. Under resubmission to *IEEE Communication Letters*. 2013.
  - M. Hekrdla and J. Sykora. Optimized Constellation Prerotation for 3-Terminal 1-Relay Network with Wireless Network Coding. In *IEEE Communication Letters*, pages 1200 - 1203, vol. 16, no. 8, August 2012.
  - M. Hekrdla and J. Sykora. Design of Uniformly Most Powerful Alphabets for HDF 2-Way Relaying Employing Non-Linear Frequency Modulations. In *EURASIP Journal on Wireless Communications and Networking (J-WCN)*, pages 1-18, no. 128/2011, October 2011.
- Local Journals
  - M. Hekrdla. Numerically Optimized Uniformly Most Powerful Alphabets for Hierarchical-Decode-and-Forward Two-Way Relaying. In *Acta Polytechnica*, vol. 51, no. 5/ 2011.
  - M. Hekrdla. Constellation space dimensionality reduced sub-optimal receiver for orthogonal STBC CPM modulation in MIMO channel. In *Acta Polytechnica*, vol. 49, no.2-3/ 2009.

- Conference Papers

- M. Hekrdla and J. Sykora. On Indexing of Lattice-Constellations for Wireless Network Coding with Modulo-Sum Decoding. In *Proc. IEEE Vehicular Technology Conf. (VTC)*, pages 1-6, Dresden, Germany, June 2013.
- M. Hekrdla and J. Sykora. Uniformly Most Powerful Alphabet for HDF Two-Way Relaying Designed by Non-linear Optimization Tools. In *IEEE International Symposium on Wireless Communication Systems (ISWCS)*, pages 1-5, Aachen, Germany, November 2011.
- J. Sykora and M. Hekrdla. Determinant criterion optimizing linear subspace projector for burst orthogonal STC CPM modulation in MIMO channel. In *Proc. IEEE Vehicular Technology Conf. (VTC)*, pages 1-6, Barcelona, Spain, April 2009.

- Workshop Papers

- M. Hekrdla and J. Sykora. Lattice-Constellation Indexing for Wireless Network Coding 2-Way Relaying with Modulo-Sum Relay Decoding. In **COST IC1004 MCM**, pages 1-10, Bristol, United Kingdom, September 2012, TD(12)05057.
- M. Hekrdla and J. Sykora. Suppression of Relative-Fading by Diversity Reception in Wireless Network Coding 2-Way Relaying. In **COST IC1004 MCM**, pages 1-8, Lyon, France, May 2012, TD(12)04033.
- M. Hekrdla. Numerically Optimized Uniformly Most Powerful Alphabets for Hierarchical-Decode-and-Forward Two-Way Relaying. In **Poster 2011**, pages 1-5, Prague, May 2011. **\*\*\* Dean award for the best paper in section Communications in Poster 2011 \*\*\***
- M. Hekrdla, T. Uricar, P. Prochazka, M. Masek, T. Hynek and J. Sykora. Cooperative Communication in Wireless Relay Networks. In **Workshop 2011**, pages 1-18, Prague, February 2011.
- M. Hekrdla and J. Sykora. Channel parameter invariant network coded FSK modulation for hierarchical decode and forward strategy in wireless 2-way relay channel. In **COST 2100 MCM**, pages 1-8, Aalborg, Denmark, June 2010, TD-10-11087.
- M. Hekrdla. On design of channel parameter invariant FSK in two-way relay channel. In **Poster 2010**, pages 1-7, Prague, May 2010.
- T. Uricar, J. Sykora and M. Hekrdla. Example design of multi-dimensional parameter-invariant hierarchical exclusive alphabet for layered HXC design in 2-WRC. In **COST 2100 MCM**, pages 1-7, Athens, Greece, February 2010. TD-10-10088.
- M. Hekrdla. Constellation space dimensionality reduced sub-optimal receiver for orthogonal STBC CPM modulation in MIMO channel. In **Poster 2009**, pages 1-6, Prague, May 2009. **\*\*\* Dean award for the paper in section Communications in Poster 2009 \*\*\***
- M. Hekrdla and J. Sykora. CPM constellation subspace projection maximizing average minimal distance - sufficiency condition and comparison to PC analysis. In **COST 2100 MCM**, pages 1-8, Valencia, Spain, May 2009. TD-09-870.
- J. Sykora and M. Hekrdla. Determinant maximizing and rank preserving waveform subspace linear projector for burst Alamouti STC MSK modulation. In **COST 2100 MCM**, pages 1-7, Lille, France, October 2008. TD-08-655.

## Projects:

- International Projects

- FP7 ICT-2011-8/2009.1.1: DIWINE - Dense Cooperative Wireless Cloud Network, 2013 – *present*

- EU COST-IC1004: Cooperative Radio Communications for Green Smart Environments, 2011 – *present*
  - FP7 ICT/STREP (INFISO-ICT-248001): SAPHYRE — Sharing Physical Resources Mechanisms and Implementations for Wireless Networks, 2010 – 2012
  - FP7 ICT/STREP (INFISO-ICT-215669): EUWB — Coexisting Short Range Radio by Advanced Ultra-WideBand Radio Technology, 2010 – 2011
  - EU COST 2100: Pervasive Mobile & Ambient Wireless Communications, 2006 – 2010
- Local Projects
    - Ministry of Education, Youth and Sports (LD 12062): WNC and Signal Processing in Cooperative Distributed Multi-node Multi-source Communication Systems, 2012 – *present*
    - Grant Agency of the Czech Technical University in Prague (SGS 13/083/OHK3/1T/13): Wireless Network Coding based Multi-node Dense Networks, 2013 – *present*
    - Grant Agency of Czech Republic (GACR 102/09/1624): Mobile radio communication systems with distributed, cooperative and MIMO processing, 2009 – 2012
    - Grant Agency of the Czech Technical University in Prague (SGS 10/287/OHK3/3T/13): Distributed, Cooperative and MIMO (Multiple-Input Multiple-Output) Physical Layer Processing in General Multi-Source Multi-Node Mobile Wireless Network, 2010 – 2012
    - Ministry of Education, Youth and Sports (OC 188): Signal Processing and Air-Interface Technique for MIMO radio communication systems, 2007 – 2010

### **Professional Service:**

- Technical Program Committee:
  - *IEEE International Symposium on Personal, Indoor and Mobile Radio Communications (PIMRC)*, London, United Kingdom, 2013.
- Review Effort:
  - *IEEE International Symposium on Personal, Indoor and Mobile Radio Communications (PIMRC)*,
  - *IEEE Global Telecommunications Conf. (GLOBECOM)*,
  - *IEEE Vehicular Technology Conf. (VTC)*,
  - *International Symposium on Wireless Communication Systems (ISWCS)*,
  - *Radioengineering*.

### **Languages:**

- Czech: *Native*,
- English: *Professional working proficiency* (FCE Certificate, Private Language Summer Schools in UK (2x)),
- German: *Limited working proficiency* (Erasmus Study in Germany, Private Language Courses at Goethe Institute in Prague (2 years)).